

**SIMULATION OF SAMPLING DISTURBANCE  
IN SOFT CLAYS  
USING TRIAXIAL ELEMENT TESTS**

by

**Maria Caterina Santagata**

Laurea in Ingegneria Civile, Università di Ancona  
Ancona, Italia  
(1990)

Submitted to the  
Department of Civil and Environmental Engineering  
in partial fulfillment of the requirements for the degree of  
Master of Science in Civil and Environmental Engineering

at the

**MASSACHUSETTS INSTITUTE OF TECHNOLOGY**

May, 1994

© Massachusetts Institute of Technology, 1994

Signature of Author.....  
Department of Civil and Environmental Engineering, May 20, 1994

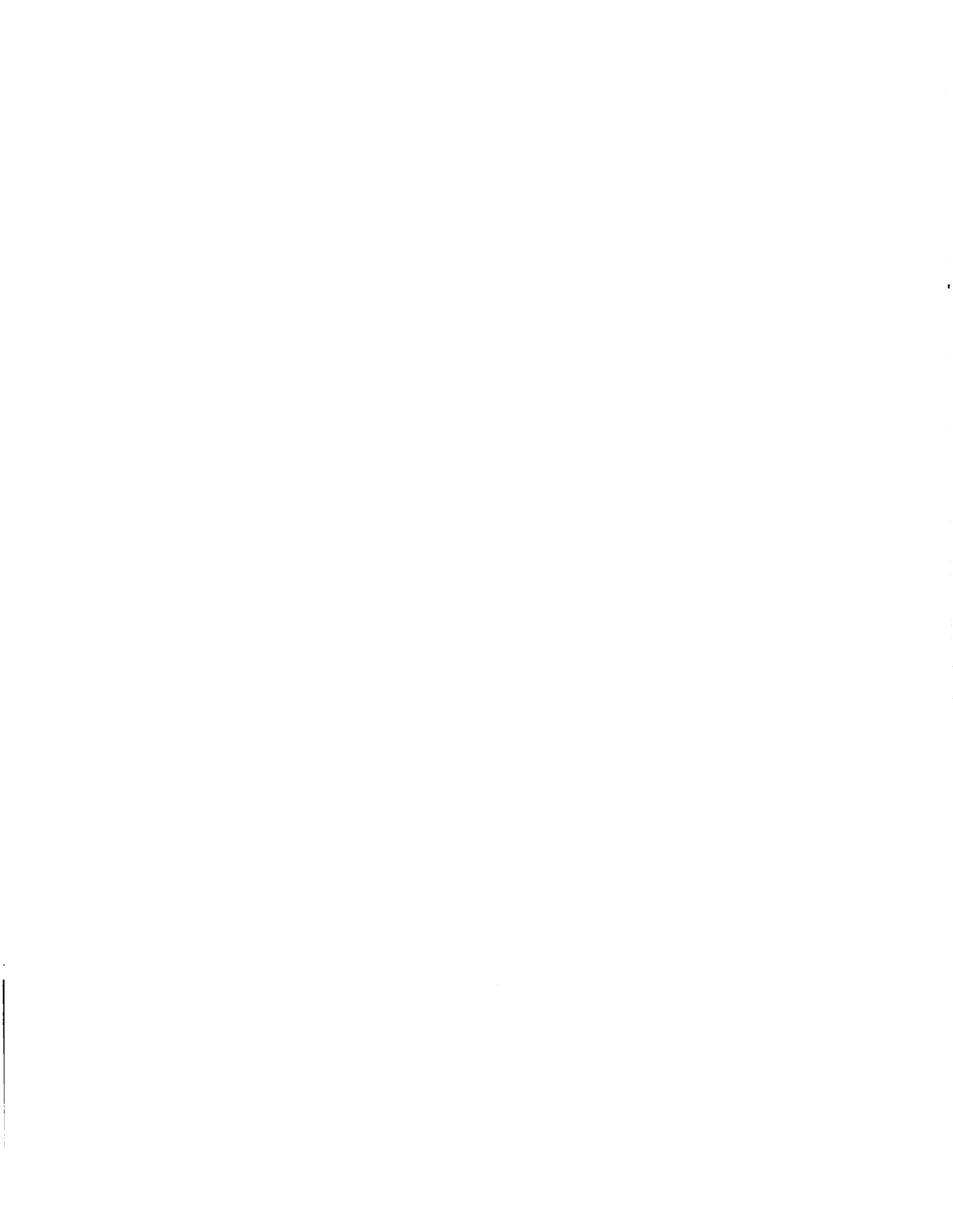
Certified by.....  
Dr. John T. Germaine, Thesis Supervisor

Accepted by.....  
Joseph M. Sussman  
Chairman, Departmental Committee on Graduate Studies

ARCHIVES  
MASSACHUSETTS INSTITUTE  
OF TECHNOLOGY

JUN 29 1994

LIBRARIES



# **SIMULATION OF SAMPLING DISTURBANCE IN SOFT CLAYS USING TRIAXIAL ELEMENT TESTS**

by

**Maria Caterina Santagata**

Submitted to the Department of Civil and Environmental Engineering on  
May 20, 1994 in partial fulfillment of the requirements  
for the degree of Master of Science in Civil and Environmental Engineering

## **ABSTRACT**

The problem of sampling disturbance was investigated with single element triaxial tests performed on Resedimented Boston Blue Clay. Intact specimens were disturbed according to the Perfect Sampling Approach (PSA) and the Ideal Sampling Approach (ISA) to simulate specific aspects of disturbance. Each test was continued to measure the mechanical properties of the soil after disturbance. The testing program included a total of 46 triaxial tests with OCR between 1 and 8.

The effects of PSA and ISA disturbance on the compression and undrained shear behavior of the soil were quantified by comparison with the intact behavior of the soil. Results indicate that PSA disturbance produces limited damage on NC RBBC and has no effect on the behavior of OC RBBC. ISA disturbance produces a reduction in the effective stresses and a degradation of the material properties. These adverse effects increase with the magnitudes of the disturbance strains. NC RBBC appears to be more susceptible to disturbance than the OC soil.

Neither the decrease in the effective stresses, nor the loss in undrained strength caused by ISA disturbance are as severe as typically observed in field samples. However the strength of the disturbed soil is well represented by a SHANSEP type equation by introducing the Induced Overconsolidation Ratio (IOCR).

Increasing disturbance causes a decrease in the compression ratio of the soil and an increase in the strains at any given stress, but does not significantly affect the preconsolidation pressure which for all levels of disturbance is estimated within  $10 \pm 5\%$ . In all cases disturbance leads to an overestimation of  $\sigma'_p$ .

The work performed also provides a preliminary assessment of the applicability of the Recompression and SHANSEP (for NC RBBC only) techniques to recover the intact behavior of the soil. Test results indicate that Recompression yields an unsafe estimate of the strength for NC RBBC and a poor description of the stress strain behavior of the soil for all OCRs. Reconsolidation through SHANSEP provides, for all magnitudes of disturbance, an accurate and safe estimate of the undrained strength of the NC soil, and for moderate disturbance furnishes a realistic description of its stress strain behavior.

This research has also isolated several new aspects of the intact behavior of RBBC. In particular, it was shown that within a wide range of values of  $K_0$  there is a clear relationship between the pre-shear lateral stress ratio and the undrained strength ratio of NC RBBC, with  $c_u/\sigma'_{vc}$  decreasing with increasing  $K_0$ . It was also pointed out that stress path consolidation produces significant variations in the compression behavior of RBBC obscuring the stress history and causing a marked decrease of the compression ratio.

Thesis Supervisor: Dr. John T. Germaine.

Title: Principal Research Associate in Civil and Environmental Engineering







## Table of Contents

<b>Abstract</b>	<b>3</b>
<b>Acknowledgments</b>	<b>5</b>
<b>Table of Contents</b>	<b>7</b>
<b>List of Tables</b>	<b>13</b>
<b>List of Figures</b>	<b>15</b>
<b>1 Introduction</b>	<b>27</b>
1.1 Problem Statement	27
1.2 Research Objectives	29
1.3 Organization	30
<b>2 Background</b>	<b>33</b>
2.1 Introduction	33
2.2 Hvorslev's Work	34
2.3 The Perfect Sampling Approach	38
2.4 The Ideal Sampling Approach	40
2.5 Reconsolidation Procedures	43
2.5.1 Recompression	43
2.5.2 SHANSEP	44
2.5.3 Recompression vs. SHANSEP	45
2.6 Other Research on Sampling Disturbance of Cohesive Soils	46 47
2.6.1 Sampling Techniques	47

2.6.1.1	Traditional Sampling Methods for Undisturbed Samples	47
2.6.1.2	The Laval Sampler	49
2.6.1.3	The Sherbrooke Sampler	51
2.6.2	Effects of Disturbance	52
2.6.2.1	Effective Stresses	52
2.6.2.2	Bounding Surface	54
2.6.2.3	Undrained Strength	55
2.6.2.4	Undrained Stiffness	56
2.6.2.5	Compression Curve and Preconsolidation Pressure	59
2.6.3	Factors Influencing Disturbance	60
2.6.3.1	Borehole Advancement	60
2.6.3.2	Sampler Penetration	61
2.6.3.3	Storage Method and Time	64
2.6.3.4	Specimen Preparation Method	65
2.6.4	Assessment of Sample Quality	67
<b>3</b>	<b>Supporting Technology</b>	<b>95</b>
3.1	Introduction	95
3.2	Resedimented Boston Blue Clay	96
3.2.1	Introduction	96
3.2.2	Resedimentation procedure	96
3.2.3	Material Index Properties	98
3.3	MIT Automated Stress Path Triaxial Apparatus	100
3.4	Testing Procedure	103



<b>4</b>	<b>Research Approach</b>	<b>115</b>
4.1	Introduction	115
4.2	Description and Motivation of the Testing Program	116
4.2.1	"Disturbed" and "Undisturbed" Tests	116
4.2.2	Simulation of Disturbance According to the PSA and ISA	119
4.2.3	Motivation of the Testing Program	120
<b>5</b>	<b>Intact Behavior of RBBC</b>	<b>131</b>
5.1	Introduction	131
5.2	Intact Compression Behavior	133
5.2.1	Typical Compression Behavior	133
5.2.2	Compression Ratio	135
5.2.3	Lateral Stress Ratio $K_0$	136
5.3	Intact Shear Behavior	139
5.3.1	General Undrained Behavior	139
5.3.2	Undrained Strength Ratio	140
5.3.3	Effective Stress Failure Envelope	142
5.3.4	Strain at Peak	143
5.3.5	Stiffness	143
<b>6</b>	<b>Effect of Disturbance on the Engineering Properties of RBBC</b>	<b>169</b>
6.1	Introduction	169
6.2	Effect of Disturbance on the Initial Effective Stresses	172
6.3	Effect of Disturbance on the Undrained Strength	177
6.4	Effect of Disturbance on the Strain at Peak	182

6.5	Effect of Disturbance on the Undrained Modulus Eu(50)	183
6.6	Effect of Disturbance on the Intermediate Strain Stiffness	185
6.7	Effect of Disturbance on the Compression Behavior	188
6.7.1	Effect of Disturbance on the Compression Curve and the Compressibility Parameters	188
6.7.2	Effect of Disturbance on the Reconsolidation Strains	191
6.7.3	Effect of Disturbance on the Maximum Past Pressure	192
6.8	Effect of Stress Relief due to Borehole Drilling	199
7	<b>Effect of Recompression and SHANSEP Reconsolidation on the Undrained Behavior of RBBC</b>	235
7.1	Introduction	235
7.2	Recompression	236
7.2.1	General Undrained Behavior	236
7.2.2	Undrained Strength	239
7.2.3	Strain at Peak	242
7.2.4	Undrained Stiffness	243
7.3	SHANSEP	244
7.3.1	General Undrained Behavior	244
7.3.2	Undrained Strength	246
7.3.3	Strain at Peak	247
7.3.4	Undrained Stiffness	248

<b>Chapter 8</b>	<b>Summary, Conclusion, and Recommendations</b>	<b>267</b>
8.1	Introduction	267
8.2	Summary of the Results	268
8.2.1	Intact Behavior of Resedimented Boston Blue Clay	268
8.2.2	Effects of Disturbance on the Undrained Shear Behavior of RBBC	271
8.2.3	Effects of Disturbance on the Compression Behavior of RBBC	275
8.2.4	Effect of Recompression Reconsolidation on the Undrained Behavior of RBBC	277
8.2.5	Effect of SHANSEP Reconsolidation on the Undrained Behavior of NC RBBC	278
8.3	Conclusions	279
8.4	Recommendations for Future Research	282

## References

## Appendix A



## List of Tables

Table 2.1:	Variation of Strength and Stiffness as a Function of Tube Diameter and Tip Geometry (from La Rochelle et al. 1981)	71
Table 4.1:	Summary of Testing Program	123
Table 4.2:	Test Classification	124
Table 6.1:	Changes in the Effective Stresses due to Disturbance	202
Table 6.2:	Comparison of True and Estimated Values of the Preconsolidation Pressure for ISA $\pm$ 1, ISA $\pm$ 2 and ISA $\pm$ 5 Tests on NC RBBC	203
Table 6.3:	Comparison of True and Estimated Values of the Preconsolidation Pressure for ISA $\pm$ 1 Tests on RBBC with OCR=1, 1.89 and 4.4	204



## List of Figures

Figure 2.1a	Shape of the Simple Sampler	72
Figure 2.1b	Detail of the Tip of the Simple Sampler	72
Figure 2.2a	Contours of $\epsilon_{rr}$ Produced by Penetration of the Simple Sampler (from Baligh et al. 1985)	73
Figure 2.2b	Contours of $\epsilon_{\theta\theta}$ Produced by Penetration of the Simple Sampler (from Baligh et al. 1985)	73
Figure 2.2c	Contours of $\epsilon_{rz}$ Produced by Penetration of the Simple Sampler (from Baligh et al. 1985)	73
Figure 2.2d	Contours of $\epsilon_{zz}$ Produced by Penetration of the Simple Sampler (from Baligh et al. 1985)	73
Figure 2.3	Straining History at Centerline of Simple Samplers (from Baligh et al. 1985)	74
Figure 2.4	Consolidation Procedures for Recompression and SHANSEP $CK_0U$ Testing (from Ladd 1987)	75
Figure 2.5	Geometrical Characteristics of Tube Samplers (from Sinfield 1994)	76
Figure 2.6	Thin-Wall Open Drive Sampler (from Hvorslev 1949)	77
Figure 2.7	Piston Sampler with Stationary Piston (from Hvorslev 1949)	78
Figure 2.8	Schematic of the Laval Sampler (from La Rochelle et al. 1981)	79

Figure 2.9	Phases of Operation of the Laval Sampler (from La Rochelle et al. 1981)	80
Figure 2.10	Schematic of the Sherbrooke Sampler (from Lefebvre and Poulin, 1979)	81
Figure 2.11	Comparison of Mean Effective Stresses in Situ and after Sampling for Bothkennar Clay (a), Offshore Clayey Silts (b), London Clay (c) (from Hight 1992)	82
Figure 2.12	Variation of Water Content within (a-b) Soft (LL=92%, PL=33%) and (c-d) Stiff (LL=81%, PL=30%) Clay Samples due to Tube Sampling (from Vaughan et al 1992)	83
Figure 2.13	Sources of Variation of the Mean Effective Stress (from Hight et al. 1992)	84
Figure 2.14	Comparison of the Bounding Surfaces of Saint Louis Clay Obtained from Laval and Piston Samplers (from Tavenas and Leroueil 1987)	85
Figure 2.15	Comparison of UU Test Results on Bothkennar Clay Specimens Obtained from Piston and Laval Samples (from Hight et al. 1992)	86
Figure 2.16	$E_{50}/\sigma'_{vc}$ versus OCR for Recompression and SHANSEP Tests on Boston Blue Clay (from Estabrook 1990)	87
Figure 2.17	Operations Influencing Disturbance	88
Figure 2.18	Comparison of Strength Profiles from UU Tests on Samples Obtained Using Different Boring and Sampling Methods (from Adachi 1981)	89



Figure 2.19	Mean Effective Stress Profiles Determined from Piston, Laval, and Sherbrooke Samples (from Hight et al. 1992)	90
Figure 2.20a	Effect of Trimming Method on the Stress-Strain Behavior of Bothkennar Clay (from Atkinson et al. 1992)	91
Figure 2.20b	Effect of Trimming Method on the Stiffness of Bothkennar Clay (from Atkinson et al. 1992)	91
Figure 2.20c	Effect of Trimming Method on the Bounding Surface of Bothkennar Clay (from Atkinson et al. 1992)	91
Figure 2.21	Effect of the Tube Trimming Method on the Mean Effective Stress Determined on Piston, Laval and Sherbrooke Samples (from Hight et al. 1992)	92
Figure 2.22	Volumetric Strains During Reconsolidation of Tube and Sherbrooke Samples (from Lacasse et al. 1985)	93
Figure 3.1	Schematic of the Equipment Used for Resedimentation of Boston Blue Clay	109
Figure 3.2	Results of Grain Size Analysis on RBBC Series III (after Seah 1990)	110
Figure 3.3	Results from Atterberg Limit Tests on Series III RBBC (modified from Cauble 1993)	111
Figure 3.4	Plasticity Chart with Data from RBBC Series III (Modified from Cauble 1993)	112
Figure 3.5	Schematic Representation of the MIT Automated Stress Path Triaxial Apparatus (from de La Beaumelle 1991)	113

Figure 4.1a	Phases of a ISA $\pm$ 2 "UU" Test on NC RBBC: e- log $\sigma'_v$ Curve	125
Figure 4.1b	Phases of a ISA $\pm$ 2 "UU" Test on NC RBBC: Stress Path	125
Figure 4.2a	Phases of a ISA $\pm$ 2 "Recompression" Test on NC RBBC: e- log $\sigma'_v$ Curve	126
Figure 4.2b	Phases of a ISA $\pm$ 2 "Recompression" Test on NC RBBC: Stress Path	126
Figure 4.3a	Phases of a ISA $\pm$ 2 "SHANSEP" Test on NC RBBC: e- log $\sigma'_v$ Curve	127
Figure 4.3b	Phases of a ISA $\pm$ 2 "SHANSEP" Test on NC RBBC: Stress Path	127
Figure 4.4a	Examples of Stress Strain Curves during PSA and ISA Disturbance of NC RBBC	128
Figure 4.4b	Examples of Stress Paths during PSA and ISA Disturbance of NC RBBC	128
Figure 4.5a	Examples of Stress Strain Curves during PSA and ISA Disturbance of OCR4 RBBC	129
Figure 4.5b	Examples of Stress Paths during PSA and ISA Disturbance of OCR4 RBBC	129
Figure 5.1a:	Selection of Compression Curves from Tests on BBC216: TX115, 117, 118, 119, 120, 121, 123	145
Figure 5.1b:	Selection of Compression Curves from Tests on BBC217: TX124, 125, 127, 130, 131	146
Figure 5.1c:	Selection of Compression Curves from Tests on BBC218: TX134, 140, 142, 145, 177	147

<b>Figure 5.1d:</b>	Selection of Compression Curves from Tests on BBC219: TX182, 186, 196, 199, 208, 210	148
<b>Figure 5.1e:</b>	Selection of Compression Curves from Tests on BBC220: TX219, 224, 231, 235, 237, 238, 242	149
<b>Figure 5.2:</b>	Lateral Stress Ratio vs. Vertical Effective Stress During $K_0$ - Consolidation of RBBC	150
<b>Figure 5.3:</b>	Scatter in the Measured Values of $K_{0(NC)}$ for Batches 216-220	151
<b>Figure 5.4:</b>	Selection of Stress Paths for One Dimensional Consolidation of RBBC (Batches 216-219)	152
<b>Figure 5.5a:</b>	Comparison of $K_0$ (TX118) and Stress Path Consolidation (TX172): $K$ vs. $\sigma'_v$ Curves	153
<b>Figure 5.5b:</b>	Comparison of $K_0$ (TX118) and Stress Path Consolidation (TX172): Compression Curves	153
<b>Figure 5.5c:</b>	Comparison of $K_0$ (TX118) and Stress Path Consolidation (TX172): Stress Paths	153
<b>Figure 5.6</b>	Intact Undrained Shear (TXC) Behavior of RBBC (OCR=1, 2, 4, 8): Stress Paths	154
<b>Figure 5.7:</b>	Intact Undrained Shear Behavior (TXC) of RBBC (OCR=1, 2, 4, 8): Stress Strain Curves	155
<b>Figure 5.8a:</b>	Intact Undrained Shear (TXC) Behavior of RBBC (OCR=1, 2, 4, 8): Normalized Shear Induced Pore Pressure vs. Axial Strain	156
<b>Figure 5.8b:</b>	Intact Undrained Shear (TXC) Behavior of RBBC (OCR=1, 2, 4, 8): Normalized Excess Pore Pressure vs. Axial Strain	157

<b>Figure 5.9:</b>	Selection of Stress Paths for Undrained Shear (TXC) of Intact NC RBBC (Batches 216-219)	158
<b>Figure 5.10:</b>	Selection of Stress Strain Curves for Undrained Shear (TXC) of Intact NC RBBC (Batches 216-219)	159
<b>Figure 5.11:</b>	Relationship between the Pre-Shear Lateral Stress Ratio $K_{0(NC)}$ and the Undrained Strength Ratio for NC RBBC	160
<b>Figure 5.12:</b>	Correction of the Undrained Strength of NC RBBC to account for the Variation of the Lateral Stress Ratio $K_{0(NC)}$	161
<b>Figure 5.13:</b>	Effect of $K_{0(NC)}$ on the Strength of OC RBBC	162
<b>Figure 5.14:</b>	$C_u/\sigma'_{vc}$ versus OCR: Determination of the SHANSEP Parameters for Intact RBBC	163
<b>Figure 5.15:</b>	Friction Angle at Maximum Obliquity for Intact RBBC (OCR=1, 2, 4, 8)	164
<b>Figure 5.16:</b>	Strain at Peak versus $K_0$ for NC RBBC	165
<b>Figure 5.17:</b>	Strain at Peak versus OCR for RBBC	165
<b>Figure 5.18:</b>	$E_{u(50)}/\sigma'_{vc}$ versus Overconsolidation Ratio for Intact RBBC	166
<b>Figure 5.19:</b>	Normalized Undrained Modulus versus Axial Strain for Intact RBBC (OCR=1, 2, 4, 8)	167
<b>Figure 6.1a:</b>	Effect of PSA and ISA Disturbance on the Stress Strain Curves of Normally Consolidated RBBC	205

<b>Figure 6.1b</b>	Effect of PSA and ISA Disturbance on the Stress Paths of Normally Consolidated RBBC	205
<b>Figure 6.2a</b>	Effect of PSA and ISA Disturbance on the Stress Strain Curves of OCR4 RBBC	206
<b>Figure 6.2b</b>	Effect of PSA and ISA Disturbance on the Stress Paths of OCR4 RBBC	206
<b>Figure 6.3</b>	Effect of ISA <sub>+2</sub> Disturbance on the Compression Behavior of NC RBBC	207
<b>Figure 6.4a</b>	Stress Strain Curves for PSA, ISA <sub>+1</sub> , ISA <sub>+2</sub> and ISA <sub>+5</sub> Disturbance of OCR4 RBBC	208
<b>Figure 6.4b</b>	Stress Paths for PSA, ISA <sub>+1</sub> , and ISA <sub>+2</sub> and ISA <sub>+5</sub> Disturbance of OCR4 RBBC	208
<b>Figure 6.4c</b>	Shear Induced Pore Pressure During PSA, ISA <sub>+1</sub> , ISA <sub>+2</sub> and ISA <sub>+5</sub> Disturbance of NC RBBC	209
<b>Figure 6.5a</b>	Stress Strain Curves for PSA, ISA <sub>+1</sub> , and ISA <sub>+2</sub> Disturbance of OCR4 RBBC	210
<b>Figure 6.5b</b>	Stress Paths for PSA, ISA <sub>+1</sub> , and ISA <sub>+2</sub> , ISA <sub>+5</sub> Disturbance of OCR4 RBBC	210
<b>Figure 6.5c</b>	Shear Induced Pore Pressure During PSA, ISA <sub>+1</sub> , and ISA <sub>+2</sub> Disturbance of OCR4 RBBC	211
<b>Figure 6.6</b>	Loss in Mean Effective Stress due to PSA and ISA Disturbance in NC RBBC	212
<b>Figure 6.7</b>	Loss in Mean Effective Stress due to PSA and ISA Disturbance for NC and OC RBBC	213
<b>Figure 6.8</b>	Loss in Mean Effective Stress due to Disturbance as a Function of the OCR and the Amplitude of the Disturbance Cycle	214

<b>Figure 6.9a</b>	Schematic Representation of Effects of Swelling and Disturbance: NC RBBC	215
<b>Figure 6.9b</b>	Schematic Representation of Effects of Swelling and Disturbance: OC RBBC	215
<b>Figure 6.10</b>	Decrease in Strength of NC RBBC due to PSA and ISA Disturbance	216
<b>Figure 6.11</b>	Effect of PSA and ISA Disturbance on the Undrained Strength of NC and OC RBBC	217
<b>Figure 6.12</b>	SHANSEP Relationship between $C_u/\sigma'_s$ and IOCR for Disturbed NC RBBC	218
<b>Figure 6.13</b>	SHANSEP Relationship for Disturbed RBBC	219
<b>Figure 6.14</b>	Strain at Peak after PSA and ISA Disturbance of RBBC	220
<b>Figure 6.15</b>	Strain at Peak versus AOCR for Intact and Disturbed RBBC	221
<b>Figure 6.16</b>	Effect of ISA Disturbance on $Eu_{50}$ for NC RBBC	222
<b>Figure 6.17</b>	Decrease of $Eu_{50}$ due to Disturbance in RBBC	222
<b>Figure 6.18</b>	Effect of Disturbance on the Intermediate Strain Stiffness of NC RBBC	223
<b>Figure 6.19</b>	Effect of Disturbance on the Intermediate Strain Stiffness of RBBC with $OCR=2$	223
<b>Figure 6.20</b>	Effect of Disturbance on the Intermediate Strain Stiffness of RBBC with $OCR=4$	224

<b>Figure 6.21</b>	Effect of ISA Disturbance on the Compression Behavior of NC RBBC	225
<b>Figure 6.22</b>	Effect of Disturbance on the Compressibility of NC RBBC	226
<b>Figure 6.23</b>	Effect of ISA $\pm$ 2 Disturbance on the Compressibility of RBBC with OCR=1, 1.89, and 4.4	226
<b>Figure 6.24</b>	Effect of ISA $\pm$ 2 Disturbance on the Compression Behavior of RBBC with OCR=1, 1.89, 4.4	227
<b>Figure 6.25</b>	Volumetric Reconsolidation Strains after PSA and ISA Disturbance of RBBC	228
<b>Figure 6.26a</b>	Determination of the Preconsolidation Pressure by the Strain Energy Method after ISA $\pm$ 1 Disturbance of NC RBBC (TX134)	229
<b>Figure 6.26b</b>	Determination of the Preconsolidation Pressure by the Strain Energy Method after ISA $\pm$ 2 Disturbance of NC RBBC (TX142)	229
<b>Figure 6.26c</b>	Determination of the Preconsolidation Pressure by the Strain Energy Method after ISA $\pm$ 5 Disturbance of NC RBBC (TX260)	230
<b>Figure 6.27</b>	Simplified Models Describing the Effects of Disturbance on the Compression Curve	231
<b>Figure 6.28a</b>	Determination of the Preconsolidation Pressure by the Strain Energy Method after ISA $\pm$ 2 Disturbance of OCR2 RBBC (TX236)	232
<b>Figure 6.28b</b>	Determination of the Preconsolidation Pressure by the Strain Energy Method after ISA $\pm$ 2 Disturbance of OCR4 RBBC (TX140)	232

<b>Figure 6.29a</b>	Special Test TX120 with Shear Stress Release Prior to ISA $\pm$ 1 Disturbance: Stress Strain Curve	233
<b>Figure 6.29b</b>	Special Test TX120 with Shear Stress Release Prior to ISA $\pm$ 1 Disturbance: Stress Path	233
<b>Figure 6.30a</b>	Comparison of TX120 with Two ISA $\pm$ 1 Tests: Stress Strain Curves	234
<b>Figure 6.30b</b>	Comparison of TX120 with Two ISA $\pm$ 1 Tests: Stress Paths	234
<b>Figure 7.1a</b>	Effect of PSA Disturbance and Recompression on the Undrained Shear Behavior of NC RBBC: Stress Strain Curve	249
<b>Figure 7.1b</b>	Effect of PSA Disturbance and Recompression on the Undrained Shear Behavior of NC RBBC: Stress Path	249
<b>Figure 7.2a</b>	Effect of ISA $\pm$ 1 Disturbance and Recompression on the Undrained Shear Behavior of NC RBBC: Stress Strain Curve	250
<b>Figure 7.2b</b>	Effect of ISA $\pm$ 1 Disturbance and Recompression on the Undrained Shear Behavior of NC RBBC: Stress Path	250
<b>Figure 7.3a</b>	Effect of ISA $\pm$ 2 Disturbance and Recompression on the Undrained Shear Behavior of NC RBBC: Stress Strain Curve	251
<b>Figure 7.3b</b>	Effect of ISA $\pm$ 2 Disturbance and Recompression on the Undrained Shear Behavior of NC RBBC: Stress Path	251



Figure 7.4a	Effect of ISA $\pm$ 2 Disturbance and RBBC with Nominal OCR equal to 4: Stress Strain Curve	252
Figure 7.4b	Effect of ISA $\pm$ 2 Disturbance and Recompression on the Undrained Shear Behavior of RBBC with Nominal OCR equal to 4: Stress Path	252
Figure 7.5	Change in Strength due to Recompression of Disturbed NC and OCR4 RBBC	253
Figure 7.6	Strain at Peak from Undisturbed, UU and Recompression Tests on NC RBBC	254
Figure 7.7	Strain at Peak from Undisturbed, UU and Recompression Tests on OCR4 RBBC	255
Figure 7.8	Effect of Disturbance and Recompression on the Stiffness of NC RBBC	256
Figure 7.9a	Effect of Disturbance and Recompression on the Stiffness of NC RBBC: PSA	256
Figure 7.9b	Effect of Disturbance and Recompression on the Stiffness of NC RBBC: ISA $\pm$ 1	257
Figure 7.9c	Effect of Disturbance and Recompression on the Stiffness of NC RBBC: ISA $\pm$ 2	257
Figure 7.10	Effect of Disturbance and Recompression on the Stiffness of RBBC with Nominal OCR=4	258
Figure 7.11a	Effect of ISA $\pm$ 1 Disturbance and SHANSEP on the Undrained Shear Behavior of NC RBBC: Stress Strain Curve	259

Figure 7.11b	Effect of ISA $\pm$ 1 Disturbance and SHANSEP on the Undrained Shear Behavior of NC RBBC: Stress Path	259
Figure 7.12a	Effect of ISA $\pm$ 2 Disturbance and SHANSEP on the Undrained Shear Behavior of NC RBBC: Stress Strain Curve	260
Figure 7.12b	Effect of ISA $\pm$ 2 Disturbance and SHANSEP on the Undrained Shear Behavior of NC RBBC: Stress Path	260
Figure 7.13a	Effect of ISA $\pm$ 5 Disturbance and SHANSEP on the Undrained Shear Behavior of NC RBBC: Stress Strain Curve	261
Figure 7.13b	Effect of ISA $\pm$ 5 Disturbance and SHANSEP on the Undrained Shear Behavior of NC RBBC: Stress Path	261
Figure 7.14	Applicability of the $K_{0(NC)}$ vs. $C_u/\sigma'_{vc}$ Relationship to the SHANSEP Tests	262
Figure 7.15	Strain at Peak from Undisturbed, UU, SHANSEP, and Recompression Tests on NC RBBC	263
Figure 7.16	Validity of the $K_{0(NC)}$ versus $\epsilon_{peak}$ Relationship for SHANSEP tests	264
Figure 7.17	Effect of Disturbance and SHANSEP Reconsolidation on the Stiffness of NC RBBC	265
Figure 7.18	Stiffness for ISA $\pm$ 1 Disturbed SHANSEP Test on NC RBBC	265
Figure 7.19	Stiffness for ISA $\pm$ 2 Disturbed SHANSEP Test on NC RBBC	266
Figure 7.20	Stiffness for ISA $\pm$ 5 Disturbed SHANSEP Test on NC RBBC	266

# Chapter 1 Introduction

## 1.1 Problem Statement

Laboratory tests on samples obtained from the field are routinely performed to evaluate the engineering properties of soils. These tests have the advantages of providing well-defined, controlled boundary and drainage conditions as well as uniform stresses within the soil, therefore allowing easy interpretation of the results. However there may be significant differences between the actual soil properties and those that are measured in the laboratory. In fact during the retrieval of the sample from the ground and the installation of the soil specimen in the testing device, the soil undergoes changes in stress, water content and structure which are generally referred to as sampling disturbance effects.

The geotechnical profession has long recognized the influence of sampling disturbance on the engineering properties of soils. However, most of the research performed in the last 40 years to establish the nature and extent of disturbances associated with sampling has been limited to comparative experimental investigations, and Hvorslev's 1949 "Subsurface Exploration and Sampling of Soils for Civil Engineering Purposes" still represents the most comprehensive study on the subject.

There is still large disagreement as to how sampling disturbance affects the engineering properties and how the intact behavior of the soil can be recovered in the laboratory. This is partially due to the fact the quality of a sample is the result of many factors before, during and after the

actual sampling operations: drilling, penetration and retrieval of the sampling tube, transportation, storage, extrusion, trimming and other operation required to prepare the specimens for laboratory testing.

It is useful however to separate the causes of disturbance as suggested by Baligh et al. (1987). These authors distinguish between the operator dependent and the unavoidable sampling disturbances. The first are mainly dependent on the performance of the operator, and can be reduced by close adherence to good practices of sampling. The second, considered the minimum possible disturbances, cannot be reduced by improving sampling operations for given equipment, and are primarily due to the penetration of the sampler, the water redistribution within the tube and the extrusion of the sample.

The only two efforts of rationally quantifying the effects of minimum sampling disturbance are represented by the Perfect Sampling Approach (PSA: Ladd and Lambe 1963) and the Ideal Sampling Approach (ISA: Baligh et al. 1987), which apply to block and tube sampling respectively. The PSA accounts for no disturbance except the undrained removal of the in situ shear stresses. The ISA incorporates the effects of tube penetration, sample retrieval to the surface and sample extrusion and provides a rational framework for predicting minimum disturbance effects in tube samples.

## 1.2 Research Objectives

This research expects to contribute to the fundamental understanding of the mechanisms causing sampling disturbance in soft clays. The experimental program is designed to simulate simple aspects of the field process using single element triaxial tests, making use of one clay with very well documented behavior: Resedimented Boston Blue Clay (RBBC). The simulation of disturbance is performed in accordance with the Perfect Sampling Approach and the Ideal Sampling Approach to model block and tube sampling, respectively. The sampling simulation is carried out using automated triaxial equipment.

The research intends to quantify the effects of disturbance, as defined by the PSA and the ISA, on the compression and undrained properties of soft clays as a function of the OCR. These properties include the initial effective stresses, the undrained strength, the stiffness, the strain at peak, the preconsolidation pressure, and the compressibility parameters of the soil.

A second objective of the research relates to evaluating the applicability of the two available reconsolidation techniques, Recompression and SHANSEP, in order to define the most appropriate means of recovering the intact behavior of the soil after disturbance.

On a secondary basis this work intends to perform a thorough evaluation of the behavior of intact RBBC.

### 1.3 Organization

Chapter 2 contains background information relative to sampling disturbance of clays. The first sections present the most significant contributions to the topic: a brief overview of Hvorslev's work, the Perfect Sampling Approach and the Ideal Sampling Approach. This is followed by a review of the reconsolidating techniques most used in practice: SHANSEP and Recompression. The chapter ends with a summary of prior investigations regarding the development of sampling methods particularly used in research, the effects of disturbance on the engineering properties of clays, the factors influencing the degree of disturbance and the methods used to assess disturbance.

Chapter 3 reviews the components of the technology available at MIT and used for this research. The Resedimentation Technology for obtaining Resedimented Boston Blue Clay, the material used for all the experimental program, is first presented followed by a description of the MIT Automated Stress Path Triaxial Cells employed to perform all the tests.

Chapter 4 discusses the rationale of the testing program. It also introduces the terminology used in the following chapters and provides a description of the different types of tests, distinguishing between Standard Undisturbed and Disturbed UU, Recompression, and SHANSEP tests.

The results of the triaxial experimental program are presented and discussed in the following three chapters.

Chapter 5 is dedicated to introducing the basic features of the "undisturbed" compression and shear behavior of RBBC determined

through tests run as part of this research and from previous data available on RBBC.

Chapters 6 and 7 present the original work performed in this thesis. Chapter 6 discusses the results of the tests conducted to evaluate the effect of disturbance, as described by the Perfect Sampling and the Ideal Sampling Approach on the engineering properties of RBBC. The first part of the chapter discusses the effects of disturbance on the undrained behavior of the soil including the pre-shear effective stresses, the undrained strength, the strain at peak and the stiffness characteristics. The second part of the chapter summarizes the more limited results obtained on the effects of disturbance on the compression behavior of the soil. In particular it is discussed how disturbance affects the estimates of the preconsolidation pressure and of the compressibility parameters (CR and RR). The chapter ends with the review of one special test performed to evaluate the effect of shear stress release prior to sampling on the magnitude of disturbance.

A limited number of tests were run to investigate to what degree reconsolidation by Recompression or SHANSEP is able to erase the effects disturbance and provide reliable estimates of the intact engineering properties. These tests are presented and discussed in Chapter 7.

Chapter 8 summarizes the most important results presented, draws the conclusions and examines the possible future directions of this research.





# Chapter 2 Background

## 2.1 Introduction

Sampling disturbance includes the changes in stresses, water content and structure undergone by a sample of soil during its retrieval from the ground and its installation in a testing device, which cause the properties measured in the lab to differ from the actual in situ values.

Many research efforts have been directed towards understanding the effects of disturbance on the engineering properties of sampled soils in response to the need for reliable and safe estimates of design parameters.

This chapter presents an overview of the most significant contributions relative to sample disturbance in soft clays, however is not intend to be a comprehensive summary.

Section 2.2 summarizes the main points of Hvorslev's 1949 report on soil sampling and subsurface exploration which represents the most comprehensive study on soil sampling and that contains recommendations for drilling, sampling and handling samples many of which are still used today.

The following two sections describe in some detail the main concepts of the Perfect Sampling Approach (PSA: Ladd and Lambe 1963) and of the Ideal Sampling Approach (ISA: Baligh et al. 1987), which are especially relevant to this research.

The concepts at the base of the two most used reconsolidation procedures, Recompression and SHANSEP, are summarized in Section 2.5.

The last section reviews other significant contributions in the field of sample disturbance regarding development of new sampling techniques, the effects of disturbance on the engineering properties of soft clays, the factors during the sampling and handling operations that influence the degree of disturbance and, finally, the methods used to assess disturbance.

## 2.2 Hvorslev's Work

In 1949, J. Hvorslev published "Subsurface Exploration and Sampling of Soils for Civil Engineering Purposes" which was the final report of the Committee of Sampling and Testing of the Soil Mechanics and Foundation Engineering Division of ASCE constituted with the goals of investigating the effects of sampling disturbance, critically reviewing the existing methods and equipment for soil sampling and developing improved methods and equipment. This represents the first and only comprehensive study on the subject of sample disturbance.

Of particular interest for the purpose of this research are the observations made by Hvorslev regarding the different types of disturbance to which the soil is subjected during sampling and their effects on engineering properties.

Hvorslev classified sample disturbance into the following types:

- a) change in stress conditions,
- b) change in water content and void ratio,
- c) disturbance of the soil structure,

- d) chemical changes and
- e) mixing and segregation of soil constituents.

Hvorslev observes that the sample may be subjected to both stress increases and decreases during the boring and sampling operations and is the first to recognize that "although most disturbances can be avoided or reduced by use of appropriate methods and equipment and careful work, ultimately the external stresses on the sample will be reduced from those acting in the ground to atmospheric pressure". While observing that in saturated clays the change in stress conditions will lead to the decrease of the shearing resistance observed in unconfined compression tests, Hvorslev suggests that the temporary stress reduction will have limited impact on the results of tests, consolidation, triaxial, direct shear, in which the specimen is subjected to stresses in excess of the original stresses in the ground.

Regarding the second class of disturbance, Hvorslev observes that changes in volume and void ratio will occur before, during and after sampling. Volume changes before sampling are hard to estimate and according to Hvorslev affect only the upper portion of the sample. The volume changes during sampling should not represent a major concern for saturated soils unless the sampler's advance is too slow to ensure fully undrained conditions. Hvorslev also recognizes the difficulty in determining the changes in water content caused by internal migration of water after sampling.

Hvorslev focuses most of his interest on the disturbance associated with disruption of the soil structure, described as the weakening of the inter-particle bonds or the rearrangement of the soil grains, and discusses

its effect on the results of consolidation tests as well as on UU and CU tests is discussed. Observation of compression curves allows to qualitatively judge the amount of disturbance that the soil structure has undergone: larger disturbance will produce more rounded compression curves and obscure the stress history. Disturbance will generally cause the unconfined strength to decrease. In CU tests this loss in strength may be balanced and even erased by the increase in strength caused by the decrease in void ratio during laboratory consolidation.

The processes which cause changes of the soil chemistry are covered in detail. They are related generally to storage of samples in untreated containers, oxidation caused by prolonged exposure of the soil to the air and penetration of salts from the wash water or of ingredients from the drilling mud into the soil at the bottom of the borehole.

The last type of disturbance, mixing and segregation, is generally caused by improper cleaning of the borehole, use of an open sampler or by piping or partial liquefaction caused by creation of vacuum over the sample. It is a gross form of disturbance which in most cases can be avoided with use of appropriate equipment.

According to Hvorslev a sample should be considered undisturbed when it suffers:

- a) no alteration of the soil structure,
- b) no change in water content or void ratio and
- c) no change in constituents or chemical composition

Considering it is nearly impossible to make sample by sample evaluation based on these three necessary requirements, Hvorslev defines the

following "practical requirements" which *can* be verified on a sample basis.

- a) the specific recovery ratio, defined as the ratio between the penetration of the sampler below the bottom of the borehole and the length of the recovered sample, should be very close to 1;
- b) no distortions or other signs of disturbance should be visible;
- c) the net length and weight of the sample should not change during shipment, storage and handling .

These requirements are to be considered complimentary: it is possible, for example that the soil structure has undergone significant disturbance and the recovery ratio is still very close to one.

Further qualitative indications of the disturbance suffered by the sample may be obtained by :

- a) examining the shape of the compression curve as well as the stress strain curve for compression tests,
- b) observing the variation in results within a sample
- c) comparing the quality of samples taken by various methods
- d) comparing samples of various diameters.

The magnitude of disturbance and consequently its influence on the engineering properties measured in lab tests depend on the equipment and on the characteristics of the soil. A critical review of the sampling techniques existing at the time, suggestions as to the most proper to use for different purposes and in different soil types and indications to reduce disturbance in practice are presented by Hvorslev. Particular emphasis is placed on the use of drilling fluid to prevent the caving of the borehole

and on performing the sampling operations as quickly as possible so that the swelling caused by the excavation of the borehole is limited.

### 2.3 The Perfect Sampling Approach

The Perfect Sampling Approach, the first effort to rationally quantify the minimum sampling disturbance effects, was proposed by Ladd and Lambe (1963). The Perfect Sampling Approach suggests that the only disturbance that cannot be avoided during sampling operations is the one produced by the release of the anisotropic in situ stresses. When all the sources of disturbance are eliminated, that is in the case of Perfect Sampling, it is possible to predict the effective stress after sampling from the following equation:

$$\sigma'_{ps} = \sigma'_{vo}[K_0 + Au(1-K_0)]$$

where  $\sigma'_{ps}$  is the effective stress at the end of perfect sampling,  $\sigma'_{vo}$  is the in situ vertical effective stress,  $K_0$  is the lateral stress ratio and  $Au$  is the  $A$  parameter for the undrained release of the shear stresses. Using typical values of  $K_0$  and  $Au$ , the equation predicts values of  $\sigma'_{ps}/\sigma'_{vo}$  equal to 0.35-0.8 for normally consolidated and slightly overconsolidated clays.

Measurements of residual pore pressures show however that actual sampling may cause a much more marked decrease in the effective stresses. The authors report measured pore pressures equal to 20%±20% of the theoretical value. The ratio  $\sigma'_{ps}/\sigma'_s$ , where  $\sigma'_s$  is the effective stress measured during setup, is suggested as a useful indicator of the additional disturbance to which the soil has been subjected during actual sampling.

Ladd and Lambe observe the similarity between the results of UU tests on NC clay, which carry the imprint of the disturbance to which the soil has been subjected, and CU tests on overconsolidated clays.

The reduction in effective stress from  $\sigma'_{ps}$  to  $\sigma'_s$  caused by sample disturbance and the decrease in stresses due to swelling appear to have comparable effects on the undrained strength of the soil. It is suggested that UU tests be regarded as tests performed on overconsolidated specimens with a maximum past pressure  $\sigma'_{ps}$  and an overconsolidation ratio equal to  $\sigma'_{ps}/\sigma'_s$ . This ratio is termed Apparent Overconsolidation Ratio.

Based on these considerations Ladd and Lambe propose a method to correct the undrained shear strength of the soil measured in UU tests by which the reduction in strength due to the decrease of the effective stresses is predicted from the decrease in strength with rebound, determined from CIU test results.

It must be pointed out that the idea of correcting UU data was not developed any further: UU results are influenced by other factors such as strain rate during shearing and the measurement of the residual stress requires the use of techniques not always precise and available. On the other hand the Perfect Sampling Approach constitutes the first effort of rationally quantifying sampling disturbance effects and the observation of the similarity between UU tests and CU tests on OC clay represents the basis for the development of the SHANSEP reconsolidation procedure which will be discussed in Section 2.5.2.

Since the introduction of the Perfect Sampling Approach, it has been recognized (Baligh et al. 1987) that the release of the in situ shear stress is not the only "unavoidable" disturbance occurring during tube sampling.

Perfect Sampling represents however an exhaustive model for the case of block sampling.

## 2.4 The Ideal Sampling Approach

The Ideal Sampling Approach (ISA: Baligh et al. 1987) represents an extension of the Perfect Sampling Approach discussed in the previous section. Relying on solutions based on the Strain Path Method (Baligh 1985), Baligh et al. (1987) suggest that tube sampling causes other "inevitable" disturbance besides that produced by the release of the in situ shear stresses. In fact the straining of the soil induced by tube penetration represents a dominant source of disturbance and must be considered in the rational formulation and prediction of minimum disturbance effects due to tube sampling of clays.

During the process of tube penetration, the soil is subjected to a complex strain path history, dependent on the position of the soil element within the sampler and the tube geometry expressed as a thickness to diameter ratio. The solutions presented by Baligh et al. are obtained with the Strain Path Method, by superimposing the effects of a ring source and a uniform flow. The geometry of the sampler is that of the "simple-sampler" (S-sampler) (Figure 2.1). The walls of the S-sampler have curved tips and involve a slight reduction of the inner diameter. The geometrical characteristics, thickness, inside clearance ratio, can be varied by changing the power of the ring source and using more sources.



Figure 2.2 presents contours of the different strain components produced by the penetration of an S-sampler with  $B/t=40$  (typical of thin-walled tube samplers).  $\epsilon_{rr}$ ,  $\epsilon_{zz}$  and  $\epsilon_{\theta\theta}$  represent respectively the radial, vertical and tangential normal strains, while  $\epsilon_{rz}$  is the meridional shear strain. These contours show the magnitude and extent of straining due to the steady state penetration of the S-sampler and indicate the complexity of the strain field around the tip. The three normal components are all of comparable magnitude. The shear strain is very large in vicinity of the sampler wall and is sharply reduced after passing the tip. The different sign of this strain inside and outside of the sampler wall is caused by the different shearing direction in the two zones. Soil disturbance, as described by the level of shear distortions, decreases towards the center of the sample. In the inner half of the sample the variations in the soil strains are minor: the dominant straining component is  $\epsilon_{zz}$ ,  $\epsilon_{rr}=\epsilon_{\theta\theta}$  and  $\epsilon_{rz}$  is very close to zero. In the outer half of the sampler soil disturbances involve significant nonuniformities. Baligh et al. suggest that a reasonable estimate of soil disturbance within the sampler can be obtained from results at the sample centerline.

The ISA adopts the undrained strain paths of soil elements located at the centerline of a simple-sampler to describe the effect of the tube penetration, while the retrieval and extrusion of the sample are modeled, as in the FSA, by an undrained shear stress release. Figure 2.3 shows the vertical straining to which an element of soil located at the centerline is subjected. There are three distinct phases of undrained triaxial shearing: initially ahead of the sampler the soil is subjected to compression until  $\epsilon_{max}$  is reached at about  $0.35 B$  below the tip; in a second phase there is

reversal of the straining,  $\epsilon_{zz}$  decreases rapidly, attains the value zero at the tip of the sampler and  $\epsilon_{min}$  is reached at about  $0.35B$  inside the sampler; in the last phase the soil element is once again subjected to compression and  $\epsilon_{zz}$  approaches zero. The figure shows strain paths for three different geometries of the simple sampler:  $B/t=20, 40, 50$ . The thicker the sampler, the higher the straining caused in the soil. The analysis predicts that a standard thin-walled Shelby tube with  $B/t$  approximately equal to 40 causes a maximum compressive strain of about 1%. For NC and low OCR clays the axial strain at peak is significantly exceeded during the initial compression phase and the soil fails before even entering the sampler.

In proposing the ISA, Baligh et al. also presented the results of a limited experimental program conducted at MIT. Triaxial tests performed on  $K_0$  consolidated NC RBBC show that soil disturbances predicted by the ISA have significant effects on the undrained behavior of the clay. The ISA predicts significant reduction in the mean effective stresses due to sampling disturbances compared to the PSA. Comparison to results of UU tests on BBC shows that the ISA describes the behavior, in terms of residual effective stress, undrained strength, strain at peak, stiffness, post peak behavior and stress path, more accurately than the PSA. The results of the triaxial tests also give an indication that tube-sampling disturbance effects are primarily due to tube-penetration disturbance.

Based on these results it is suggested that for tube samples, the ratio between the effective stress  $\sigma'_s$  in the sample and  $\sigma'_{is}$ , the value predicted by the ISA, be used as a measure of the "avoidable" disturbance undergone by the sample and possibly to correct the normalized strength parameters obtained in UU tests.

## 2.5 Reconsolidation Procedures

The selection of a suitable reconsolidation procedure of the soil that will enable to reconstruct the in situ behavior represents one of the most challenging problems of laboratory testing.

In practice one of the two following procedures is adopted: the Recompression (Bjerrum 1973) procedure in which the specimen is reconsolidated back to the in situ effective stresses or the SHANSEP (Ladd and Foott, 1974) procedure in which consolidation proceeds much past the in situ stresses.

This section will briefly summarize the basis of the two reconsolidation procedures and review their relative advantages.

### 2.5.1 Recompression

The Recompression method was proposed in 1973 by Bjerrum to reconstruct prior to shearing the original structure of the soil damaged by disturbance and was developed in response to the need for reliable engineering parameters for foundation design on soft clay.

The method suggests that the detrimental effects of swelling caused by disturbance can be limited if prior to shear the specimen is consolidated to the in situ stresses (point 3 in Figure 2.4). By these means also the excess water adsorbed during sampling is squeezed out of the soil.

Bjerrum also recognizes that recompression is applicable to cases in which "the swelling is so small that it is of elastic nature and that the mechanical disturbance of the sample is relatively small". If, in fact, the

disturbance from sampling is too large, reconsolidation to the in situ stresses involves strains much larger than the ones caused by swelling and therefore the water content at the end of consolidation will be much lower than the in situ value leading to an unsafe estimate of the undrained strength.

## 2.5.2 SHANSEP

The SHANSEP (Stress History and Normalized Soil Engineering Properties, Ladd and Foott 1974) reconsolidation technique was sparked by the observation of the similarity in behavior between UU tests which carry the full imprint of disturbance and CU tests on overconsolidated clays and is based on the assumption that natural soil exhibits normalized behavior influenced only by the value of the OCR. In this framework the effects of disturbance can be erased by reconsolidating the soil to the pre-disturbance OCR, that is by eliminating the AOCR caused by disturbance. This is achieved by reconsolidating the soil well into the virgin compression stress range and then rebounding it to the desired OCR (point C or D, figure 2.4). The assumption of normalized behavior of the soil guarantees that the soil will behave in identical way if sheared starting from '1' or from the point on the BD curve with OCR equal to that of '1'.

By performing  $CK_0U$  Tests on clay consolidated to points B, C, D it is possible to establish the normally consolidated and the overconsolidated behavior. The results can be expressed in terms of the parameters S and m of the equation:

$$c_u/\sigma'_{vc}=S \cdot (OCR)^m$$

which can be used to predict the undrained strength for any value of the OCR. From the above it appears clear that the SHANSEP technique is strictly applicable only to mechanically overconsolidated and truly normally consolidated soils and that, in the case of highly structured, sensitive clays and naturally cemented deposits it may lead to erroneous results, even though always on the safe side.

### 2.5.3 Recompression vs. SHANSEP

The issue of the selection of the most appropriate laboratory reconsolidation procedure has been widely discussed (Jamiolkowski et al. 1985, Tavenas and Leroueil 1985, Jamiolkowski et al. 1985b etc.) and is certainly not resolved.

It is generally recognized that the Recompression technique should be used in the case of highly structured and sensitive clays and for highly overconsolidated deposits. In the first case in fact consolidation well past the maximum past pressure causes complete destructuring of the soil, while in the second case the SHANSEP technique is difficult to employ due to the high stresses that need to be applied.

There is instead large dissent on what reconsolidation procedure should be adopted in the case of medium to low plasticity clays which represent the focus of this research. It is recommended by many (Jamiolkowski et al. 1985, Ladd 1986) that the recompression technique be used only when high quality samples are available. Jamiolkowski et al. (1985) suggest that in the case of disturbed samples the change in water

content during reconsolidation may lead to overestimating the undrained strength of the soil, even though no evidence of this has been shown.

On the other hand it has been shown (Estabrook 1991, Clayton et al. 1992) that the SHANSEP procedure does not lead to an accurate evaluation of the stiffness of the soil.

In practice block sampling or large diameter samplers are either too expensive or technically not feasible as in the case of deep sampling or offshore exploration. In these cases the focus of the discussion should shift as pointed out by Jamiolkowski et al. (1985b) to examining to which degree the SHANSEP reconsolidation procedure provides reasonable estimates of relevant design parameters.

## **2.6 Other Research on Sampling Disturbance of Cohesive Soils**

This section reviews the most important aspects of sample disturbance on cohesive soils through an extensive review of the pertinent literature. The Section is composed of four different parts.

A lot of the research effort in the area of sampling disturbance has been aimed at the development of special sampling equipment capable of reducing the disturbance induced in the soil. Section 2.6.1 presents, after a very brief description of the thin walled open and fixed piston samplers, the techniques most commonly used in practice to obtain undisturbed samples, a quick overview of two of the most significant apparatuses developed in the last 20 years, the Laval sampler and the Sherbrooke

sampler. These apparatuses have been extensively employed for research purposes and much data regarding their use is available.

Section 2.6.2 reviews the most important effects of disturbance on measured soil properties presenting the relevant data existing in literature.

The factors influencing disturbance during the sampling operations starting from the drilling of the borehole to the setup of the specimen are summarized in Section 2.6.3.

Finally the methods employed to assess sample quality are discussed in Section 2.6.4.

## **2.6.1 Sampling Techniques**

### **2.6.1.1 Traditional Sampling Methods for Undisturbed Samples**

This section will review the sampling techniques most commonly used in practice to obtain undisturbed samples, which can be used for shear strength tests. Figure 2.5 shows the parameters most commonly used to describe the geometry of samplers which will be referenced very frequently throughout this thesis.

#### **Open Thin-Walled/'Shelby' Tube Samplers**

The thin wall sampler, introduced in 1936 for obtaining undisturbed drive samples, consists of a section of thin-walled seamless tubing which is attached to a sampler head or adapter containing a check valve and vents for escape of air or water. Sampler tubes are generally fabricated of steel, but the use of brass and stainless steel has become more common to

avoid corrosion especially when samples are stored for long periods of time before being tested.

Figure 2.6 shows a schematic of a thin walled sampler. The Shelby tube is characterized by a sharp, drawn in cutting edge, by  $B/t < 40$ , by a value of the area ratio between 10% and 13% and a value of the inside clearance ratio between 1% and 3%.

Thin walled tubes are available with diameters varying from 2 to 6 inches, and length from 24 to 30 inches.

The thin walled sampler is generally employed for sampling of soft to stiff clays. The samples are also used for shear strength tests even though this practice is not optimal except in the case of uniform, insensitive, highly plastic clays.

### **Stationary Piston Samplers**

A piston sampler is a thin walled sampler in which the lower end of the sampling tube is closed with a piston which prevents the entrance of excess soil and mud during sampling. Figure 2.7 shows a scheme of the mechanical sampler and of the steps of the sampling procedure. When the sampler is lowered into the borehole, the piston is located at the base of the sampling tube. Once the sampler has reached the bottom of the borehole the piston rod is held fixed relative to the ground surface and the thin walled tube is pushed into the soil by hydraulic pressure or mechanical jacking. The sampler is never hammered. When the sampler is removed from the borehole, the vacuum between the piston and the top of the sample is broken with a vacuum breaking device.

The most frequently used sizes is 3 inside diameter and 30 inches long.



The stationary piston sampler is employed for sampling of soft to stiff cohesive soils and according to Hvorslev (1949) generally produces samples of much higher quality than those obtained with the Shelby samplers.

#### 2.6.1.2 The Laval Sampler

The Laval sampler (La Rochelle et al. 1981) was the result of a large effort undertaken at the university of Laval to study the effects of disturbance on the behavior of highly sensitive Canadian clays.

This sampler is characterized by the following characteristic features:

- large diameter (200 mm);
- elimination of the inside clearance,
- elimination of the piston,
- sharp cutting edge,
- overcoring technique around the sampling tube.

The choice of the large diameter as well as the elimination of the inside clearance aim to reduce the area ratio and therefore the magnitude of disturbance. According to LaRochelle et al. , the elimination of the inside clearance ratio reduces disturbance because it prevents lateral expansion of the soil once inside the tube .

A very sharp angle of attack is chosen so that the change of volume occurs towards the outside of the tube, and, to reduce the effect of the thickness of the tube.

The fact that specimens located in the middle part of tubes are generally of higher quality than those at the ends is attributed by La

Rochelle et al. to the action of the piston and to the effects of suction during extraction of the tube. For this reason the piston is eliminated in the Laval sampler and suction is avoided by overcoring around the sampler while keeping the borehole filled with bentonite.

Figure 2.8 shows the three main parts of the Laval sampler: the sampling tube, the sampler head, and the coring tube. The phases of operation of the sampler are described in Figure 2.9a-d. Once the borehole is prepared the sampler assembly is lowered (Fig.2.9a). The tube is unhooked from the coring tube and pushed into the soil while the mud flows out of the tube through the head of the sampler. To avoid any piston effect the advance of the tube is stopped when the head reaches an elevation of about 5 cm above the top of the sample (Fig.2.9b). The head valve is then closed and coring takes place while at the same time injecting under pressure the bentonite mud. The coring is stopped when the ring has reached a depth of ~20 cm below the sampler (Fig.2.9c). The sample is rotated and pulled up, hooked back to the coring tube and pulled out of the ground (Fig.2.9d).

Even though the quality of the samples obtained with the Laval technique is certainly higher than for thin walled samplers the use of this sampler is still not economically feasible for routine investigations. The Laval sampler has however been used extensively for sampling of highly sensitive Canadian clays.

### 2.6.1.3 The Sherbrooke Sampler

The Sherbrooke Sampler (Lefebvre and Poulin, 1979) was developed at the University of Sherbrooke, to obtain, from the surface, samples of quality comparable to that of block samples when the sampling depth is such that costs and practical difficulties do not allow the use of standard block sampling technique as is the case of clay deposits in eastern Canada, usually covered by a weathered crust deeper than 3 or 4 m.

Figure 2.10 shows a schematic of the apparatus. The sampler is placed in a hole of about 40 cm in diameter which is kept full of drilling fluid. The sampler is rotated by means of a vertical rod powered by an electrical motor and a sample of about 25 cm in diameter and 35 cm in height is carved by the annular motion of three cutting tools located at the bottom of 3 arms. The separation of the "sample" from the underlying soil is obtained by the penetration of horizontal diaphragms, initially located in an annular slot, which also support the sample while it is lifted out of the borehole. This last operation needs to be performed very slowly to permit good circulation of the water under the sample and avoid suction. The carving technique is very similar to the one used to obtain block samples, except that the sample obtained is cylindrical.

Strains associated with the penetration of a sampling tube into the ground are avoided with this method of sampling but the soil block is exposed to drilling muds during carving and on withdrawal from the boring hole.

As for the Laval sampler, also the Sherbrooke sampler is used, at this point, mainly for research purposes.

## 2.6.2 Effects of Disturbance

The major disadvantage of laboratory testing is that sampling disturbance effects generally cause significant differences between the measured properties of soil specimens and the in situ foundation soils.

All engineering properties of the soil are affected to a smaller or larger degree by disturbance. The following sections summarize the existing knowledge of the effects of sample disturbance on the engineering properties of soft clays through a review of the pertinent literature.

### 2.6.2.1 Effective Stresses

The change in the effective stresses during sampling is dependent on the overconsolidation ratio of the soil, its plasticity, as well as on the details of sampling.

For soft low OCR clays the mean effective stress  $p'$ , equal to  $(\sigma'_v + 2\sigma'_h)/3$ , is generally reduced by an amount dependent on the sampling method and the geometric characteristics of the sampler. The decrease of  $p'$  is more marked as the plasticity of the soil decreases. For heavily overconsolidated clays especially those with low plasticity there is generally no significant change in the mean effective stress and in some cases,  $p'$  may actually increase with sampling due to the dilatancy in the peripheral zone. Figure 2.11, from Hight (1992) shows these general trends for a low plasticity clay (Bothkennar Clay with  $PI=18-22\%$ ), an offshore clayey silt ( $PI=5-15\%$ ) and a much stiffer overconsolidated clay (London Clay). The decrease of the stresses is more distinct as the plasticity index

decreases. In the case of the heavily overconsolidated clay the mean effective is not reduced, but because of dilatancy in the peripheral zone.  $p'$  may actually increase.

Hight et al. (1985) and Vaughan et al. (1992) attempt to separate the effect of the straining in the central part of the sample from that of the side shear, on the variation of the mean effective stress. The central part of the sample is subject to straining similar to the compression-extension-compression straining described by Baligh et al. (1987) which will lead to generation of positive pore pressures in low OCR clays. In stiffer clays the effect of compression/extension strains on pore pressures is less marked and the decrease in  $p'$  will be smaller.

According to Vaughan the effect of the side shear is much greater. For contractant soils positive pore pressures will be generated in the peripheral zone of the sample due to side shear while for stiff dilatant clay it is hypothesized that the shearing will cause negative pore pressures. After dissipation of the excess pore pressure, there will be an overall reduction of pore pressure in the heavily overconsolidated soil and an overall increase in the normally consolidated clay. Correspondingly, there will be redistribution of the water content.

As indirect evidence of this phenomenon Vaughan et al. (1993) present measurements of the water content at varying radii of a 100 mm sample. The results are shown in Figures 2.12a-d. In the case of soft Thames alluvial clay (Figure 2.12a-b) the water content is reduced at the periphery of the sample. The opposite behavior is exhibited by a sample of stiff London clay (Figure 2.12c-d).

Finally, Clayton et al. (1992) have performed tests similar to the ones presented in this report subjecting triaxial specimens to the straining cycle suggested by the Ideal Sampling Approach. For Bothkennar clay they have shown that increasing disturbance causes a larger loss of mean effective stress. These results will be compared to the ones performed at MIT in Section 6.2.

Figure 2.13 from Hight et al. (1992) summarizes the factors that can lead to variation of  $p'$  during sampling, handling and setup.

#### 2.6.2.2 Bounding Surface

Evidence for shrinking of the bounding surface due to sample disturbance has been presented by La Rochelle et al. (1981), Tavenas and Leroueil (1987) and Hight et al. (1992).

Figure 2.14 from Tavenas and Leroueil (1987) compares the bounding surfaces for Saint Louis Clay obtained from 50 mm piston samples and 200 mm Laval samples. The results presented in the figure indicate that as the strains imposed on the soil during sampling increase, the bounding surface contracts. It also appears that there is no significant difference between the results obtained from block and Laval samples.

Hight et al. (1992) have suggested that there is a hierarchy of bounding surfaces, each surface being associated with a particular sampling method, and with the contraction of the surface being directly related to the level of disturbance or destructuring. For increasing disturbance then shrinking of the bounding surface increases and, according to the model

presented by Burland (1990), converges towards the bounding surface for reconstituted soil.

### 2.6.2.3 Undrained Strength

The effect of disturbance on the undrained strength can be evaluated by observing the results of UU tests which reflect the effects of both the changes in the mean effective stress and of any destructuring caused by sampling and preparation of the specimens. In UU tests, as first observed by Hvorslev (1949), disturbance causes a decrease of the undrained strength. This is shown very clearly in the results presented by Hight et al. (1992) (Figure 2.15) which compare the behavior of specimens obtained with different sampling techniques. Specimens obtained from the higher quality samples show a much higher value of the undrained strength.

Ladd (1986) observes that the restructuring of the soil on the migration of water often produce highly variable strength from UU type tests and recommends that CU type tests must be employed to estimate the undrained strength of clays. Even though the common practice in performing Consolidated Undrained is to make use of either the Recompression or the SHANSEP technique to reconsolidate the soil, it is not fully understood to what extent these two procedures lead to recovery of the intact behavior of the soil and in particular yield accurate and safe estimated of the undrained strength.

Results from Hight et al. (1992) and Clayton et al. (1992) indicate that for Bothkennar clay, recompression partially erases the effects of disturbance, but does not recover the intact strength. These results are in

disagreement with the limited experimental program conducted by Baligh et al. (1985) as well as with the results presented in this thesis. For NC Resedimented Boston Blue Clay the change in water content during reconsolidation compensates for the damage done to the soil structure during sampling and recompression leads to an unsafe estimate of the undrained strength.

#### 2.6.2.4 Undrained Stiffness

There is agreement on the fact that disturbance during tube sampling causes a decrease in the measured stiffness of clays and that stiffness is more sensitive to disturbance than some other parameters such as undrained strength.

However, it is not easy to quantify the absolute loss in stiffness due to the uncertainties associated with the definition of the intact stiffness behavior. Another issue is the choice of the parameter to use when assessing the degree of disturbance.

While  $E_{u50}/\sigma'_v$  is the parameter most often used to evaluate the effects of disturbance on the stiffness of the soil, it must be pointed out that comparisons involving this parameter must be considered with care. Due to the large changes in the stress strain behavior of the soil caused by increasing disturbance, the increment to failure varies greatly and the strain level at which the modulus is compared varies over a very wide range. It is therefore more significant to evaluate the effects of disturbance by comparing the values of the stiffness at the same strain level.

The effect of disturbance on the undrained modulus after



recompression to the in situ stresses is studied by Clayton et al (1992). Specimens obtained from undisturbed Laval samples of Bothkennar clay (OCR~1.5) were subjected to ISA straining of varying amplitude to simulate the effect of sampling and then reconsolidated to the in situ stresses and sheared undrained. The results obtained indicate that increasing disturbance is associated with decreasing values of the stiffness between 0.01 and 1%. For low levels of disturbance ( $\pm 0.5\%$ ), reconsolidation leads to an increase of the normalized stiffness  $E_u/p'$ , due to the reduction in volume during reconsolidation which compensates the damage to the soil structure. Moderate disturbance ( $\pm 1\%$ ) does not significantly affect the stiffness but, as the magnitude of the strain imposed increases ( $\pm 2\%$ ), reconsolidation cannot erase the effect of disturbance on the undrained modulus.

The results presented by Clayton et al. (1992) must be considered with care. The reference behavior to which the tests are compared cannot be considered truly representative of the undisturbed behavior of Bothkennar clay having been determined from recompression tests on Laval samples. These samples are subject to some straining during the penetration of the tube (estimated by Hight et al. 1992 in the order of 0.5%). Also the effect of any level of disturbance is probably less marked when acting on already disturbed clay.

Clayton et al. (1992) investigate also the effect of consolidating the soil to  $2\sigma'_p$  following a constant K path. For Bothkennar clay this reconsolidation procedure produces further destructuring and the values of the normalized stiffness represent a lower bound.

These results are consistent with those presented by Estabrook (1991) for Boston Blue Clay. Figure 2.16 plots the values of  $E_{u50}/\sigma'_{vc}$  determined from both Recompression and SHANSEP tests and points out how the second reconsolidation procedure causes destructuring of the clay. This is especially evident in the results of the extension tests.

Hight et al. (1985) present some results of a UU test and a recompression test performed on  $OCR=1.1$  clay from two identical tube samples taken at the same depth from the seabed in the Northern North Sea. The value of the normalized stiffness at 0.01% strain  $E_{u0.01\%}/p'_o$  is equal to 1080 for the UU test and 1460 for the recompression test. It appears that reconsolidation is able to recuperate part of the stiffness lost during sampling. In the same paper Hight et al. make an interesting observation regarding the different effect of perfect sampling on the stiffness of NC and OC clay. For reconstituted North Sea clay with  $OCR=1$ ,  $(E_u)_{0.01\%}/p'_o$  after perfect sampling is higher than the intact value; the opposite is true for  $OCR=7.4$ . It is suggested that the direction of the final stress path relative to that followed in the subsequent triaxial tests represents an important aspect of sampling. When the soil is unloaded it carries the small strain zone. When the direction of the stress path reverses, as in the NC case, the full small-strain zone can be traversed and this can result in an increase of the stiffness even if the overall size of the zone is smaller. When the direction of the stress path in triaxial compression is a continuation of that followed during sampling, as for  $OCR=7.4$ , some or all of the small strain zone is missing.

It should be pointed out that in the results discussed in this chapter the stiffness is always normalized by the consolidation stresses. This is not

a truly valid procedure due to the fact that the modulus does not exhibit normalized behavior.

#### 2.6.2.5 Compression Curve and Preconsolidation Pressure

It is quite well established that the shape of the compression curve as well as the values of the compressibility parameters give useful indications to assess sample quality. Disturbance typically tends to increase the recompression ratio and decrease the compression ratio.

There is not, however, full agreement on the effects caused by disturbance on the preconsolidation pressure even though it is generally thought that increasing disturbance is associated with lowering of the  $\sigma'_p$  (e.g. Jamiolkowski et al. 1985, Peters 1988).

Results for quick and sensitive clays presented by Lacasse et al. (1985) and La Rochelle et al. (1981) based on the comparison of tests on block and 90 mm tube samples indicate that even though the values of the preconsolidation pressure estimated from the piston samples are lower than those obtained by testing the block samples, very small differences are observed in the preconsolidation pressure profiles. These observations are supported also by the results of oedometer tests performed on block and piston samples presented by Holtz et al. (1986).

The preconsolidation pressure should normally be located on the limit state curve at the intersection with the  $K_0$  line. Hight et al. (1992) note that the stress path followed in an oedometer test will depend on such factors such as  $p'_i$  and the disturbance of the sample. It is therefore possible that in different quality samples not only will the location of the boundary

surface differ but also the region in which the oedometer path meets the bounding surface will vary. For this reason the effects of disturbance on the preconsolidation pressure will not always be apparent.

In most cases the effects of increasing disturbance appear to reduce the preconsolidation pressure.

### **2.6.3 Factors Influencing Disturbance**

As indicated in Figure 2.17 many factors affect the quality of a sample before, during and after the actual sampling operations: borehole excavation, penetration and retrieval of the sampling tube, transportation, storage, extrusion, trimming and other operations required to prepare the specimens for laboratory testing .

This section reviews, through a review of the existing literature, the most significant factors that can affect sample quality.

#### **2.6.3.1 Borehole Advancement**

As Hvorslev (1949) first pointed out, disturbance can be produced even before sampling is started due to the advancement of the borehole as well as to the use of a drilling mud of adequate weight.

Indication on the importance of the boring method is offered, for example, by the results, presented by Adachi et al. (1981), of a large site investigation program for a reclamation project in Singapore marine clay in which the following boring and sampling methods were used:

- percussion boring from a pontoon with open-drive sampler (group I),

- percussion boring from a pontoon with free piston thin-walled sampler (group II),
- rotary boring from a fixed platform with fixed piston thin-walled sampler (group III).

Figure 2.18 shows the strength profiles obtained from UU tests performed on samples obtained with the three different methods. The results presented indicate that quality sample is greatly influenced by the method of boring and sampling. The strength obtained by percussion borings with the open drive sampler are in fact much lower than those obtained by rotary borings with the fixed piston, thin walled sampler. Significant differences are observed also in the stress strain curves.

### 2.6.3.2 Sampler Penetration

#### *Sampler Type*

It has been observed in Section 2.6.2.1 that in low OCR clays increasing disturbance produces more marked loss of effective stress .

The decrease in effective stresses produced in Bothkennar clay ( $OCR < 2$ ) by the sampling operations is compared by Hight et al. (1992) for 3 sampling methods: the Laval sampler, the Sherbrooke sampler and a standard piston sampler. The profiles of the mean effective stress obtained from tests on the different samples are shown together with the estimated mean  $p'$  profile in Figure 2.19. Piston samplers show, in Bothkennar clay, a reduction in mean effective stress generally greater than 50%. Specimens obtained from Laval samples retain higher effective stress and to a lesser degree so do the specimens trimmed from the Sherbrooke samples. This is

however attributed to problems which occurred during the sampling operations at the Bothkennar site.

Evidence of the larger disturbance produced by piston sampling appears also in the results of the UU tests performed on both Laval and piston samples from the Bothkennar site and presented by Hight et al (1992) (Figure 2.15). Specimens cut from piston samples have, compared to those obtained from Laval samples, lower residual effective stress, lower peak strength, larger strain at peak and, lower stiffness and brittleness. The difference in behavior is a result not only of the differences in effective stresses but is an indication of the larger destructuring associated with piston sampling.

Hight et al. (1992) also compare the bounding surfaces from Sherbrooke and Laval samples from similar depths and observe that Laval samples are subjected to some destructuring and shrinking of the bounding surface.

Comparisons between Sherbrooke samples and 95 mm piston samples are presented by Lacasse et al. (1985) for low OCR (from 2 to 5) sensitive clays and quick clays with PI varying between 3 and 44. In the data presented by Lacasse et al. (1985), the effect of sample disturbance appears to be very limited in the oedometer tests with small differences in the preconsolidation stress profiles, but increases dramatically for unconfined compression tests.

### *Sampler Geometry*

The amount of disturbance produced in the soil is very strongly dependent on the geometric characteristics of the sampler. Among these

the most important ones are diameter, length  $L$ , wall thickness,  $B/t$ , area ratio, inside clearance ratio ICR (Figure 2.5).

Figure 2.3 showed the vertical straining for an element located at the centerline of a tube sample predicted by the Strain Path Method for different values of the  $B/t$  ratio. As the  $B/t$  value increases the vertical straining induced at the centerline of the sampler decreases, and therefore the magnitude of disturbance also decreases.

Results presented by Vaughan et al. (1992), based on measurements on samples taken by jacking from a block of London clay, show that in general effective stress after sampling increases with increasing  $B/t$ .

In most cases there are practical limitations to the reduction of the thickness of the sampler below certain values and the  $B/t$  ratio can only be decreased by using larger diameter samples.

In the research performed prior to the development of the Laval sampler (LaRoche 1981) the influence of the inside clearance ratio was investigated by the Laval group. Table 2.1 extracted from LaRoche et al. (1981), presents, for three clays, the results of unconfined compression tests performed on clay sampled with four different tubes. If, for example, the tangent modulus is compared for the different cases it appears that the reshaped tube, i.e. the one in which the inside clearance ratio has been eliminated, induces less disturbance than the standard tube of the same diameter (54 mm). As expected, an increase in the diameter of the tube leads to a decrease of disturbance.

### 2.6.3.3 Storage Method and Time

Graham and Lau (1988) compared the effect of storage in drained and undrained conditions for different storage times for NC and OCR=2 clay. Triaxial specimens were prepared from blocks of reconstituted grundite clay. The specimens were set up in the triaxial apparatus, consolidated well past the preconsolidation pressure and finally unloaded in undrained conditions to simulate the effect of sampling. At this point undrained and drained storage was simulated keeping the drainage lines closed in the first case and allowing the specimens to freely absorb water from the drainage lines in the second case. "Storage" times were varied from 15 minutes to 7 days. The swelling increased with increasing storage time and the NC specimens swelled slightly more than the overconsolidated ones. The results presented by Graham and Lau show that access to water during storage causes quite large changes in the soil parameters even after reconsolidation. In the case of "drained storage" increasing storage time produce increasing reconsolidation strains, decreasing strength and stiffness. Most of the changes take place quickly and the 1 day and 7 day strength envelope are very close. The samples with undrained storage showed, instead, no variation in strength with increasing storage time.

Quite clearly the test conditions do not model exactly what happens in sample tubes and the storage times examined may not correspond to the rates at which samples can drain or equalize their pore pressure in sampling tubes. However the drained and undrained storage conditions considered, form bounds to what might be expected in practice and the



results presented by Graham et al. (1988) reinforce the understanding that samples taken from the field be stored at constant volume and water content as soon as possible, and tested without delay.

Hight et al. (1992) present some results regarding the effect of undrained storage time on the effective stresses. Their results, obtained from tests performed at different times in the range of approximately 2 years on Bothkennar clay specimens obtained from Laval samples at similar depths, show that with appropriate sealing and waxing there is virtually no change in mean effective stress over the long term (up to 600 days).

It is generally recommended that samples be stored in conditions of 100% RH to avoid drying if the soil were to be exposed to the air and at temperature close to the value in situ to avoid bacteria growth.

Storage time may become an issue for tube samples in the case of tubes which are subject to corrosion. In this case rapid testing may prevent deterioration of the samples due to chemical reactions with the sampling tube.

#### **2.6.3.4 Specimen Preparation Method**

The preparation of soil specimens from the samples may cause significant disturbance that in some cases may erase the benefits of using high quality sampling techniques. It is generally recommended (Jamiołkowski et al. 1985) that the extrusion, for tube samples, and the trimming operations be performed in such a way as to minimize any further straining.

Atkinson et al. (1992) have investigated the effect of the trimming technique on the behavior of Bothkennar Clay by analyzing four different techniques:

- trimming by wire saw;
- trimming by pushing a tube into a larger tube sample;
- trimming according to the Landva method A (Landva 1964), in which the subsample is trimmed ahead of the cutting edge of the tube which is then advanced past the trimmed surface;
- trimming according to the Landva method B (Landva 1964), in which the cutting edge of the tube is advanced up to 4 mm into the sample while the trimmed material is cut away with the wire saw.

The results presented indicate that there is no clear relationship between the values of the mean effective stress measured after setting up and the preparation method used. On the other hand observation of the stress paths, of the stress-strain curves and of the stiffness versus axial strain curves shows that the specimens prepared by wire saw trimming have the higher peak deviator stress and the greatest stiffness at small strains, while samples prepared by the Landva methods exhibit the poorest behavior (Figures 2.20 a-c).

The disadvantages of using a trimming method involving the penetration of a thin walled tube in the clay are pointed out also by Hight et al. (1992) who present results regarding the decrease in mean effective stress caused by sampling and trimming. Figure 2.21 shows the initial effective stresses measured from specimens prepared by tubing and trimming obtained from Laval, Sherbrooke and Piston samples. The effective stresses are all much lower than the estimated in situ values and

there is no influence of the sampler used. It is concluded that the penetration of the tube during specimen preparation causes large disturbance and erases the advantages of using a high quality sampling technique such as the Laval or the Sherbrooke sampler. Hight et al. also observe that the reduction in  $p'$  due to the trimming operations is generally larger than 50% for the Laval samples but not very significant for the piston samples which have undergone the most significant portion of disturbance during tube sampling.

Kimura and Saitoh (1984) have measured the variation of the pore pressures during extrusion from a large consolidometer consolidometer and trimming for clays with plasticity index varying from 10 to 50%. They found that the reduction of the effective stress due to extrusion decreases with increasing plasticity, while the effect of trimming is independent of the plasticity of the soil.

#### **2.6.4 Assessment of Sample Quality**

The high quality sampling methods such as the Laval sampler or the Sherbrooke sampler described above are not used very frequently in the common geotechnical practice due to the high costs involved. In other cases, such as for deep sampling offshore, their use is not feasible. Most sampling programs employ procedures that yield samples of less than ideal quality. It becomes therefore important to assess sample quality to be able to evaluate critically test results.

The most used techniques to assess sampling disturbance are presented in the following.

## **Radiography**

Radiography has been used at MIT for the past 15 years to evaluate the quality of soil samples. By means of this technique it becomes possible to detect particularly disturbed zones and to, nondestructively, select the most representative soil for the, often expensive, consolidation and strength tests. It also facilitates the planning of the testing program, especially in projects for which the high quality samples are limited. In some offshore projects onboard radiography has been employed to provide an immediate assessment of sample quality.

Radiography allows to identify features which cannot always be captured by simple visual inspection of the extruded samples without trimming or breaking the sample apart. Among these:

- variations in soil type,
- macrofabric features resulting from bedding planes, varves, fissures and shear planes
- presence of intrusions such as sand lenses, stones, shells, drilling mud etc.
- variation in the degree of sample disturbance ranging from the curvature adjacent to the sample edges to cracks and voids more often present at the ends of the tube.

It must be pointed out however that structural damage of the clay will not always result in distortions visible by means of radiography especially in uniform deposits.

The straining history for the soil at the centerline of a tube sampler as determined by Baligh (1980) shows that, after the initial compression-

extension phases the soil is subject to a last phase of compression during which the axial strain goes back to zero. In this case, even though the soil might have even failed during the penetration of the sampler no distortion would appear from a radiography of the sample.

### **Measurement of Strains During Reconsolidation**

During reconsolidation to the in situ stresses, in oedometer, DSS or triaxial tests, more disturbed specimens experience larger straining.

Figure 2.22 from Lacasse et al. (1985) shows, for example, how 95 mm tube samples systematically give reconsolidation strains larger than those obtained on 300 mm Sherbrooke samples.

Andresen and Kolstad (1979) have suggested a criterion for sample quality evaluation based on the magnitude of these strains. It is the opinion of the author that such an absolute criterion is of little use if it isn't adapted based on the nature of the soil (OCR, St, etc.) and that the measurement of "reconsolidation" strains should be seen solely as a simple means to evaluate the relative disturbance affecting tests performed on the same soil.

The increase of the reconsolidation strains with disturbance is discussed also by Clayton et al. (1992) who correlate the reconsolidation strains to the amplitude of the strain cycle in the ISA disturbance simulation on Bothkennar clay. These results will be compared to the values measured in the tests presented in Chapter 6.

### **Measurement of the Initial Effective Stress**

The use of the residual effective stress after sampling  $\sigma'_s$  as a measure of the degree of sample disturbance was first proposed by Ladd and Lambe (1963). These measurements are however not performed routinely due to the fact that they require the use of non-standard equipment such as a fine ceramic porous stone or a mid height probe.

The measurement of  $\sigma'_s$  is in general not sufficient to evaluate the amount of disturbance to which the sample has been subjected because it cannot indicate the amount of destructuring. Moreover, it loses any significance in cemented clays since the effective stress can approach zero without seriously affecting the structure of the soil.

### **Comparison of Tube Sampling Strains and Yield Strains**

Hight (1993) suggests that by comparing the maximum center-line strain imposed by a particular sampler with the critical strains in the soil, it is possible to derive an indication of whether or not destructuring has taken place during sampling. Research to relate the geometry of the sampler to the level of straining caused during penetration is currently being carried on at MIT (Sinfield 1994).

Site	Type of tube	$c_{ur}/c_{uv}$	$E_u$ (kPa)
Saint-Vallier (7.9 m)	54 mm standard	0.32	1800
	54 mm reshaped	0.66	3500
	75 mm reshaped	0.81	4100
	100 mm reshaped	0.80	5200
Saint-Vallier (14.0 m)	54 mm standard	0.75	4100
	54 mm reshaped	0.90	7600
	75 mm reshaped	0.88	5900
	100 mm reshaped	0.84	9000
Yamaska (6.1 m)	54 mm standard	1.02	5500
	54 mm reshaped	1.24	8300
	75 mm reshaped	1.11	7200
	100 mm reshaped	1.57	9000

Table 2.1 Variation of Strength and Stiffness as a Function of Tube Diameter and the Tip Geometry (from La Rochelle et al. 1981)

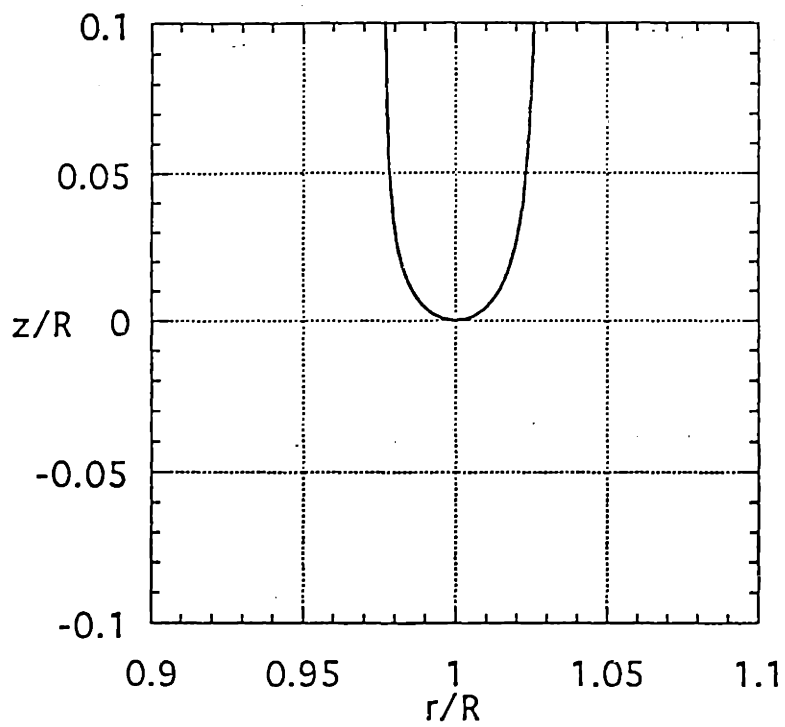
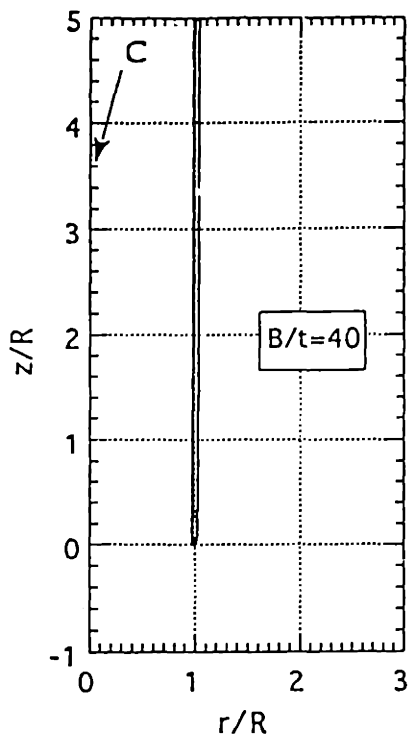
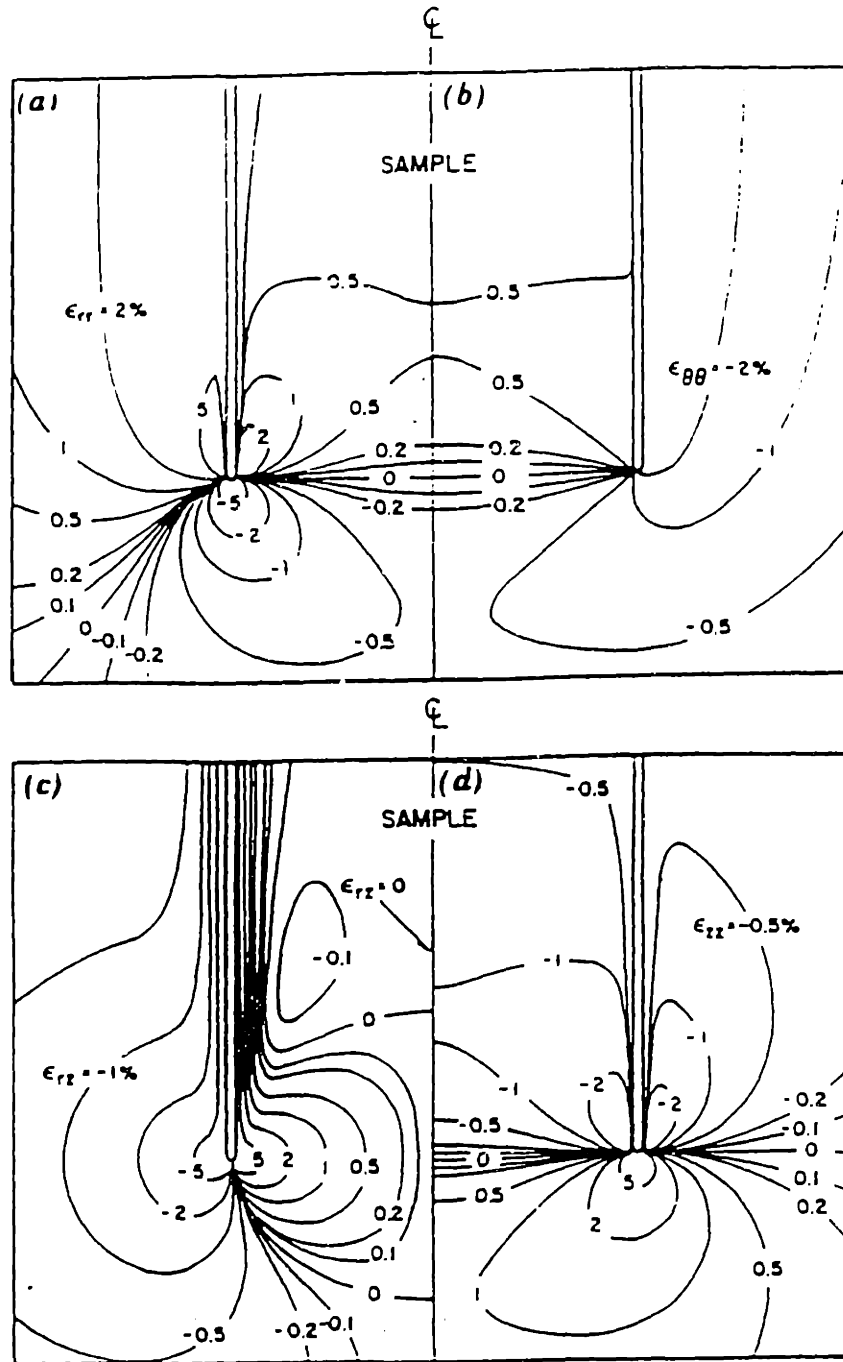


Figure 2.1 Shape (a) and Detail of the Tip (b) of the Simple Sampler





$B/t = 40, \text{ICR} \approx 1\%$

Figure 2.2 Contours of  $\epsilon_{rr}$ ,  $\epsilon_{\theta\theta}$ ,  $\epsilon_{rz}$  and  $\epsilon_{zz}$  produced by penetration of the Simple Sampler (from Baligh et al. 1985)

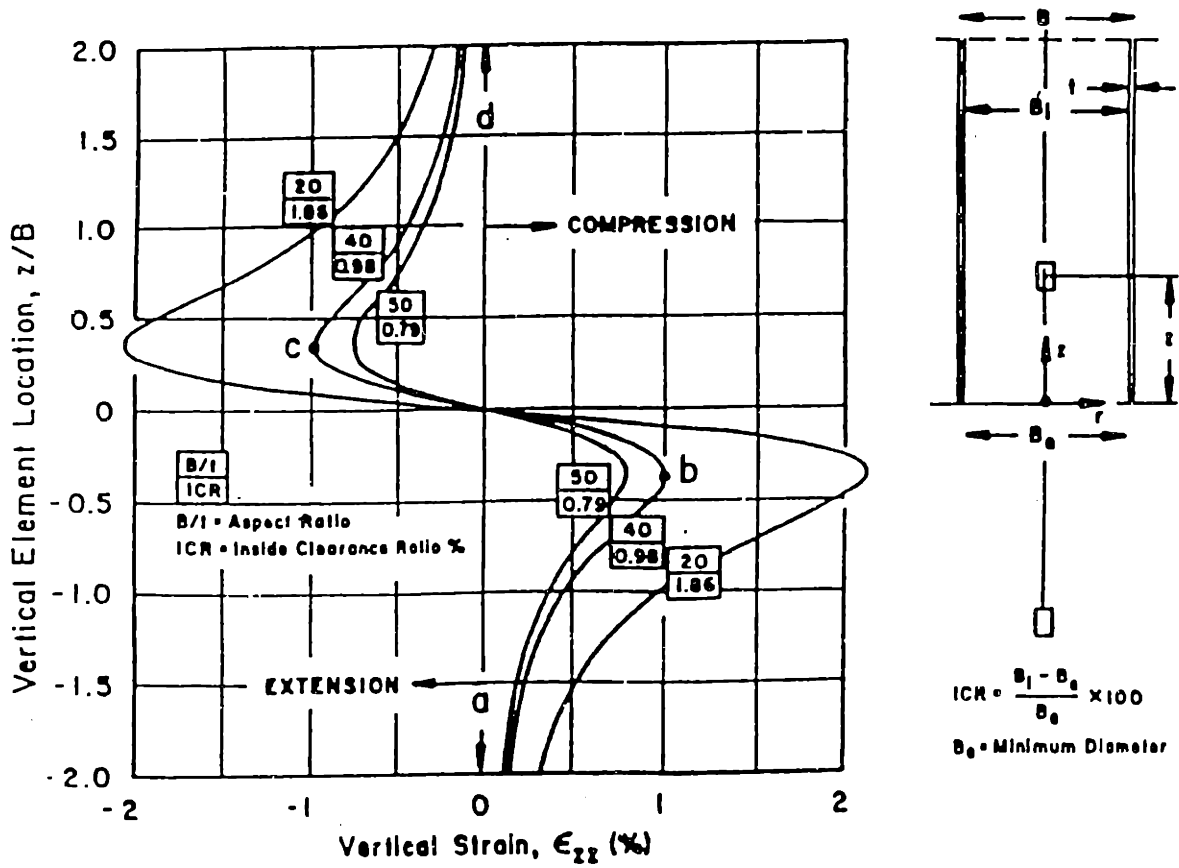


Figure 2.3 Straining History at Centerline of Simple Samplers (from Baligh et al. 1985)

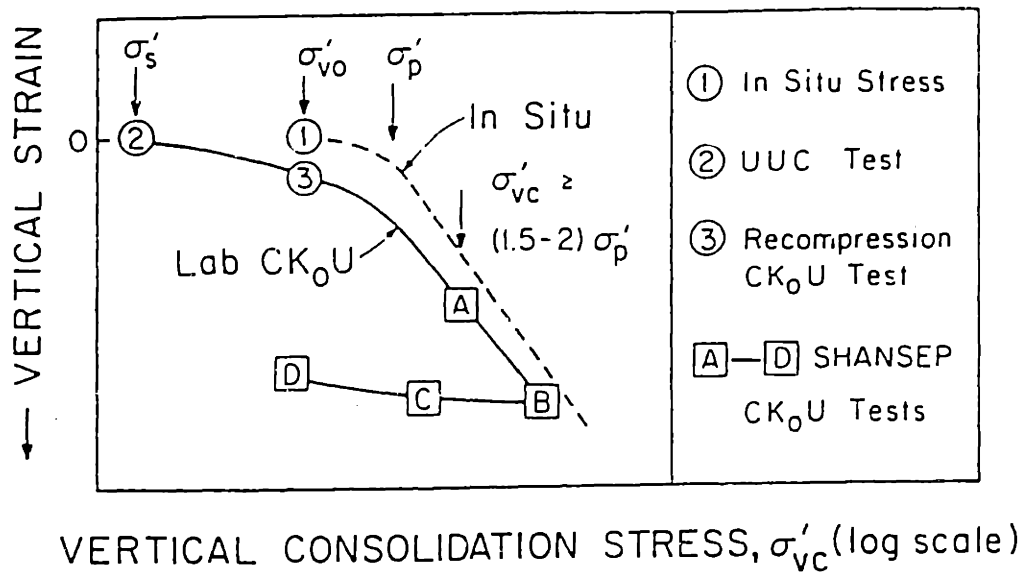
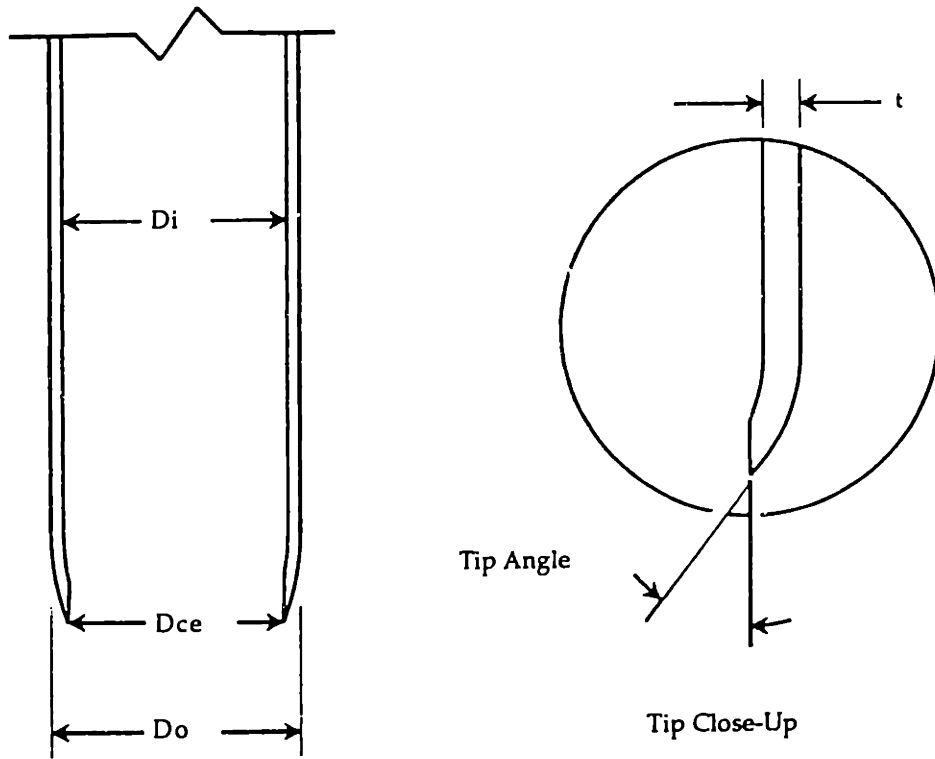


Figure 2.4 Consolidation Procedures for Recompression and SHANSEP CK<sub>0</sub>U Testing (from Ladd 1987)



$D_o$  = Outside Tube Diameter  
 $D_i$  = Inside Tube Diameter  
 $D_{ce}$  = Cutting Edge Diameter

$$B = \frac{D_{ce}}{(D_o - D_{ce})/2}$$

$$ICR = \frac{D_i - D_{ce}}{D_{ce}}$$

$$Area\ Ratio = \frac{D_o^2 - D_{ce}^2}{D_{ce}^2}$$

Figure 2.5 Geometrical Characteristics of Tube Samplers (from Sinfield 1994)

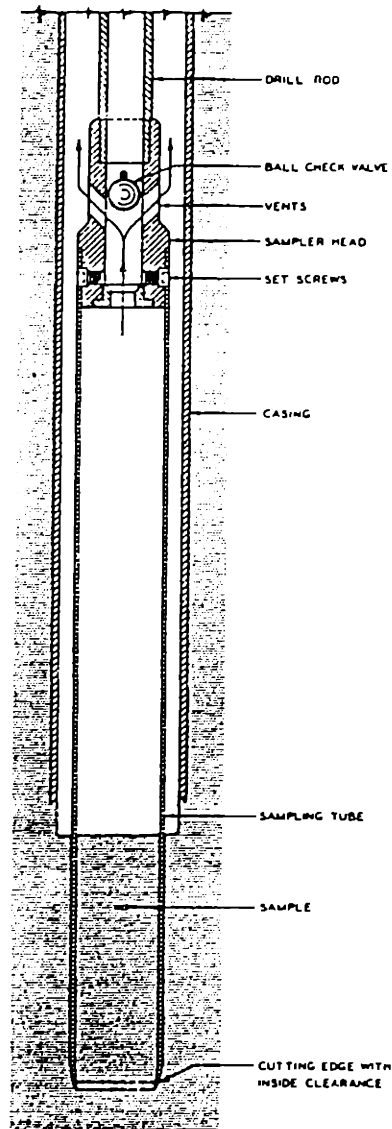


Figure 2.6 Thin-Wall Open Drive Sampler (from Hvorslev 1949)

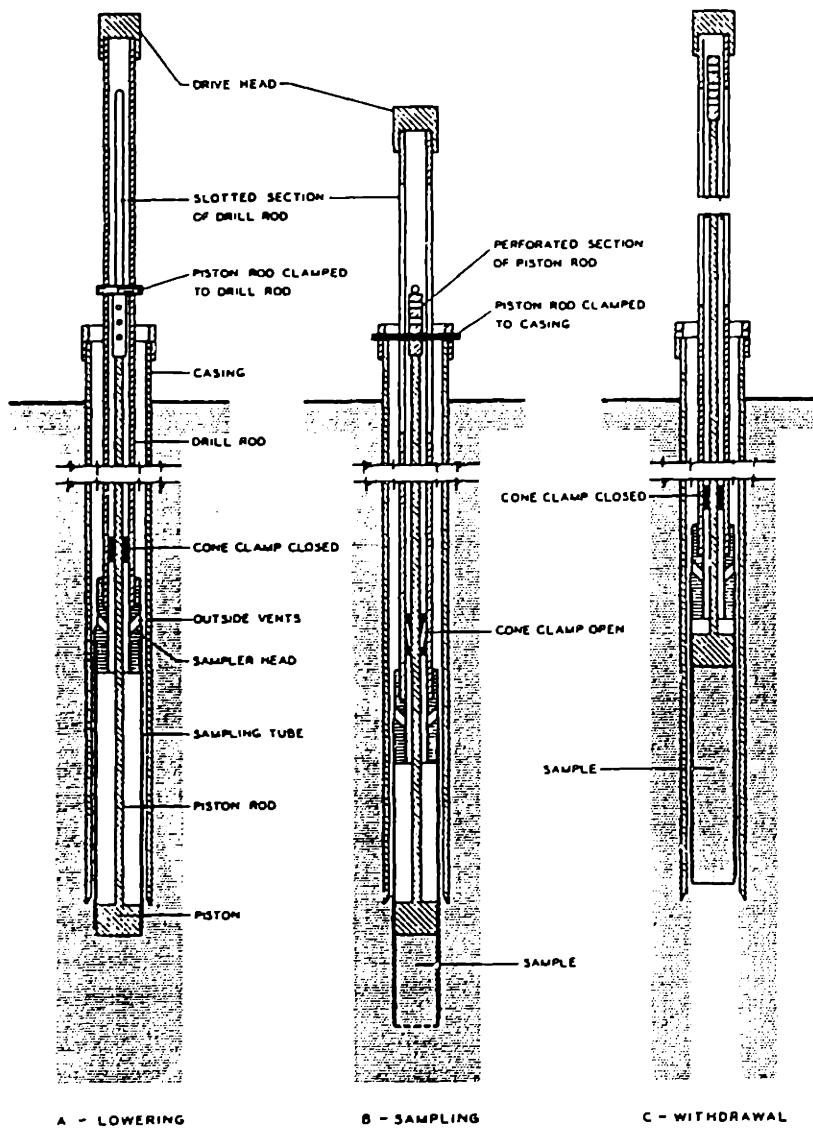


Figure 2.7 Piston Sampler with Stationary Piston  
(from Hvorslev 1949)

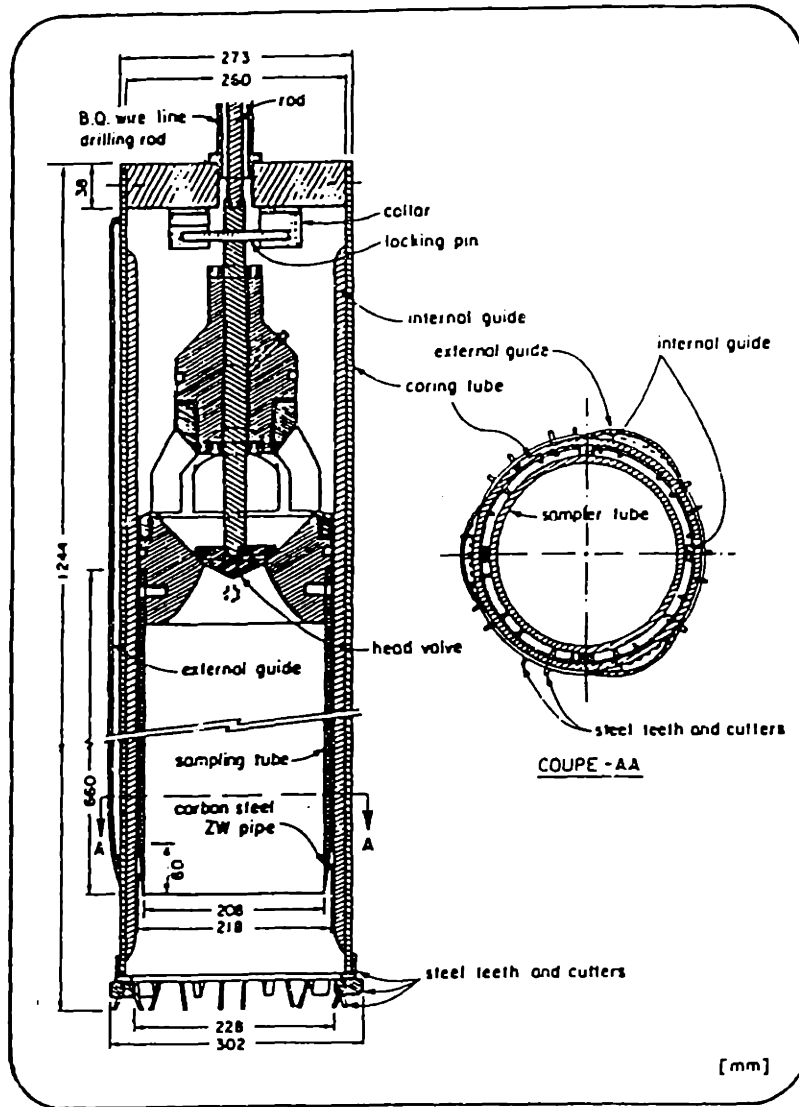


Figure 2.8 Schematic of the Laval Sampler  
(from La Rochelle et al. 1981)

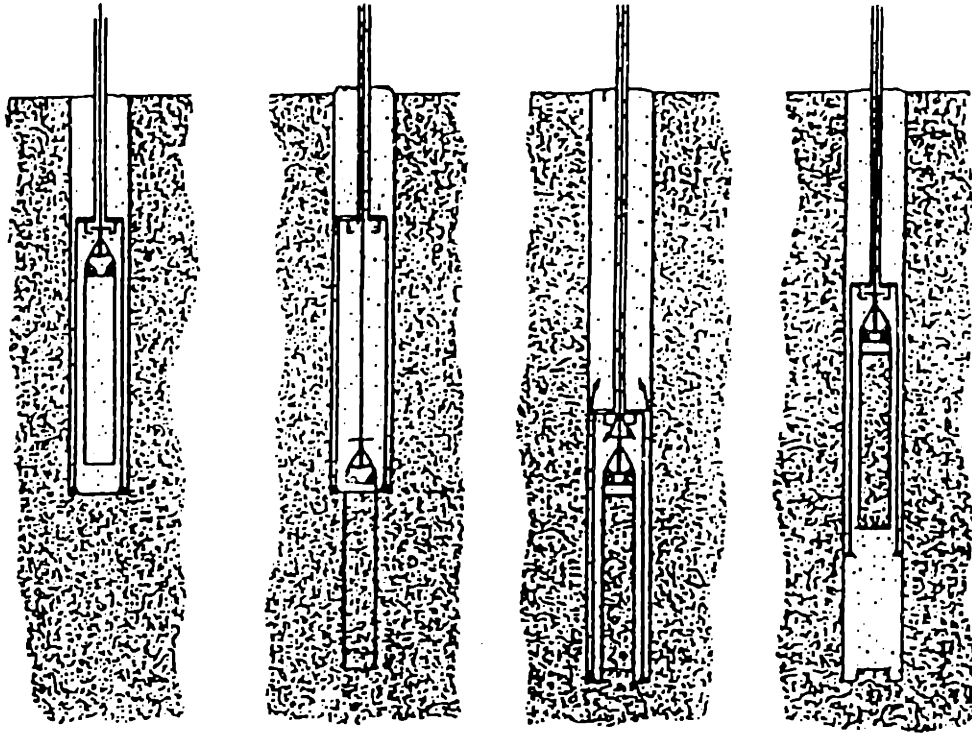


Figure 2.9 Phases of Operation of the Laval Sampler  
(from La Rochelle et al. 1981)



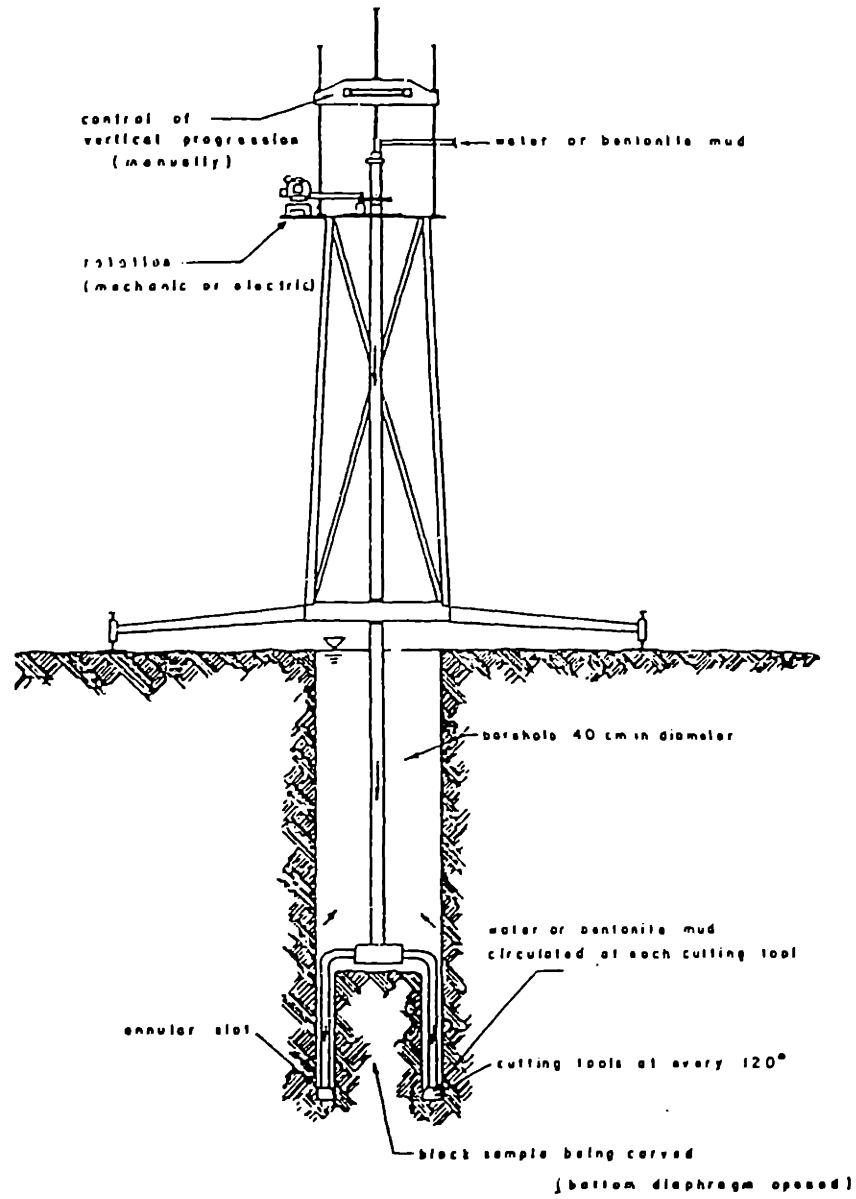


Figure 2.10 Schematic of the Sherbrooke Sampler (from Lefebvre and Poulin, 1979)

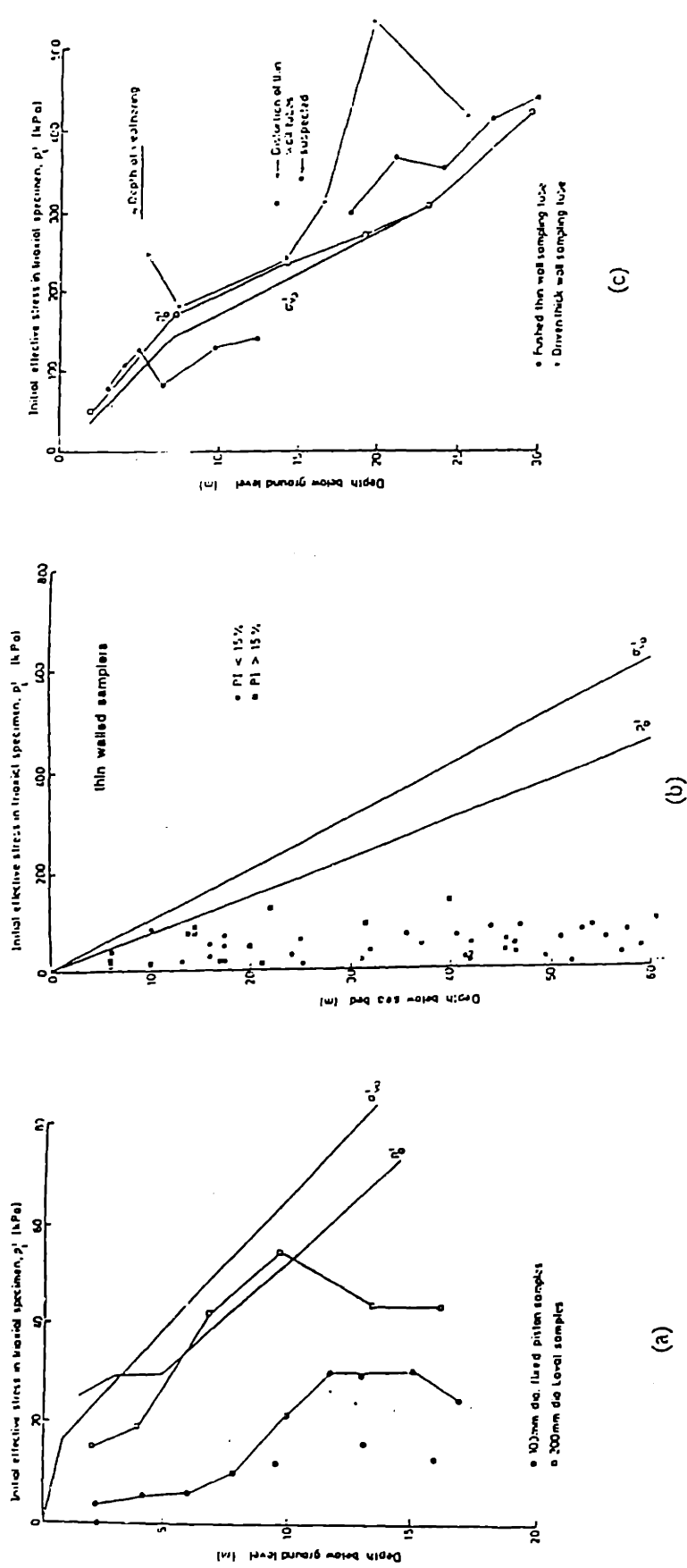


Figure 2.11 Comparison of Mean Effective Stresses in Situ and after Sampling for Bothkennar Clay (a), Offshore Clayey Silts (b), London Clay (c) (from Hight 1992)

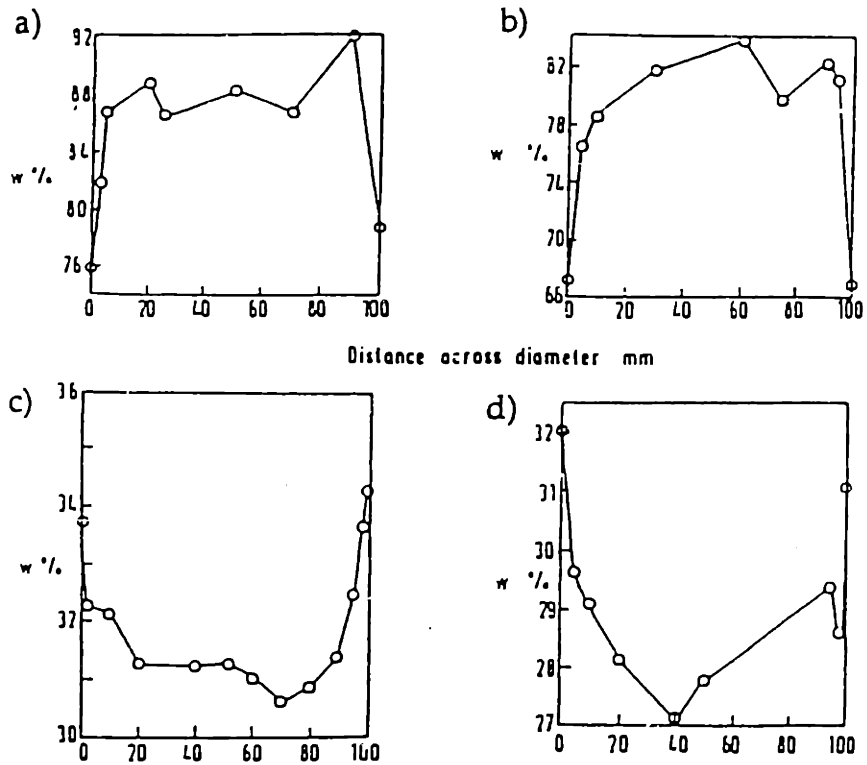


Figure 2.12 Variation of Water Content within (a-b) Soft (LL=92%, PL=33%) and (c-d) Stiff (LL=81%, PL=30%) Clay Samples due to Tube Sampling (from Vaughan et al. 1992)

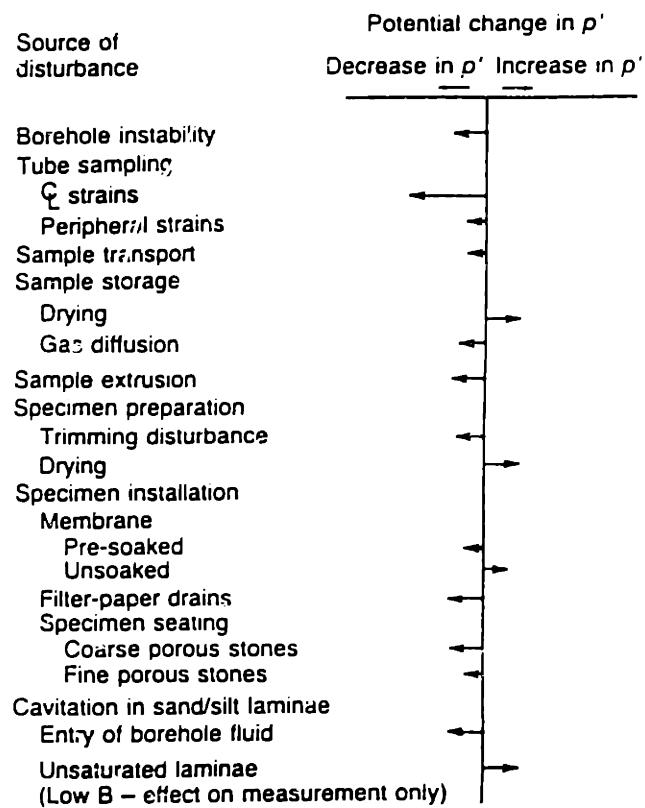


Figure 2.13 Sources of Variation of the Mean Effective Stress  
(from Hight et al. 1992)

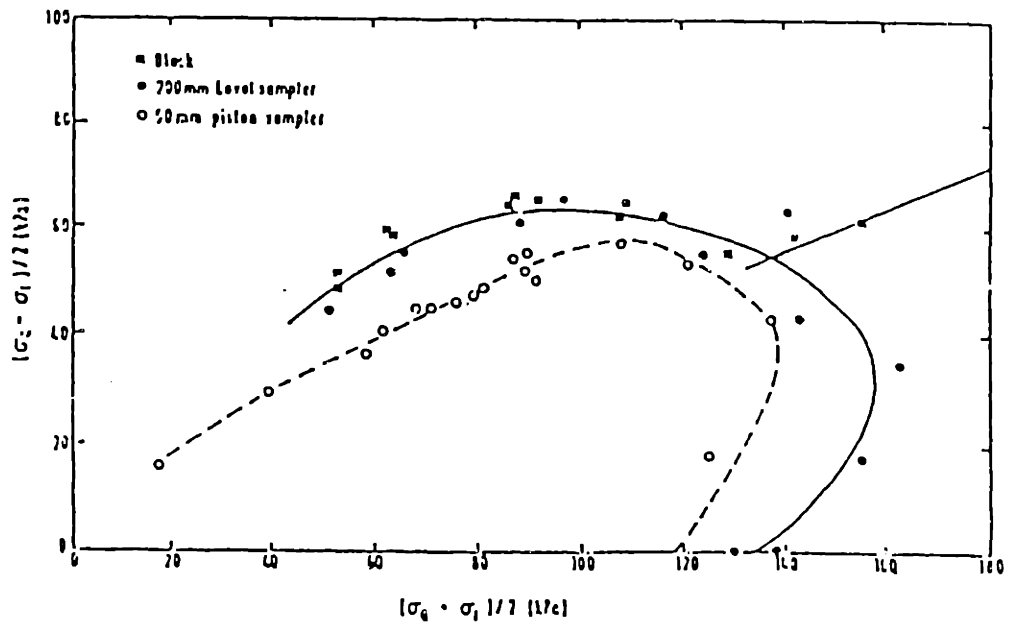


Figure 2.14 Comparison of the Bounding Surfaces of Saint Louis Clay Obtained from Laval and Piston Samplers (from Tavenas and Leroueil 1987)

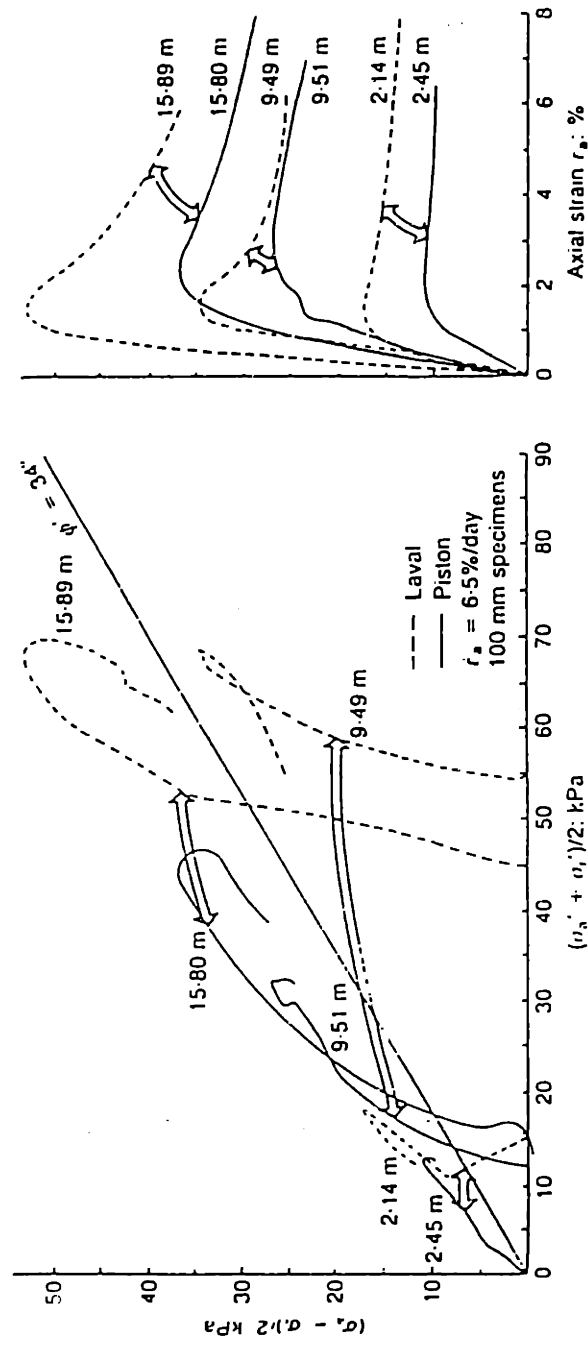


Figure 2.15 Comparison of UU Test Results on Bothkennar Clay Specimens Obtained from Piston and Laval Samples (from Hight et al. 1992)

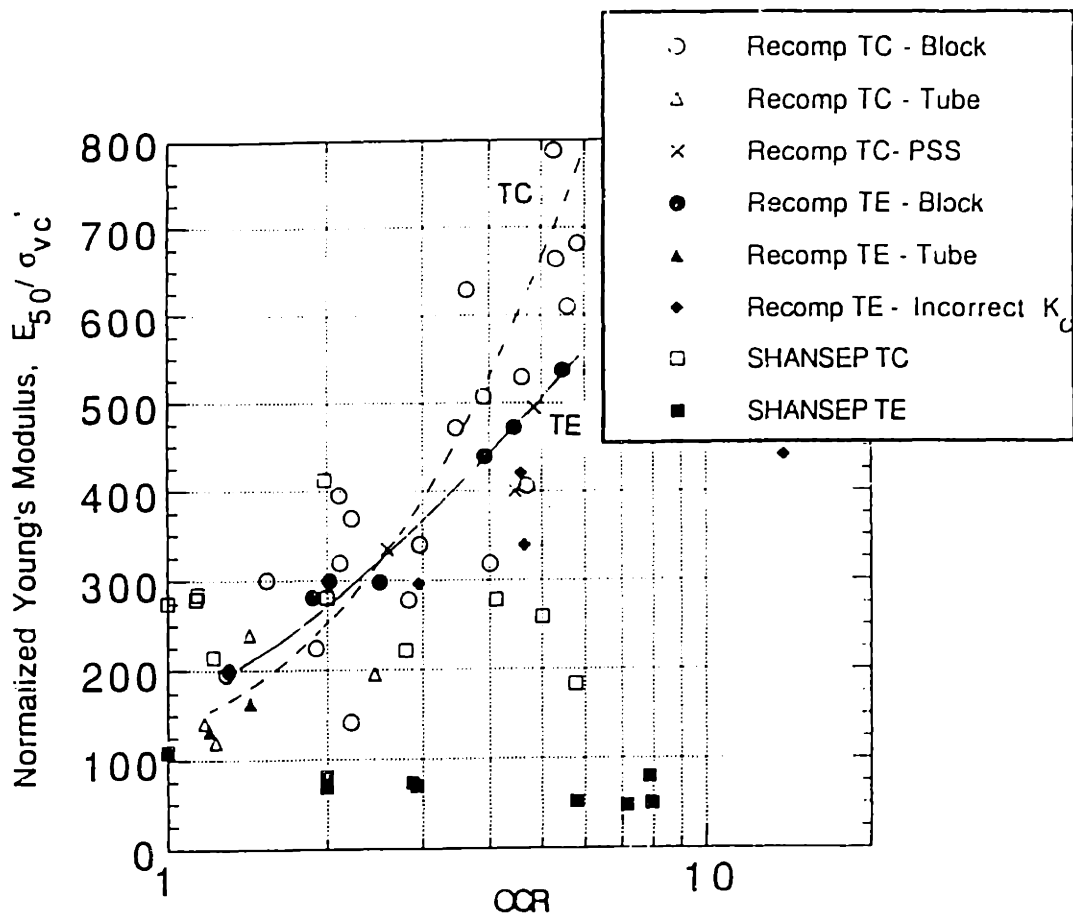


Figure 2.16  $E_{50}/\sigma'_{vc}$  versus OCR for Recompression and SHANSEP Tests on Boston Blue Clay (from Estabrook 1990)

## OPERATIONS INFLUENCING DISTURBANCE

### BOREHOLE ADVANCEMENT

- METHOD OF ADVANCING BOREHOLE
- TYPE OF DRILLING MUD

### TUBE PENETRATION AND RETRIEVAL

- SAMPLER GEOMETRY
- METHOD OF ADVANCING SAMPLER
- METHOD OF EXTRACTION

### SAMPLE TRANSPORT

- SHOCKS
- TEMPERATURE SHOCKS (FREEZING/THAWING)

### SAMPLE STORAGE

- TEMPERATURE
- HUMIDITY
- CHEMICAL REACTIONS
- TIME

### SAMPLE EXTRUSION

- METHOD OF EXTRUSION

### SPECIMEN PREPARATION

- TRIMMING
- DRYING
- SETUP (MEMBRANES, FILTER PAPER DRAINS, POROUS STONES)

Figure 2.17 Operations Influencing Disturbance



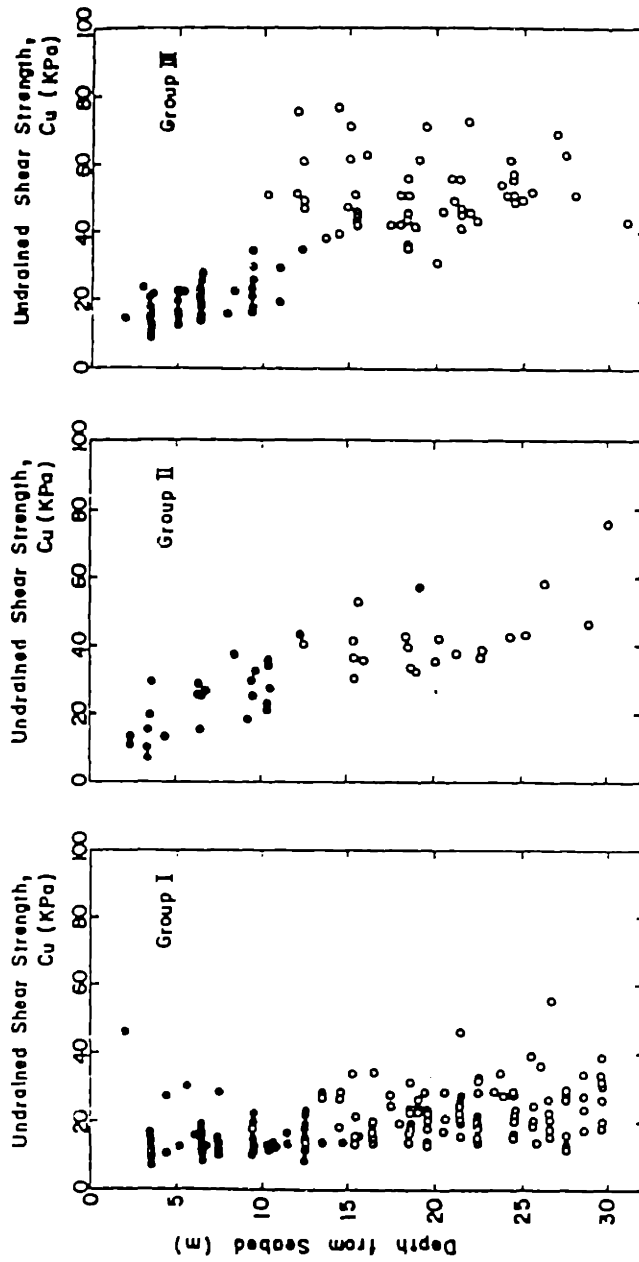
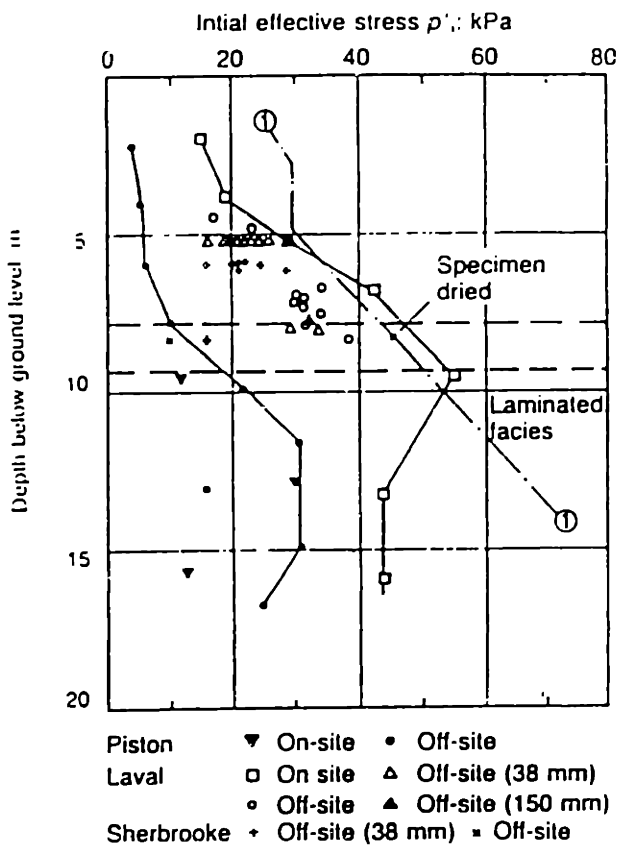


Figure 2.18 Comparison of Strength Profiles from UU Tests on Samples Obtained Using Different Boring and Sampling Methods (from Adachi 1981)



①-② Estimated mean effective stress in situ based on spade cell and self-boring pressuremeter measurements

Figure 2.19 Mean Effective Stress Profiles determined from Piston, Laval, and Sherbrooke Samples (from Hight et al. 1992)

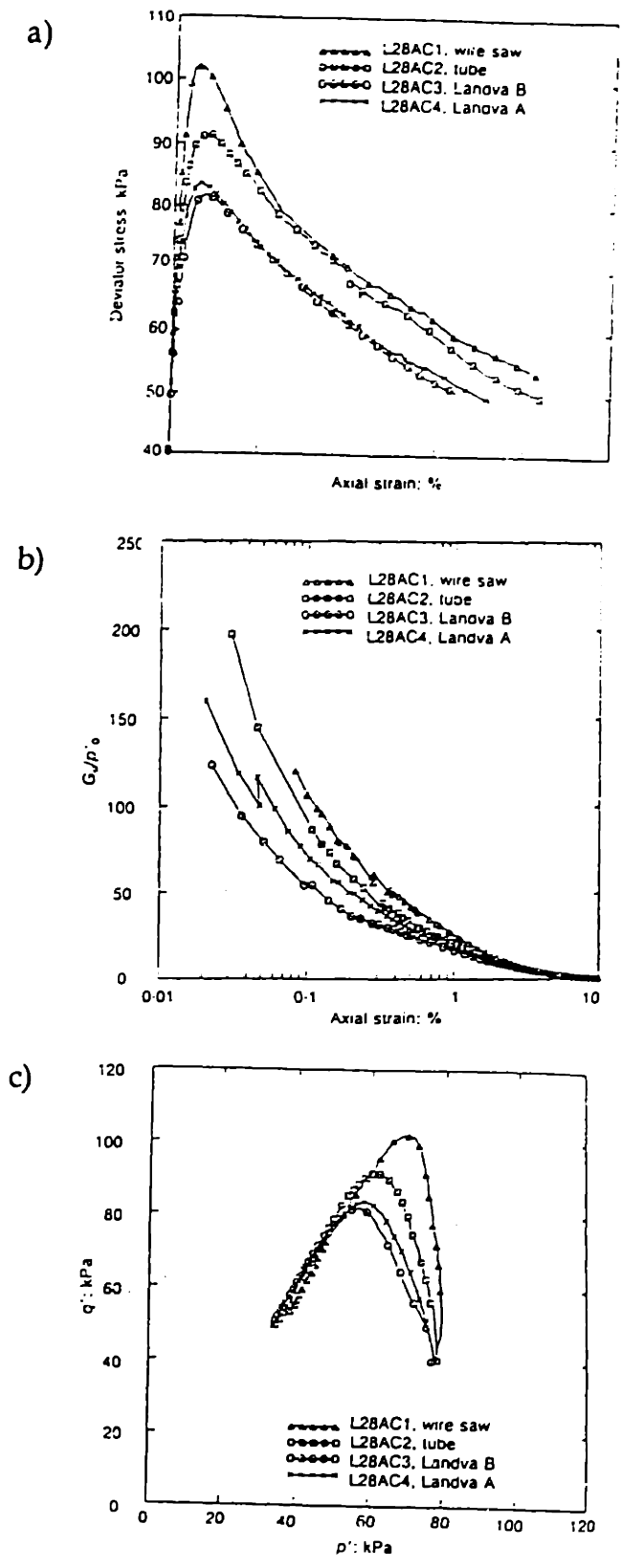


Figure 2.20 Effect of Trimming Method on (a) the Stress-Strain Behavior, (b) the Stiffness, and (c) the Bounding Surface of Bothkennar Clay (from Atkinson et al. 1992)

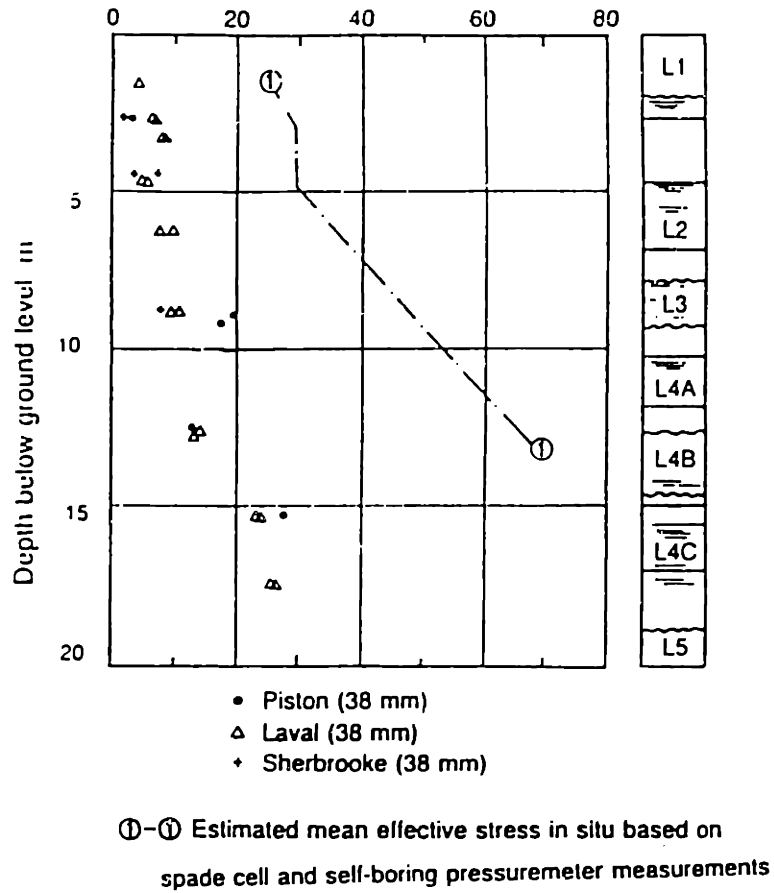


Figure 2.21 Effect of the Tube Trimming Method on the Mean Effective Stress Determined on Piston, Laval and Sherbrooke Samples (from Hight et al. 1992)

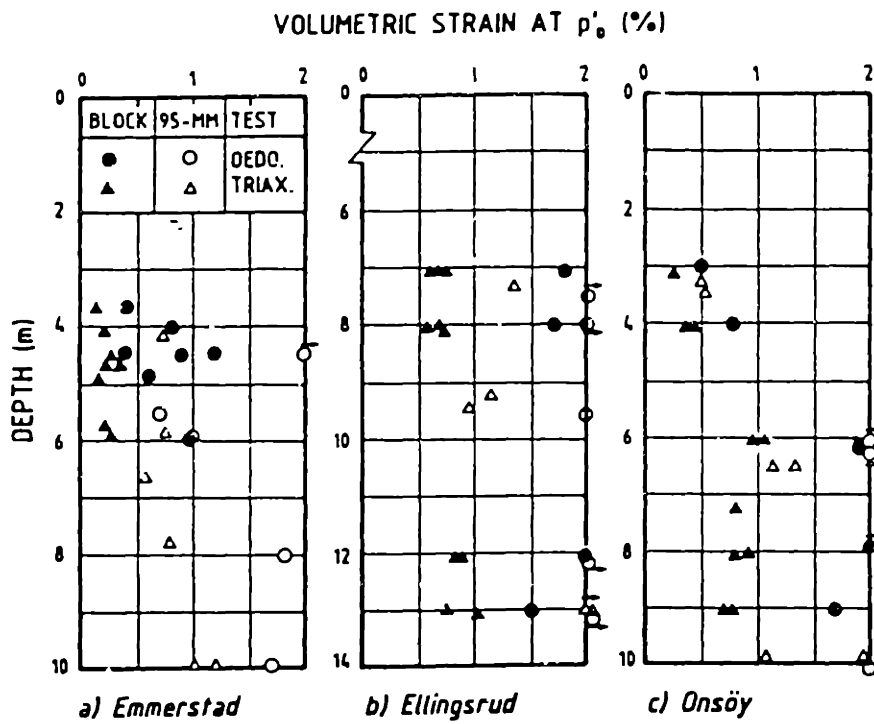


Figure 2.22 Volumetric Strains During Reconsolidation of Tube and Sherbrooke Samples (from Lacasse et al. 1985)



## Chapter 3 Supporting Technology

### 3.1 Introduction

The experimental program consists of performing single element triaxial tests which simulate the operation of sampling an intact clay.

The "intact" material tested is Resedimented Boston Blue Clay (RBBC). This clay has several advantages over natural material. It exhibits more uniform characteristics, it is completely saturated and it has a controlled stress history while maintaining the structure and the fabric of natural soil. Use of RBBC also allows easy comparison with the results of a parallel project which investigates the effects of sampler geometry (Sinfield 1994) and makes use of the same soil. Section 3.2 describes the RBBC used in this testing program, including resedimentation procedure and index properties.

As will be discussed in more detail in Section 3.4 and in Chapter 4, the tests performed in this research project entail subjecting the soil to complex strain and stress paths. The automated triaxial cells used in this research, and described in Section 3.3, allow these processes to be performed easily and accurately.

The testing procedure followed in performing the tests is outlined in Section 3.4.

## **3.2 Resedimented Boston Blue Clay**

### **3.2.1 Introduction**

Resedimented Boston Blue Clay has been used at MIT for research purposes for the last 30 years. Since 1961, resedimentation of BBC has produced over 50 recorded batches of testing material from 3 different natural sources. The material is a low to medium sensitive, CL clay, deposited in the Boston basin about 12000-14000 years ago during the deglaciation that followed the Wisconsin glacial period (Kenney 1964). This has resulted in an extensive database of material index and engineering properties.

All the triaxial test results presented in this thesis refer to specimens obtained from batches belonging to Series III. The natural material for this series was extracted from a depth of about 75 feet during construction of a parking garage near Kendall Square, Cambridge, MA.

The following section briefly reviews the procedure followed to produce the RBBC soil cakes from which the test specimens are trimmed, starting from the collection of the natural material. Section 3.2.3 summarizes the index properties of RBBC focusing on the comparison of the results from the different series and batches.

### **3.2.2 Resedimentation procedure**

Over the last 30 years the resedimentation procedure of Boston Blue Clay has been revised and improved by a large number of researchers.



The clay used in this program was resedimented according to the procedure developed mostly by Germaine (1982) and Seah (1990).

The resedimentation procedure can be divided into four steps: powdering, resedimentation, consolidation and storage.

a) Powdering

After retrieving Boston Blue Clay from the ground, the soil is cleaned and powdered. Soil particles larger than medium sand and foreign objects such as wood and shells are removed by wet sieving the natural BBC through a U.S. Standard #40 sieve. The soil is then oven-dried, pre-crushed and pulverized into powder, to pass a #100 sieve.

b) Resedimentation

Resedimentation takes place making use of the equipment showed in Figure 3.1. Fifteen kg of oven-dried soil are mixed with approximately 15 kg of deaired water under a vacuum to create a soil slurry. About 100 g of sodium chloride (a flocculant) and 2 ml of phenol (a bacterial growth inhibitor) are also added to the slurry. These components are combined using blades rotating at ~ 60 rpm in the upper chamber while maintaining a constant water content of 100%. The slurry is then mixed for about 30 minutes at 120 rpm and finally sprayed through the lower free-fall chamber into the consolidometer by opening the valve between the two chambers.

c) Consolidation

After removal of the free fall chamber, the slurry is incrementally loaded (LIR=1) in the consolidometer to a maximum vertical stress of 1 ksc and then unloaded to 0.25 ksc to produce an OCR of 4.

Except for the initial low stress increments, each load increment is maintained at least until the end of primary, while the maximum stress is kept for one cycle of secondary compression. The consolidation process in the consolidometer, which has double drainage, is completed in about 19 days. At  $OCR=4$  the soil is close to hydrostatic conditions ( $K_0 \approx 1$ ) and the shear strains due to the removal of the soil cake from the consolidometer are minimal. In this sense it is said that RBBC is characterized by low sample disturbance.

#### d) Storage

After completion of consolidation the soil cake is removed from the consolidometer and prepared for storage. The cake is cut into smaller pieces making use of a wire saw. Each piece is stored with a 4-layer protection: a layer of cellophane, a layer of a 50/50 mixture of paraffin wax and petroleum jelly, a second layer of cellophane and a second layer of the wax-jelly mixture.

The pieces are stored in a room maintained at 90-100% relative humidity until they are used to make test specimens.

### 3.2.3 Material Index Properties

To establish fundamental soil behavior through experimental testing, it is necessary to ensure test material uniformity from specimen to specimen. This section reviews the uniformity of the RBBC used in this experimental program through the index properties of the different RBBC batches.

The triaxial testing program for this project used RBBC from batches 216-220 of BBC Series III soil. Several other tests all performed on clay specimens from previous batches of Series III RBBC, part of previous experimental programs, are used in the following chapters for comparison purposes.

Figure 3.2 provides a summary of the grain size data from Series III RBBC. The data, obtained by Seah (1990) compares the grain size distribution before and after processing through the pulverizer. It appears that the reprocessed curve falls within the band of the original batch data. Seah also tested samples taken from different depths in the resedimented soil batch and found no significant change in the grain size curve, therefore concluding that there was no segregation.

Figure 3.3 plots available index properties from all the RBBC batches manufactured from Series III BBC. Water contents ( $w_i$ ) are mean values reported from batch and individual test trimmings. Liquid limits were performed using the Casagrande cup, while the "rolling" method (ASTM D4318 1992) was used to obtain values of the plastic limit,  $w_p$ . It is important to note that batches 214-220 used BBC that was reprocessed from specimens and trimmings of specimens from batches 200-210. These batches are all characterized by slightly lower water content. Except for the lower values of the liquid limit for batches 217-220, which have not been explained, there is satisfactory uniformity in the results.

Figure 3.4 plots the values of the liquid limit and the plasticity index for all the batches from Series III on the Plasticity Chart from which it results that RBBC is, just as the parent soil, a CL clay. It can be observed

that, due to the lower value of the liquid limit, the soil from batches 217-220 plots slightly off from the other batches and from the source material.

### **3.3 MIT Automated Stress Path Triaxial Apparatus**

A large effort has been invested at MIT over the past 5 years into automating the existing conventional testing equipment. The result of this effort is the Flexible Automation Technology for Computer Assisted Testing: the FATCAT, characterized by increased versatility and productivity, dramatic labor reduction and exceptional quality control.

Figure 3.5 shows a schematic representation of the new system for computer controlled triaxial testing (Sheahan and Germaine 1992) which represents one of the most recent contributions to FATCAT and which, consistent with the FATCAT concept, combines existing MIT testing equipment with some innovative new components.

All the tests performed for this experimental program were run making use of these Automated Stress Path Triaxial Cells. At the time in which the tests were performed four identical triaxial cells (MIT03-MIT06) were available.

The system shown in Figure 3.5 can be divided into 5 main parts:

- a) the triaxial cell itself,
- b) the pressure control devices,
- c) the motor control box,
- d) the personal computer, and
- e) the data acquisition control unit.

The mechanical system is housed in an environmental chamber maintained at a temperature of  $25^{\circ}\text{C}\pm 0.2$  SD.

The triaxial cell is composed of a Wykeham Farrance base dating back to the mid 1960's with customized features such as linear ball bearing bushings and a rolling diaphragm seal to reduce piston friction, a fixed top cap for testing on clay, top and bottom drainage, ball valves, copper tubing and silicon oil as cell pressure fluid to eliminate the problem of leakage through the membrane. The cell is mounted on a Wykeham Farrance load frame and is attached to an external load cell. The pore and cell pressure transducers are placed on the base of the cell so as to reduce the system compliance. Axial strains are measured externally by means of a DCDT.

The pressure control devices are equipped with DC electric servo motors and control the pore and the cell pressure. These two motors as well as the motor which drives the load frame are controlled by the MIT-designed motor control box which receives orders from the personal computer, the controller of the system.

Automated control is carried out by a control program written in BASIC running on the PC. The program is very flexible and user-friendly and able to perform all phases of a triaxial test including initial pressure up, back pressure saturation, B-value check, consolidation along any stress path or  $K_0$  consolidation and shear in extension or compression.

During each phase of the test, signals from the pressure and displacement transducers and the load cell are converted from analog to digital by an MIT designed (Sheahan 1991), 22 bit integration card. The software in the PC processes the digital information. The current values of

the stresses and the displacements in engineering units are determined and compared with the target values. Based on this comparison the computer calculates the subsequent control signals which are sent via a Strawberrytree 12 bit digital to analog converter to the motor control box.

At regular intervals, chosen by the tester, transducer readings are also taken by the "test witness", the Hewlett Packard 3497A Data Acquisition Control Unit which transforms the information (A/D) and stores the data. The same central data acquisition system is used for the entire geotechnical laboratory. The resolution of this unit is 0.1 mV for the DCDTs and 1  $\mu$ V for the pressure transducers which exceed the sensitivity of the triaxial control program. The readings are collected into a data file and used to calculate the stresses and strains in the specimen by means of a reduction program.

Two programs were used to reduce the tests presented in this thesis. The first group of tests (TX115-TX200) were reduced making use of the BASIC program written by Sheahan and Germaine (Sheahan 1991). The rest of the tests were reduced using an improved Quick BASIC version of this program formulated by Sinfield (Sinfield 1994).

The most recent improvements of the triaxial equipment include lubricated end platens, on-specimen axial strain measurements, and utilization of specially designed pedestals capable of measuring the sampling effective stresses in conjunction with UU testing (Sinfield 1994).

### 3.4 Testing Procedure

This section reviews the testing procedure followed in running the tests here presented.

#### *Specimen Preparation and Setup*

Upon removal of the sample from the wax and plastic film, a specimen is trimmed using a wire saw and a miter box. The operation takes place in two stages: first the excess material is removed and then the final trimming is carried out to the correct diameter. The ends of the specimen are then squared off using a wire saw and a straight edge. The resulting final specimen is approximately 3.6 cm in diameter and 8 cm long. Water contents are taken using material from the final trim stage and the ends of the specimen, and the initial mass of the specimen is also measured.

After ensuring that all lines in the triaxial cell are saturated and after cleaning the porous stones and filter papers with the ultra-sound, the stones, filters and the specimen can be placed in the cell. Eight 0.5 cm wide vertical filter strips positioned around the periphery of the specimen ensure radial drainage. Two prophylactic membranes are rolled around the specimen and secured at the base and on the top cap by greased o-rings to provide an impermeable barrier between the soil and the pressured fluid during the test. Once the Plexiglas chamber is placed and the remaining equipment assembled, the triaxial cell is filled with silicone oil. The specimen height and the zeros and the calibration factors of the transducers and load cell are input into the set-up program.

## *Testing*

As will be discussed in the following chapter different types of triaxial tests (Undisturbed, UU, SHANSEP and Recompression) were performed for this experimental program. The following summary provides a review of the phases of each type of test.

### a) Pressure Up

This phase consists of applying a hydrostatic total stress (usually about 0.3 ksc) for about 12 hours with the drainage lines closed to establish positive pore pressure in the specimen.

The initial effective stress equal to the difference between the cell pressure and pore pressure is recorded.

### b) Back Pressure Saturation and B-Value Check

After equalizing the pore pressure in the back pressure line to the value existing in the specimen at the end of pressure up, the drainage lines are opened. The back pressure is then gradually increased in increments of 0.5 ksc, to 2-3 ksc, while maintaining constant the initial effective stress. The pore pressure parameter B is then checked to ensure that the specimen is fully saturated. If necessary, saturation is carried on to higher effective stress until B is greater than 95%.

### c) Consolidation ( $K_0$ or Stress Path)

This testing program has made use of both  $K_0$  and stress path consolidation. In both cases a constant rate of axial deformation of approximately 0.1%/hr was used to ensure that there was no pore pressure build up. During one dimensional consolidation, the computer increases



the cell pressure so that until the desired vertical stress is reached, the area of the specimen remains constant and  $K_0$  conditions are maintained. The maximum stress is held constant for at least 24 hours. For overconsolidated tests the specimen is then rebounded to the appropriate OCR using the same constant rate of axial deformation. Once again the stress is held for 24 hrs.

In the case of stress path consolidation the desired vertical  $\sigma'_{vfin}$  and horizontal  $\sigma'_{hfin}$  stresses are reached in two steps. In the first step the soil is consolidated by increasing the vertical stress only (stress path at  $45^\circ$ ) until  $\sigma'_v = \sigma'_h / K_{fin}$ , with  $K_{fin} = \sigma'_{hmax} / \sigma'_{vmax}$ . Then, the desired values of both the final vertical and horizontal stresses are input in the computer and the specimen is consolidated following a the  $K = K_{fin}$  path. Also in this case, the maximum stress at the end of consolidation is maintained for at least 24 hrs to allow secondary compression.

While phases (a) through (c) are common to all tests, the following phases depend on the type of test.

d) Standard Undrained Shear (Standard Undisturbed Tests)

Before performing the undrained shearing process the drainage lines are closed and the change in pore pressure is monitored for 30 minutes to check for possible leakage. The specimen is then sheared undrained at a constant rate of axial deformation of approximately 0.5%/hr until 10-15% axial strain.

(e) PSA Disturbance (PSA Disturbed Tests)

At the end of phase (c) after checking the possibility of a pressure leak as described in (d), the specimen is unloaded in extension at a constant rate of axial deformation of approximately 0.5%/hr, with a total vertical stress target value equal to the cell pressure at the end of the previous testing phase (consolidation or swelling for the OC tests).

(f) ISA Disturbance (ISA Disturbed Tests)

At the end of phase (c) the possibility of a pressure leak is checked as described in (d). Then the specimen is sheared undrained in a cycle of compression (from 0 to  $\epsilon_{\max}$  axial strain), extension (from  $\epsilon_{\max}$  to  $-\epsilon_{\max}$ ), and compression (from  $-\epsilon_{\max}$  to 0 strain) at a constant rate of axial deformation of either 0.5%/hr or 1%/hr. Finally the specimen is unloaded in extension at the same strain rate to hydrostatic conditions. The turnaround points in the straining cycle are specified by the operator (e.g.  $\pm 1.0\%$ ) and the actual reversal of the axial deformation is performed under manual control.

(g) Undrained Shear after Disturbance (Disturbed PSA/ISA UU Tests)

In this case the shear is performed as described at point (d) except that no pressure leak check is performed.

(h) One Dimensional Reconsolidation after Disturbance

(Disturbed PSA/ISA SHANSEP Tests)

At the end of either PSA or ISA disturbance, the pressure on the back pressure line is equalized to the pore pressure of the specimen. The specimen height and area are calculated based on the deformations of the

specimen and on the outflow of water during the first consolidation. These updated values are input in the set up program of the computer.

The specimen is then  $K_0$  consolidated as described in (c) to the desired stress, usually 9 ksc or higher. The maximum stress is held constant for at least 24 hours. In the OC tests the specimen is swelled to the pre-disturbance OCR. The end of swelling stress is held constant for at least 24 hours.

(i) Stress Path Reconsolidation after Disturbance

(Disturbed PSA/ISA Recompression Tests)

As described above for the one-dimensional consolidation, at the end of the disturbance phase, the pressure on the back pressure line is equalized to the pore pressure of the specimen. The specimen height and area are calculated based on the deformations of the specimen and on the outflow of water during the first consolidation, and these updated values are input in the set up program of the computer.

The specimen is then consolidated to the pre-disturbance state of stress at a constant strain rate of about 0.1%/hr by inputting the desired values of the vertical and the horizontal effective stresses.

(j) Final Undrained Shear after Reconsolidation

(Disturbed SHANSEP and Recompression Tests)

After checking for a possible pressure leak as described in (d) the soil is sheared at a constant rate of strain of 0.5%/hr until the axial strain reaches 10-15%.

After the apparatus is disassembled, the final specimen dimensions and the weight of the specimen are measured. From the final weight of the specimen it is possible to determine the water content and the dry mass of the specimen which are used for phase relation calculation.

In summary the different types of test are characterized by the following phases:

Standard Undisturbed Tests: (a), (b), (c), (d)

Disturbed PSA UU Tests: (a), (b), (c), (e), (g)

Disturbed ISA UU Tests: (a), (b), (c), (f), (g)

Disturbed PSA SHANSEP Tests: (a), (b), (c), (e), (h), (j)

Disturbed ISA SHANSEP Tests: (a), (b), (c), (f), (h), (j)

Disturbed PSA Recompression Tests: (a), (b), (c), (e), (i), (j)

Disturbed ISA Recompression Tests: (a), (b), (c), (f), (i), (j)

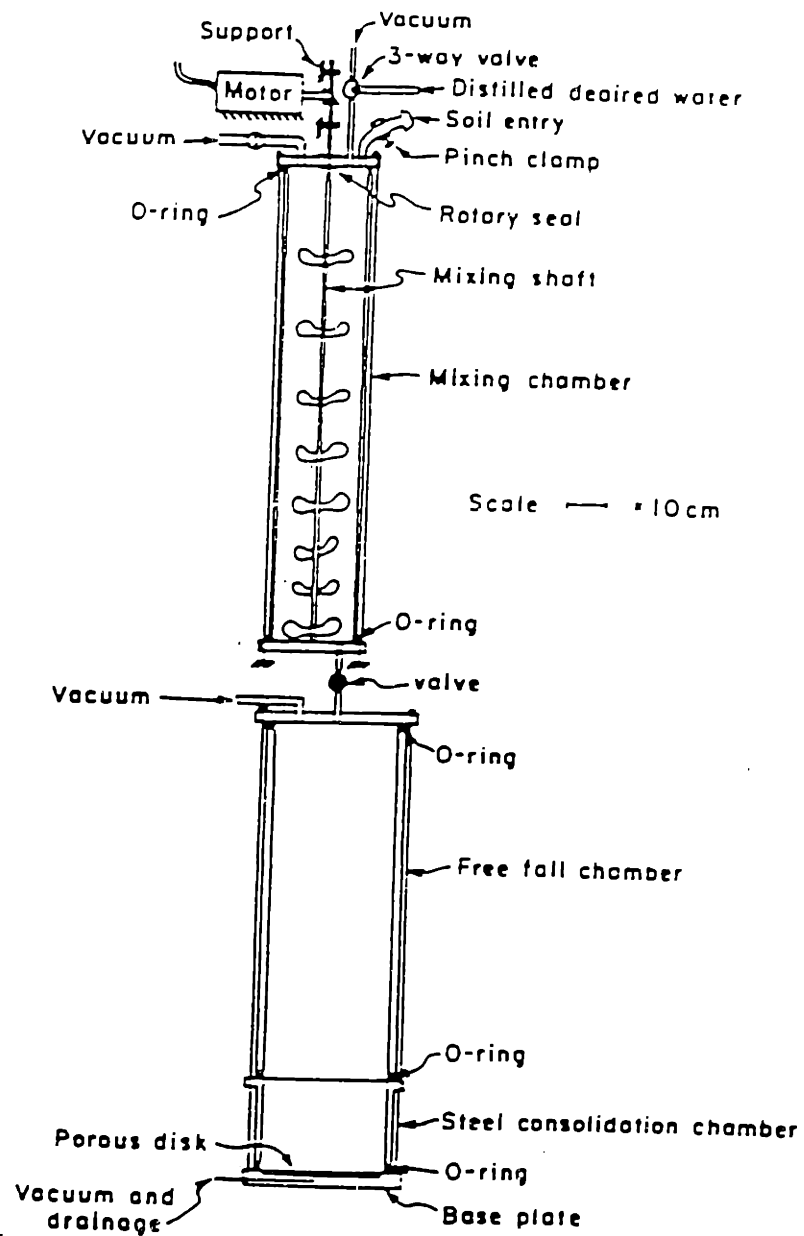


Figure 3.1: Schematic of the Equipment Used for the Resedimentation of Boston Blue Clay

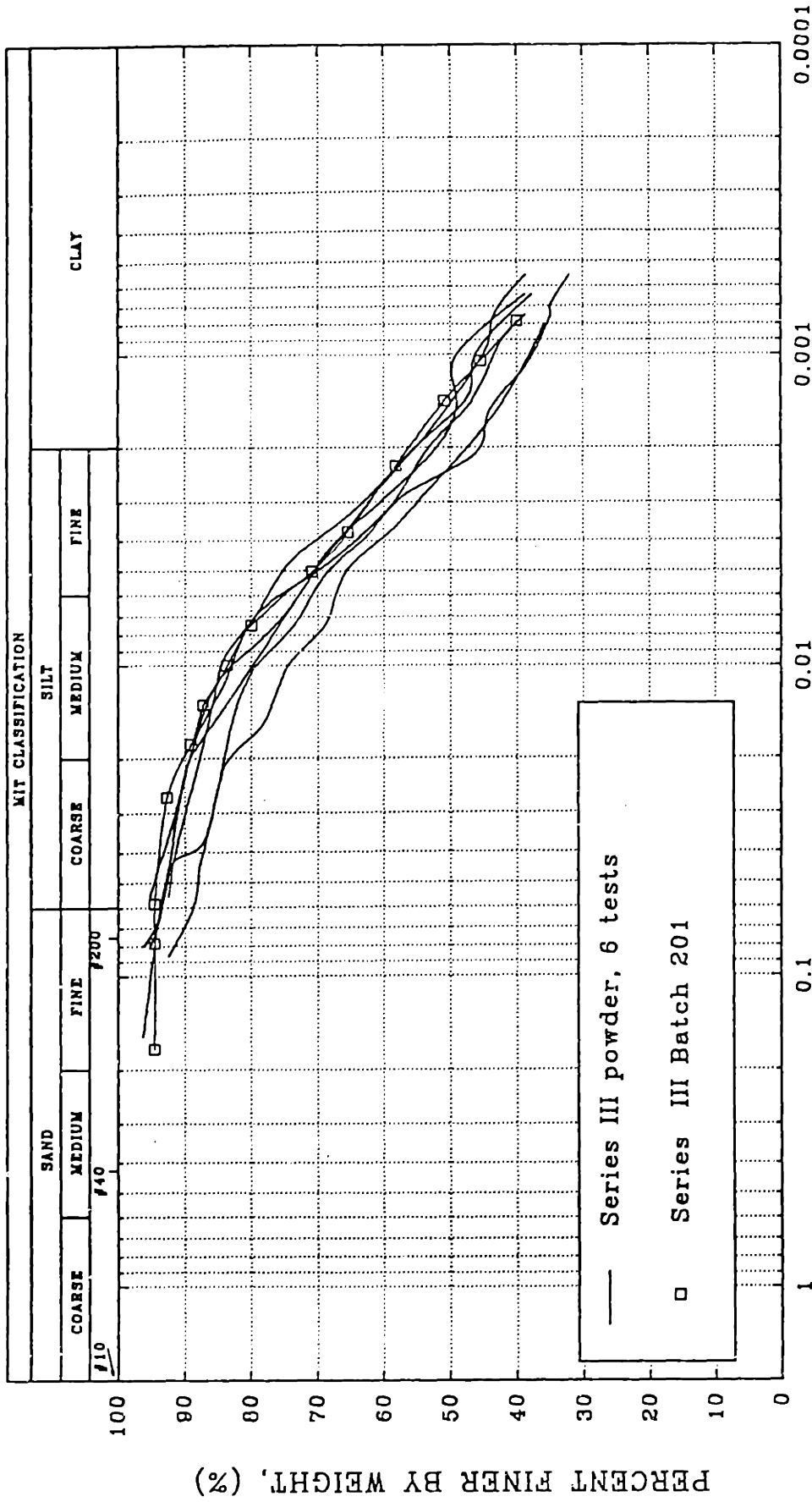


Figure 3.2: Results of Grain Size Analysis on RBBC Series III  
(after Seah 1990)

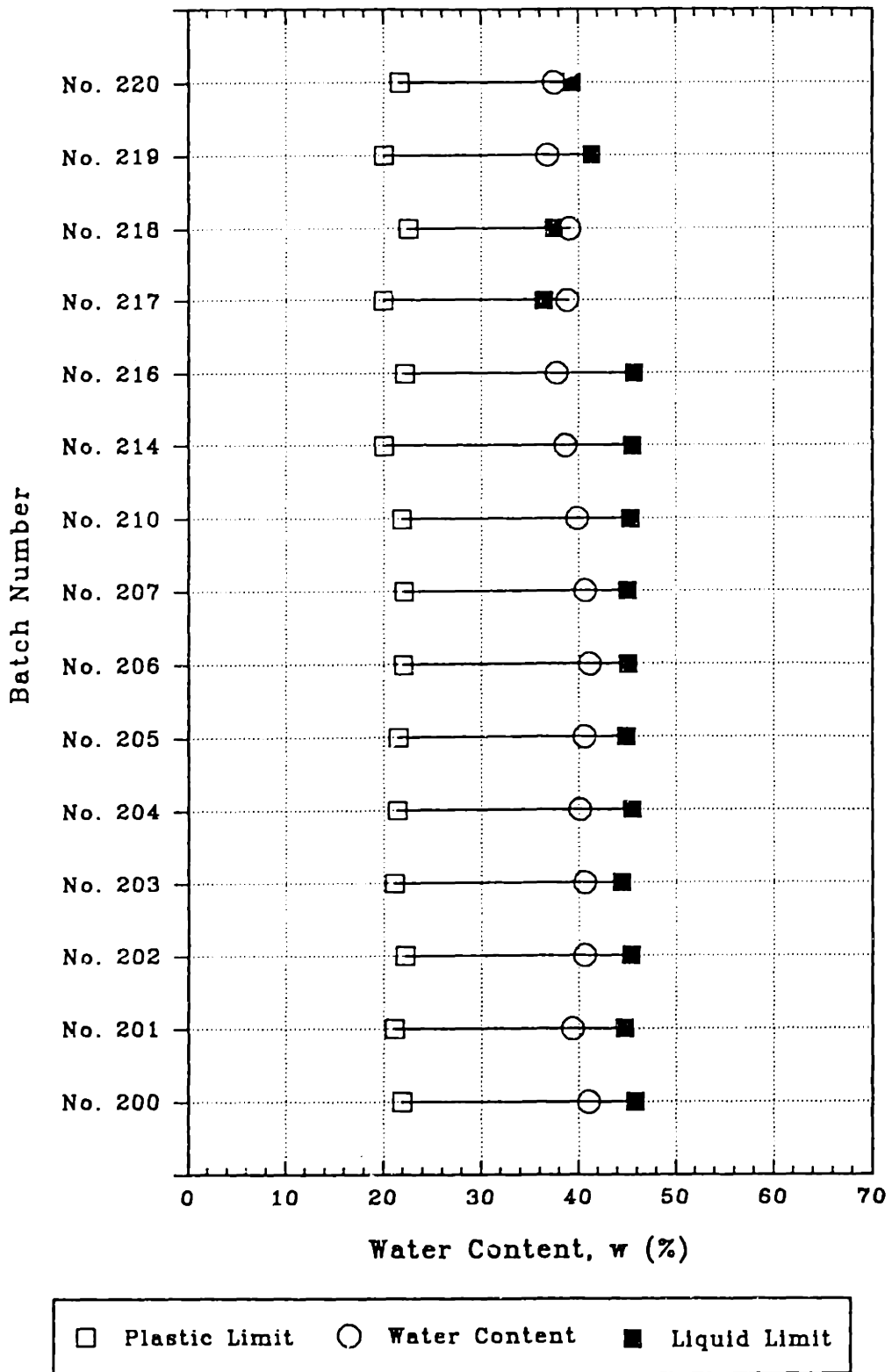


Figure 3.3: Results from Atterberg Limit Tests on Series III RBBC (Modified from Cauble 1993).

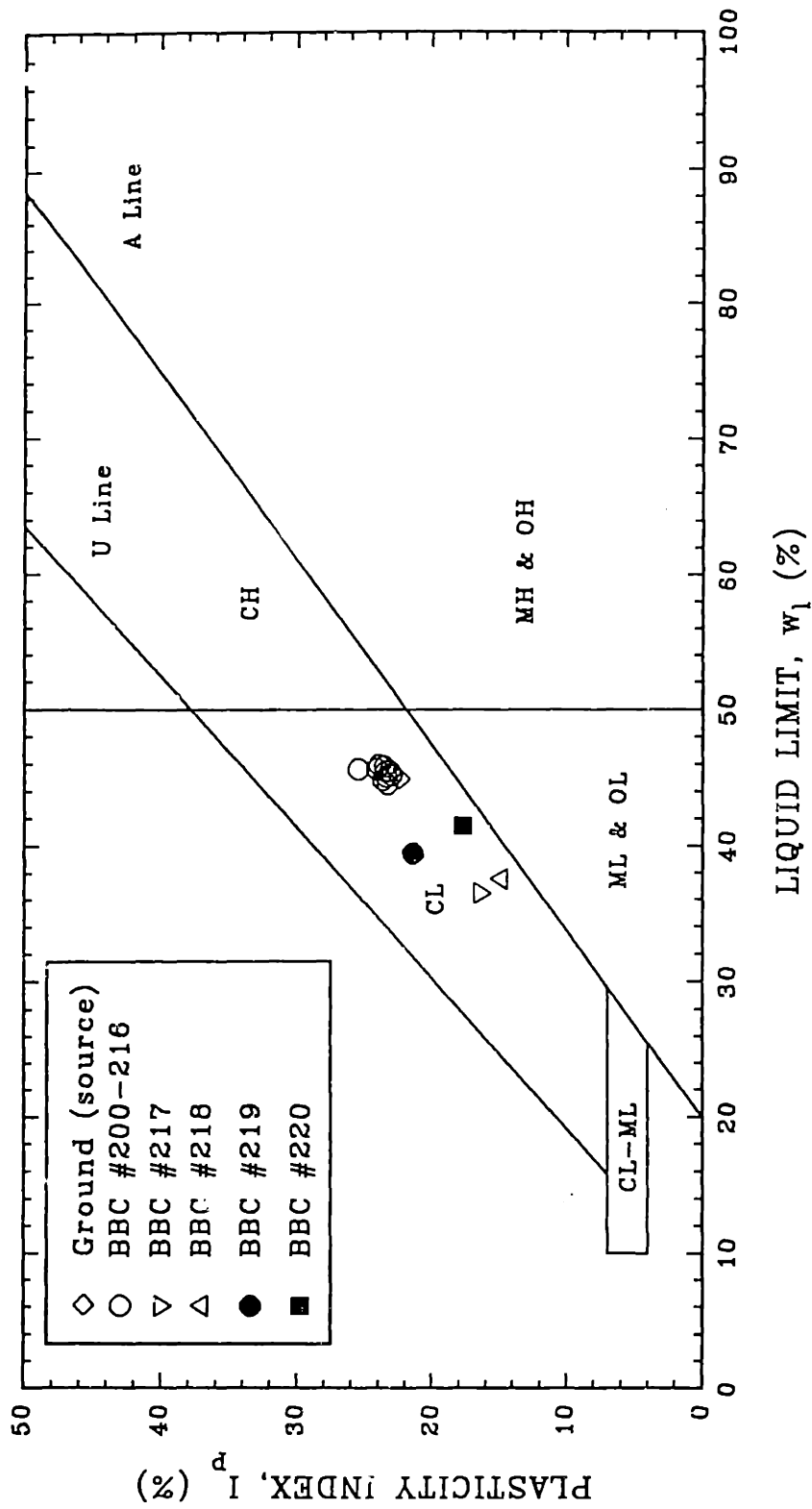


Figure 3.4: Plasticity Chart with Data from RBBC Series III  
(Modified from Cauble 1993)



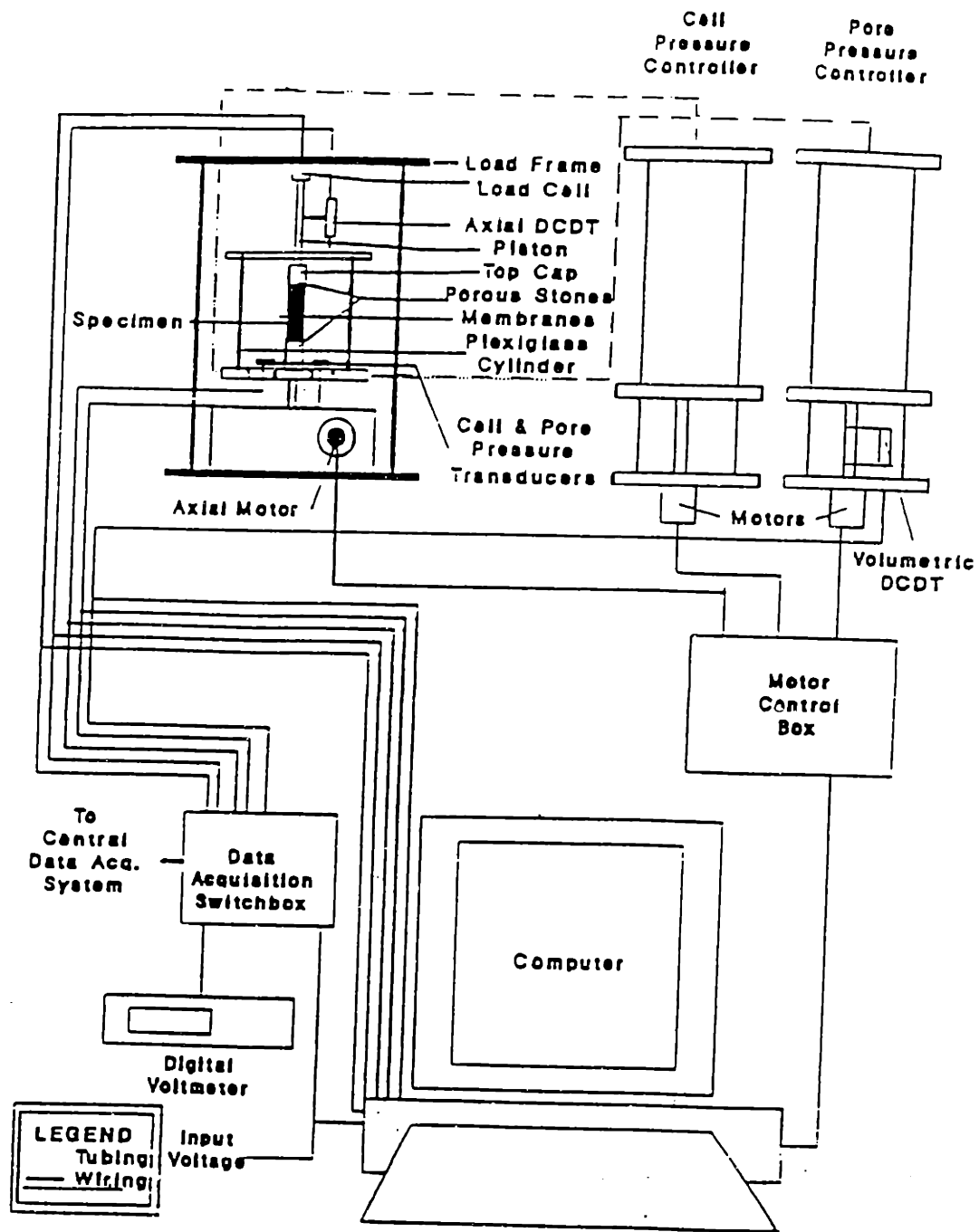


Figure 3.5: Schematic Representation of the MIT Automated Stress Path Triaxial Apparatus (from de La Beaumelle 1991)



# Chapter 4 Research Approach

## 4.1 Introduction

The experimental program presented in this thesis is designed to simulate simple aspects of the sampling process using single element triaxial tests. It is based on the assumptions that sampling can be considered an undrained process and that the disturbance undergone by a soil element during sampling can be simulated in a triaxial experiment. Further, the simulation of tube sampling disturbance in the triaxial cell is based on analytical solutions obtained making use of the Strain Path Method (Baligh 1985) and presented by Baligh et al. (1987) within the framework of the "Ideal Sampling Approach".

In clays, due to the low permeability of the soil and to the rapid penetration rates associated with the sampling operations, sampling can be considered an undrained process, therefore supporting the first assumption of this analysis. The second assumption quite obviously does not apply to all soil elements of a sample. In fact during penetration of a sampler, each soil element is subjected to a complex strain path history dependent on its position within the sampler and on the geometry of the tube. Only soil elements positioned along the centerline of the sampler are sheared in the triaxial mode.

Results obtained making use of the Strain Path Method (Chin 1985 and Baligh et. al 1987) indicate, however, that  $\epsilon_{zz}$  is the dominant straining component in the inner half of the sample and that, as suggested

by the Ideal Sampling Approach, reasonable estimates of soil disturbance within the sampler can be obtained from results at the sample centerline.

The Strain Path Method represents the analytic basis for the work presented here and tube sampling disturbance is simulated in accordance with the Ideal Sampling Approach. The simulation of block sampling relies instead on the Perfect Sampling Approach. More details on the simulation of disturbance in the triaxial tests for both of these cases are furnished in the following section which describes in depth the different types of tests performed and discusses the rationale of the triaxial experimental program.

## **4.2 Description and Motivation of the Testing Program**

### **4.2.1 "Disturbed" and "Undisturbed" Tests**

Tables 4.1 and 4.2 summarize the triaxial tests performed as part of the Sample Disturbance project.

The tests are subdivided into the following types:

- Standard "Undisturbed" Tests
- "Disturbed Tests" which include :
  - "UU" Tests
  - "Recompression" Tests
  - "K<sub>0</sub> Consolidation or SHANSEP" Tests

It must be noted that the terms used above to characterize the different types of tests are not used in their traditional sense. For this reason the different phases of each test will be described in detail. The procedure followed for testing is described in Chapter 3 and is only briefly summarized here. After back pressure saturation the specimen is consolidated in oedometric conditions to a maximum stress of 3-4 ksc using a constant rate of axial deformation of about 0.1%/hr. The maximum stress is maintained for 24 hours. Past research has shown that RBBC exhibits normalized behavior. Therefore consolidation to 3-4 ksc allows to erase the limited disturbance caused by the removal of the soil cake from the consolidometer and the set-up operations. At the end of consolidation the specimen can be considered in an undisturbed state equal to that of an element of normally consolidated soil in the field prior to sampling. In the OC tests the specimen is swelled to the desired OCR and the stresses are held constant for 24 hours.

The conditions at the end of consolidation, or swelling for the OC tests, will always be referred to as the "in situ" stresses.

In the Standard "Undisturbed" Tests, without allowing any change in the in situ conditions or in the water content the specimen is sheared. The test is considered representative of the intact behavior of Resedimented Boston Blue Clay. The results of these tests are presented and discussed in Chapter 5.

Figures 4.1a-b, 4.2a-b, and 4.3a-b summarize the stress paths and the compression curves for the three types of "disturbed" tests for NC RBBC. Similar paths apply in the case of OC tests.

In the "Disturbed" Tests, at the end of consolidation, or swelling for  $OCR > 1$ , the specimen is subjected to an undrained shearing process simulating the disturbance produced by the sampling operations. According to whether disturbance is simulated according to the Perfect Sampling Approach or to the Ideal Sampling Approach, the tests are denoted as PSA or ISA tests. As will be discussed in the following section, the PSA tests intend to simulate the effect of block sampling, while the ISA tests are aimed at investigating the disturbance produced by tube sampling. The details of the undrained process simulating disturbance are provided in the following section.

Following disturbance, in the "UU Tests" the specimen is sheared undrained. The properties such as undrained strength, modulus, etc., measured during the undrained shear, are considered to be equal to those that would be measured if a UU test were performed on a specimen obtained from a block (PSA tests) or tube (ISA tests) of RBBC.

In the "Recompression Tests" the specimen is reconsolidated back to the "in situ" conditions making use of stress path consolidation which reinstates both the vertical and the horizontal in situ stresses. The specimen is then sheared undrained.

In the " $K_0$ -consolidation Tests or SHANSEP" the specimen is  $K_0$ -consolidated well past the "in situ" effective stress to at least 9 ksc. This stress is held constant for 24 hours. In the OCR tests the soil is then unloaded to the "in situ" OCR and maintained at constant stresses for at least one cycle of secondary compression. Finally the specimen is sheared undrained.

In all tests the final undrained shear is performed in compression with a strain rate approximately equal to 0.5%.

#### 4.2.2 Simulation of Disturbance According to the PSA and ISA

In this testing program disturbance is simulated according to either the Perfect Sampling Approach (PSA tests) or the Ideal Sampling Approach (ISA) which have been introduced in Sections 2.3 and 2.4.

In the first case the disturbance phase involves only the release of the in situ shear stress which occurs when the soil passes from the anisotropic in situ stress state to the isotropic state of stress after extrusion.

In the second case the disturbance phase simulates both the penetration of the tube sampler and the extrusion of the soil from the tube. Consequently the specimen is first subjected to the compression-extension-compression straining history, determined by the Strain Path Method, for a soil element located at the centerline of the sampler (see Figure 2.3), and then unloaded to isotropic conditions.

The different phases of the ISA disturbance cycle can be isolated in Figures 4.4 a and b which show the stress strain curve and the stress path relative to the disturbance phase of an ISA test on NC RBBC. The figures present also example curves for a PSA test. During ISA disturbance the soil is initially sheared in compression to a maximum strain which depends on the geometry of the sampler. In this particular case  $\epsilon_{\max}$  is equal to approximately 2% corresponding to  $B/t \sim 20$ . According to the Strain Path Method this compression corresponds to the sampler advancing towards the soil element. An extension phase (2-3) to  $\epsilon = -|\epsilon_{\max}|$  follows. Finally the

soil is compressed again to  $\varepsilon=0\%$ . The last portion of this undrained process (4-5) simulates the effect of the extrusion of the sample from the tube which results in the release of the shear stresses.

Figures 4.5a-b present similar plots to those presented in Figures 4.4a-b in the case of a PSA and an ISA test on RBBC with  $OCR=4$ .

### **4.2.3 Motivation of the Testing Program**

In the past (Ladd and Lambe 1963), it was suggested that if the degradation of the undrained strength produced by sampling disturbance could be quantified, UU test results could be corrected and the in situ strength of the soil predicted without the need of performing CU tests. Since then it has been recognized that the results of UU tests are influenced by other factors such as the strain rate during shear.

The purpose of the "UU" tests performed in this testing program is to understand and quantify, by comparison with the undisturbed tests, the effects of disturbance on parameters such as the mean effective stress, the undrained strength, the strain at peak strength, the stiffness characteristics, etc. as a function of the type (PSA or ISA) and the magnitude (level of straining) of disturbance and the overconsolidation ratio of the soil. The results of these tests along with the comparison to the "undisturbed" tests are presented in Chapter 6.

Comparison of the "Recompression Tests" and to the "Undisturbed Tests" makes it possible to evaluate the effect of this reconsolidation procedure on the engineering properties of RBBC as a function of the OCR of the soil and the level of disturbance.



The "K<sub>0</sub>-Consolidation/SHANSEP" Tests were conducted to measure the effect of disturbance on the compression characteristics of the clay and on the determination of the maximum past pressure. This is achieved by analyzing the compression curve relative to the K<sub>0</sub>-consolidation performed after the disturbance cycle. The undrained shear following reconsolidation to 9-10 ksc provides a measure of the effects of this type of reconsolidation on the undrained behavior of disturbed RBBC.

Few "Undisturbed" tests were performed as part of this research as can be observed from Table 4.1. This is due to two reasons: in the first place extensive research has been performed over the last 20 years at MIT making use of RBBC and therefore a large database is available for standard tests. In the second place, much information on the intermediate strain intact behavior of RBBC can be derived from the first compression phase of all the ISA tests which is identical to the initial portion of an undisturbed test. In particular, for NC RBBC, the peak strength and the corresponding strain can be measured because the failure strain, which is approximately equal to 0.1%, is always smaller than the maximum strain of the disturbance cycle.

One "special test" TX120 on NC RBBC appears in Tables 4.1 and 4.2. In this test the specimen was unloaded to zero shear stress prior to being subjected to the ISA disturbance cycle to estimate the effect produced by the use of a drilling mud with a unit weight equal to  $K_0 \cdot \gamma_{soil}$ . The results of this test are presented and discussed in Section 6.8.

As mentioned above the intent in performing PSA and ISA disturbed tests was to simulate the effects of block and tube sampling respectively.

As part of this testing program ISA tests were performed with nominal value of  $\epsilon_{\max}$  ranging from 0.5% to 8%. According to the Strain Path Method the magnitude of the straining to which the soil is subjected during tube penetration depends on the geometric characteristics of the sampler. For standard thin-walled Shelby tubes with  $B/t=40$ , the results of the Strain Path Method indicate that  $|\epsilon_{\max}|$  is close to 1%, while  $|\epsilon_{\max}|=2\%$  corresponds approximately to  $B/t=20$ .

The purpose of the tests with higher  $|\epsilon_{\max}|$  is not only to investigate the effect of thicker tubes but also to gain some insight into the degradation of the engineering properties for soil elements not located at the centerline, which are subjected to higher vertical strains, even though they are not sheared in the triaxial mode during the penetration of the sampler. In the following chapters which discuss the effect of disturbance the value of  $|\epsilon_{\max}|$  will be used to quantify the magnitude of disturbance undergone by the soil.

	OCR=1			OCR=2			OCR=4			OCR=8		
UNDISTURBED	1			-			3			-		
DISTURBED	UU	REC	SH	UU	REC	SH	UU	REC	SH	UU	REC	SH
PSA	5	1	-	1	-	-	1	1	-	-	-	-
ISA+0.5	1	-	-	-	-	-	-	-	-	-	-	-
ISA+1	7	1	1	1	-	-	2	1	-	1	-	-
ISA+1.5	1	-	-	-	-	-	-	-	-	-	-	-
ISA+2	4	1	1	-	-	1	1	1	1	1	-	-
ISA+5	2	-	1	-	-	-	-	-	-	-	-	-
ISA>5	-	-	-	-	-	-	-	1	-	-	-	-
SPECIAL	-	-	-	-	-	-	1	-	-	-	-	-
SUBTOTAL	20	3	3	2		1	5	4	1	2		
TOTAL	27			3			13			2		

Table 4.1: Summary of Testing Program

TEST	OCR	TEST TYPE	DIST. TYPE	TEST	OCR	TEST TYPE	DIST. TYPE
115	1.00	UNDISTURBED	-	182	1.00	W	ISA+5
117	1.00	W	PSA	183	1.00	W	ISA+0.5
118	1.00	W	ISA+1	186	1.00	W	ISA+1
119	1.00	W	PSA	187	1.00	W	ISA+1
120	1.00	W	PSA	196	4.13	W	ISA+8
121	1.00	W	ISA+1	199	4.12	W	ISA+1
122	1.00	W	ISA+2	200	1.00	FEC	ISA+2
123	1.00	W	ISA+1	208	1.00	W	ISA+1
124	4.30	W	ISA+1	210	4.58	UNDISTURBED	-
125	3.93	W	PSA	211	1.00	FEC	PSA
126	4	(INCOMPLETE)	-	213	1.00	FEC	ISA+1
127	4.44	W	ISA+2	219	2.02	(INCOMPLETE)	ISA+1
130	1.00	W	ISA+2	224	4.24	FEC	ISA+2
131	4.00	UNDISTURBED	-	231	4.11	FEC	ISA+1
134	1.00	SH	ISA +1	232	4.15	(INCOMPLETE)	ISA+5
140	4.40	SH	ISA+2	235	2.02	(INCOMPLETE)	ISA+2
142	1.00	SH	ISA+2	236	1.89	SH	ISA+2
145	4.40	(INCOMPLETE)	ISA+1	237	8.59	(INCOMPLETE)	ISA+1
164	1.00	W	ISA+1.5	238	4.00	FEC	PSA
168	1.00	W	ISA+2	239	4.00	FEC	ISA+5
171	1.00	W	PSA	241	2.03	W	ISA+1
172	1.00	W	ISA+2	242	8.78	W	ISA+1
175	1.00	W	PSA	243	7.76	W	ISA+2
177	1.00	W	ISA+1	244	1.98	W	PSA
179	1.00	W	ISA+5	260	1.00	SH	ISA+5
180	4.00	UNDISTURBED	-	-	-	-	-

Table 4.2: Test Classification

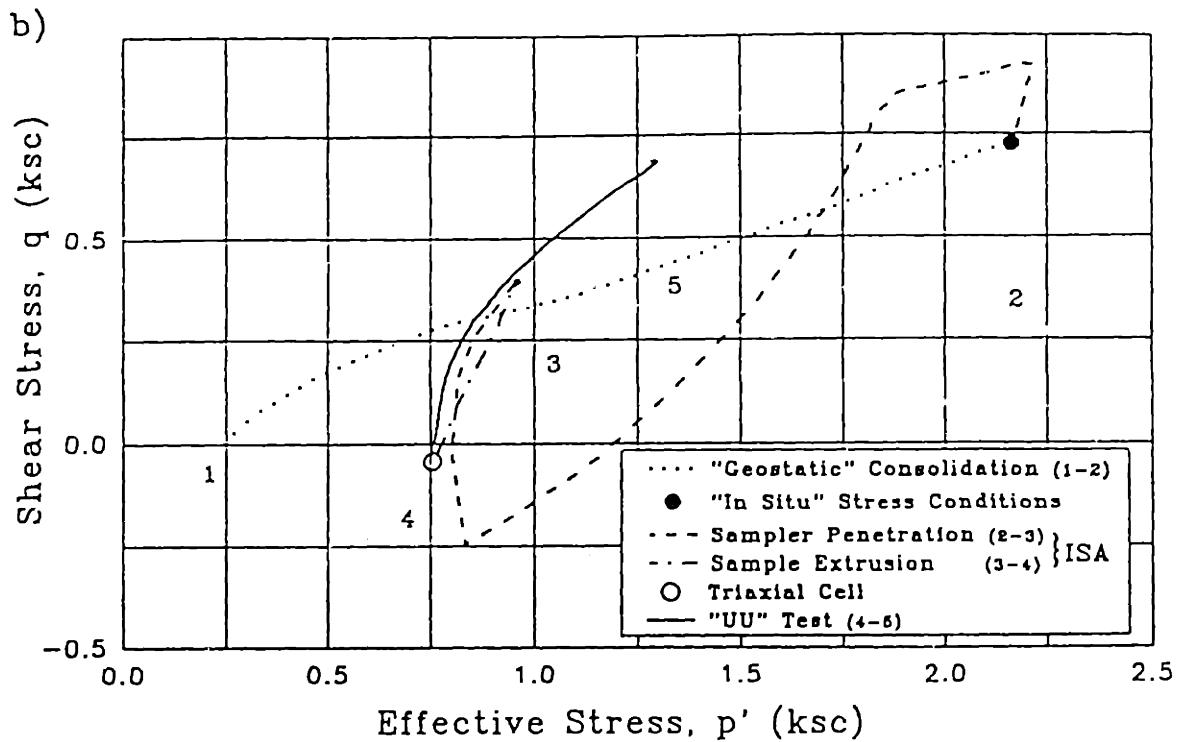
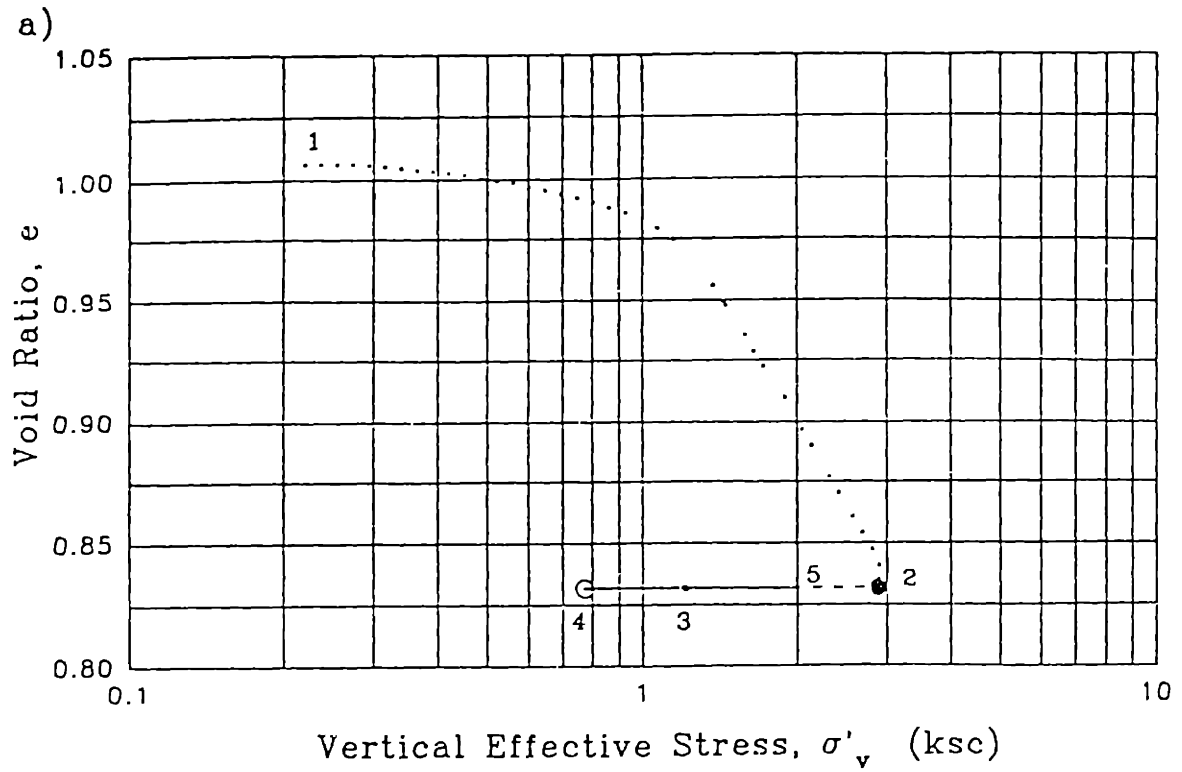


Figure 4.1: Phases of a  $ISA_{\pm 2}$  "UU" Test on NC RBBC:  
 (a)  $e - \log \sigma'_v$  Curve and (b) Stress Path

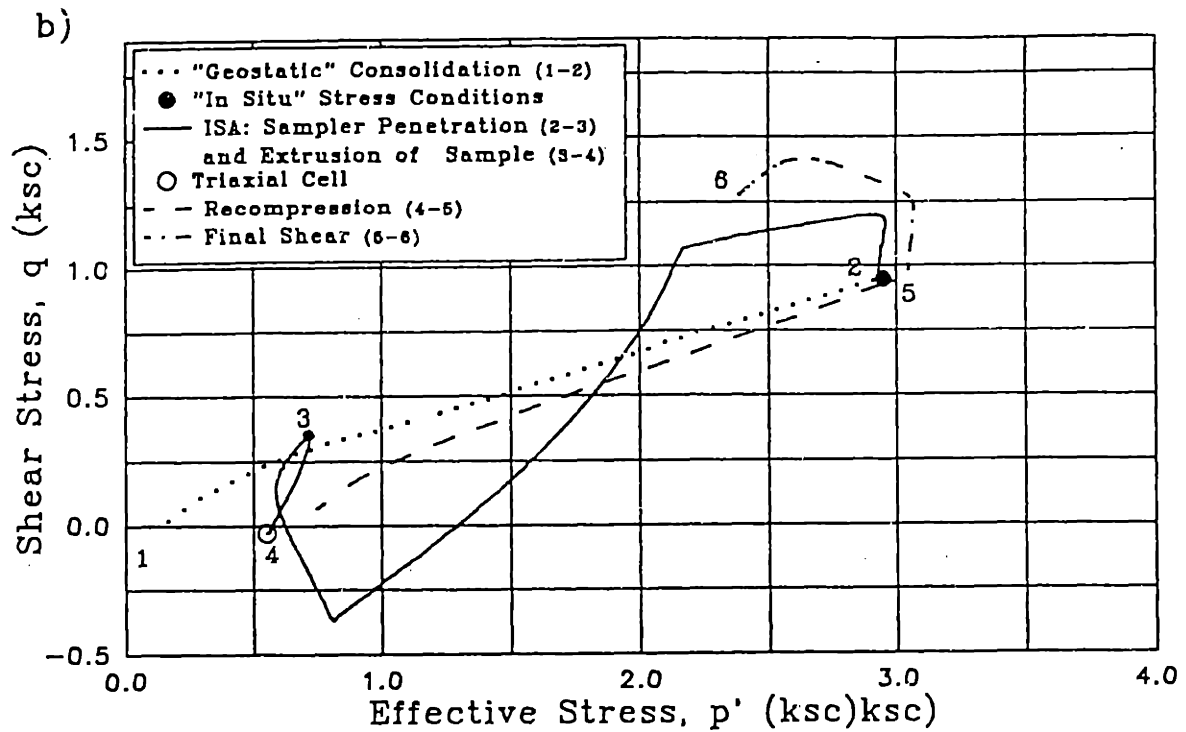
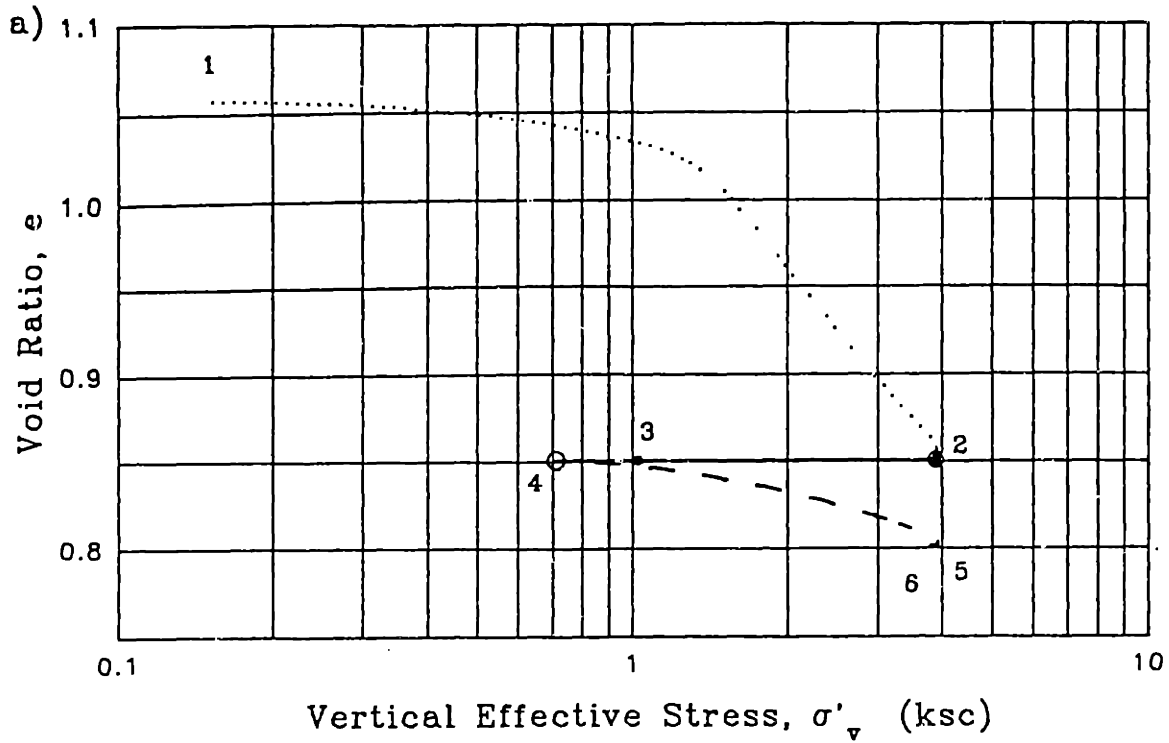


Figure 4.2: Phases of a  $ISA_{\pm 2}$  "Recompression" Test on NC RBBC: (a)  $e - \log \sigma'_v$  Curve and (b) Stress Path

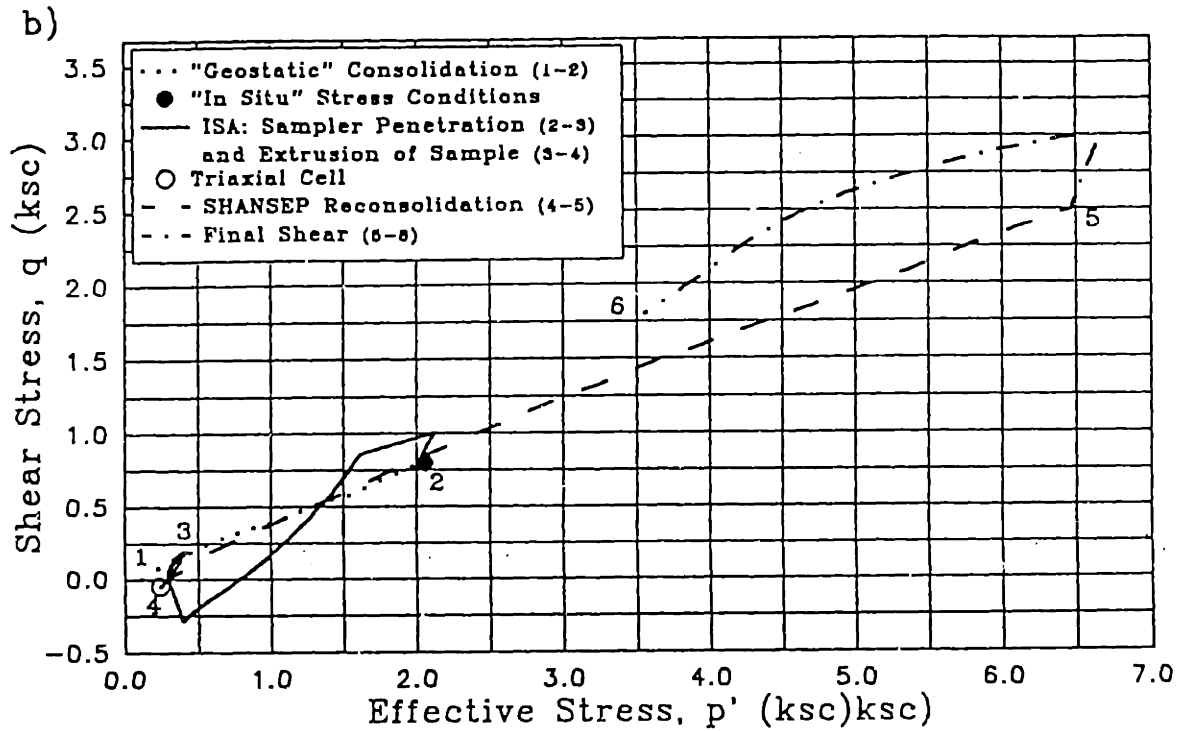
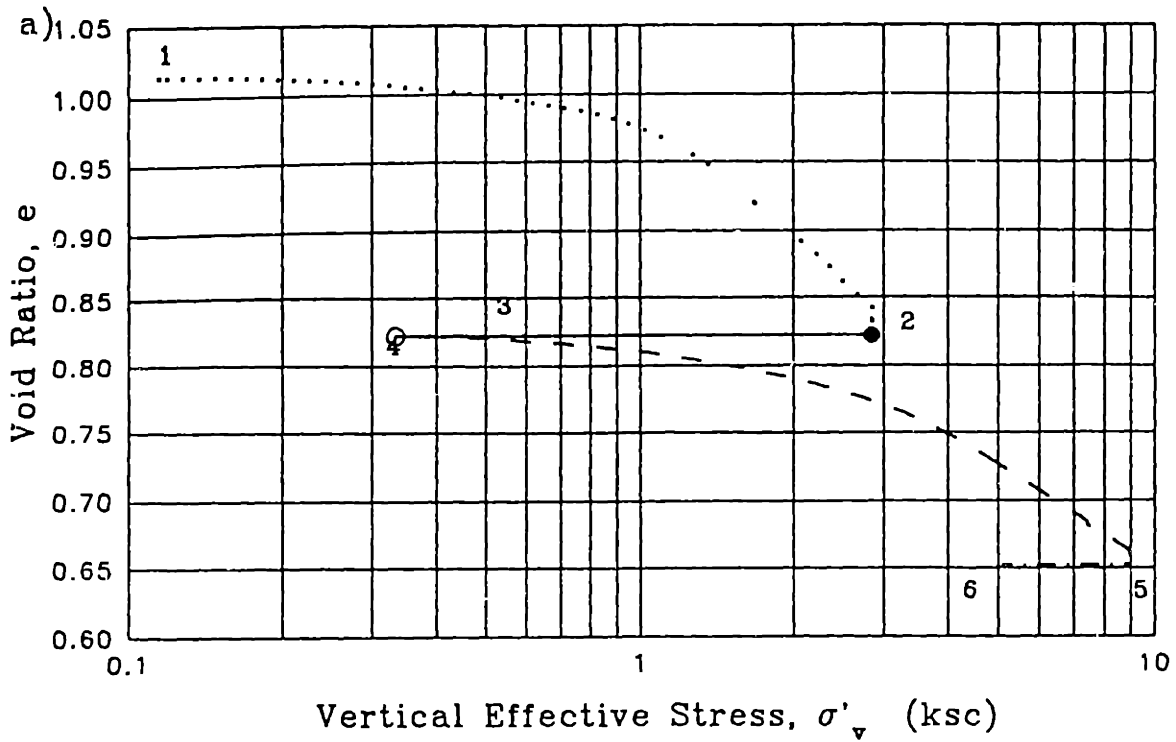


Figure 4.3: Phases of a ISA±2 "SHANSEP" Test on NC  
 (a)  $e - \log \sigma'_v$  Curve and (b) Stress Path

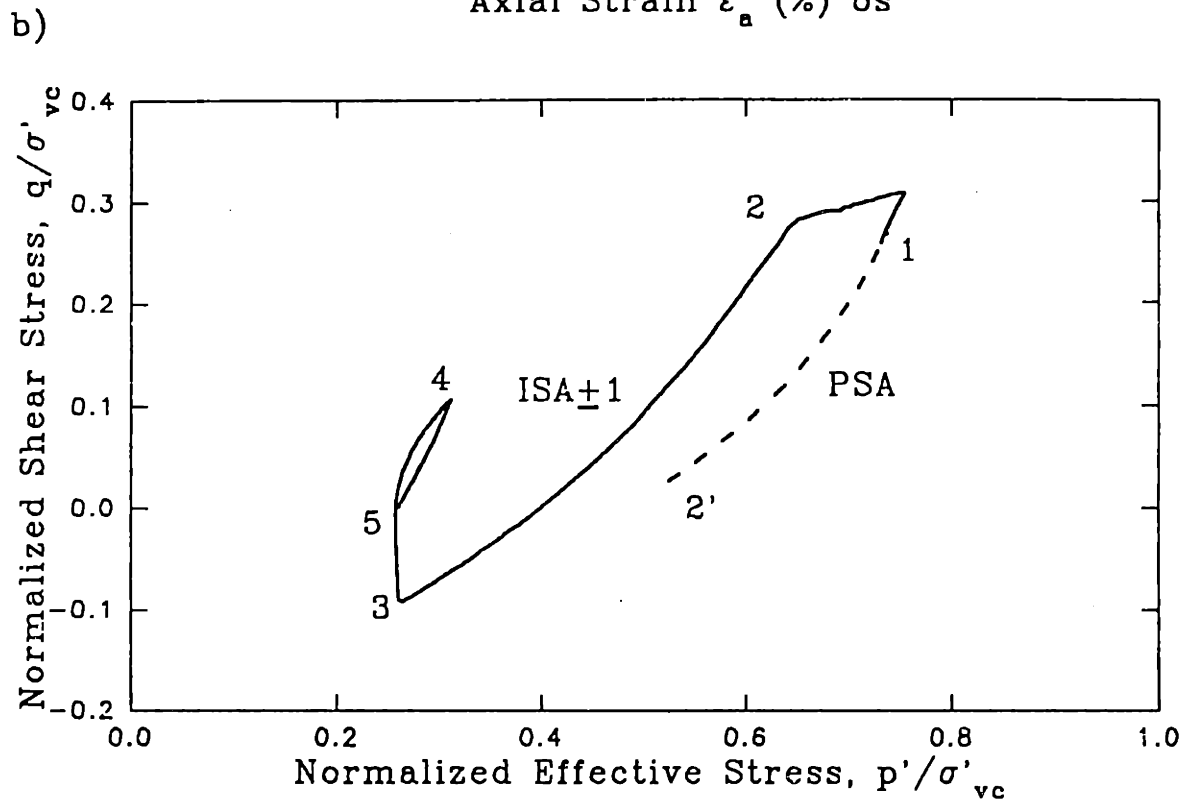
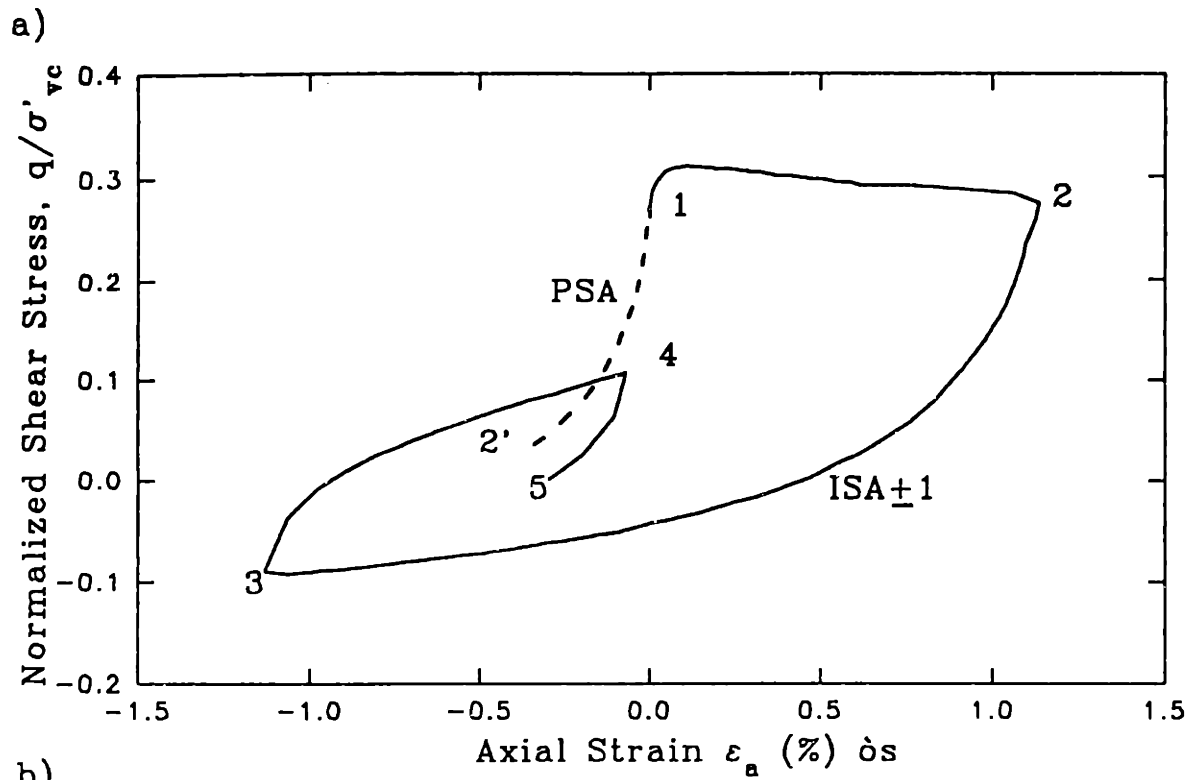


Figure 4.4: Examples of (a) Stress Strain Curves and (b) Stress Paths during PSA and ISA Disturbance of NC RBBC



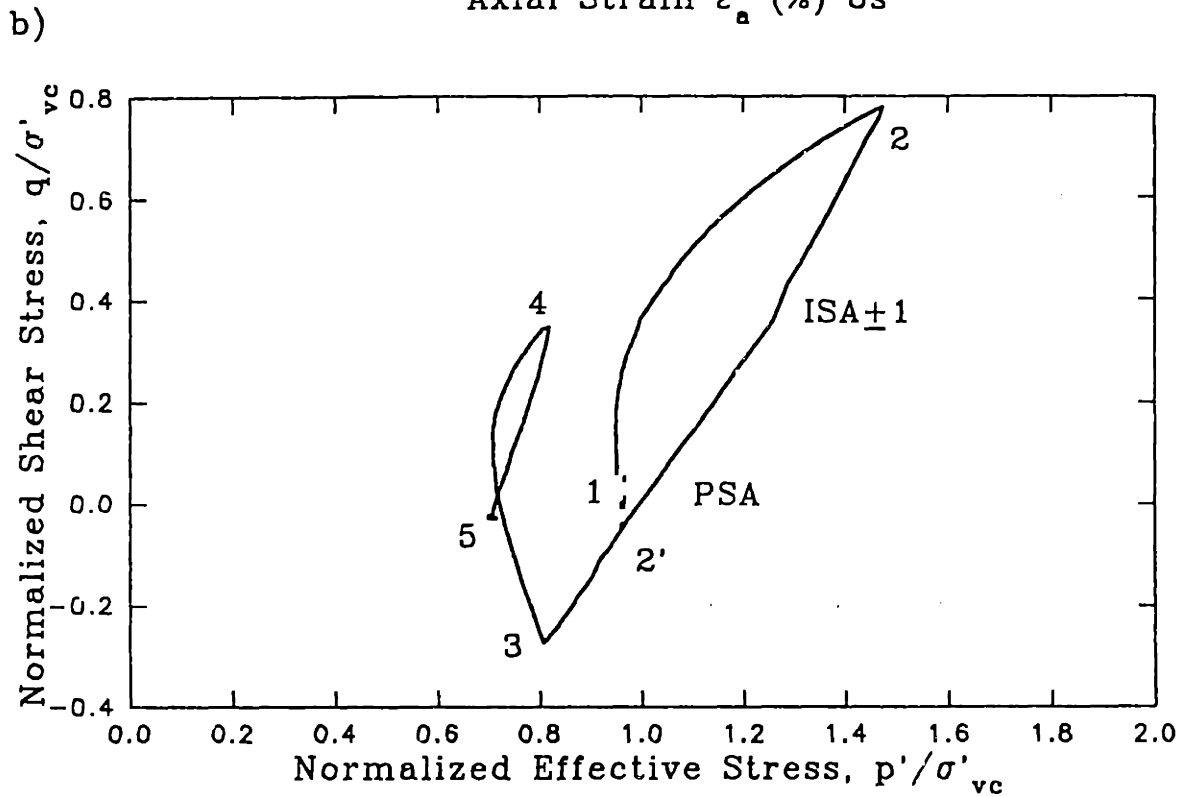
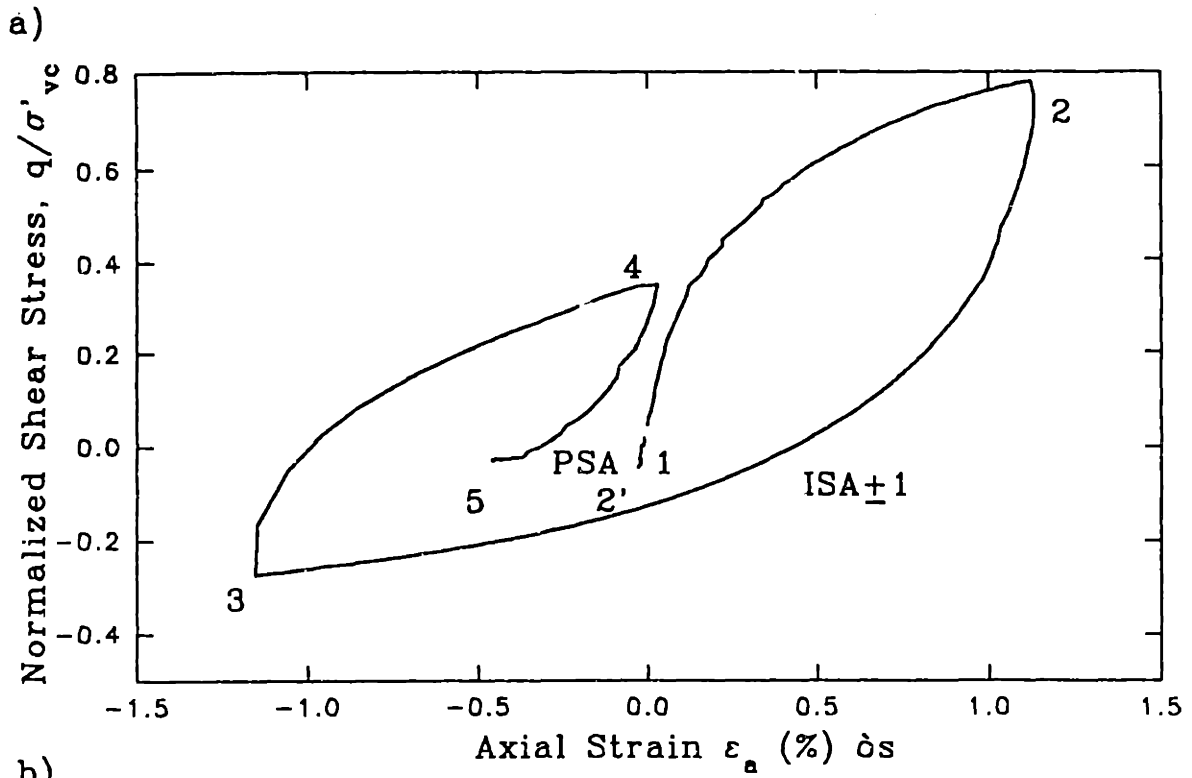


Figure 4.5: Examples of (a) Stress Strain Curves and (b) Stress Paths during PSA and ISA Disturbance of OCR4 RBBC



# Chapter 5 Intact Behavior of RBBC

## 5.1 Introduction

One of the first goals of this research project was to characterize the intact behavior of RBBC to use as a reference when investigating the effects of disturbance. This proved to be a challenge greater than expected as will become apparent in the following sections.

Previous research performed at MIT has shown that, within the range of stresses considered in this experimental program, RBBC exhibits normalized behavior. It is therefore assumed that the soil, when reconsolidated to 3-4ksc ( $3-4 \sigma'_p$ ), reaches the virgin compression line, and that the effects of the disturbance caused by the removal of the soil cake from the consolidometer, as well as by the trimming and setup operations, are thus erased. The behavior exhibited by the soil during the undrained shear after consolidation to 3-4 ksc can therefore be considered representative of the true intact shear behavior of RBBC.

Similar information on the compression behavior of the intact normally consolidated soil, such as the compression ratio CR and the lateral stress coefficient  $K_0$ , can be derived from the analysis of the last part of the consolidation phase. When necessary for comparison purposes, data on the compression behavior of RBBC was derived from CRS tests and the consolidation phase of DSS tests performed on RBBC (Ortega 1992, Cauble 1993).

Most of the triaxial test results presented in this chapter refer to tests run specifically for this research project. The results of a few triaxial tests, (all those characterized by numbers lower than 100) were part of a previous experimental program performed at MIT to investigate the effect of strain rate on the behavior of soft clays. Of these last tests only the ones run at standard strain rate are taken into account in the present analysis. All the tests used for this analysis were run making use of the automated triaxial equipment developed at MIT and described in Section 3.3. The data presented here refer to specimens obtained from 8 different batches of Resedimented Boston Blue Clay (BBC 216-220 for tests which are part of the "sample disturbance program" and BBC 210, 214, for tests which are part of the "strain rate effect" experimental program). All the soil comes from Series III RBBC.

Significant scatter in the behavior of RBBC was shown by the results of the tests. Quite surprisingly, even specimens obtained from the same batch of RBBC often exhibited quite different behavior during compression as well as during shear. Along with trying to define reference properties for intact RBBC, this chapter will also address the issue of the scatter of some of the engineering properties which proved to be larger than what was expected based on previous experience with RBBC.

The variation in the behavior appeared especially significant during the consolidation phase. The first part of the Section 5.2 which analyzes the consolidation results presents and discusses the variability in the compression behavior of RBBC. The second part of the section presents the best estimates for the engineering properties of interest, such as  $K_0$  and CR.

Section 5.3 discusses the most significant features of the undrained behavior of intact RBBC. Some of the tests used to define the intact shear behavior of RBBC are classified in Table 4.2 as "ISA Disturbed Tests". The reason for including them in this section is that some information on the intact behavior of RBBC can be derived from the first compression phase of the ISA disturbance cycle. In particular it is always possible to evaluate the stiffness at small strains. For clay with  $OCR=1$  and, whenever the peak strength is reached before the reversal of the straining it is also possible to measure the  $C_{upeak}$ ,  $\epsilon_{peak}$  and  $E_{u(50)}$ .

The results for all the tests are summarized in a separate report (Santagata and Germaine 1994) which presents phase relations calculations, summary of the consolidation data and of the undrained shear data and summary plots for every test performed.

## 5.2 Intact Compression Behavior

### 5.2.1 Typical Compression Behavior

According to the procedure described in Chapter 3, during resedimentation of BBC, the soil cake is always loaded in the consolidometer to a maximum stress of 1 ksc and maintained at this stress for 24 hours before being unloaded to  $OCR=4$ . In practice however it is possible that in some cases the stress applied is slightly different or that the maximum stress is left on for a longer period of time. Therefore

specimens obtained from different batches may have a slightly different preconsolidation pressure. It has also been observed that some batches have exhibited index properties different from the ones usually found for RBBC and this may have an impact on the compressibility characteristics of the soil. Figures 5.1a-e present examples of compression curves during one dimensional consolidation from tests on Batches 216-220. It can be seen that, except for Batch 219 for which the variability of the compression behavior is limited, all batches show some scatter in the compression behavior.

Some of the curves appear more rounded but in most cases they exhibit a clear break which allows determination, with some confidence, of the preconsolidation pressure  $\sigma'_p$ . Even though the maximum stress to which the soil has been subjected is constant for specimens obtained from the same batch, the values of the preconsolidation pressure determined for each test using the Strain Energy method (Becker et al. 1987) show some scatter. The mean values of  $\sigma'_p$  for the  $K_0$  consolidated tests performed on clay from five batches (216-220) are the following:

Batch 216:  $\sigma'_p = 1.11 \pm 0.08SD$  ksc (n=7)

Batch 217:  $\sigma'_p = 1.19 \pm 0.10SD$  ksc (n=7)

Batch 218:  $\sigma'_p = 1.27 \pm 0.08SD$  ksc (n=4)

Batch 219:  $\sigma'_p = 1.27 \pm 0.09SD$  ksc (n=11)

Batch 220:  $\sigma'_p = 1.16 \pm 0.13SD$  ksc (n=9)

These values are consistent with those determined with the same method in the case of CRS tests and in the consolidation (at constant rate of strain) phase of DSS tests on specimens obtained from the same batches (Ortega 1992, and Cauble 1993). The values of preconsolidation pressure

are consistently higher than the  $\sigma'_{vm}=1$  ksc applied to the batches of RBBC in the consolidometer. The increase in preconsolidation pressure cannot be completely explained taking into account the secondary compression ("aging") during batch consolidation at  $\sigma'_{vm}$ . The increment of preconsolidation pressure for 24 hours of secondary is in fact estimated to be approximately 0.005 ksc. According to Cauble (1993), for batches 217, 218 and 219 it is suspected that the maximum load applied during consolidation was higher than 1 ksc.

### 5.2.2 Compression Ratio

The virgin compression ratio was determined for each test from the consolidation results. In most cases it was observed that CR reached a constant value when  $\sigma'_v = 2.5$  ksc was reached, and this value was assumed to be the "intact" value of the virgin compression ratio.

The mean values of CR for the tests performed on clay from batches 216, 217, 218, 219 and 220 are the following:

Batch 216:	CR = 0.180 ± 0.015SD	(n=6)	(PI=23.54%)
Batch 217:	CR = 0.168 ± 0.016SD	(n=5)	(PI=16.41%)
Batch 218:	CR = 0.164 ± 0.012SD	(n=6)	(PI=14.91%)
Batch 219:	CR = 0.165 ± 0.008SD	(n=11)	(PI=21.38%)
Batch 220:	CR = 0.143 ± 0.011SD	(n=8)	(PI=17.71%)

It must be noted that in deriving the statistics above the only tests considered are those in which  $K_0$  consolidation was performed.

Even though the results are fairly consistent for specimens obtained from the same batch, the variation of CR between some of the batches is

very large. The results for batches 217, 218 and 219 are very consistent, despite the fact that the Plasticity Index determined for BBC219 is much higher than that of the other two batches. A slightly higher value of CR for BBC219 would have been expected, as is seen for BBC216. The higher compression ratio measured in specimens from this batch is in fact explained by the significantly higher Plasticity Index.

The CR measured for BBC220 is consistently lower than that measured for any of the other batches. In this case the difference cannot be explained by a variation in the index properties because the limits measured on clay from BBC 220 fall within the range of values measured for batches 217-219.

### 5.2.3 Lateral Stress Ratio $K_0$

The automated triaxial cells used for this research program measure the value of the coefficient of lateral stress  $K_0$  while performing one dimensional consolidation. Figure 5.2 shows the typical trend of  $K_0$  with vertical stress during consolidation displayed in all the  $K_0$  consolidated tests performed.  $K_0$  decreases during the initial loading within the overconsolidated region until approximately 1 ksc (maximum stress applied in the consolidometer), and then it increases slightly. Once the soil is consolidated into the virgin compression region  $K$  remains basically constant. The value of  $K_0$  in the virgin compression region is referred to as the normally consolidated value  $K_{0(NC)}$ . Once the specimen is consolidated to the desired maximum consolidation stress ( $\sigma'_{vm}$ ), this stress is maintained for 24 hours to allow for dissipation of the excess pore



pressures and one cycle of secondary consolidation. In this study,  $K_{0(NC)}$  was calculated as the average value of  $K$  measured during the 24 hour hold stress phase.

Quite surprisingly a significant scatter in the measured values of  $K_{0(NC)}$  was observed. The range of variation of  $K_0$  is very large even for specimens obtained from the same batch, as can be seen in Figure 5.3. Up to this moment, the reasons for this scatter are not well understood even though many possibilities have been considered. The variation of the material index properties does not seem to affect  $K_0$ . The water content and the void ratio values determined for the different specimens are fairly consistent and their limited variation cannot justify the large scatter of  $K_0$ . Consideration was also given to the possibility that  $K_0$  is related to the degree of disturbance undergone by the specimen during trimming and setup. Unfortunately there seems to be no relationship between  $K_0$  and any of the parameters quantifying disturbance such as the strain at overburden (approximately 1ksc in this case). There also appears to be no influence of the equipment used (four separate triaxial cells were used for this experimental program). Finally it wasn't possible to define any link between the slope of the compression curve and the value of  $K_0$ .

Figure 5.4 shows stress paths during consolidation for a few of the tests performed, from which it is possible to observe that due to the variation of  $K_0$  the stress state of the soil prior to shear varies considerably. When first observed, the large scatter in  $K_0$  represented a major concern primarily due to the fact that the preshear value of  $K_0$  dramatically affects the value of the undrained strength and it is therefore impossible to define a unique value of  $C_u/\sigma'_{vc}$  to use as reference when investigating the

effects of disturbance. The effect of  $K_0$  on the undrained strength will be discussed in detail in Section 5.3.2. Consequently for a few of the tests, the specimen was consolidated to the maximum stress by stress path consolidation. In this case a value of  $K$  equal to 0.48 was chosen and the soil was consolidated by first increasing the vertical stress only (stress path at  $45^\circ$ ) until the  $K=0.48$  line was reached and then by following the  $K=0.48$  line until the desired stress. Figure 5.5a plots  $K$  versus the vertical effective stress for one of these tests (TX172). The figure also presents the curve relative to a  $K_0$  consolidated specimen (TX118) with  $K_{0(NC)}$  approximately equal to 0.48. The curve for TX118 shows the trend described above with  $K_0$  decreasing to a minimum value at approximately 0.9 ksc, then increasing until the vertical stress reaches 1.5 ksc after which  $K$  does not change significantly. For TX172, instead,  $K$  decreases very rapidly and then remains basically constant after  $\sigma'_v$  reaches about 0.4 ksc. The compression curves for the same two tests are plotted in the following figure. Both the axial and volumetric strain are plotted versus the vertical effective stress for both tests. While for TX118 the two lines ( $\epsilon_a$  vs.  $\sigma'_v$  and  $\epsilon_v$  vs.  $\sigma'_v$ ) superimpose perfectly, the same quite obviously is not true for TX172. Regardless of the fact that the stress paths for the two tests are (see Figure 5.5c) extremely similar, the effect of stress path consolidation on the compression behavior is much larger than anticipated. The compression curve shifts towards the lower effective stresses and its slope decreases significantly. All four specimens consolidated at constant  $K$  to the maximum stress were obtained from batch 219. The values of the compression ratio measured in all the four stress path consolidated tests

are all much lower ( $0.142 \pm 0.004$ ) than the average CR for BBC219 indicated above as  $0.165 \pm 0.008$ .

Stress path consolidation was limited to just four tests due to its consequences just described on the compression behavior of the soil. Further, the most significant problem associated with the variation of  $K_0$  was resolved, as is described in Section 5.3.2.

### 5.3 Intact Shear Behavior

#### 5.3.1 General Undrained Behavior

Figures 5.6, 5.7 and 5.8 illustrate the typical undrained triaxial compression behavior of RBBC at nominal OCRs of 1, 2, 4, and 8. Figure 5.6 presents the effective stress paths normalized to the maximum vertical consolidation stress ( $\sigma'_{vm}$ ), Figure 5.7 presents the stress strain curves ( $q/\sigma'_{vm}$  vs.  $\epsilon_a$ ) and Figures 5.8a and 5.8b plot respectively the shear induced and the excess pore pressures generated during shear ( $u_s/\sigma'_{vc}$  vs.  $\epsilon_a$ ).

One can observe the following:

- a) the effective stress paths approach a common failure envelope at large strains;
- b) increasing OCR causes;
  - a decrease in the peak value of the strength normalized to the maximum vertical stress;
  - less strain softening;
  - an increase in the axial strain at failure;

- a decrease of the shear induced pore pressure at large strains.

### 5.3.2 Undrained Strength Ratio

Figure 5.9 and 5.10 present stress paths and strain curves relative to the undrained shear of several specimens of NC RBBC. It is evident that the value of the undrained strength varies over a large range. While this initially appeared to be a serious impediment to the definition of a reference NC undrained strength, it was also observed that the variation in  $C_u/\sigma'_{vc}$  was related to the scatter in the value of the lateral stress ratio. Consequently, the relationship between  $K_0$  and the NC undrained strength was investigated.

As mentioned above, when performing  $K_0$  consolidation it was observed that the preshear value of  $K_0$  for the NC specimens showed significant scatter the reasons for which are, at this point, still not understood. Most importantly, it appears that an increase of the preshear lateral stress ratio  $K_{0(NC)}$  is associated with a decrease of the undrained strength of NC RBBC as is illustrated in Figure 5.11. The results are quite consistent and a linear regression through the data yields the following equation:

$$S_c = 0.56 - 0.49 \cdot K_{0(NC)} \quad r^2 = 0.80$$

Apart from the tests consolidated at constant  $K=0.48$  described above, a few other tests were run using stress path consolidation for values of  $K$  outside the range of the values measured in the NC tests, to verify that the same relationship between  $K$  and  $C_u/\sigma'_{vc}$  was valid. This was indeed the case, and thus the  $K$  values for these tests should not be considered part of the

scatter. It is important to point out that the relationship presented should not be extrapolated beyond the range here investigated.

To establish a reference undisturbed strength for NC RBBC the values of the undrained strength were corrected to account for the difference in  $K_0$  by:

- 1) choosing a reference value of  $K_0$  equal to 0.48;
- 2) assuming that the expression  $S_c = 0.56 - 0.49 \cdot K_{0(NC)}$  accurately describes the relationship between  $K_0$  and the NC strength;
- 3) and considering the distance along the vertical axis from the regression line as a measure of the scatter around the average.

Figure 5.12 shows the procedure to correct the undrained strength data: each data point is moved parallel to the regression line, to a value of  $K_0$  equal to 0.48.

The variation  $K_{0(NC)}$  was shown to have no influence on the strength of the overconsolidated clay. Figure 5.13 plots in full symbols the undrained strength normalized by the consolidation stress versus the OCR.

For every test based on the value of  $K_0$  prior to swelling, a value of  $S_c$  was determined from the equation presented above. The undrained strength ratio  $c_u / \sigma'_{vc}$  was then normalized by this number and is plotted in Figure 5.13 in hollow symbols. The figure also presents the regression lines through the two sets of points. It is apparent that the normalization does not reduce the scatter, i.e. the  $r^2$ , of the regression and it is therefore concluded that  $K_{0(NC)}$  does not influence the value of the undrained strength of overconsolidated RBBC.

Figure 5.14 presents the values of  $C_u/\sigma'_{vc}$ , the undrained strength normalized to the consolidation stress, plotted versus the OCR. The parameters necessary for the SHANSEP equation can be determined from the regression through these points. The SHANSEP equation relates the soil's normalized undrained strength to its overconsolidation ratio in the following manner:

$$c_u/\sigma'_{vc} = S (\text{OCR})^m$$

where:  $m$  is the slope of the line plotted in Figure 5.14 and  $S$ , the normally consolidated undrained strength ratio, is the intercept on the vertical axis. The values of  $c_u/\sigma'_{vc}$  for NC RBBC were corrected as described above to account for the difference in  $K_0$ . The regression yielded the following parameters:  $S=0.33$  and  $m=0.71$  with  $r^2=0.99$ , in perfect agreement with previous data on RBBC (Sheahan 1991).

### 5.3.3 Effective Stress Failure Envelope

The normalized shear stress versus the normalized effective stress at maximum obliquity is presented in Figure 5.15.

A linear regression through these data is used to define the  $q$ - $p'$  effective stress failure envelope at maximum obliquity:

$$q/\sigma'_{vm} = a'/\sigma'_{vm} + (p'/\sigma'_{vm}) \cdot \sin\phi'$$

The corresponding Mohr-Coulomb relationship commonly used to describe the stresses on the failure plane ( $\tau_f$  and  $\phi'_f$ ) is:

$$\tau_f/\sigma'_{vm} = c'/\sigma'_{vm} + (\sigma'_f/\sigma'_{vm}) \cdot \tan\phi'$$

The linear regression through the data yields the following:

$$q/\sigma'_{vm} = 0.009 + (p'/\sigma'_{vm}) \cdot \sin 31.06^\circ \quad \text{with } r^2=0.97$$

### 5.3.4 Strain at Peak

The results of this testing program indicate that for Intact NC RBBC the values of the strain at peak cover a relatively wide range, between 0.09% and 0.26%. Most likely much of the scatter ( $\pm 0.03\%$ ) is associated with the strain measurement. There may also be an effect of the lateral stress ratio: as is shown in Figure 5.16 which plots  $\epsilon_{\text{peak}}$  versus the pre-shear lateral stress ratio  $K_0$ . The results are quite scattered but there appears to be a trend of increasing  $\epsilon_{\text{peak}}$  with increasing  $K_0$ . Although the trend is not too clear for lower values of  $K_0$ , it can be observed that the higher values of the strain at peak are all associated with the unusually high values (larger than 0.5) of  $K_0$ .

Figure 5.17 plots on a semi-logarithmic plot the strain at failure versus the OCR. The data indicates that the strain at failure increases with increasing OCR.

### 5.3.5 Stiffness

Figure 5.18 presents the data of  $E_{u(50)}/\sigma'_{vc}$ , the undrained modulus at 50% of the stress increment to reach failure ( $0.5 \Delta q_f$ ) normalized by the consolidation stress, plotted versus the overconsolidation ratio. The results are extremely scattered and do not seem to indicate any trend of this parameter with overconsolidation ratio.

Figure 5.19 plots the undrained modulus normalized by the consolidation stress versus the axial strain (0.01% to 1%) for NC and OC RBBC. The data for NC RBBC is extremely consistent at all strain levels. In

most of the OC tests unreliable measurements of the modulus were obtained under  $\epsilon_a=0.05\%$ . From the data presented it can be deduced that the stiffness at the lower strains decreases with increasing OCR. Around  $\epsilon_a=0.1\%$  the NC soil reaches the peak strength and then strain softens. Consequently the stiffness of the soil becomes lower than that of the OC RBBC. The data show a consistent trend and suggests that inside the yield surface the normalized modulus does not change with position.



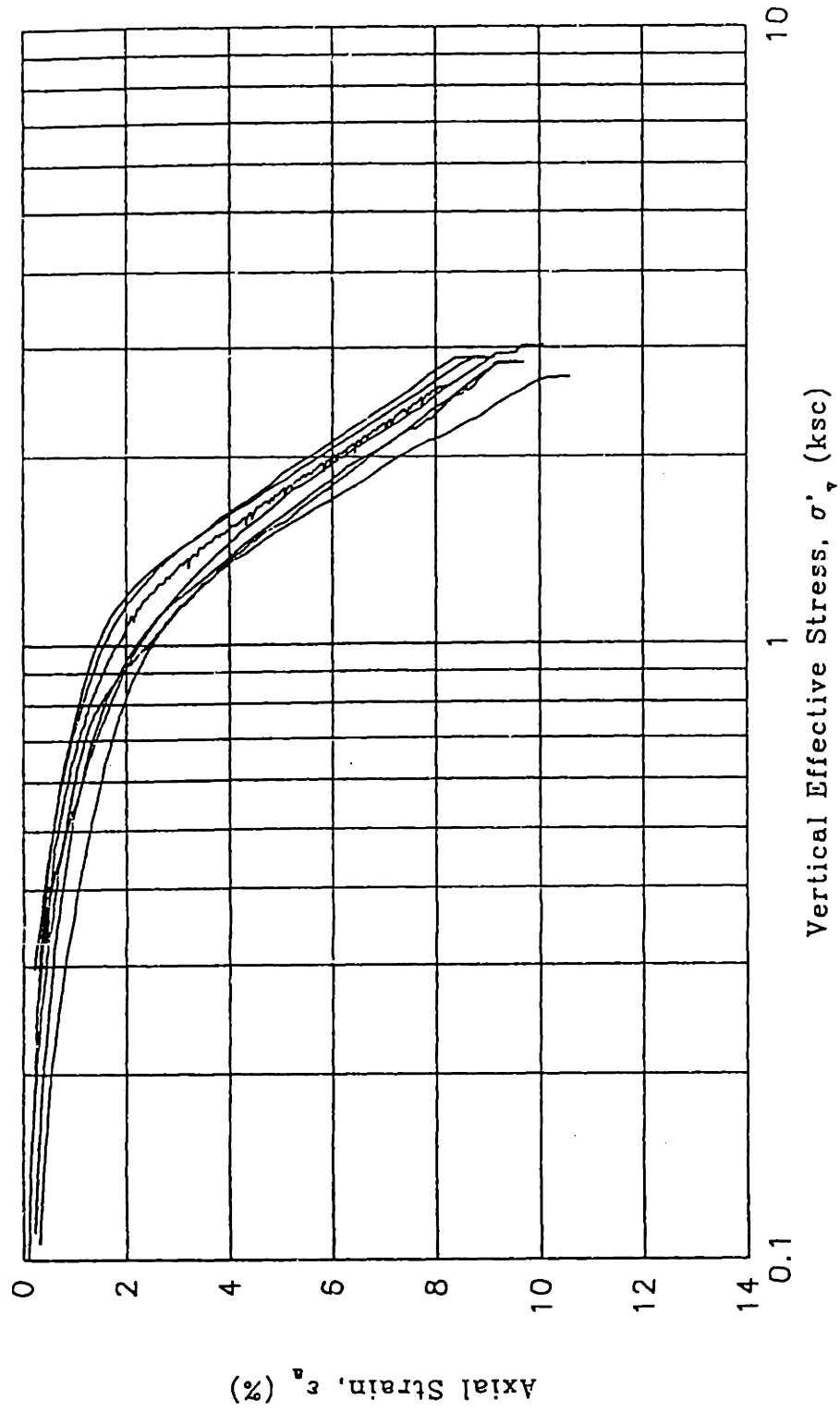


Figure 5.1a: Selection of Compression Curves from Tests on BBC216: TX115, 117, 118, 119, 120, 121, 123

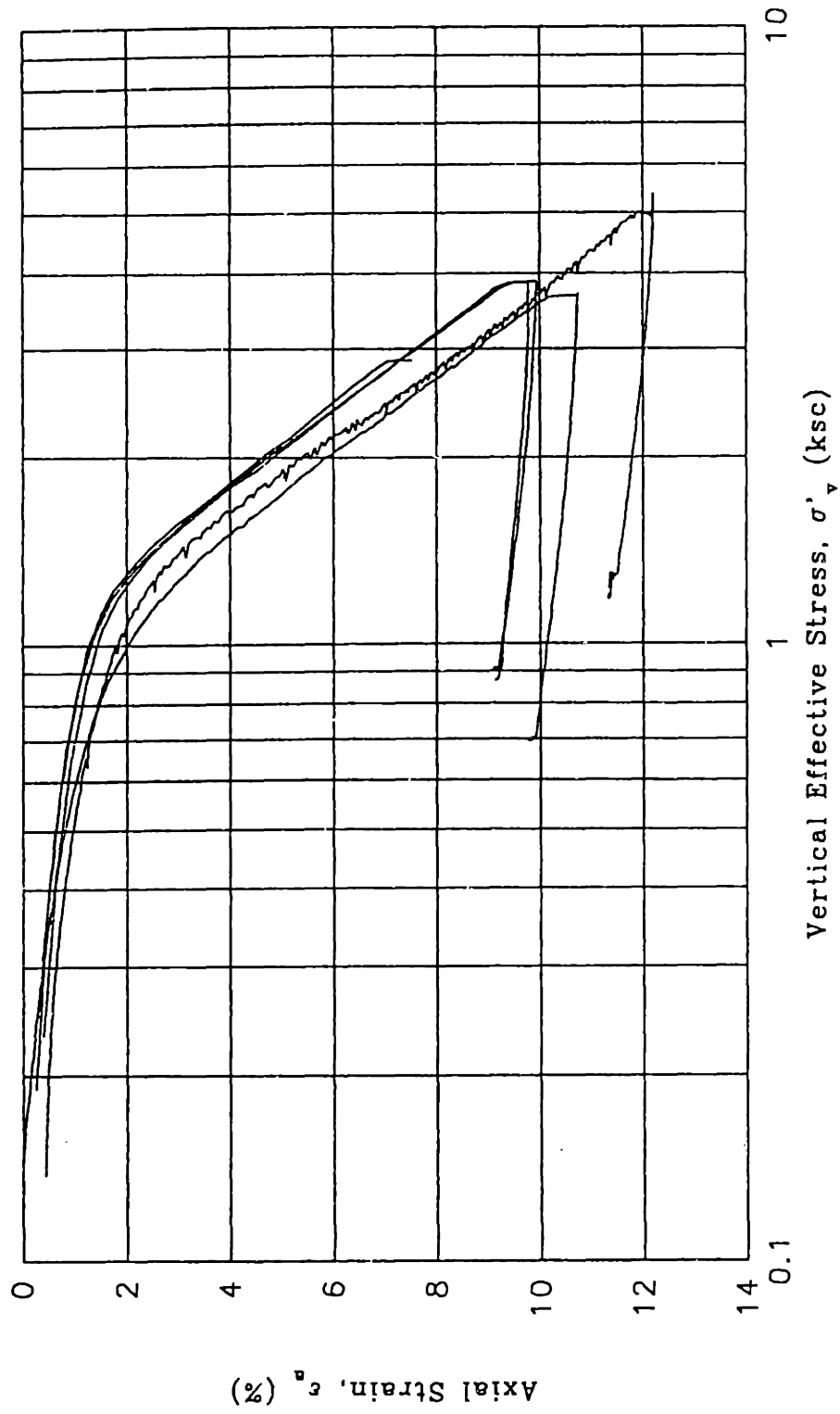


Figure 5.1b: Selection of Compression Curves from Tests on BBC217: TX124, 125, 127, 130, 131

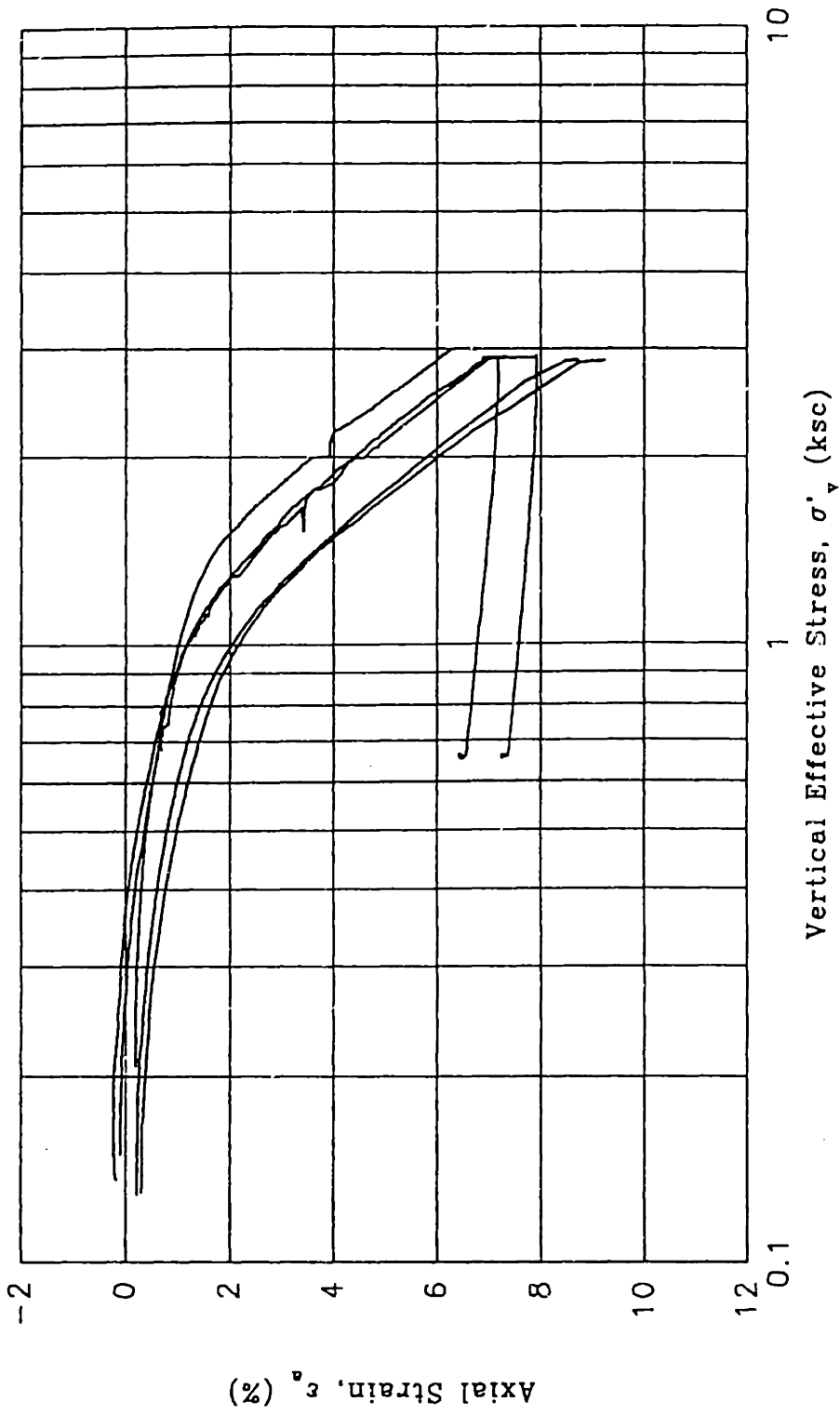
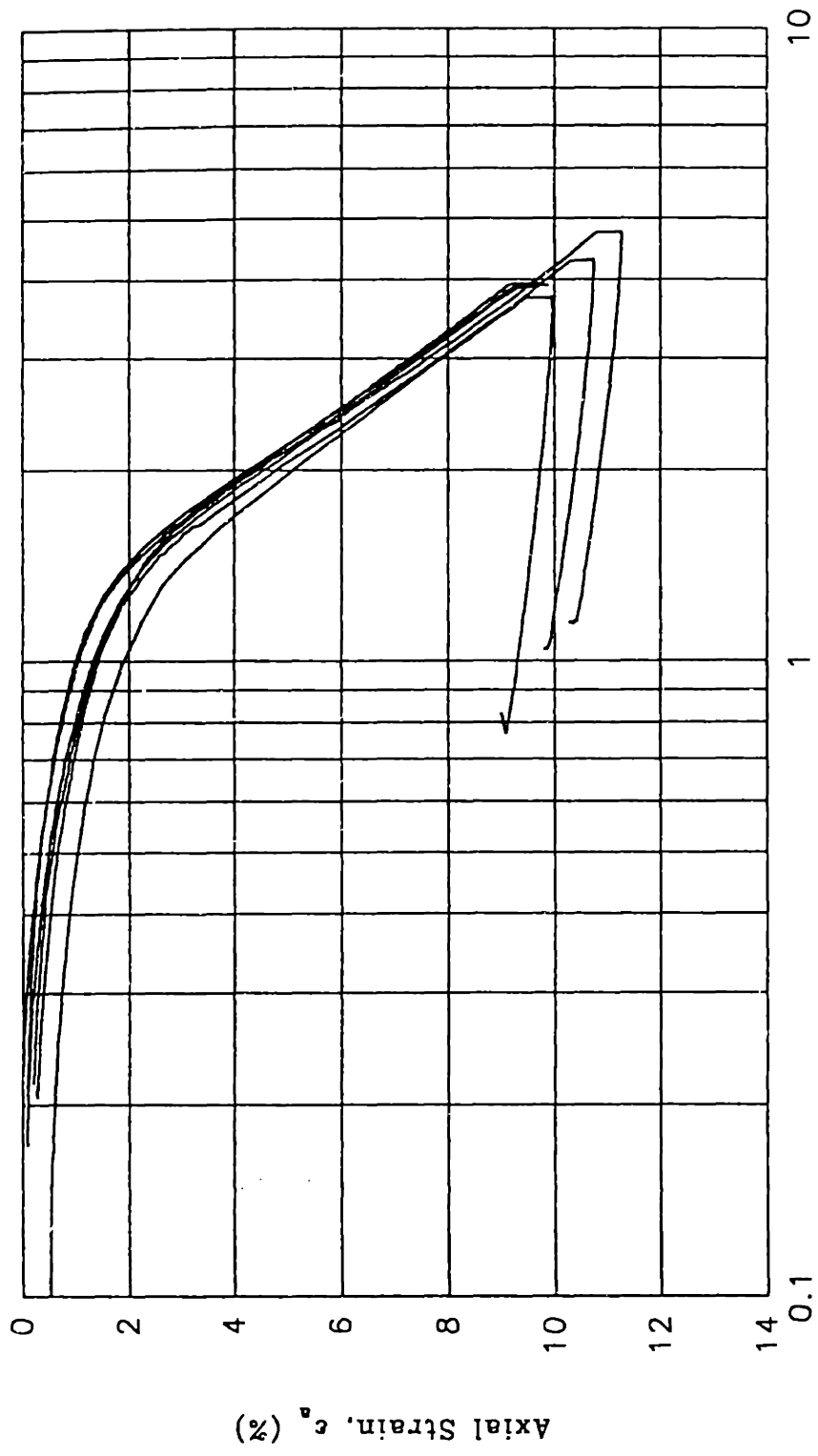


Figure 5.1c: Selection of Compression Curves from Tests on BBC218: TX134, 140, 142, 145, 177



Vertical Effective Stress,  $\sigma'_v$  (ksc)

Figure 5.1d: Selection of Compression Curves from Tests on BBC219: TX182, 186, 196, 199, 208, 210

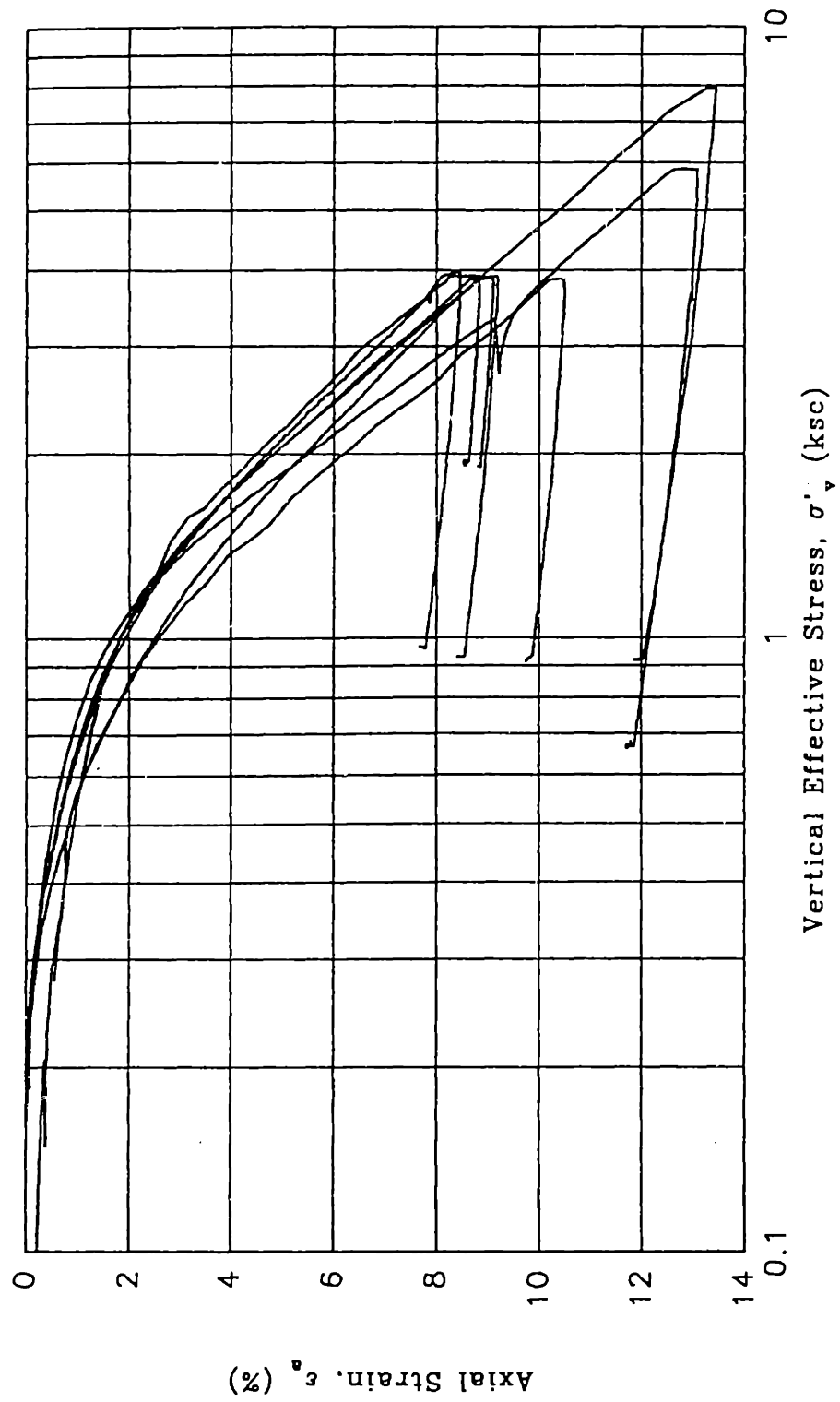


Figure 5.1e: Selection of Compression Curves from Tests on BBC220: TX219, 224, 231, 235, 237, 238, 242

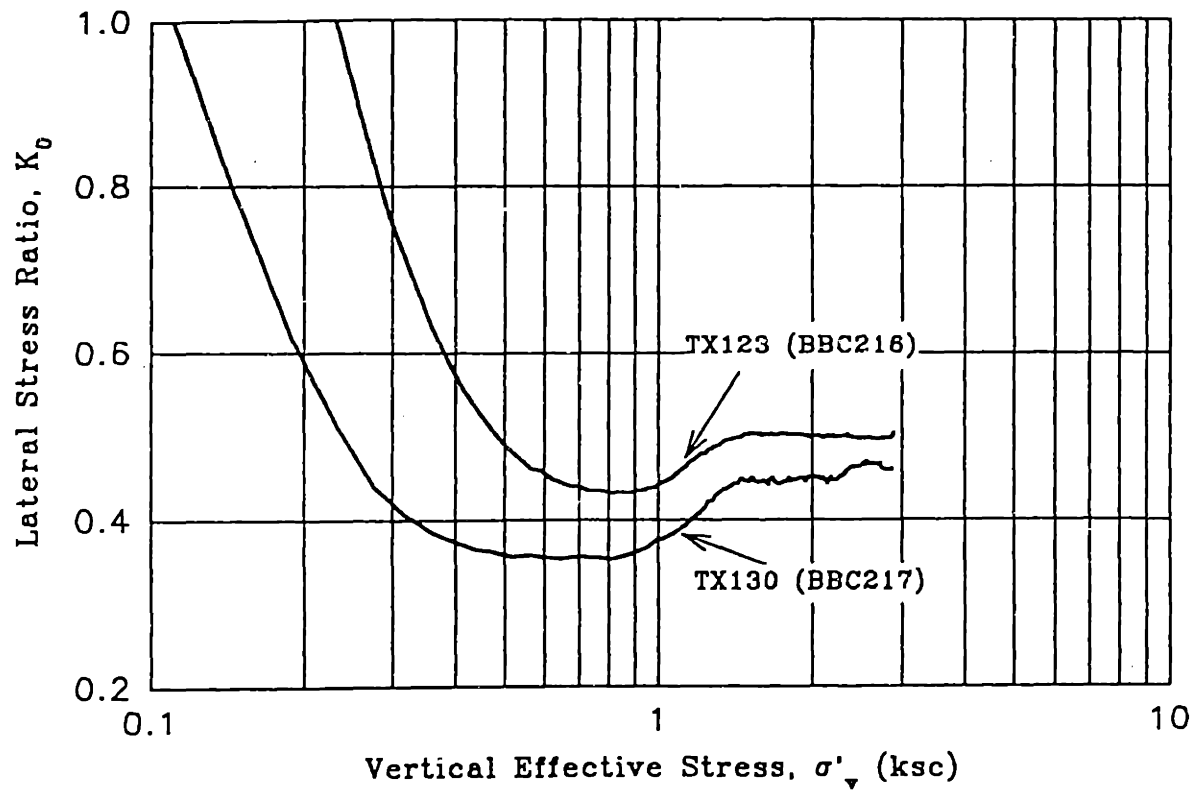


Figure 5.2: Lateral Stress Ratio vs. Vertical Effective Stress During  $K_0$ - Consolidation of RBBC

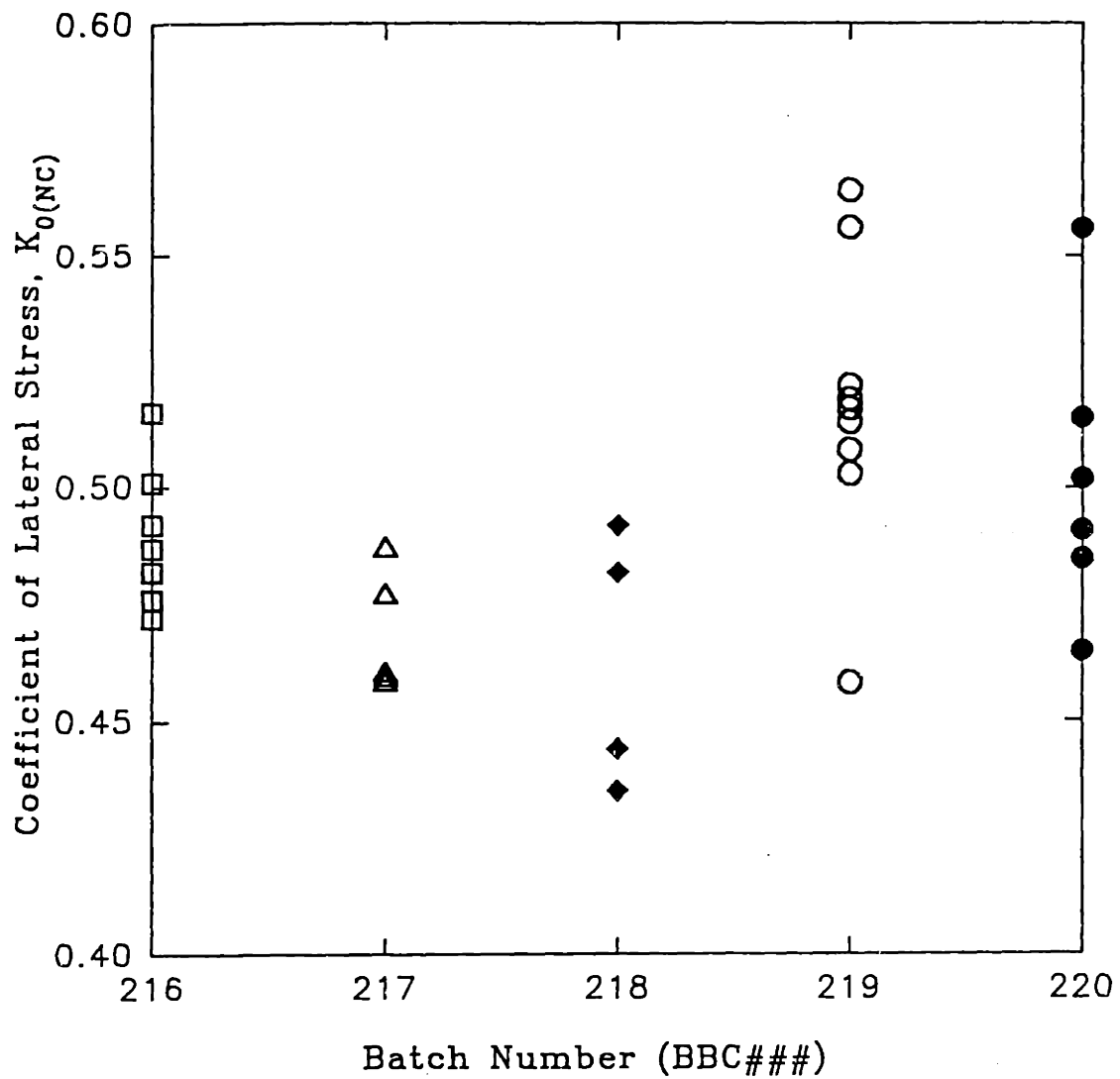


Figure 5.3: Scatter in the Measured Values of  $K_{0(NC)}$  for Batches 216-220

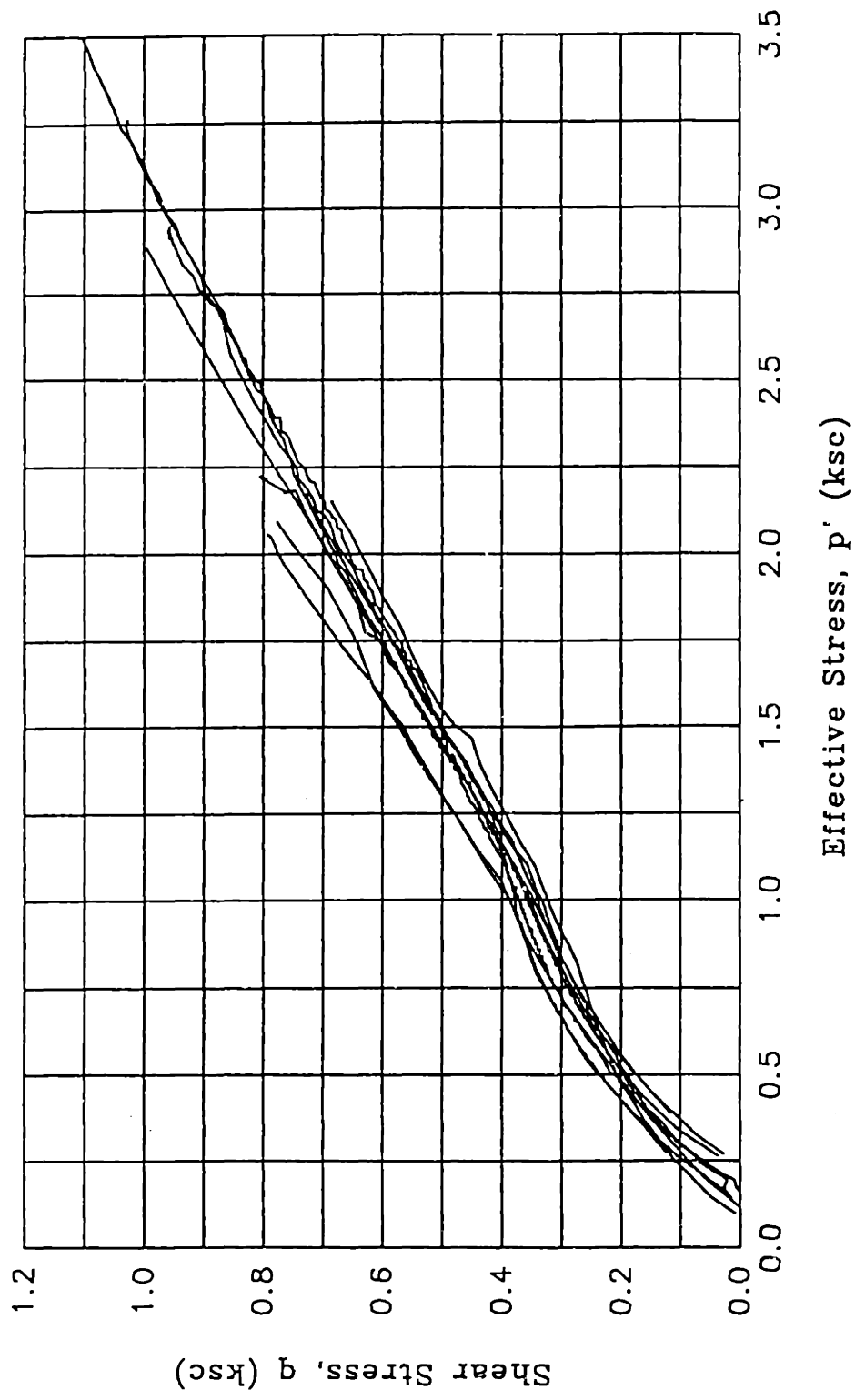


Figure 5.4: Selection of Stress Paths for One-Dimensional Consolidation of RBBC (Batches 216-219)



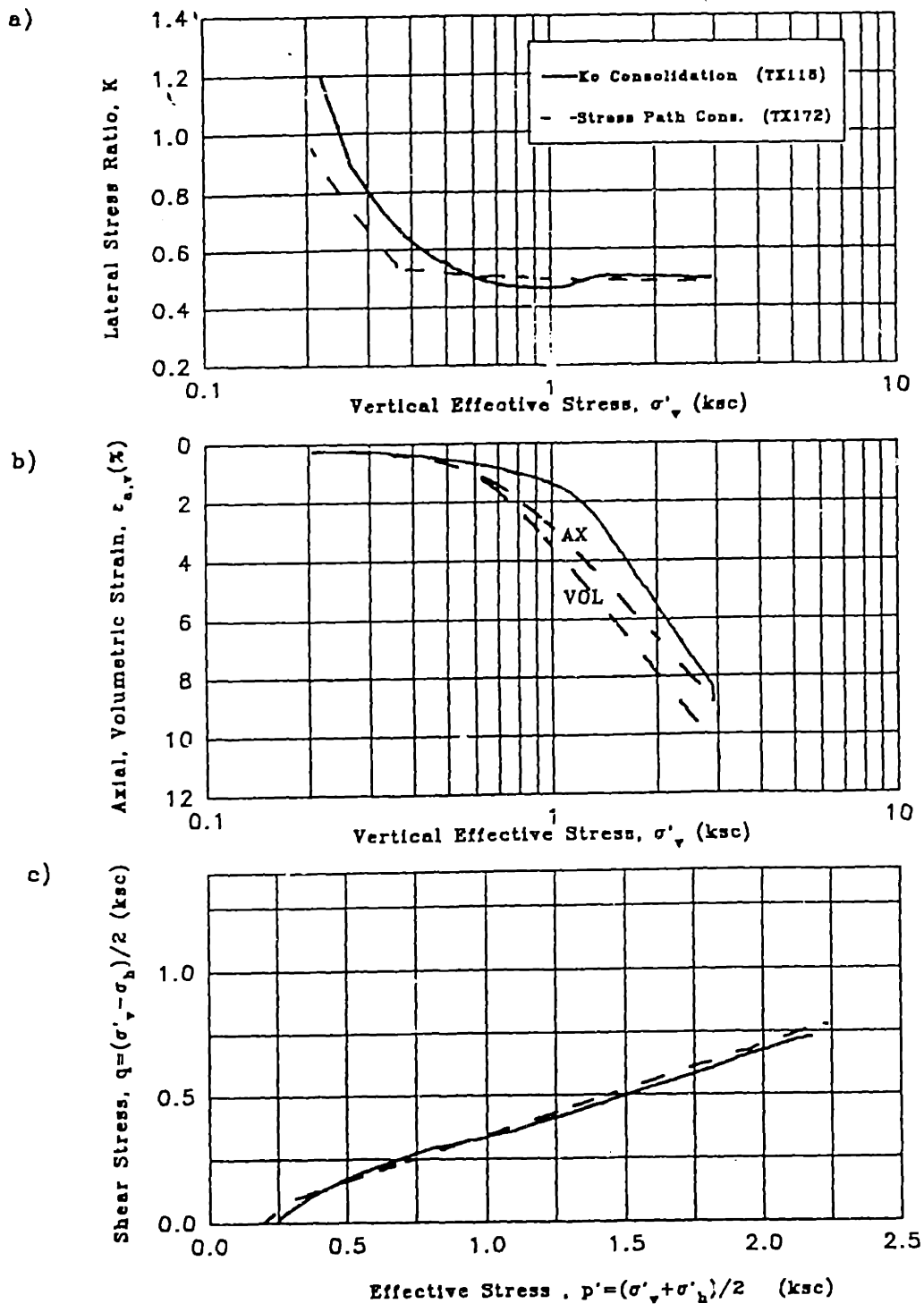


Figure 5.5: Comparison of  $K_0$  (TX118) and Stress Path Consolidation (TX172): a)  $K$  vs.  $\sigma'_v$  Curves; b) Compression Curves; c) Stress Paths

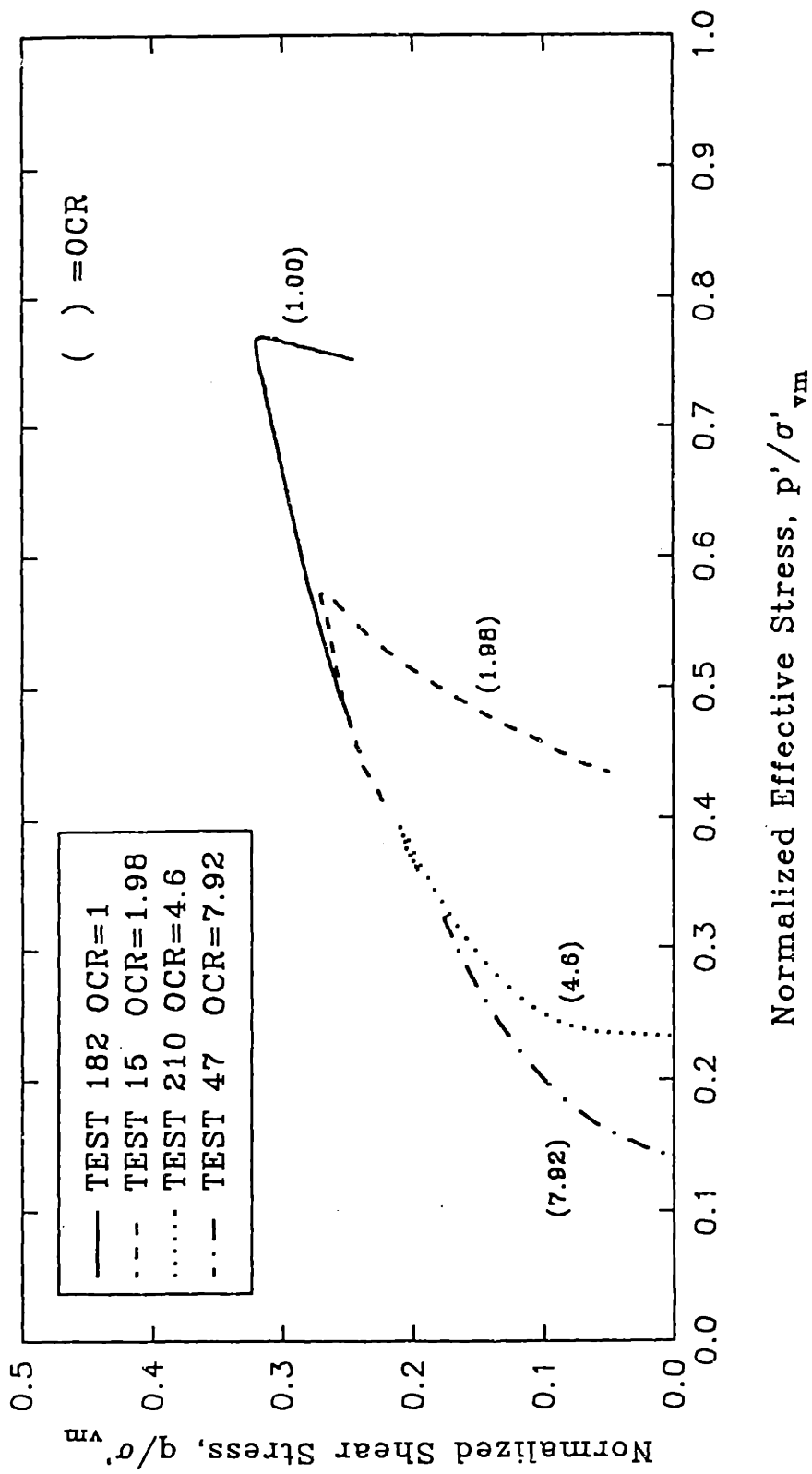


Figure 5.6: Intact Undrained Shear (TXC) Behavior of RBBC (OCR=1,2,4,8): Stress Paths

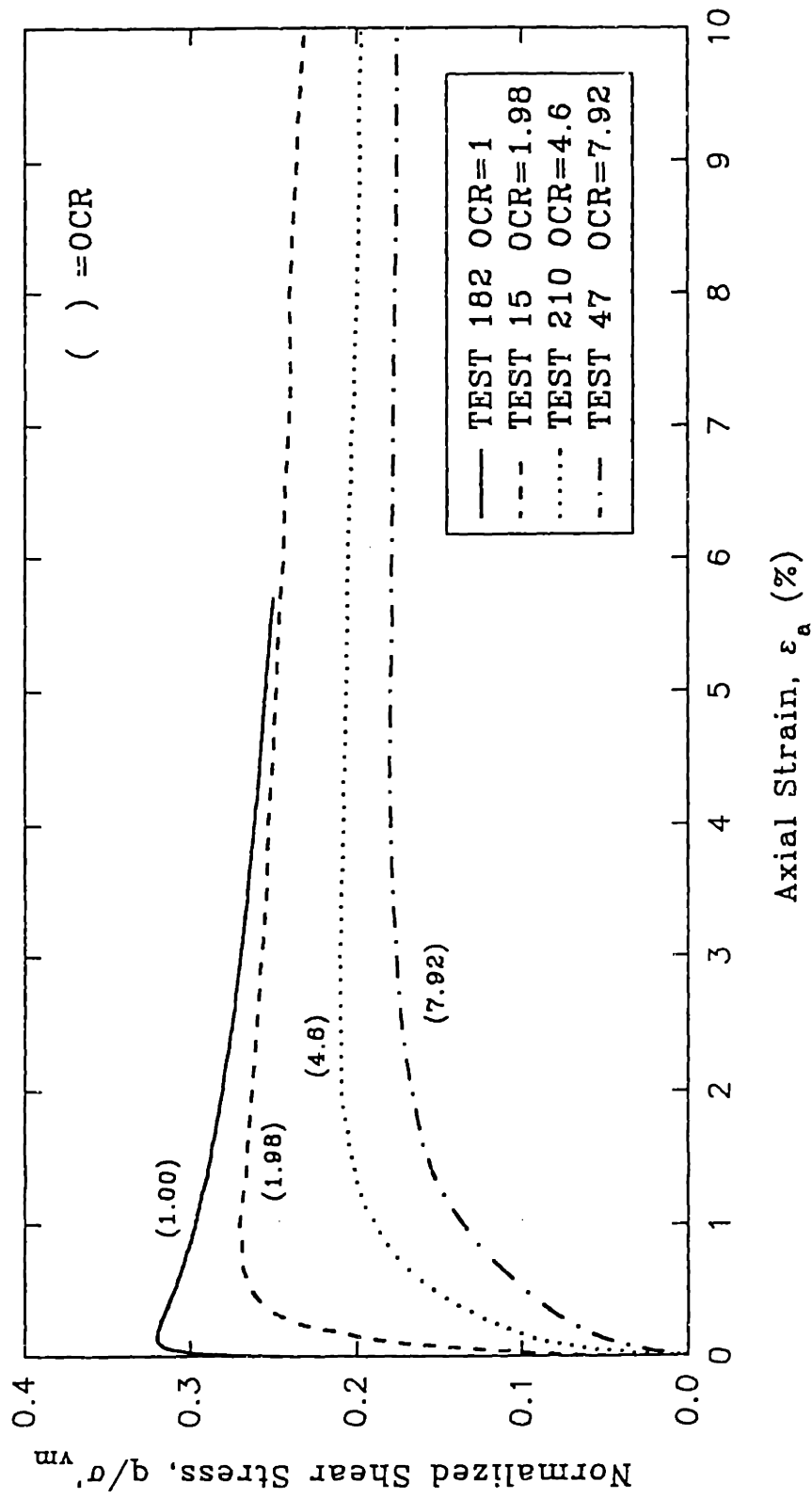


Figure 5.7: Intact Undrained Shear Behavior (TXC) of RBBC (OCR=1,2,4,8):  
Stress Strain Curves

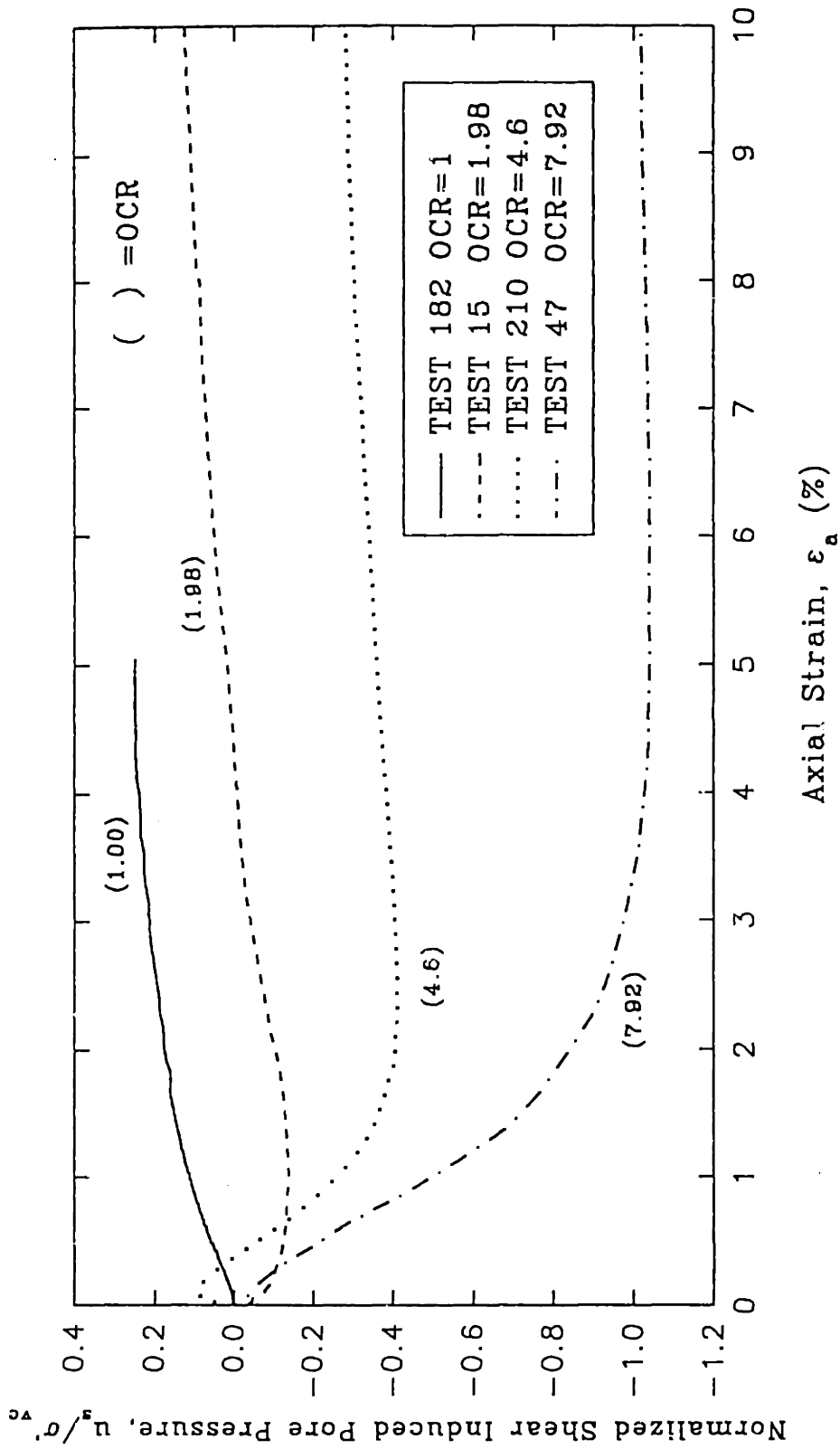


Figure 5.8a: Intact Undrained Shear (TXC) Behavior of RBBC (OCR=1,2,4,8):  
Normalized Shear Induced Pore Pressure vs. Axial Strain

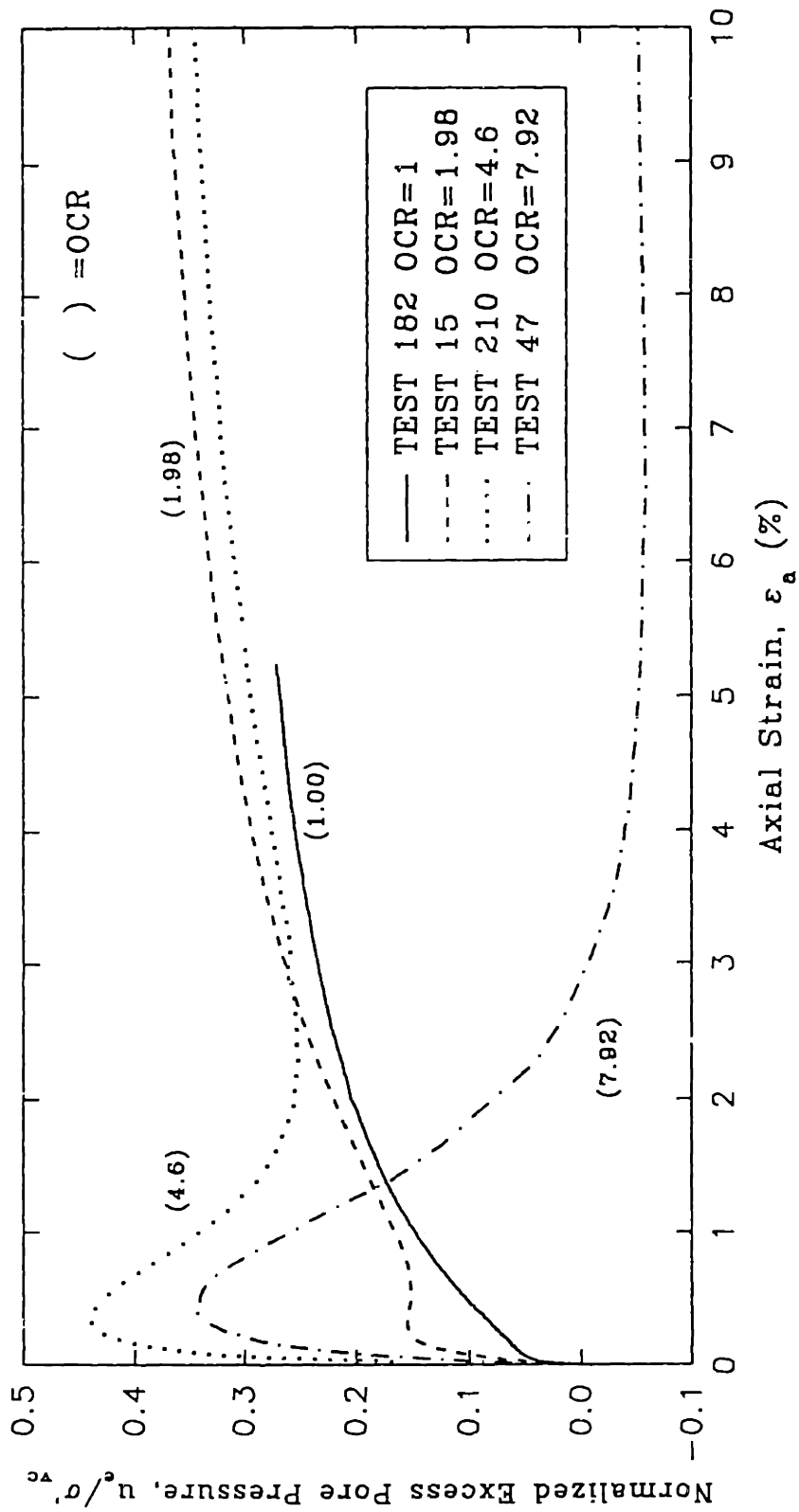


Figure 5.8b: Intact Undrained Shear (TXC) Behavior of RBBC (OCR=1,2,4,8):  
Normalized Excess Pore Pressure vs. Axial Strain

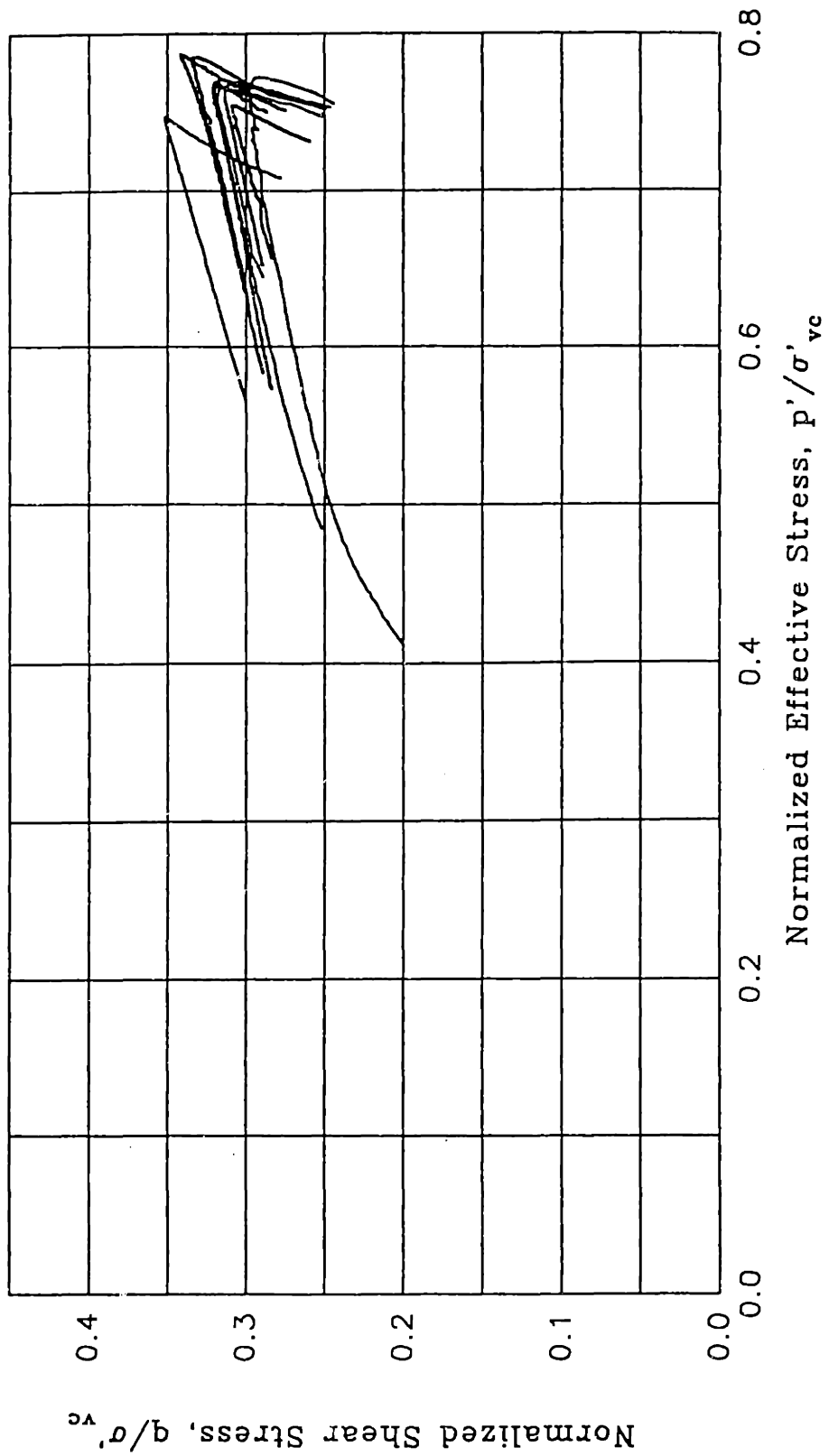


Figure 5.9: Selection of Stress Paths for Undrained Shear (TXC) of Intact NC RBBC (Batches 216-219)

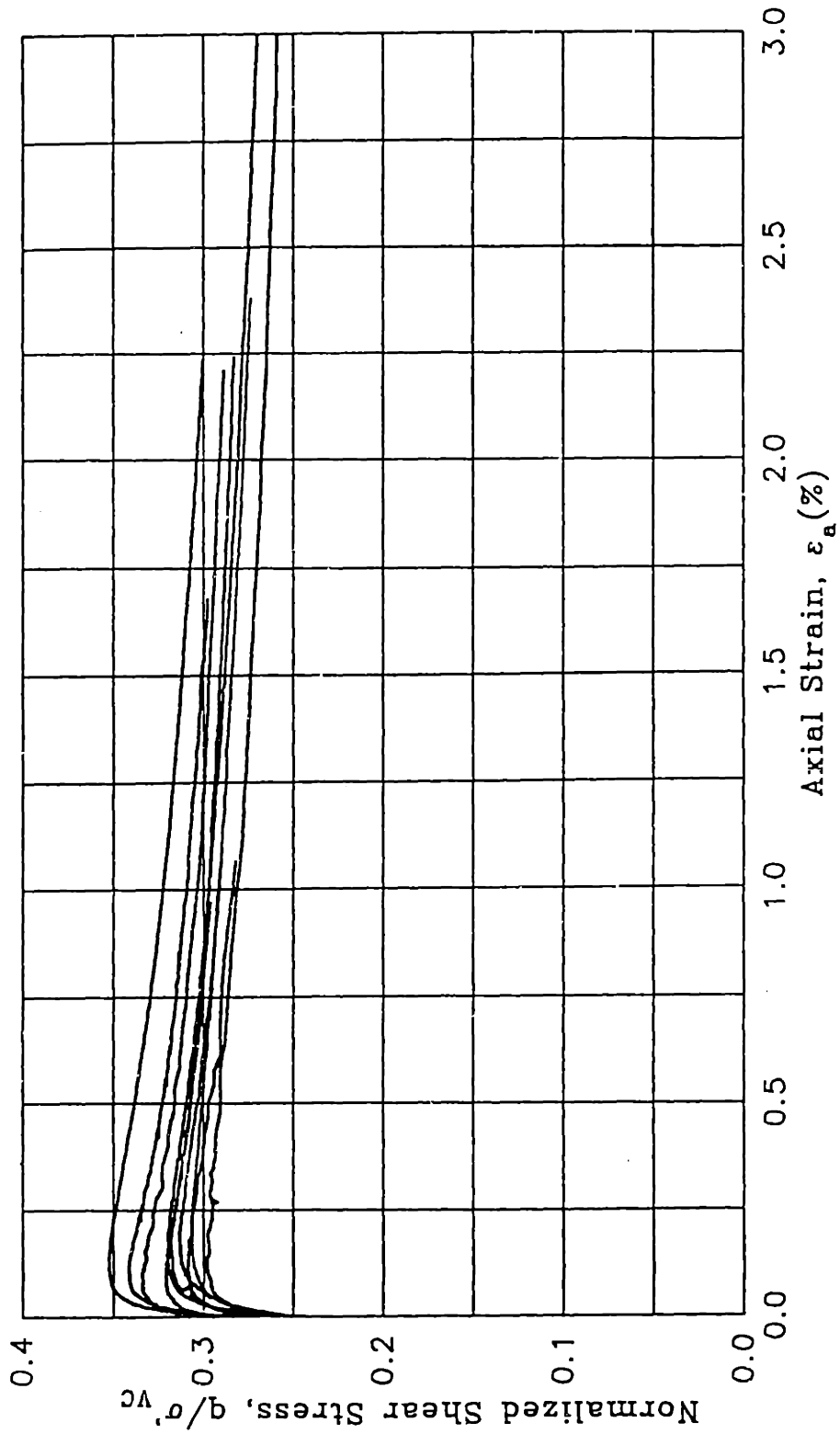


Figure 5.10: Selection of Stress Strain Curves for Undrained Shear (TXC) of Intact NC RBBC (Batches 216-219)

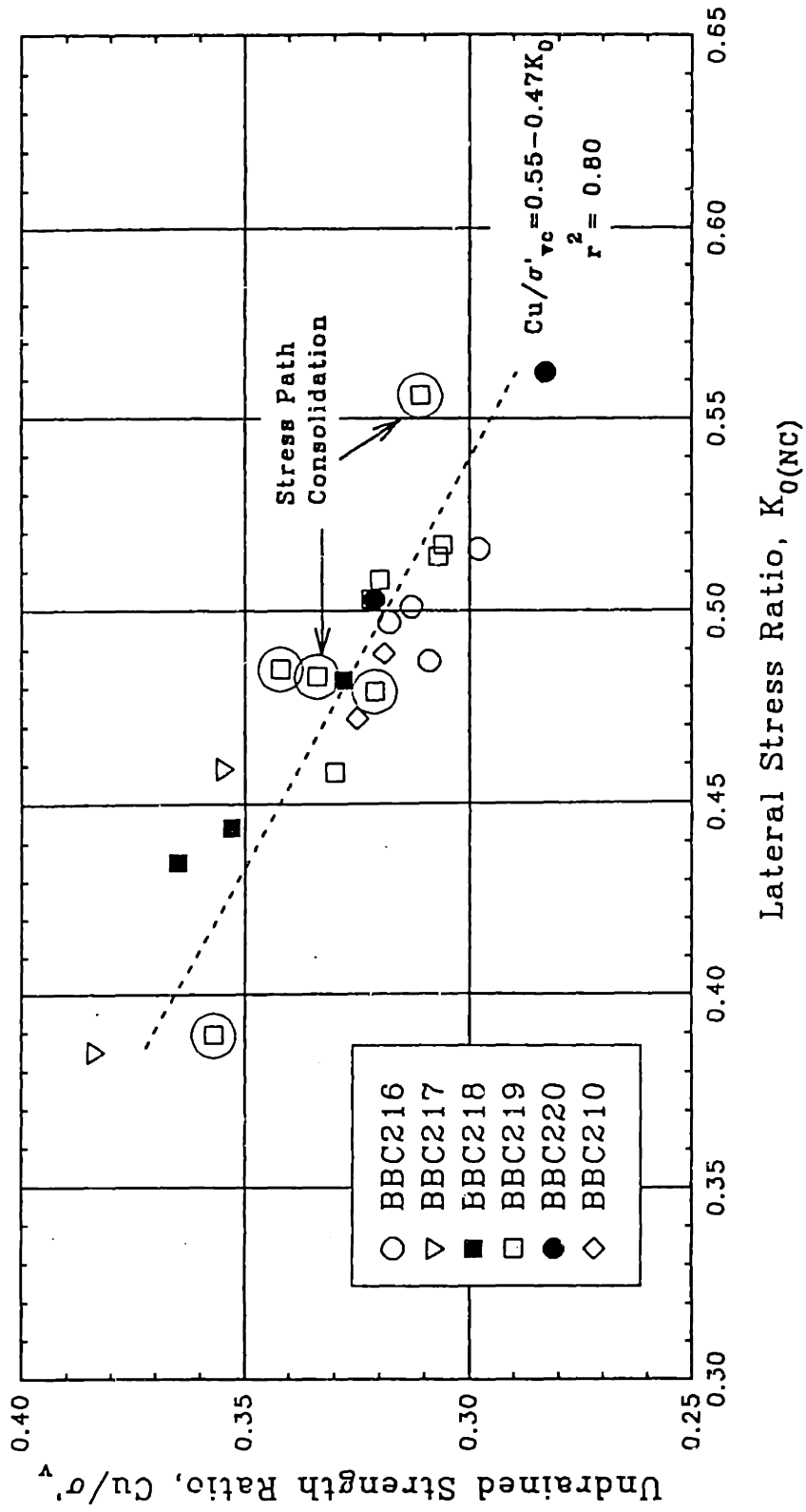


Figure 5.11: Relationship between the Pre-Shear Lateral Stress Ratio  $K_{0(NC)}$  and the Undrained Strength Ratio for NC RBBC



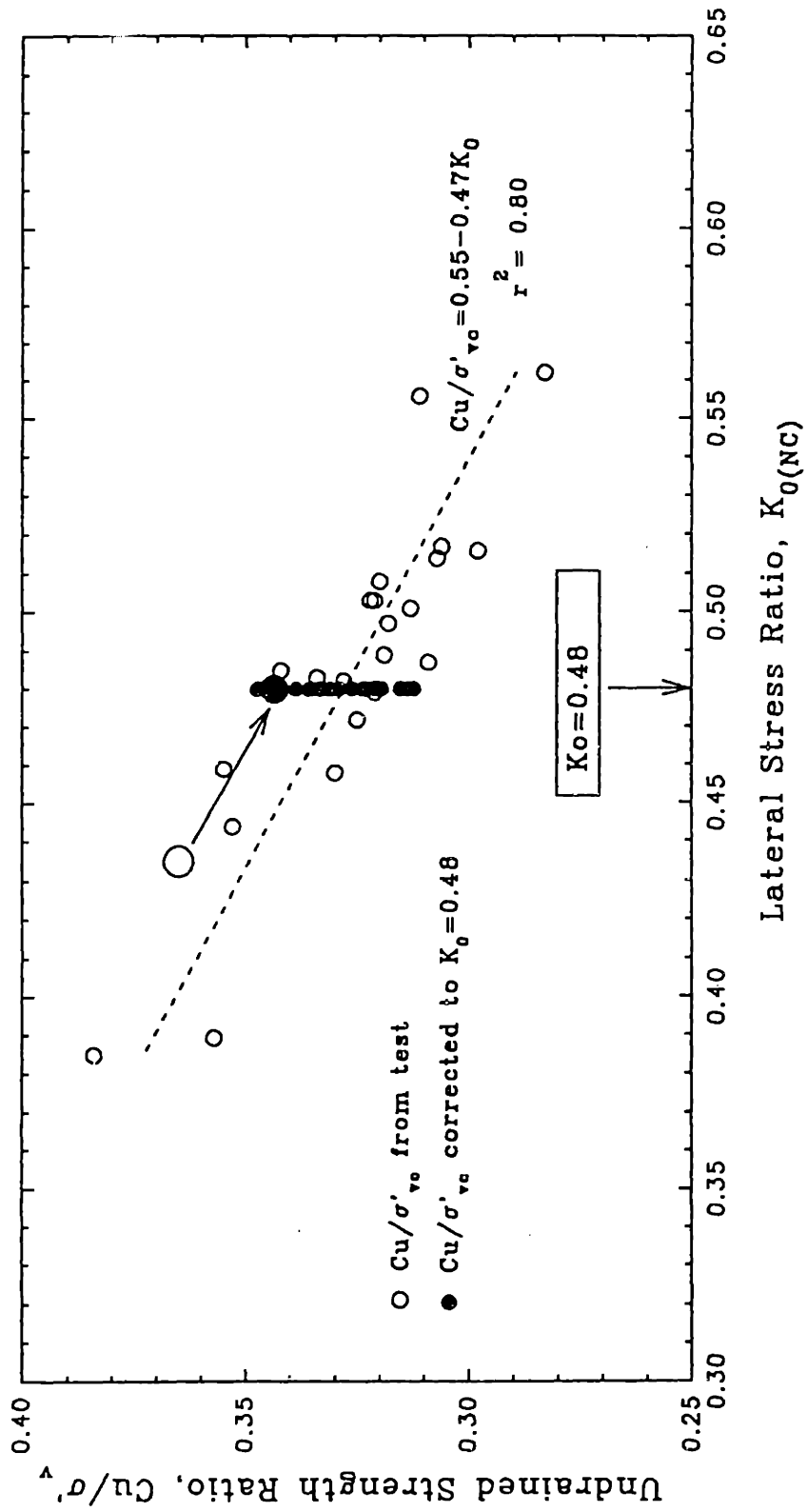


Figure 5.12: Correction of the Undrained Strength of NC RBBC to account for the Variation of the Lateral Stress Ratio  $K_{0(NC)}$

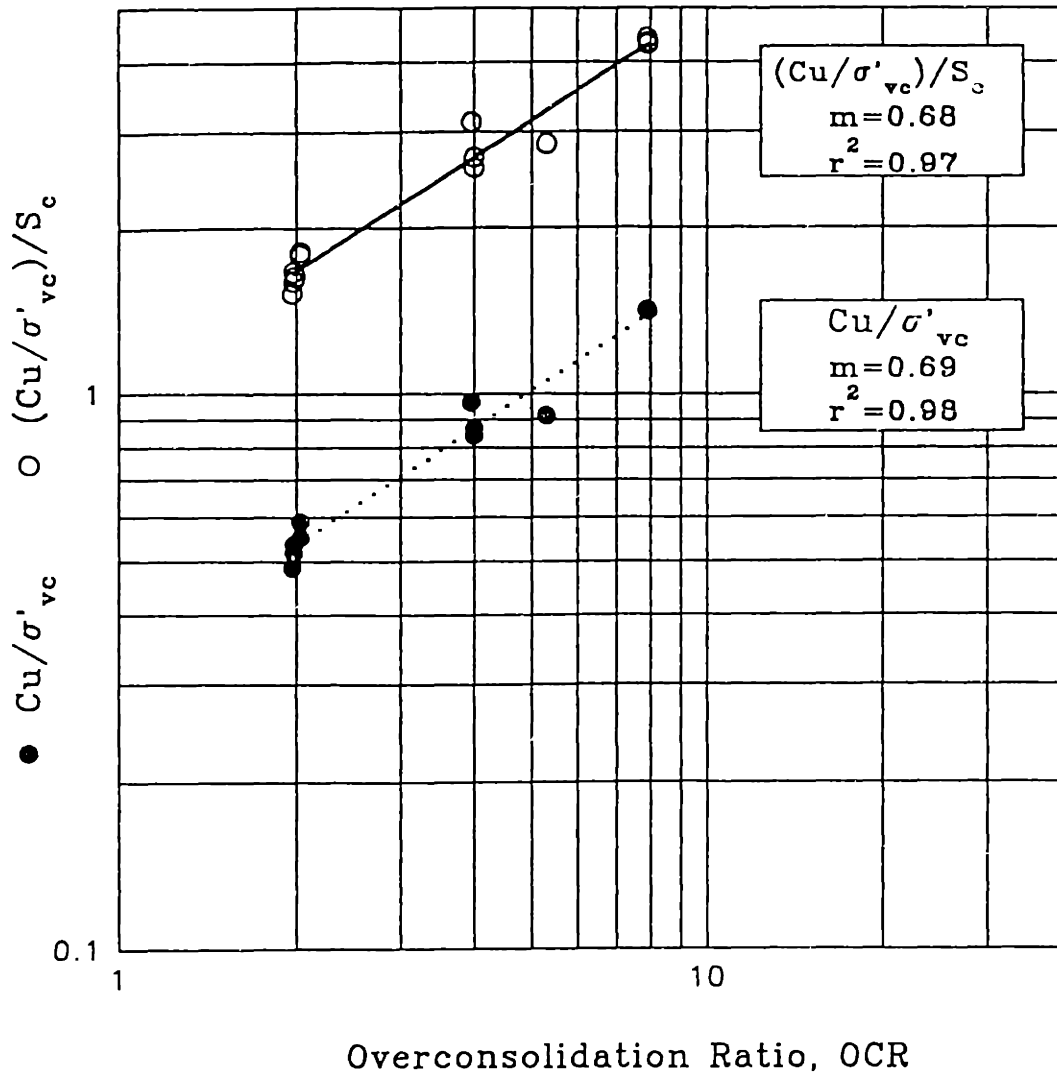


Figure 5.13: Effect of  $K_{0(NC)}$  on the Strength of OC RBBC

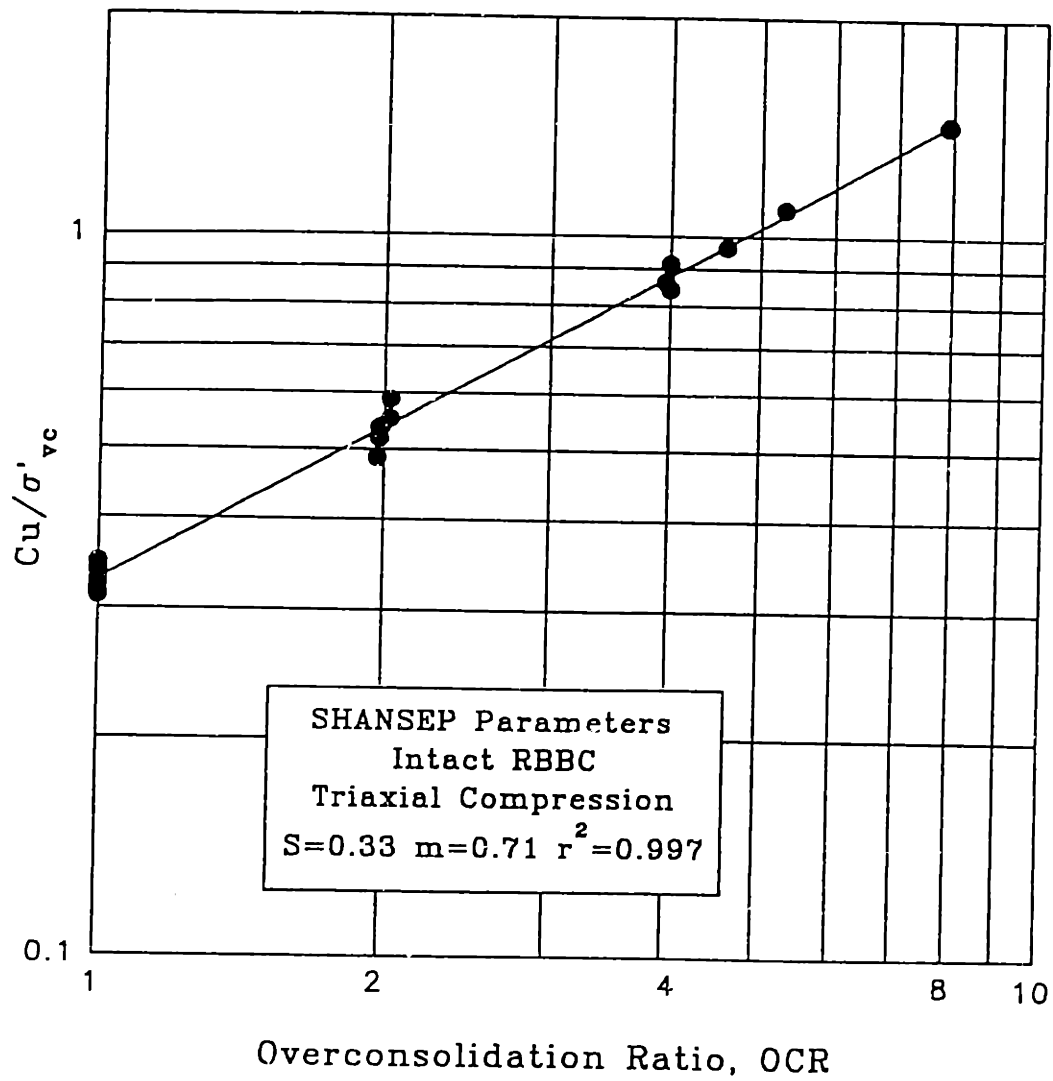


Figure 5.14:  $C_u/\sigma'_{vc}$  versus OCR: Determination of the SHANSEP Parameters for Intact RBBC

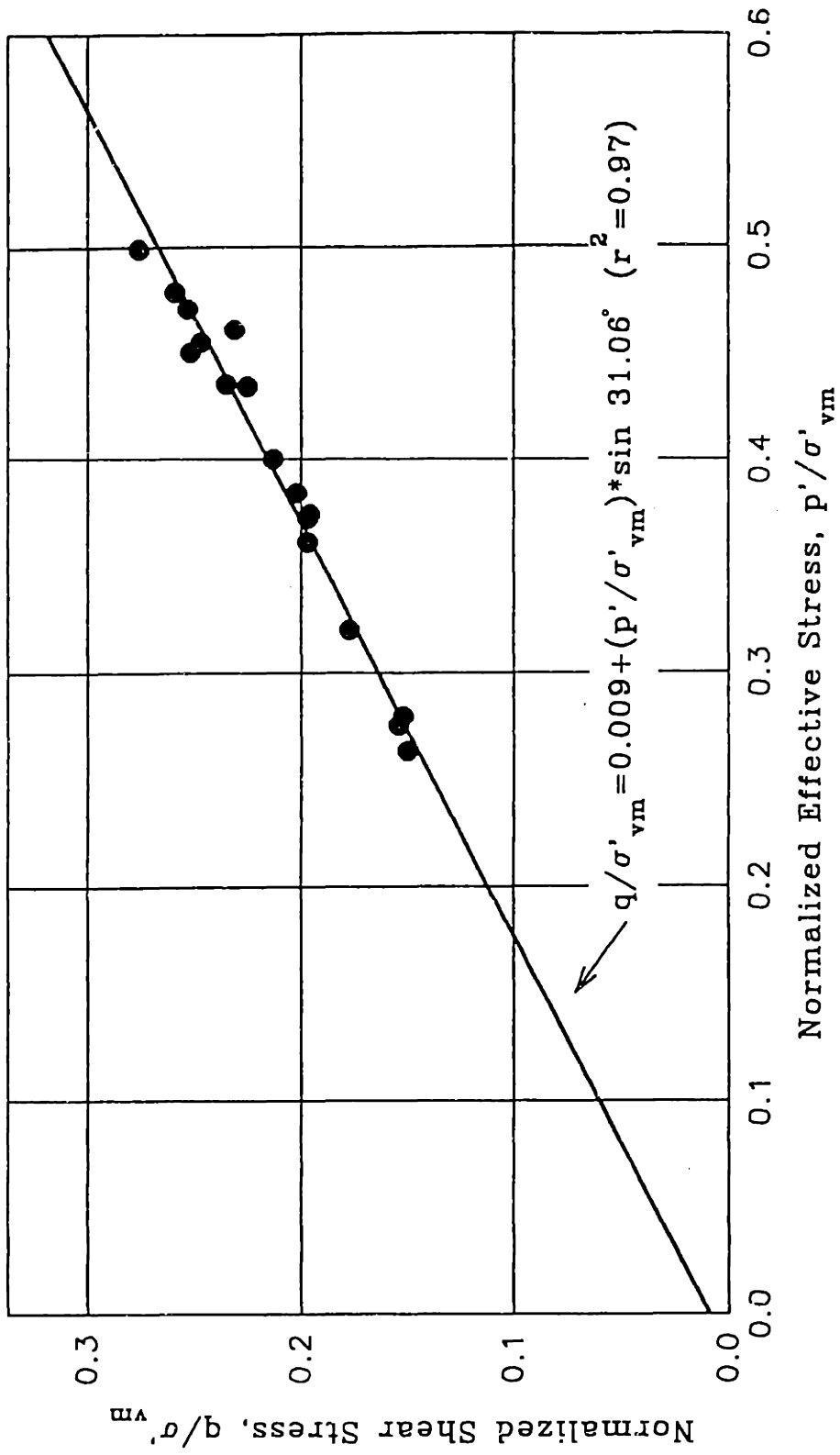


Figure 5.15: Friction Angle at Maximum Oblliquity for Intact RBBC (OCR=1,2,4,8)

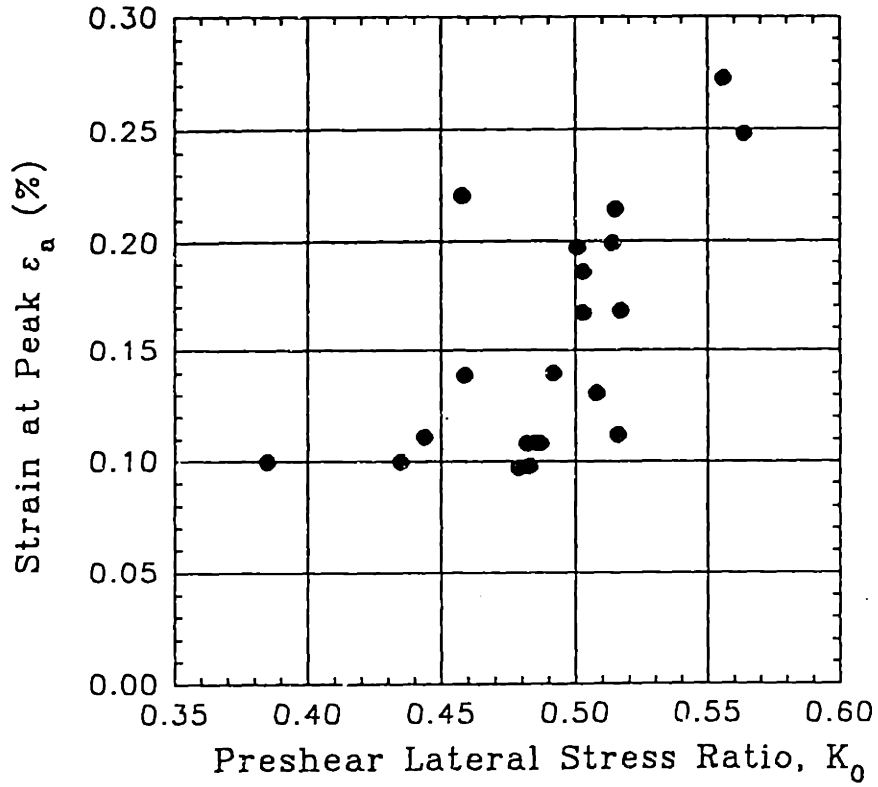


Figure 5.16: Strain at Peak versus  $K_0$  for NC RBBC

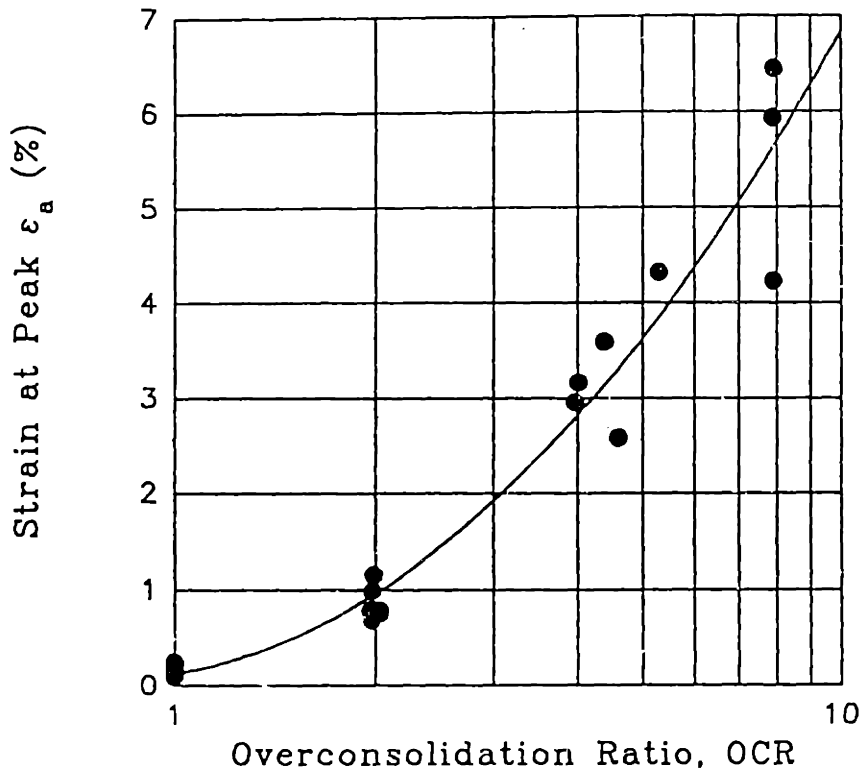


Figure 5.17: Strain at Peak versus OCR for RBBC

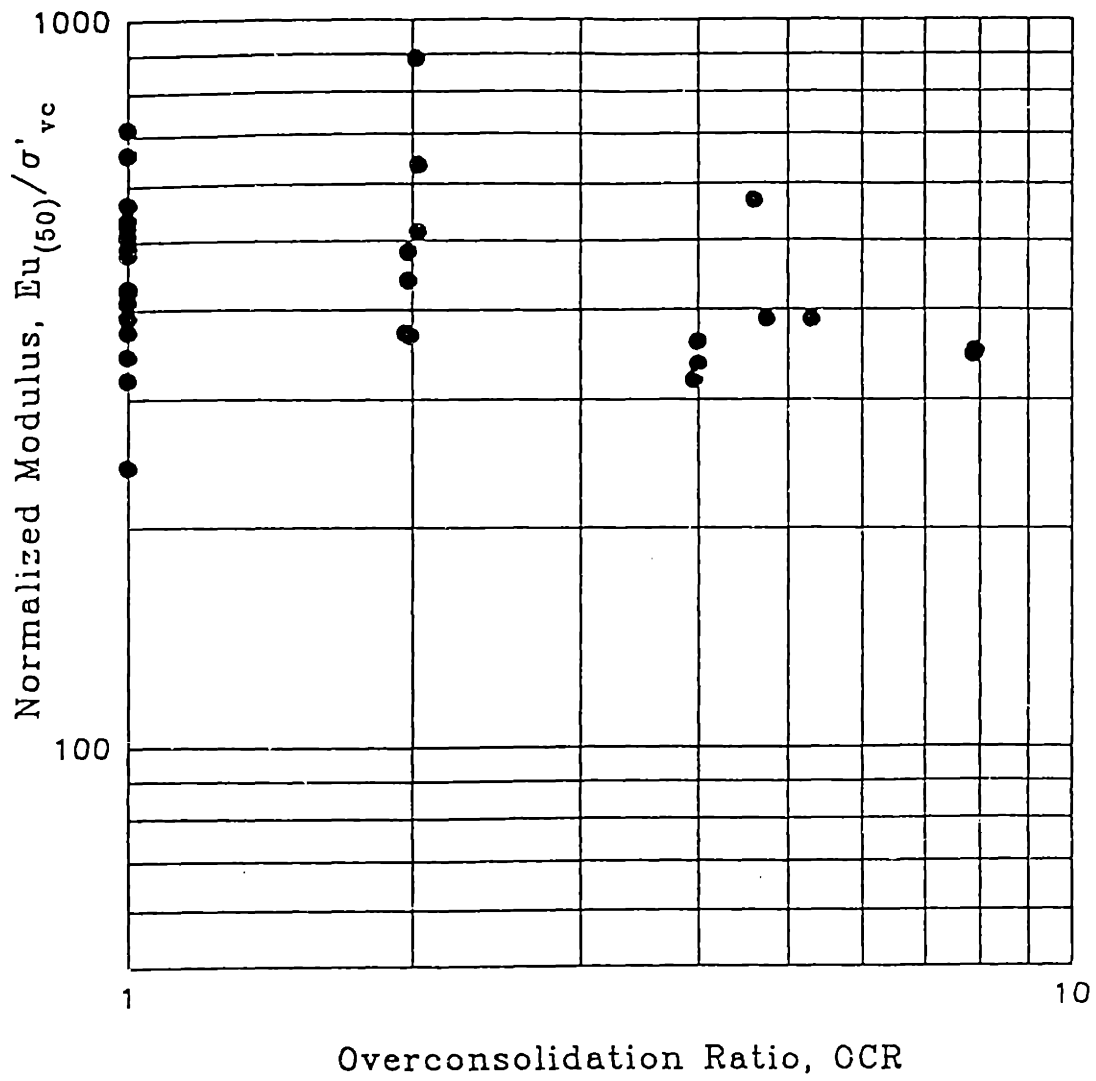


Figure 5.18:  $E_{u(50)}/\sigma'_{vc}$  versus Overconsolidation Ratio for intact RBBC

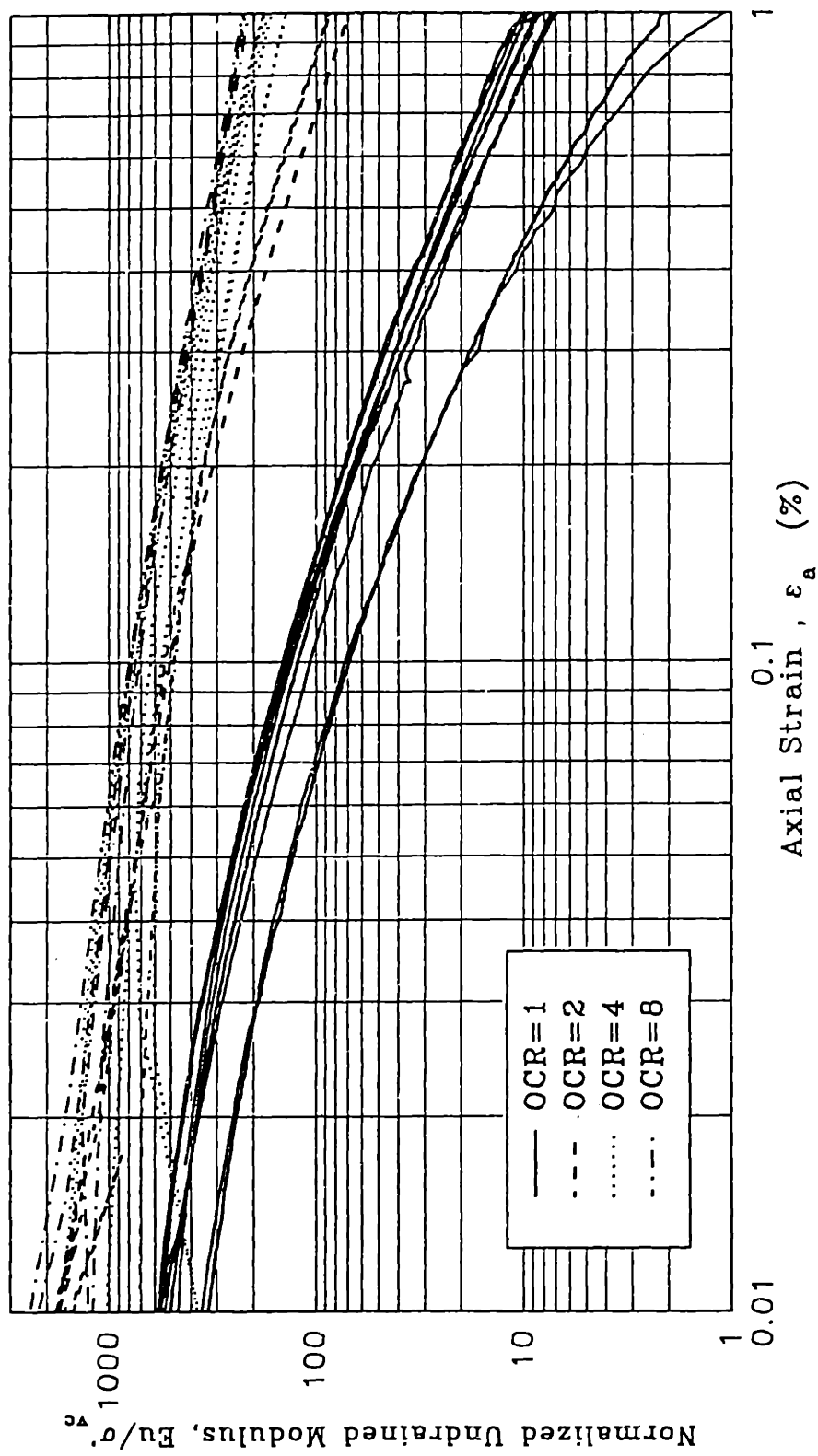


Figure 5.19: Normalized Undrained Modulus versus Axial Strain for Intact RBBC (OCR=1,2,4,8)





# Chapter 6 Effect of Disturbance on the Engineering Properties of RBBC

## 6.1 Introduction

The following sections analyze the results of a series of triaxial tests performed to investigate the effects of disturbance on the engineering properties of Resedimented Boston Blue Clay with OCR equal to 1, 2, 4 and 8. The tests analyzed in the present chapter have been classified in Chapter 4 as "UU" tests and "K<sub>0</sub>-consolidation" tests. The rationale followed in developing the testing program and the detailed phases of each test type have been described in depth in Chapter 4 and are only briefly reviewed here.

In both the "UU" and the "K<sub>0</sub>-consolidation" the soil reaches the "in situ" stress state following consolidation to 3-4ksc (and subsequent swelling to the desired consolidation stress for the OC tests). This phase is then followed by an undrained shearing cycle which simulates sampling disturbance according to the Perfect Sampling Approach (PSA tests) or the Ideal Sampling Approach (ISA tests).

In case of the "UU" tests the soil is sheared immediately after the disturbance cycle and thus the properties measured carry the full imprint of disturbance. Comparison of the results of this undrained shear with the shear properties of the intact material makes it possible to assess the effects of disturbance on the undrained behavior of the soil.

In contrast, when performing a "K<sub>0</sub>-consolidation" test, after the simulation of disturbance, the soil is reconsolidated to about 9 ksc under K<sub>0</sub> conditions (and swelled to the desired OCR in the OC tests). Thus an analysis of the resulting compression curve provides insight into the effects of disturbance of the compression behavior of RBBC.

In order to illustrate the typical behavior of disturbed material, Figures 6.1a and b show stress strain curves and stress paths relative to the final shear of one standard NC undisturbed test and six "UU" tests performed after the NC specimens had been subjected to different types and amounts of disturbance. It can be observed that, in NC clays, increasing amplitudes of imposed strains during the undrained strain path cycle are associated with:

- increased reduction of the effective stresses;
- increased reduction of the undrained strength;
- increased strain at peak;
- loss of the strain softening;
- increased reduction of the soil stiffness.

In the case of the PSA test the loss in strength and the increase in the strain at peak are minimal and the soil still exhibits some strain softening.

For increased disturbance, however, the stress-strain curves lose all the characteristics typical of normally consolidated RBBC and the stress strain curves and the stress paths are more similar to those typical of OC RBBC (see Figure 5.6). It appears that disturbance has effects on the undrained behavior of the soil similar to those produced by swelling as in fact is suggested by Ladd and Lambe (1963).

Figures 6.2a-b present equivalent plots showing the effect of disturbance on overconsolidated clay with nominal OCR equal to 4. One can observe that PSA disturbance has no effects on the behavior of the clay, while ISA disturbance causes a decrease of the effective stresses, the undrained strength, and the stiffness and an increase of the strain at peak. For any level of disturbance these effects are however less marked than those observed with NC RBBC.

Figure 6.3 shows the compression curves from the two consolidation phases of a " $K_0$ -consolidation" test performed on a specimen consolidated to an "in situ" stress equal to  $\sim 2.86$  ksc and, after 24 hours of secondary, subjected to  $ISA \pm 2$  disturbance cycle. It can be observed that for NC RBBC disturbance causes the following:

- more rounded compression curve and less defined break with consequent obscuring of the stress history;
- large strains at any given consolidation stress;
- lower compression ratio.

The following sections will discuss in more detail, for different values of the overconsolidation ratio, the effects of disturbance level and type on the effective stresses, the undrained strength, the strain at peak, the intermediate strain stiffness and the compression curve of RBBC. When possible the effects of disturbance will be compared to those produced by swelling.

The last section of this Chapter analyzes the results of TX120 a test conducted to investigate the effect of stress relief prior to sampling.

## 6.2 Effect of Disturbance on the Initial Effective Stresses

It has long been recognized that one of the effects of disturbance in clays is to reduce the effective stresses. Ladd and Lambe were the first to suggest that the loss in vertical stress be used to quantify the amount of disturbance.

The stress strain curves, stress paths and shear induced pore pressures for PSA, ISA $\pm$ 1, ISA $\pm$ 2 and ISA $\pm$ 5 disturbance on NC RBBC are shown in Figure 6.4a-c. Increasing disturbance is associated with increasing loss in the effective stresses.

In the ISA $\pm$ 1 test the decrease in  $p'$  is caused mainly by the initial compression and extension phases (1-2 and 2-3). As the disturbance increases, the second compression phase, to  $\epsilon_a=0\%$ , also causes further reduction in the effective stresses. In all cases the effect of the last phase of the ISA disturbance, the release of the shear stresses, appears to be minimal.

Figures 6.5 a-c present the stress strain curves, the stress paths, and the shear induced pore pressures during PSA, ISA $\pm$ 1 and ISA $\pm$ 2 disturbance of OCR4 RBBC. In this case the straining associated with the release of the shear stresses is minimal (approximately 0.5%) due to the fact that the "in situ" stress state of the soil is very close to being hydrostatic. In the ISA tests the soil dilates during the initial compression to  $\epsilon_a=\epsilon_{max}$  with consequent increase of the effective stresses. The positive pore pressures produced during the subsequent extension to  $-\epsilon_{max}$  lead to an overall reduction of the effective stresses which are not much affected by the last two phases of the ISA disturbance cycle.

As a measure of the loss of effective stress it has been decided to use the change in the mean effective stress ( $p'_m = (\sigma'_v + 2\sigma'_h)/3$ ) normalized by its value at the end of consolidation, or swelling in the case of tests on overconsolidated RBBC. Table 6.1 presents  $\Delta p'_m / p'_{m0}$  (%) caused by the undrained simulation of disturbance in the PSA and ISA tests on RBBC with OCR varying between 1 and 8. These values are plotted, for NC RBBC, with full circles versus the strain cycle amplitude  $\epsilon_c$ , in Figure 6.6. Values obtained from the PSA tests are plotted in correspondence to  $\epsilon_c$  equal to zero. The release of the in situ shear stresses is associated, in fact, with a very small negative strain as can be observed in Figure 6.4a.

For all the levels of straining the results are extremely consistent. Changes in  $p'$  are substantial and increase with the amplitude of the strain cycle towards a limit value. The PSA tests predict a substantial decrease of  $p'$ , approximately equal to 20%. In all the ISA tests ( $\pm 0.5\%$  to  $\pm 5\%$ ) the soil is sheared past its peak strength and the decrease of the effective stress is much more significant. A straining of  $\pm 1\%$  is enough to produce a loss of  $p'$  larger than 60%. For ISA $\pm 2$  the change in mean effective stress increases to  $\sim 82\%$ , and after  $\pm 5\%$  straining,  $p'$  is down to  $\sim 7\%$  of its initial value.

Figure 6.7 incorporates the results for the tests performed on overconsolidated RBBC with nominal OCR equal to 2, 4 and 8. As above, the results for the PSA tests are plotted in correspondence to  $\epsilon_c = 0$ . Figure 6.7 also presents, along with the results for RBBC a full line taken from Clayton et al. (1992) relative to "ISA Disturbed" tests performed on Laval samples of Bothkennar clay with estimated OCR of about 1.5. Finally Figure 6.8 plots the loss in mean effective stress versus the OCR of the soil for the different disturbance cycles.

From the observation of Figures 6.4-6.8 one can conclude the following:

- the PSA predicts a loss in effective stress much lower than the ISA;
- for NC RBBC the PSA disturbance causes a loss of  $p'$ ; in the PSA tests on RBBC with  $OCR \geq 2$  instead,  $\Delta p'/p'_o$  is  $\leq 0$ ; for OCR4 the effect of PSA disturbance is negligible;
- for the ISA tests changes in mean effective stress due to disturbance are substantial and increase with the amplitude of the strain cycle towards a limit value;
- the ISA disturbance cycles lead to a decrease in the mean effective stress for all OCRs;
- the decrease of  $p'$  caused by the ISA disturbance increases dramatically as the amplitude of the strain cycle exceeds the strain at peak of the intact soil;
- larger straining is required to produce the same change in  $p'$  for increasing OCR. The soil with higher OCR appears to be less susceptible to disturbance.
- for higher straining levels there is a smaller difference between NC tests and OC tests in terms of  $\Delta p'_m/p'_m'o$ . This is apparent from Figure 6.8 in which the steepness of the lines through the data points is larger for higher strain cycle amplitudes;

Regarding the results of the ISA tests on Bothkennar clay, it appears that the trend of the mean effective stress decrease is extremely similar to the one found for RBBC especially if it is considered that due to its higher plasticity and slightly overconsolidated state, Bothkennar clay is expected to be less seriously damaged by the ISA cycle than RBBC. Also, the tests

reported by Clayton et al. (1992) were performed on Laval samples and, since the clay already underwent some disturbance prior to the ISA straining, the effects of the ISA disturbance are probably underestimated.

The similarity between the results analyzed here and those presented by Clayton et al. is encouraging and suggests that some of the conclusions made here regarding the effect of disturbance on RBBC may be applicable to other soft soils with different properties.

Column 6 of Table 6.1 isolates the effect of the final deviatoric unloading after ISA disturbance on the loss of effective stress. No clear trend is apparent between the change in mean effective stress caused by shear stress release and the magnitude of the strain cycle amplitude or the OCR of the soil. However, in most cases, the final shear stress release causes a variation in  $p'_m$  smaller than 5-10%. This points out, once more, that tube sampling disturbance effects are primarily due to tube penetration disturbance.

As mentioned in Section 4.1, one NC specimen (TX120) was subjected to deviatoric unloading prior to the ISA  $\pm 1\%$  disturbance cycle and the final shear stress unloading. The initial deviatoric unloading does not seem to cause any difference in the effective stress decrease. The consequences of this result will be discussed later.

It has been observed that disturbance produces changes in the stress strain curves and the stress paths of intact RBBC similar to those caused by swelling. Just as the stress unload produced by swelling is quantified through the OCR, the undrained decrease in stresses caused by sampling disturbance can be expressed by the Induced Overconsolidation Ratio IOCR and the Apparent Overconsolidation Ratio AOOCR. The Apparent

Overconsolidation Ratio, first introduced by Ladd and Lambe (1963), is here redefined as:

$$AOCR = \sigma'_{vmax} / \sigma'_s$$

The Induced Overconsolidation Ratio, here introduced by the author, is defined in the following way:

$$IOCR = \sigma'_{vc} / \sigma'_s$$

where  $\sigma'_{vmax}$  is the maximum stress,  $\sigma'_{vc}$  is the vertical consolidation stress at the end of consolidation, or swelling for the overconsolidated specimens, and  $\sigma'_s$  is the vertical stress at the end of the sampling operations which corresponds to the end of the PSA or ISA undrained shear in this testing program.

In the case of undisturbed soil the AOCR is equal to the actual OCR, and IOCR is equal to 1. From the definitions above it is also clear that  $IOCR = AOCR / OCR$ , and that for NC clay IOCR is always equal to AOCR. Figure 6.9 schematically summarizes these quantities.

The last column of Table 6.1 presents the IOCR produced by the different disturbance cycles for RBBC. For NC RBBC the Induced Overconsolidation Ratio ranges from ~2 in the PSA tests, ~4 in the ISA $\pm$ 1 tests to approximately 10 in the ISA $\pm$ 2. The values of IOCR for overconsolidated RBBC are, as for  $\Delta p'_m / p'_{mo}$ , very much lower for any level of straining.



### 6.3 Effect of Disturbance on the Undrained Strength

Figure 6.10 plots the decrease in the undrained strength, caused by disturbance simulated according to the PSA or the ISA, normalized by the undisturbed strength versus the strain cycle amplitude  $\epsilon_c$  in the case of NC RBBC. For the ISA tests the undisturbed strength used as reference is the one measured during the first compression phase of the disturbance cycle. For the PSA tests, a value of  $Cu_{und}$  was picked based on the  $K_0$  of the soil prior to shearing using the relationship presented in Section 5.3.2. Once again the values obtained from the PSA tests are plotted in correspondence to  $\epsilon_c$  equal to zero.

The results are quite consistent for each level of straining. The loss in undrained strength increases with the level of disturbance. The specimens disturbed according to the PSA show a decrease in strength on the order of 15%. ISA disturbance with  $|\epsilon_{max}|=1\%$  is enough to cause a 25% loss of strength. For the ISA $\pm 2$  test the decrease is about 30-35%.

Figures 6.11 incorporates the results for overconsolidated clays. In most cases the strain amplitude of the ISA disturbance is less than the peak strain at failure and hence the  $Cu_{und}$  must be estimated by other means. For this figure the results of the OC tests are not normalized to the undisturbed strength. Figure 6.11 plots, in full symbols, the undrained strength normalized to the consolidation stress as a function of the strain cycle amplitude for different values of the nominal OCR. The values relative to the PSA disturbance tests are plotted in correspondence to  $\epsilon_c=0$ . The larger hollow symbols, also plotted in correspondence to  $\epsilon_c=0$  represent instead the values of  $Cu/\sigma'_{vc}$  obtained for each value of the

nominal OCR using the SHANSEP equation with the parameters determined in Section 5.3.2 for intact RBBC:

$$C_u/\sigma'_{vc} = 0.33 \cdot (\text{OCR})^{0.71}$$

Interpretation of the results for OC clay is less straightforward than for NC RBBC. While NC RBBC shows a well defined trend of decreasing strength with increasing strain cycle amplitude the same is not true for the OC clay. PSA disturbance does not produce any significant effect on the undrained strength of the soil for all OCRs. Further it appears that for OCRs larger than 2 the undrained strength is not very sensitive to disturbance for values of the strain cycle amplitude less than or equal to 2%. For OCR 4 and 8, for example, no decrease in the undrained strength is noticeable after  $ISA_{\pm 2}$  even though this level of disturbance is enough to produce a significant variation in the pre-shear effective stresses. This is probably due to the fact that at 2% strain neither the OCR4 nor the OCR8 RBBC have reached failure, while the NC and the OCR2 RBBC reach the peak strength at about 0.1% and 1% strain, respectively. More severe disturbance than  $ISA_{\pm 2}$  is needed in the case of RBBC with OCR higher than 2 for the clay to suffer a significant loss of strength as can be seen by looking at the result of the test on OCR=4 clay with  $\epsilon_c=8\%$  that shows a decrease in strength larger than 40%.

It must also be observed that in some cases the clarity of the results is clouded by the fact that the true OCR of the specimen is quite different from the value of the nominal OCR. This explains why in certain cases, for example for OCR=4, the strength actually appears to increase with increasing disturbance.

This research has established the existence of a SHANSEP type relationship between the strength of disturbed NC RBBC and the "Induced" Overconsolidation Ratio produced due to disturbance. The behavior of disturbed NC RBBC can be interpreted in this framework. In the case of intact soil, the SHANSEP equation relates the undrained strength of the soil normalized by the current consolidation stress to its overconsolidation ratio through the equation :

$$C_u/\sigma'_{vc}=S\cdot(OCR)^m$$

where  $S$  represents the normalized strength of the NC material.

When applying the SHANSEP equation to disturbance the OCR is replaced by the IOCR and  $S$ , which represents the strength in correspondence to IOCR=1, is the intact strength of NC RBBC. The strength is now no longer normalized by the stress at the end of swelling ( $\sigma'_{vc}$ ) but by the stress at the end of disturbance ( $\sigma'_s$ ).

Figure 6.12 presents, in hollow symbols, the data points used to define the SHANSEP parameters for intact RBBC. The figure plots in full symbols, on a log-log scale,  $C_u/\sigma'_s$  versus the Induced Overconsolidation Ratio, where  $\sigma'_s$  is the vertical effective stress at the end of the sampling operations. The points plot along a well defined line ( $r^2=0.998$ ) which has an intercept  $S=0.33$  and a slope  $m=0.82$ .

Obviously the intercept  $S$  is equal to the value for the intact material because, as mentioned above, the points plotted for IOCR=1 represent the values of the strength in the case of no disturbance and are the same points plotted for OCR=1 in Figure 5.13. The slopes ( $m$ ) of the two equations are quite different with the points obtained from the disturbed tests all plotting above the line for the intact material indicating that the

value of  $C_u/\sigma'_s$  measured in a UU test on a NC specimen with a certain IOCR is higher than the value of  $C_u/\sigma'_{vc}$  measured in a CU test on a OC specimen with  $OCR=IOCR$ .

The increased value of  $m$  can be interpreted observing that, in the case of disturbance as simulated in this testing program, the decrease of effective stress, i.e. the generation of the IOCR, takes place at constant water content. Therefore the swelling associated with the unloading of the stresses ( $\Delta w^*$  in Figure 6.9a) is inhibited leading to an increase of strength. It should be pointed out however, that, based on work performed by Sinfield (1994), there is evidence that the same "SHANSEP" equation applies also for soil disturbed under conditions of limited drainage.

Figure 6.13 incorporates the results of the overconsolidated tests. To be able to compare the results for the different OCRs,  $C_u/\sigma'_s$  has been divided by the undisturbed  $C_u/\sigma'_{vc}$  determined for the pre-disturbance OCR making use of the SHANSEP equation from Section 5.3.2 so that all the undisturbed data plots in correspondence to a value of the vertical axis equal to one. For  $OCR=1$ , for example, the same data presented in Figure 6.11 is here plotted normalized by  $S=0.33$ . For undisturbed RBBC only the SHANSEP equation is plotted here with a solid line for reference. The dashed line represents the regression through the results from the disturbed tests on NC clay.

All the points from the "UU" tests on OC RBBC, in solid symbols, lie above the line for the intact material due to the fact that the undrained nature of the disturbance process inhibits the swelling ( $\Delta w^{**}$  in Figure 6.12b) which would result from the stress unloading.

Unfortunately the data available for OCR larger than 1 are quite limited and it is hard to make a conclusive statement as to whether the same SHANSEP equation found for disturbed NC RBBC applies also to the OC soil. Based on the available data, it appears however that, except for one outlier, all the points for the OC tests are bounded by the line with slope  $m=0.82$  which represents the maximum effect of disturbance and the line with slope  $m=1$  for which disturbance has no effect on the undrained strength of the soil. Further it can be observed that for increasing values of the OCR, the data points tend to lie closer to the upper bound, i.e. the undrained strength of the soil is less and less susceptible to disturbance.

In Section 6.2 it was concluded that for increasing OCR of the soil, larger disturbance is required to produce the same decrease in effective stress, i.e. the same IOCR. Based on the discussion presented above it can also be concluded that the decrease of the undrained strength of the soil, when a certain IOCR is produced due to disturbance, is more marked in the case of NC soil and in many cases insignificant for OC soil. Note in fact from Figures 6.7 and 6.10 that in the case of OCR 4 and 8 RBBC, ISA  $\pm 1$  and ISA  $\pm 2$  disturbance lead to a significant decrease in the effective stresses but cause no decrease in the strength. The variation of the "SHANSEP" relationship with increasing OCR can be explained recalling that, as mentioned above, the disturbance process described here takes place at constant water content and therefore inhibits the increase of the water content normally associated with swelling due to the reduction of the effective stresses. Figure 6.12b shows however that, due to the fact that the swelling ratio (SR) of the soil increases for increasing OCR, for the same

decrease of the vertical stress, i.e. for the same IOCR, the  $\Delta w$  inhibited in the case of OC RBBC ( $\Delta w^{**}$ ) is larger than in the case of NC RBBC ( $\Delta w^*$ ).

#### 6.4 Effect of Disturbance on the Strain at Peak

The effect of disturbance on the stress-strain behavior of RBBC has been introduced in Section 6.1. Based on Figure 6.1 it was observed that for NC RBBC increasing disturbance led to increasing values of the strain at peak strength. The same was true for OC RBBC even though the increase in strain at peak caused by disturbance was less.

Figure 6.14 plots the strain at peak measured after disturbance versus the strain cycle amplitude. The figure shows that PSA disturbance produces an increase in the strain at peak only for NC RBBC. In the ISA tests, as the disturbance increases so does the strain at peak. For any level for disturbance the effect is less marked as the OCR increases.

As was done for strength in the previous section, it is also possible to compare the effects of disturbance and swelling on the strain at peak. Figure 6.15 plots the strain at peak measured in the disturbed "UU" tests versus the AOCR. This trend is compared to the trend of  $\epsilon_{\text{peak}}$  versus OCR (equal to AOCR when material is undisturbed) for intact RBBC (Figure 5.15). Swelling and disturbance have similar effects on the strain at peak. The two trends are very close. All the points relative to the PSA agree with the results for intact RBBC. On the other hand, the values of  $\epsilon_{\text{peak}}$  measured in the ISA disturbed tests are all larger than the values found for the intact soil. Therefore a specimen of disturbed RBBC with

AOCR=AOCR\* is less brittle than a specimen of intact RBBC with OCR=AOCR\*.

Contrary to swelling, disturbance as simulated by the Ideal Sampling Approach is associated not only with a decreases of the effective stresses but also with some restructuring of the soil due to the compression-extension-compression straining. While for OCR2 and OCR4 RBBC it is expected that PSA disturbance will not produce any increase in the strain at peak, for OCR1 it appears that there is not much difference between the swelling process and the undrained release of the shear stress, both of which take place inside the yield surface. The disturbance is limited and does not alter the fabric of the soil. In the ISA tests however the change in structure caused by the straining is dominant and causes the soil to become less brittle.

## 6.5 Effect of Disturbance on the Undrained Modulus $E_{u(50)}$

Figure 6.16 plots, for all the ISA tests on NC RBBC,  $E_{u(50)}/\sigma'_{vc}$ , the undrained modulus at 50% of the stress increment to reach failure ( $0.5 \Delta q_f$ ) measured during the shear following disturbance normalized by the value for intact RBBC. As discussed for the undrained strength, the first compression phase of the ISA disturbance cycle is used to determine the intact undrained modulus  $E_{u(50)}$ . This is not true in the case of the PSA tests and for this reason the results from these tests do not appear in the figure.

It appears clear that even minimal disturbance has a very severe effect on the undrained modulus. The decrease in  $E_{u(50)}/\sigma'_{vc}$  is smooth and consistent with the increase of the strain cycle amplitude. After  $ISA_{\pm 1}$  disturbance cycle, the modulus is, in fact, down to less than 20% of its intact value. Figure 6.17 presents the results relative to both NC and OC RBBC. As was done in Section 6.3 when presenting the strength results, the values of the modulus are not normalized to the undisturbed values. In most tests on OC RBBC in fact no information on the intact value of  $E_{u50}$  can be derived from the first compression phase of the ISA tests because the straining is reversed before reaching the peak strength. The scatter in the intact results is such that it is hard to establish a unique, reasonable estimate of  $E_{u(50)}$  for each OCR. Figure 6.17 therefore plots for each OCR the "disturbed" undrained modulus  $E_{u(50)}/\sigma'_{vc}$  normalized by the consolidation stress prior to disturbance versus the strain cycle amplitude. The mean values of the modulus for intact RBBC and their standard deviations are also plotted on the left side of the graph for comparison purposes. A logarithmic scale is used for the vertical axis because of the very wide range of the numbers. From this figure it is also possible to evaluate the results of the PSA tests, also plotted in correspondence to  $\epsilon_c=0$

While for NC clay PSA disturbance has a significant effect on  $E_{u(50)}$ , this is not true for the OC specimens due to the fact that their pre-disturbance stress state is very close to hydrostatic conditions. Therefore, PSA unloading to zero shear stress takes place with minimal straining. In the case of the ISA tests the effect of disturbance is significant for all OCRs.



The reduction in the modulus is more significant in the NC tests and becomes less pronounced as the OCR of the soil increases.

For OCR4 and OCR8 RBBC it is observed that the lower levels of disturbance, which did not for example influence the undrained strength, seriously affect the undrained modulus. The limited data available does not show any significant difference between RBBC with OCR=4 and OCR=8. The effect of disturbance on  $E_{u(50)}$  decreases with increasing OCR to what appears to be a minimum value where the OCR 4 and 8 tests plot.

It is important to point out that comparisons involving  $E_{u(50)}$  must be considered with care due to the fact that for Intact, PSA and ISA tests, the increment to failure is very different, and the strain level at which the modulus is compared varies over a very wide range. In this sense the variation in  $E_{u(50)}$  should be viewed more as a measure of the effects of disturbance on the stress strain behavior of the soil than as indicator of the variation in stiffness.

## 6.6 Effect of Disturbance on the Intermediate Strain Stiffness

To better understand the effects of disturbance on the on the soil stiffness it is necessary to compare the modulus of the disturbed and intact soil as a function of the strain level. This section investigates the effects of disturbance on the intermediate strain stiffness. The equipment employed for this research project does not in fact provide reliable estimates of the stiffness below 0.01%.

Figure 6.18 plots the modulus of NC RBBC normalized by the vertical consolidation stress versus the logarithm of the axial strain for strain between 0.01 and 0.1 %. The solid lines represent a typical range of the intact behavior of NC RBBC while all the other lines refer to the undrained shear performed after the simulation of disturbance. The results are extremely consistent. At the lower strains increasing ISA disturbance produces a drastic decrease in stiffness. The reduction in modulus increases with the amplitude of the disturbance cycle. In the ISA $\pm$ 1, ISA $\pm$ 2 and ISA $\pm$ 5 tests the stiffness at 0.01% axial strain is reduced respectively to about 50%, 35% and 15% of the intact value. Between 0.01 and 0.1% axial strain the stiffness of the disturbed soil is quite constant.

At 0.1% axial strain it is hard to determine the effect of disturbance on the stiffness except for the highly disturbed specimens (ISA $\pm$ 5). The values for the other ISA tests fall within the scatter band of the intact values. The stiffness of the intact material in fact decreases due to the post peak strain softening.

The behavior of the NC soil after PSA disturbance is very much different. In the PSA tests the soil is sheared undrained in extension with very limited straining to simulate the stress release due to extrusion and therefore, when the direction of the stress path reverses for the final shear in compression, the full small strain zone can be traversed again and this results in an increase of the stiffness. It must also be pointed out that the differences between the PSA and the intact soil increase with strain level because the PSA specimens do not strain soften as quickly.

One can observe from Figure 6.4b that the stress path reversal also exists in the case of ISA tests on NC RBBC. However, in the ISA tests the

straining results in restructuring of the soil and destruction of the soil stiffness at the small and intermediate strains.

Figures 6.18 and 6.19 present similar curves for tests performed on RBBC with OCR equal to 2 and 4. Even though the data are more limited it is possible to make some observations on the effect of disturbance on the stiffness at intermediate strains in the case of OC RBBC. It must be noted that in these case the results are plotted for a different range of strains from 0.05% to 1%. Unfortunately, in most of the OC tests, unsatisfactory measurements of the stiffness were obtained at smaller strains.

The effect of disturbance on the stiffness at intermediate strains is distinct: increasing magnitudes of disturbance cause more marked decrease of the stiffness. For OCR=2 the effects of PSA disturbance are similar to those described for NC RBBC but not as pronounced. ISA disturbance causes a significant decreases of the stiffness at the smaller strains but the stiffness does not display the linear trend with strain observed in the NC tests. At higher values of the strain (>1% axial) the curves for the disturbed and intact material converge.

For OCR=4 the results of the PSA test shown fall perfectly within the range of behavior of intact OCR4 RBBC due to the fact that the soil is already extremely close to hydrostatic conditions prior to disturbance. ISA $\pm$ 1 and ISA $\pm$ 2 disturbance produce a limited decreases of the stiffness and the disturbed behavior converges to the intact one at high strains. ISA $\pm$ 8 disturbance leads instead to a dramatic reduction of the stiffness with the modulus displaying an almost constant value for a very large range of strains and never approaching the curve of the intact material.

Comparison of the effect of the same magnitude of disturbance on the stiffness at intermediate strains for varying OCR (Figures 6.17-19) indicates that the sensitivity to disturbance decreases with increasing OCR of the soil.

## **6.7 Effect of Disturbance on the Compression Behavior**

This section examines the results of the limited number of "K<sub>0</sub>-consolidation" tests performed in this research. Based on the analysis of the one-dimensional reconsolidation following the disturbance cycle, it is possible to evaluate the effects of different magnitudes of disturbance on the compression behavior of RBBC.

### **6.7.1 Effect of Disturbance on the Compression Curve and the Compressibility Parameters**

Figure 6.21 compares the original compression curve of NC RBBC to the compression curve of the soil after disturbance for three different levels of disturbance: ISA<sub>±1</sub>, ISA<sub>±2</sub> and ISA<sub>±5</sub>. In interpreting the results of test TX260, it should be taken into account that in this test K<sub>0</sub> conditions were not well maintained during the consolidation after disturbance resulting in a difference between the axial and the volumetric strain which gradually increases to a maximum of 1%.

Figure 6.21 indicates that as the level of disturbance increases, the compression curve is more rounded and it becomes harder to identify a

break and determine the maximum past pressure. In particular, after ISA $\pm$ 5 disturbance the soil exhibits a very flat compression curve and evaluation of the maximum past pressure by means of the Casagrande construction becomes extremely subjective. Also, increasing disturbance is associated with an increase in the slope of the recompression portion of the curve, a substantial increase in the reconsolidation strains at any stress level and with a flatter compression curve after the effective stress exceeds the preconsolidation pressure ( $\sim 3$  ksc).

Figure 6.21 presents, for each plot, two lines indicating the slopes of the curves. For each test, the dotted line represents the regression through the last part of the first consolidation which identifies the virgin compression line (VCL). The dashed-dotted line is obtained from the regression over the steepest portion of the second consolidation line (after disturbance). The numbers indicated as CR<sub>1</sub> and CR<sub>2</sub> represent the compression ratios for each of the compression phases and have been determined from the corresponding  $\epsilon_v - \sigma'_v$  curves.

It must be pointed out that in test TX142 (ISA $\pm$ 2 test) the second consolidation was prolonged only to about 9 ksc ( $\sim 3 \sigma'_p$ ) while in tests TX134 (ISA $\pm$ 1) and TX260 (ISA $\pm$ 5) it was possible to consolidate to about  $3.5\sigma'_p$  and  $4 \sigma'_p$  respectively.

Because the intact compression ratios are different in the three cases (CR<sub>1</sub>=0.16 for TX134, CR<sub>1</sub>=0.18 for TX142 and CR<sub>1</sub>=0.17 for TX260), for each test the "disturbed" compression ratio CR<sub>2</sub> must be compared to the intact CR of that same test. A third, dashed, line appears on the graph for tests TX134 and TX260. This line represents the slope of the compression curve at  $\sim 3 \sigma'_p$ . The slope of the corresponding  $\epsilon_v - \sigma'_v$  curve is termed CR<sub>2b</sub>.

One can observe that increasing disturbance causes a more marked lowering of the compression ratio. At about  $3\sigma'_p$ ,  $CR_2$  has reached approximately 92% of  $CR_1$  after  $ISA_{\pm 1}$ , while for the higher magnitudes of disturbance the ratio  $CR_2/CR_1$  decreases to 85% ( $ISA_{\pm 2}$  test) and to 63% ( $ISA_{\pm 5}$  test). In all cases the disturbed compression curve does exhibit a substantial linear portion.

Figure 6.22 plots the slope of the compression curve ( $\Delta\varepsilon_v/\Delta(\log\sigma'_v)$ ) normalized by the CR of the VCL from the first compression curve, for each of the three tests, versus  $\sigma'_v/\sigma'_{vmax}$ , the current effective stress normalized by the maximum pre-disturbance "in situ" vertical effective stress. Figure 6.22 indicates that increasing disturbance is associated with a steeper recompression curve and with decreasing values of the compression ratio.

Figures 6.23 and 6.24 compare the "intact" and "disturbed" compression curves for NC and RBBC with  $OCR=1.9$  and  $4.4$  in the case of  $ISA_{\pm 2}$  disturbance. Figure 6.23 indicates that the early portion of the "disturbed" compression curve is identical for all three tests. There are however differences in the compression behavior of the soil past the preconsolidation pressure. As for NC RBBC reconsolidation to  $3\sigma'_p$  is not enough, for the OC clay, to totally erase the effect of the  $ISA_{\pm 2}$  disturbance. The effect of disturbance on the compression curve appears however to be milder for the OC clay than for NC RBBC if one compares as above the CR at  $3\sigma'_p$  to the intact value. At  $3\sigma'_p$   $CR_2/CR_1 \sim 97\%$  for  $OCR=4.4$ ,  $CR_2/CR_1 \sim 93\%$  for  $OCR=1.89$  versus  $85\%$  for  $OCR=1$ .

## 6.7.2 Effect of Disturbance on the Reconsolidation Strains

Figure 6.25 plots the volumetric strains measured during reconsolidation of the specimen to the "in situ" vertical stress as a function of the level of disturbance (amplitude of the strain cycle) for different values of OCR. In this case, information can be derived not only from the "K<sub>0</sub>-consolidation" tests, in which the "in situ" vertical stress is reached by means of K<sub>0</sub> consolidation, but also from the "Recompression" tests in which the horizontal "in situ" stress as well as the vertical one is targeted by performing linear stress path consolidation.

The data are limited but appear quite consistent. It is apparent that for any overconsolidation ratio the volumetric strain needed to bring the specimen back to the in situ stresses increases quite markedly with increasing disturbance.

For every level of disturbance the reconsolidation strain is much larger for NC RBBC compared to the same clay at OCR=4. The difference increases with the level of disturbance.

Also shown in Figure 6.25 is a line taken from Clayton et al. (1992) from similar tests on Bothkennar Clay with OCR<sub>~</sub>1.5.

Based on the results shown, it appears clear that the reconsolidation strains are closely related to the amount of disturbance undergone by the soil.

The dependence of the reconsolidation strains on the OCR of the soil confirms that it is not possible, as suggested by some researchers (Andresen and Kolstad 1979) to determine an absolute criterion for sample quality based on the magnitude of these strains. Instead the measurement

of "reconsolidation" strains should be seen as a simple means to evaluate the relative disturbance affecting tests performed on the same soil.

### 6.7.3 Effect of Disturbance on the Maximum Past Pressure

The determination of the preconsolidation pressure represents in most design problems the single most important task. No calculation of settlements or stability evaluation can in fact be performed confidently if the stress history of the soil is not known.

In Chapter 2 it was pointed out that large dissent still exists as to the effects of disturbance on the preconsolidation pressure. While in most cases it is assumed that increasing disturbance is associated with a decrease in the preconsolidation pressure, no conclusive evidence has been presented to support this theory nor has it been shown that the value determined in the case of lower disturbance is closer to the true value. In the tests presented in this section the maximum "in situ" stress is known and one can evaluate the effects of different magnitudes of disturbance.

Let us first consider the NC tests TX134, TX142 and TX260 in which the specimens were consolidated to an "in situ" vertical stress of 2.87 ksc for TX134 and TX142 and of 3.06 ksc for TX260, and then subjected to ISA disturbance with  $\epsilon_c=1\%$  in the first case,  $\epsilon_c=2\%$  in the second and  $\epsilon_c=5\%$  in the last case. Finally the soil was consolidated to approximately 10 ksc. The maximum past pressure of the soil can be estimated based on the this second consolidation phase.



It must be pointed out that prior to the disturbance cycle all the specimens were allowed some secondary compression leading to an increase in the actual preconsolidation pressure. This increase in preconsolidation pressure can be estimated making use of the following relationships presented by Mesri and Godlewski (1977)

$$\frac{\sigma'_{p'}}{\sigma'_{vi}} = \left( \frac{t}{t_p} \right)^{\left( \frac{c_{\alpha\varepsilon}}{CR} \right) \left( 1 - \frac{RR}{CR} \right)}$$

where:

$\sigma'_{p'}$  is the preconsolidation pressure accounting for secondary compression

$\sigma'_{vi}$  is the consolidation stress at which secondary compression occurred

$t_p$  is the time to end of primary consolidation;

$t$  is the entire duration of the load increment

$c_{\alpha\varepsilon}$  is the coefficient of secondary compression

CR is the compression ratio

RR is the recompression ratio.

The time to end of primary consolidation,  $t_p$ , was determined from the following expression suggested by Bishop and Henkel (1976) for triaxial specimens with both vertical and radial drainage and  $h/r$  ratio equal to two.

$$t_{100} = \pi h^2 / 100 c_v$$

A value of the coefficient of consolidation  $c_v$  equal to  $3 \cdot 10^{-3}$  cm<sup>2</sup>/sec was chosen based on the results presented by Cauble (1993). An average value of  $h$  was employed yielding a value of  $t_p$  equal to 0.19 hours. Note that this value is obtained assuming perfect radial drainage and the true  $t_p$  may

actually be higher. A ratio  $c_{\alpha\epsilon}/CR=0.017\pm 0.002$  was selected based on results of incremental consolidation tests on RBBC (Batches 217 and 218) reported by Cauble (1993).

Specimens for TX134 and TX142 were both obtained from Batch 218. The specimen for TX260 was instead obtained from Batch 220 which showed a substantial difference in the compression ratio compared to previous batches (cf. Section 5.2). It is assumed that the same factors which cause CR to vary affect also  $C_{\alpha\epsilon}$  and that the ratio of the two can be considered a constant for the soil. An unique value of  $RR/CR$  equal to 0.1 was also chosen, once again based on previous experience with RBBC.

It must be noted that since the ratio  $C_{\alpha\epsilon}/CR=0.017$  is below the range for most inorganic soft clays reported by Mesri and Godlewski (1977), the validity of the correlation might be questionable.

The "true" values of the preconsolidation pressure determined with the procedure just described are 3.15 ksc for TX134, 3.12 ksc for TX142 and 3.31 ksc for TX260.

Having determined the "true" values of  $\sigma'_p$ , it is now possible to evaluate, for different magnitudes of disturbance, how closely the preconsolidation pressure can be estimated employing the procedures most commonly used (Strain Energy and Casagrande Method) to analyze the data relative to the consolidation performed after disturbance.

Figures 6.26a-c show the determination of  $\sigma'_p$  by means of the Strain Energy (SE) method for tests TX134, TX142 and TX260 ISA $\pm$ 1, ISA $\pm$ 2 and ISA $\pm$ 5 disturbance, respectively. For tests TX134 and TX142 the preconsolidation pressure was estimated also through the Casagrande Method. For the test with higher disturbance (TX260) it appears extremely

hard to evaluate the maximum past pressure employing the Casagrande construction. Similar problems are encountered in the Strain Energy Construction in defining the initial slope. In the following, unless specified otherwise, the analysis of the results considers only the estimates of the preconsolidation pressure obtained by the Strain Energy method.

Table 6.2 summarizes the values obtained for  $\sigma'_p$  from the graphic constructions. In the case of the Strain Energy method three values of  $\sigma'_p$  are presented:  $\sigma'_{p(\min)}$ ,  $\sigma'_{p(\max)}$ , and  $\sigma'_p$  (best est). In this method the uncertainty lies mainly in the definition of the initial slope of the curve. The minimum value of  $\sigma'_p$  is obtained by assuming that this slope is zero so that the preconsolidation pressure is obtained from the intersection of the line through the steepest portion of the curve with the horizontal axis. The best estimate of  $\sigma'_p$  by the SE method is obtained by enlarging the portion of the curve at low stresses to determine the initial slope. The upper bound value for  $\sigma'_p$ ,  $\sigma'_{p(\max)}$  is obtained by choosing a higher slope for the initial slope. Also shown in Table 6.2 are the differences between  $\sigma'_{p\max}$  and  $\sigma'_{p\min}$  and between  $\sigma'_{p(\text{be})}$  and  $\sigma'_{p(\min)}$ , which quantify the uncertainty associated with the estimate of the preconsolidation pressure. As expected the estimated range of variation of the preconsolidation pressure increases for increasing value of disturbance. For example the quantity  $(\sigma'_{p\max} - \sigma'_{p\min})$  is equal to 0.3 ksc for the ISA $\pm$ 1 test, but it increases to 0.55 ksc for the ISA $\pm$ 2 test and to 1.2 ksc for the ISA $\pm$ 5 test.

We can now address the issue of how the estimates performed through this method compare with the true values of  $\sigma'_p$ . For this purpose Table 6.2 provides also the values of  $(\sigma'_{p(\text{est})} - \sigma'_{p(\text{true})}) / \sigma'_{p(\text{true})}$ . The results are quite surprising and not of easy interpretation.

The single most interesting result is that for all three levels of disturbance the preconsolidation pressure can be determined with an accuracy of  $10\pm 5\%$ . This indicates that even for high levels of disturbance, the stress history of the soil is not significantly affected by sampling disturbance and that the Strain Energy method yields a reliable value of the preconsolidation.

It is interesting to observe that for all levels of disturbance the preconsolidation pressure is overestimated. This is true also for the tests with the lowest level of disturbance (TX134). In this case even the lower estimate from the SE method is clearly in excess (11%) of the true preconsolidation pressure. This is not in accordance with what is generally assumed to be the effect of disturbance on the preconsolidation pressure.

For TX142 (ISA $\pm 2$ ) the estimates by the Strain Energy Method are instead extremely close to the true value of  $\sigma'_p$  with  $\sigma'_{p(\min)}$  underestimating  $\sigma'_p$  by only 5% and  $\sigma'_p$  (best est) overestimating it by 3%. Also the Casagrande method provides a very accurate estimate.

Even though the results for these first two tests confirm the fact that higher estimates of the preconsolidation tests are obtained from higher quality samples, they also seem to indicate that decreasing of the sample is disturbance is associated with increasing overprediction of the  $\sigma'_p$ .

In the highest disturbance case (TX260-ISA $\pm 5$ ) the results indicate a larger uncertainty in the estimate of  $\sigma'_p$  with  $\sigma'_p$  (best est) overestimating the true value of  $\sigma'_p$  by 15% and  $\sigma'_{p(\min)}$  under estimating it by 9%. It must be pointed out once again that in TX260  $K_0$  conditions were not perfectly maintained during the second consolidation.

The results just presented can be interpreted based on the following observations. It has been pointed out in the previous sections that ISA disturbance is associated with a decrease of the effective stresses as well as a restructuring of the soil and that the dominance of one or the other of these two aspects leads to different results (cf. Undrained Strength versus Strain at Peak and Stiffness). Restructuring results in what is generally described as a shrinking of the bounding surface (Burland 1990, Hight et al. 1992) which in the case of the compression behavior means that the soil is not able to reach the original VCL: the "new restructured" soil is characterized by a new relationship between the void ratio and the effective stress, therefore by a new compression curve (cf. Section 6.7.1).

Let's initially consider the limit case in which the only effect of disturbance is represented by the decrease of the effective stresses. In this case reloading to sufficiently high stresses enables the soil to reach the original virgin compression line which is not affected by disturbance. In this simplified model (Figure 6.27a), the lower the  $\sigma'_s$  from which the reloading path starts (here schematically drawn as a straight line), the higher the stress at which the VCL is intercepted. If this were the only effect of disturbance higher preconsolidation pressures would be measured for increasing disturbance.

Let's now consider a second simplified model in which the only effect of disturbance is the change in slope of the VCL resulting from the restructuring of the soil: for increasing disturbance the restructuring is larger and the slope of the "new" VCL is flatter. This simplified model also assumes that  $\sigma'_s$  is constant for any magnitude of disturbance. Figure 6.27b shows the different reloading paths from  $\sigma'_s$  to the "new" VCL

corresponding to the different magnitudes of disturbance. In this case, the value of the stress at which the reloading path intercepts the VCL decreases with increasing disturbance. This is basically the trend in the values of the maximum past pressure estimated by the Strain Energy method when assuming that the initial slope of the curve is zero (cf. Table 6.2:  $\sigma'_{p(\min)}$  is equal to  $1.11\sigma'_{p(\text{true})}$  for  $\text{ISA}\pm 1$ ,  $0.95\sigma'_{p(\text{true})}$  for  $\text{ISA}\pm 2$  and  $0.9\sigma'_{p(\text{true})}$  for  $\text{ISA}\pm 5$ ). This case neglects the initial part of the curve reflecting the different value of  $\sigma'_s$  and the estimate of the maximum past pressure  $\sigma'_{p(\min)}$  reflects only the different slope of the second part of the curve, i.e., the different value of the CR for the "new" VCL.

In reality, the reloading behavior of the soil after disturbance and the point at which the yield surface is crossed will result from a combination of these two simple models. In the case of low disturbance (TX134) for example, the restructuring is limited and the decrease of the effective stresses dominates. For higher disturbance either the restructuring as in TX142, or the stress decrease, as in TX260, may dominate. Based on the limited data it is not possible to determine with more precision the ranges of disturbance within each of the two phenomena dominate.

Figures 6.28a-b present results similar to the ones just shown for specimens of OCR 2 and 4 RBBC subjected to  $\text{ISA}\pm 2$  disturbance and then reconsolidated well past the "in situ" stresses. Comparison of the results of these two tests with those of TX142 ( $\text{ISA}\pm 2$  on NC RBBC) makes it possible to evaluate how, for the same sample quality, the OCR of the soil affects the accuracy with which  $\sigma'_p$  is determined.

The true values of the preconsolidation pressure for TX236 and TX140 are 4.34 and 3.13 ksc respectively. Table 6.3 summarizes the estimates

of the preconsolidation pressure for the three ISA $\pm$ 2 tests. For this moderate level of disturbance the preconsolidation pressure is determined with great accuracy for all three values of the OCR being overestimated by 2.6%, 10% and 2.2% in the NC, OCR2 and OCR4 tests respectively. These results confirm that the value of the preconsolidation pressure is not significantly affected by disturbance.

In conclusion the results presented in this section indicate:

- that it is possible for all levels of disturbance and regardless of the OCR of the soil to estimate the preconsolidation pressure ( $SE \sigma'_p(\text{best est.})$ ) with an accuracy of  $10\pm 5\%$  which for practical purposes is satisfactory.
- that disturbance may lead to overestimating the preconsolidation pressure.

## 6.8 Effect of Stress Relief due to Borehole Drilling

One special test (TX120) was conducted on NC RBBC to evaluate the effect of shear stress relief prior to the penetration of the sampler. The tests described to this point assume that the penetration of the sampler takes place from the ground surface and do not take into account the effects of excavation of the borehole.

In practice prior to the penetration of the sampler the soil is subjected to the disturbance caused by the excavation of the borehole. To minimize this disturbance it is generally suggested to employ heavy weight drilling mud that will partially replace the weight of the soil in the

borehole. In no case will it, however, be possible to totally compensate for the soil excavated with the drilling mud.

In the special test it was assumed that the density of the drilling mud was equal to  $\sim 0.5 \gamma_{\text{soil}}$ . In this case due to the excavation of the borehole the vertical stress at depth  $z$  in the soil changes from  $\gamma_{\text{soil}} \cdot z$  to  $0.5 \gamma_{\text{soil}} \cdot z$  while the horizontal stress is equal to  $K_0 \gamma_{\text{soil}} \cdot z$ . Therefore prior to the penetration of the sampler (ISA disturbance) the stress state of the soil is very close hydrostatic ( $K_0=0.48$  for NC RBBC).

These particular conditions were assumed in the special test TX120. The soil was initially unloaded undrained to zero shear stress to simulate the replacement of soil with the drilling fluid, then sheared following the ISA disturbance cycle (in this case with  $\epsilon_c=1\%$ ) which simulates the penetration of the sampler and the shear stress release due to extrusion from the tube. The specimen was then sheared undrained as in a UU test.

The different phases - shear stress release, ISA disturbance, final shear can be isolated in Figures 6.29a and b which plot respectively the stress strain curves and the stress paths for this complex undrained shear.

The same curves are replotted in Figures 6.30 a-b along with the corresponding curves relative to two "UU ISA $\pm$ 1" tests. It is interesting to observe that, regardless of the initial shear stress release, the values of the effective stress prior to the final shear are practically the same. Also the value of the undrained strength for the final- UU - shear does not seem to be affected by the initial unloading.

These results seem to indicate that the stress relief due to borehole drilling may not significantly affect the soil properties.



One must be careful with extrapolating this result to other situations in which  $\gamma_{\text{drilling fluid}}$  is much less than the  $\gamma_{\text{soil}}$  as is the case when water is used as drilling fluid or no drilling fluid is used at all. In these cases it is possible that the soil fails in extension due to the unloading prior to the penetration of the sampler.

Test	OCR	Test Type	(p'f-p'o)/p'o End of Dist. (%)	(p'f-p'o)/p'o End of ISA (%)	(p'f-p'o)/p'o Due to PSA (%)	IOCR End of Dist
183	1.00	ISA+0.5	44	42	2	3.00
118	1.00	ISA+1	60	58	2	3.75
121	1.00	ISA+1	61	58	3	3.85
123	1.00	ISA+1	59	57	2	3.65
134	1.00	ISA+1	71	68	3	5.37
177	1.00	ISA+1	70	76	-6	5.18
186	1.00	ISA+1	61	50	11	3.92
187	1.00	ISA+1	62	59	3	3.94
208	1.00	ISA+1	62	61	1	3.99
213	1.00	ISA+1	63	N.A	N.A	4.06
164	1.00	ISA+1.5	72	57	15	5.43
122	1.00	ISA+2	83	80	3	9.44
130	1.00	ISA+2	87	70	17	12.35
142	1.00	ISA+2	84	46	38	10.00
168	1.00	ISA+2	82	78	4	8.55
172	1.00	ISA+2	82	78	4	8.90
200	1.00	ISA+2	78	84	-6	6.80
179	1.00	ISA+5	92	90	2	25.66
182	1.00	ISA+5	94	91	3	19.67
117	1.00	PSA	19	-	19	1.96
119	1.00	PSA	23	-	23	1.98
120	1.00	PSA	23	-	23	2.00
171	1.00	PSA	22	-	22	1.95
175	1.00	PSA	23	-	23	1.87
211	1.00	PSA	15	-	15	1.74
241	2.03	ISA+1	50	48	2	2.51
219	2.02	ISA+1	73	72	1	5.24
235	2.02	ISA+2	66	70	-4	3.81
236	1.90	ISA+2	68	63	5	3.71
244	1.98	PSA	1	-	1	1.13
124	4.30	ISA+1	28	26	2	1.40
145	4.40	ISA+1	43	29	14	1.76
231	4.11	ISA+1	35	34	1	1.44
199	4.12	ISA+1	23	24	-1	1.40
127	4.44	ISA+2	65	57	8	3.23
140	4.40	ISA+2	63	58	5	2.65
224	4.24	ISA+2	59	54	5	2.45
232	4.15	ISA+5	87	83	4	8.62
239	4.00	ISA+5	85	79	6	6.62
196	4.13	ISA+8	86	85	1	7.73
125	3.93	PSA	-3	-	-3	0.96
237	8.59	ISA+1	24	35	-11	1.18
242	8.78	ISA+1	21	21	0	1.07
243	7.76	ISA+2	47	44	3	1.79

Table 6.1: Changes in the Effective Stresses due to Disturbance

Test #	OCR	Test Type	Strain Energy										Casagrande	
			$\sigma'_{true}$ (ksc)	$\sigma'_{(min)}$ (ksc)	$\sigma'_{(u)}$ (ksc)	$\sigma'_{(max)}$ (ksc)	$\frac{(\sigma'_{min}-\sigma'_{true})}{\sigma'_{true}}$ (%)	$\frac{(\sigma'_{(u)}-\sigma'_{true})}{\sigma'_{true}}$ (%)	$\frac{(\sigma'_{max}-\sigma'_{true})}{\sigma'_{true}}$ (%)	$(\sigma'_{max}-\sigma'_{min})$ (ksc)	$(\sigma'_{(u)}-\sigma'_{min})$ (ksc)	$\sigma'_{cas}$ (ksc)	$\frac{(\sigma'_{cas}-\sigma'_{true})}{\sigma'_{true}}$ (%)	
TX134	1.00	ISA+1	3.15	3.50	3.60	3.80	11.1	14.3	20.6	0.30	0.10	3.53	12.12	
TX142	1.00	ISA+2	3.12	2.95	3.20	3.50	-5.4	2.6	12.2	0.55	0.25	3.00	-3.80	
TX260	4.40	ISA+5	3.31	3.00	3.80	4.20	-9.4	14.8	27.0	1.20	0.80	N/A	N/A	

- $\sigma'_{true}$ : true preconsolidation pressure
- $\sigma'_{(min)}$ : minimum estimate of the preconsolidation pressure through Strain Energy method
- $\sigma'_{(u)}$ : best estimate of the preconsolidation pressure through Strain Energy method
- $\sigma'_{(max)}$ : maximum estimate of the preconsolidation pressure through Strain Energy method
- $\sigma'_{cas}$ : estimate of the preconsolidation pressure through the Casagrande method

Table 6.2: Comparison of True and Estimated Values of the Preconsolidation Pressure for ISA+1, ISA+2 and ISA+5 Tests on NC RBBC

Test #	OCR	Test Type	Strain Energy								
			$\sigma'_{true}$ (ksc)	$\sigma'_{min}$ (ksc)	$\sigma'_{(u)}$ (ksc)	$\sigma'_{(max)}$ (ksc)	$\frac{(\sigma'_{min}-\sigma'_{true})}{\sigma'_{true}}$ (%)	$\frac{(\sigma'_{(u)}-\sigma'_{true})}{\sigma'_{true}}$ (%)	$\frac{(\sigma'_{(max)}-\sigma'_{true})}{\sigma'_{true}}$ (%)	$(\sigma'_{max}-\sigma'_{min})$ (ksc)	$(\sigma'_{(u)}-\sigma'_{min})$ (ksc)
TX142	1.00	ISA+2	3.12	2.95	3.20	3.50	-5.4	2.6	12.2	0.55	0.25
TX236	1.89	ISA+2	4.34	4.20	4.80	4.90	-3.2	10.6	12.9	0.70	0.40
TX140	4.40	ISA+2	3.13	3.00	3.20	3.45	-4.0	2.2	10.2	0.45	0.20

- $\sigma'_{true}$ : true preconsolidation pressure
- $\sigma'_{(min)}$ : minimum estimate of the preconsolidation pressure through Strain Energy method
- $\sigma'_{(be)}$ : best estimate of the preconsolidation pressure through Strain Energy method
- $\sigma'_{(max)}$ : maximum estimate of the preconsolidation pressure through Strain Energy method
- $\sigma'_{cas}$ : estimate of the preconsolidation pressure through the Casagrande method

Table 6.3: Comparison of True and Estimated Values of the Preconsolidation Pressure for ISA+2 Tests on RBBC with OCR=1, 1.89 and 4.4

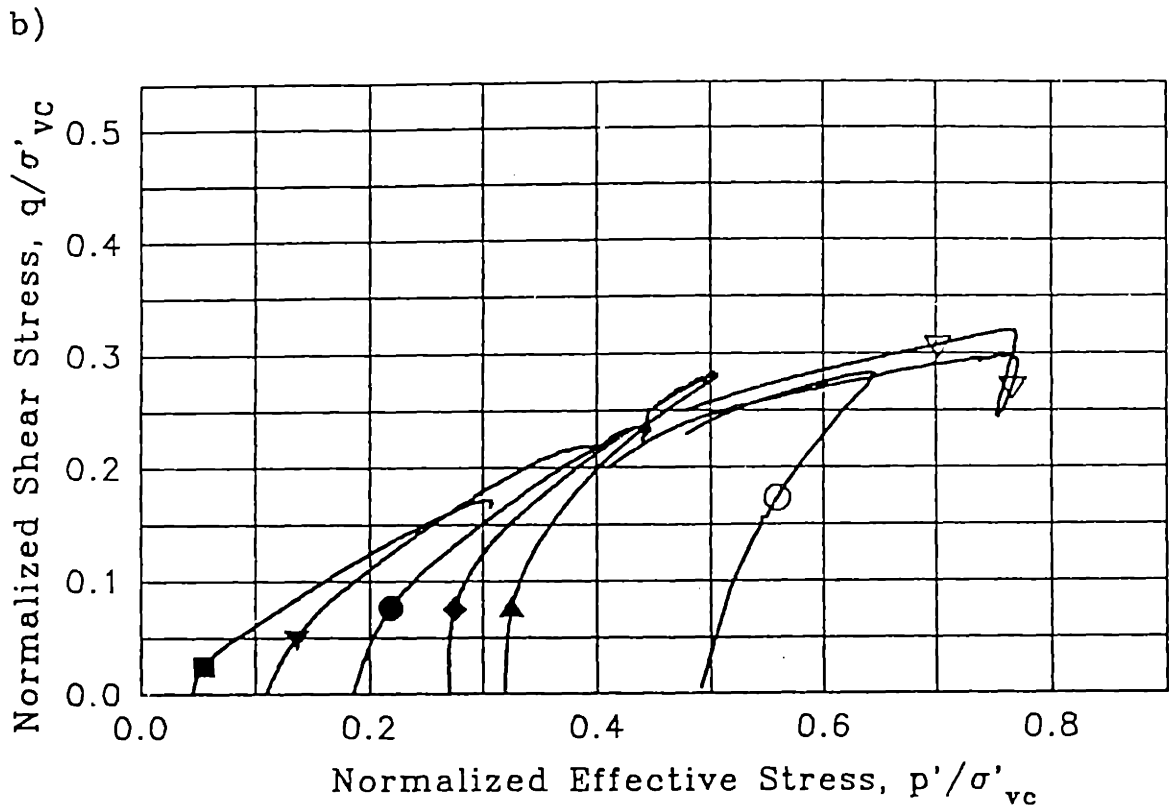
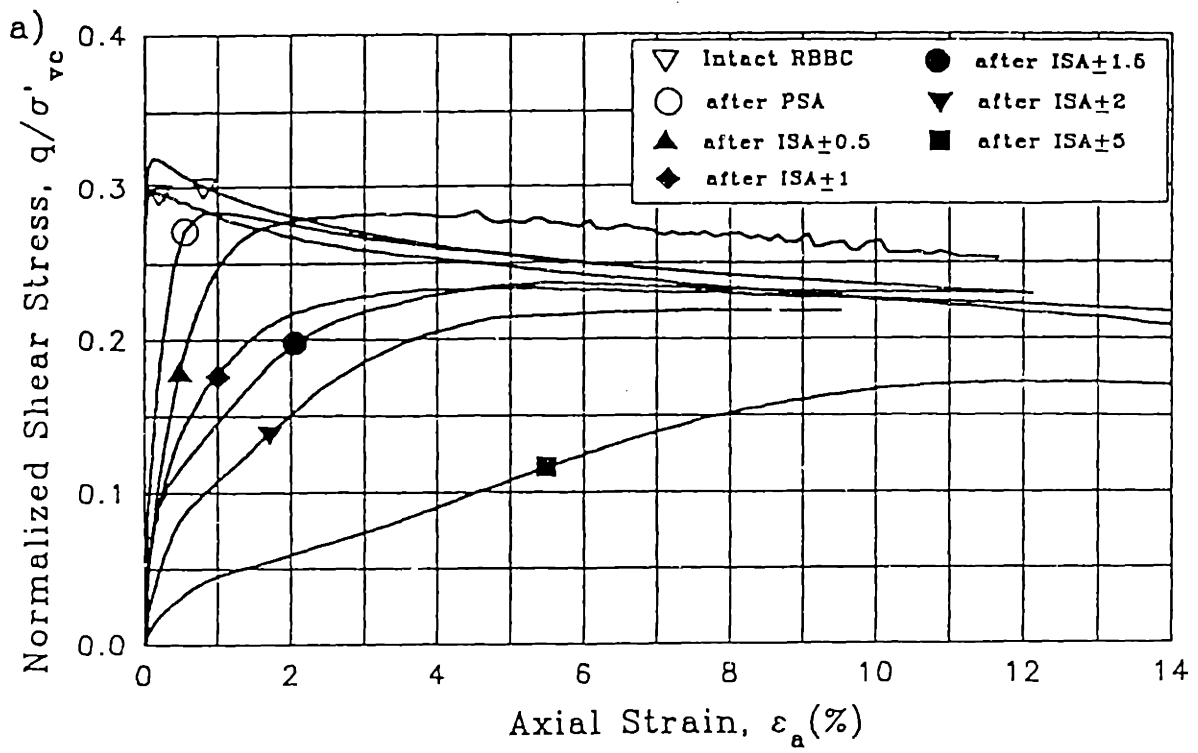


Figure 6.1: Effect of PSA and ISA Disturbance on (a) the Stress Strain Curves and (b) on the Stress Paths of Normally Consolidated RBBC

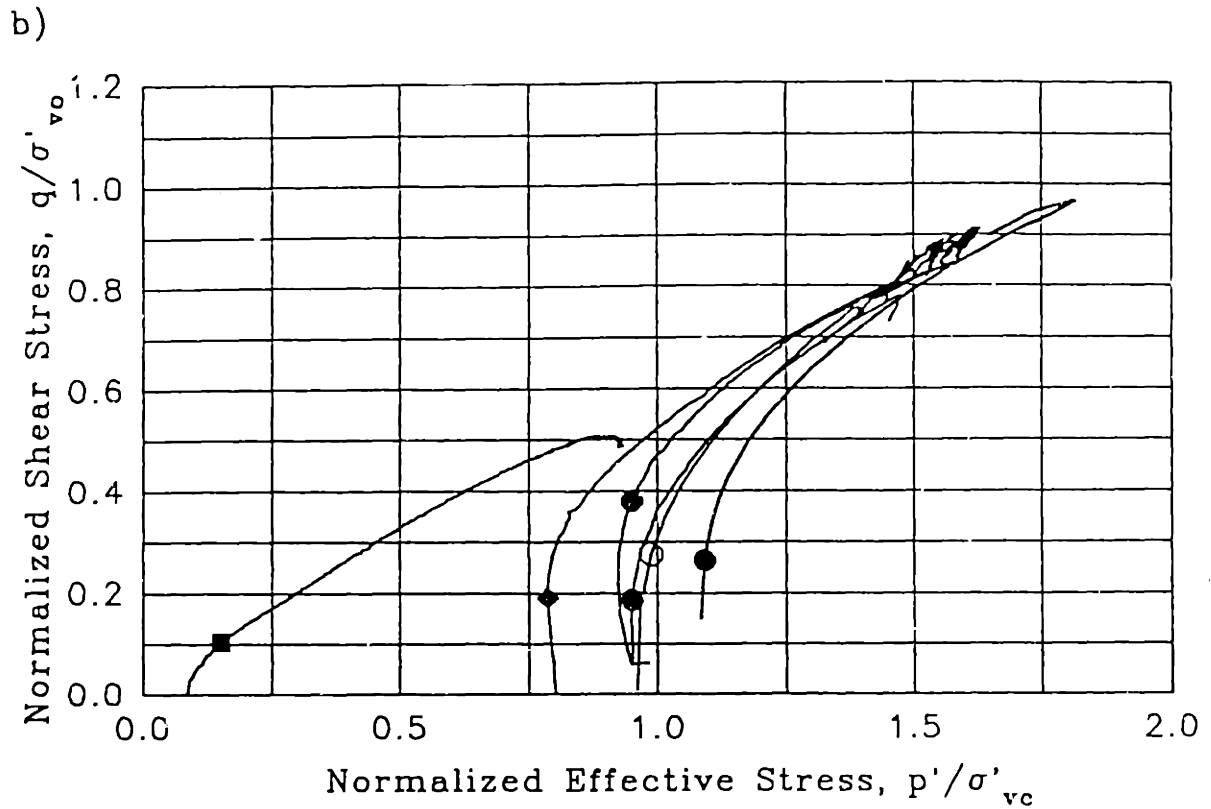
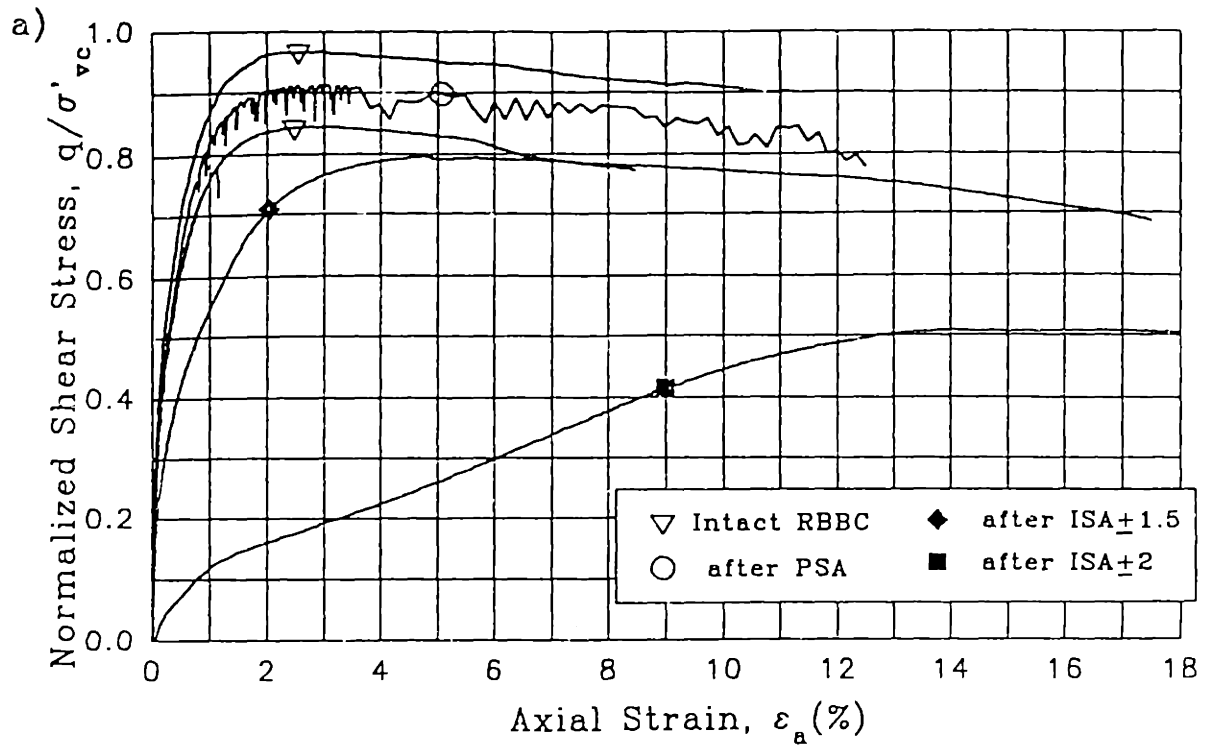


Figure 6.2: Effect of PSA and ISA Disturbance on (a) the Stress Strain Curves and (b) on the Strain Paths of OCR4 RBBC

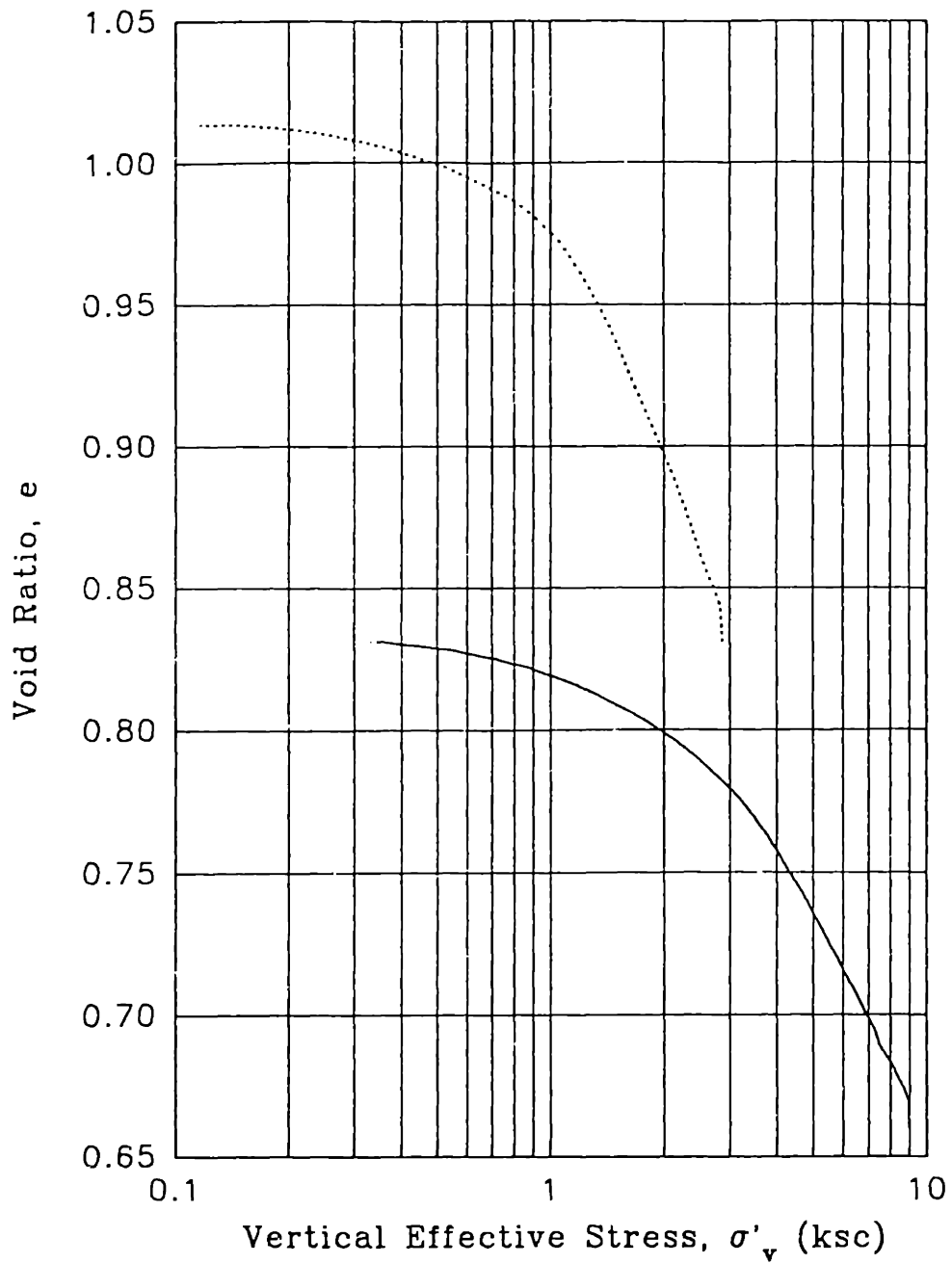


Figure 6.3: Effect of ISA<sub>+2</sub> Disturbance on the Compression Behavior of NC RBBC

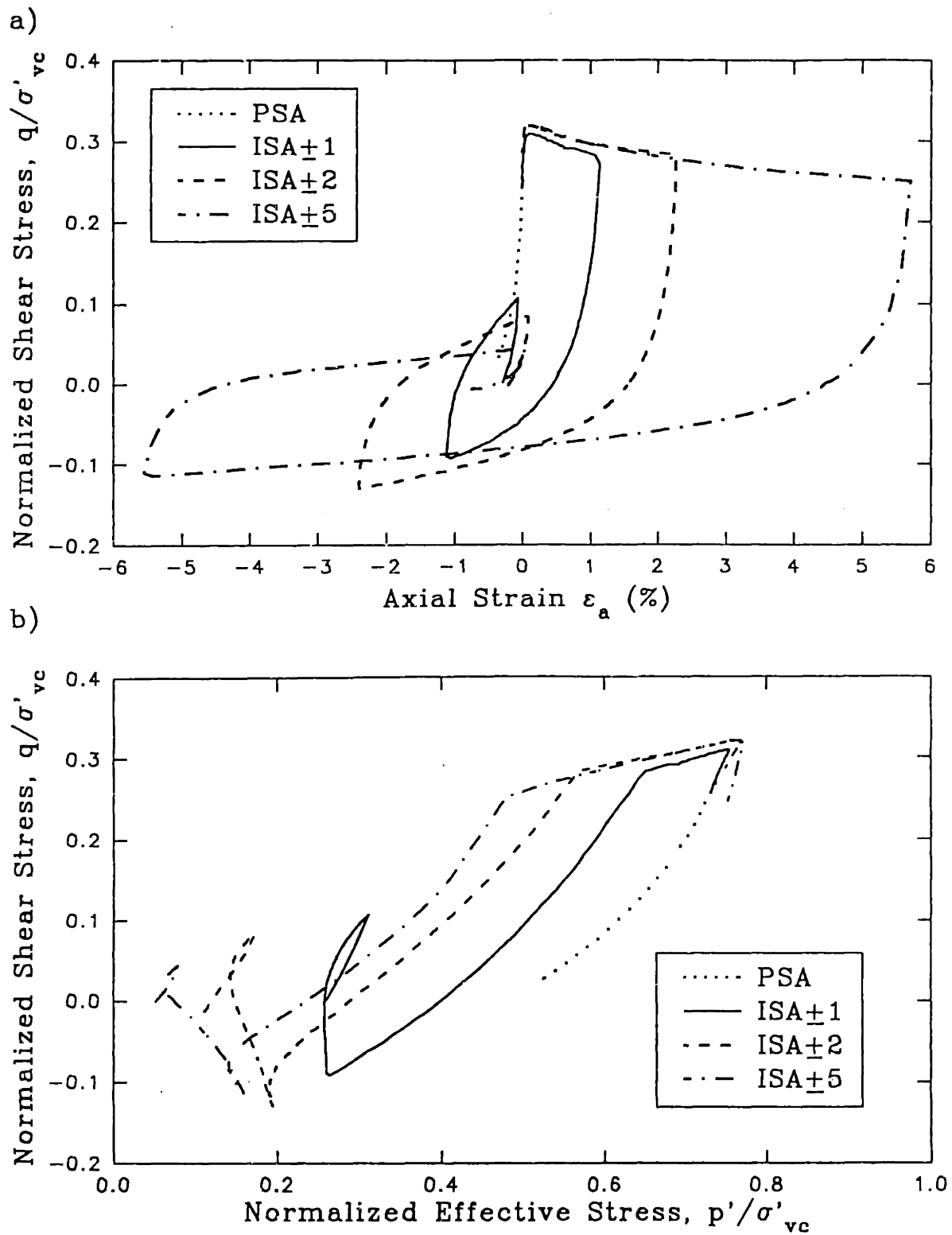


Figure 6.4: Stress Strain Curves (a) and Stress Paths (b) for PSA, ISA±1, ISA±2, and ISA±5 Disturbance of NC RBBC



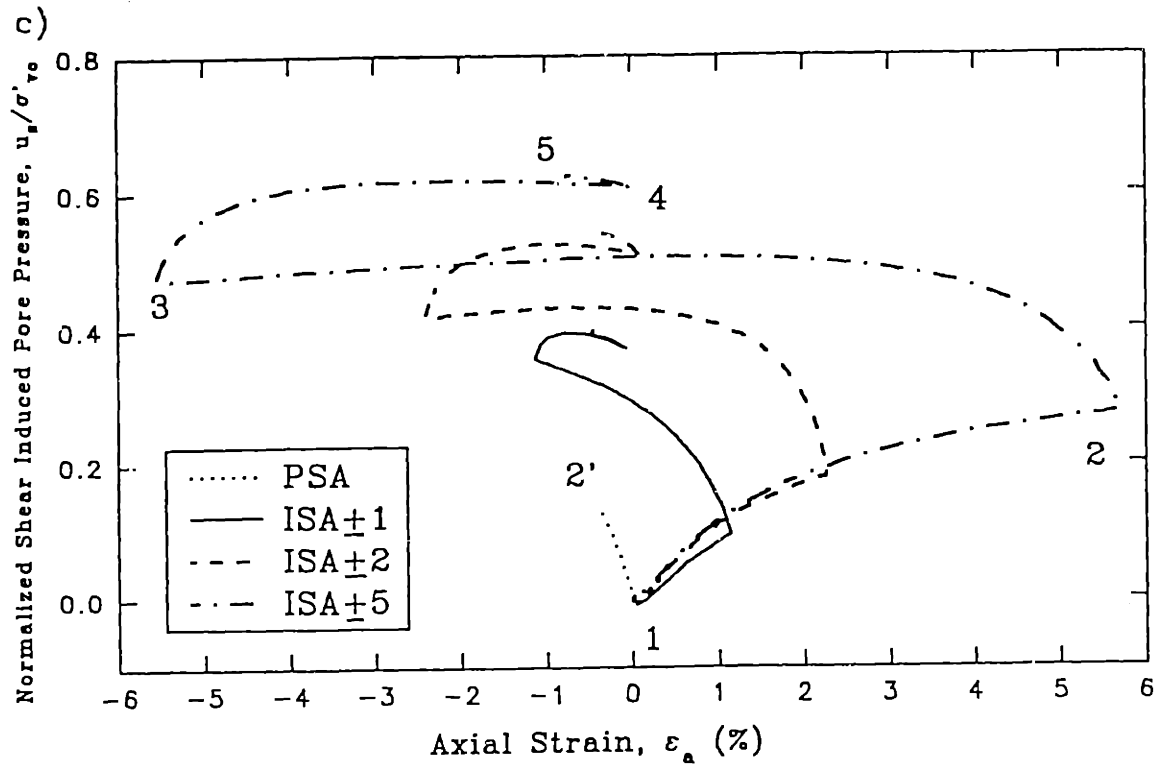


Figure 6.4: (c) Shear Induced Pore Pressure During PSA, ISA $\pm$ 1, ISA $\pm$ 2 and ISA $\pm$ 5 Disturbance of NC RBBC

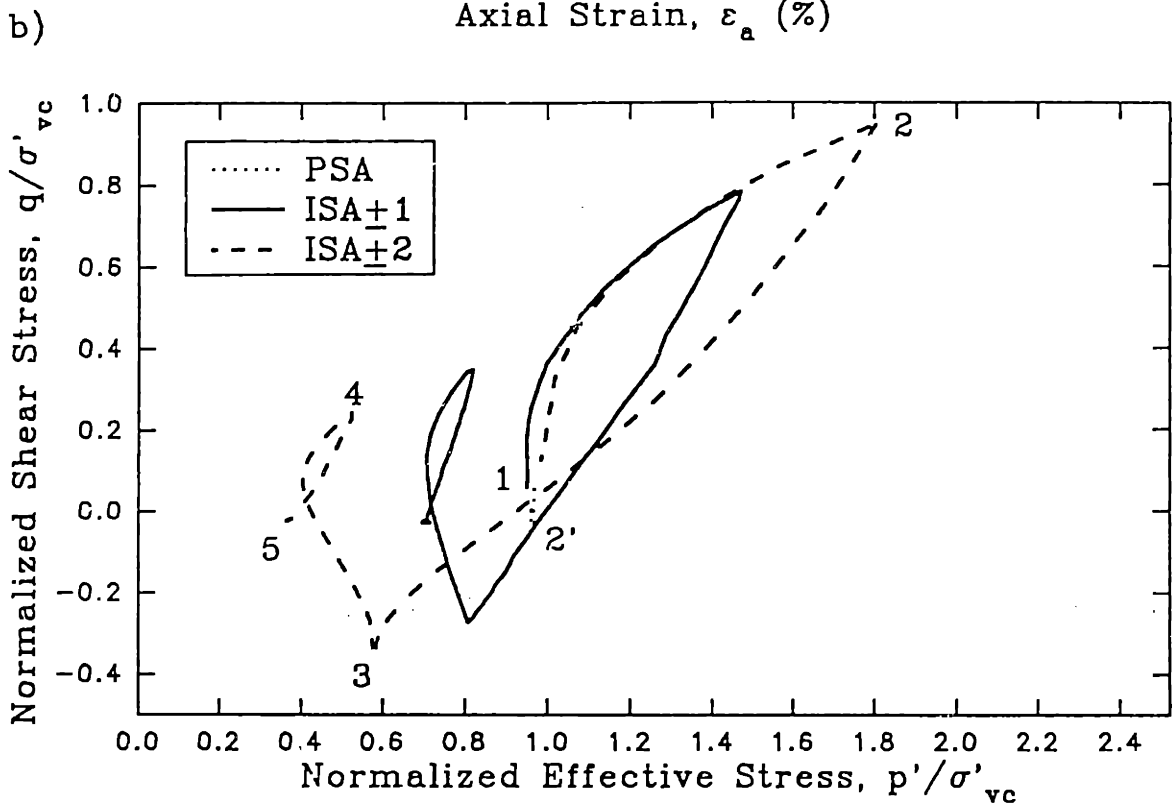
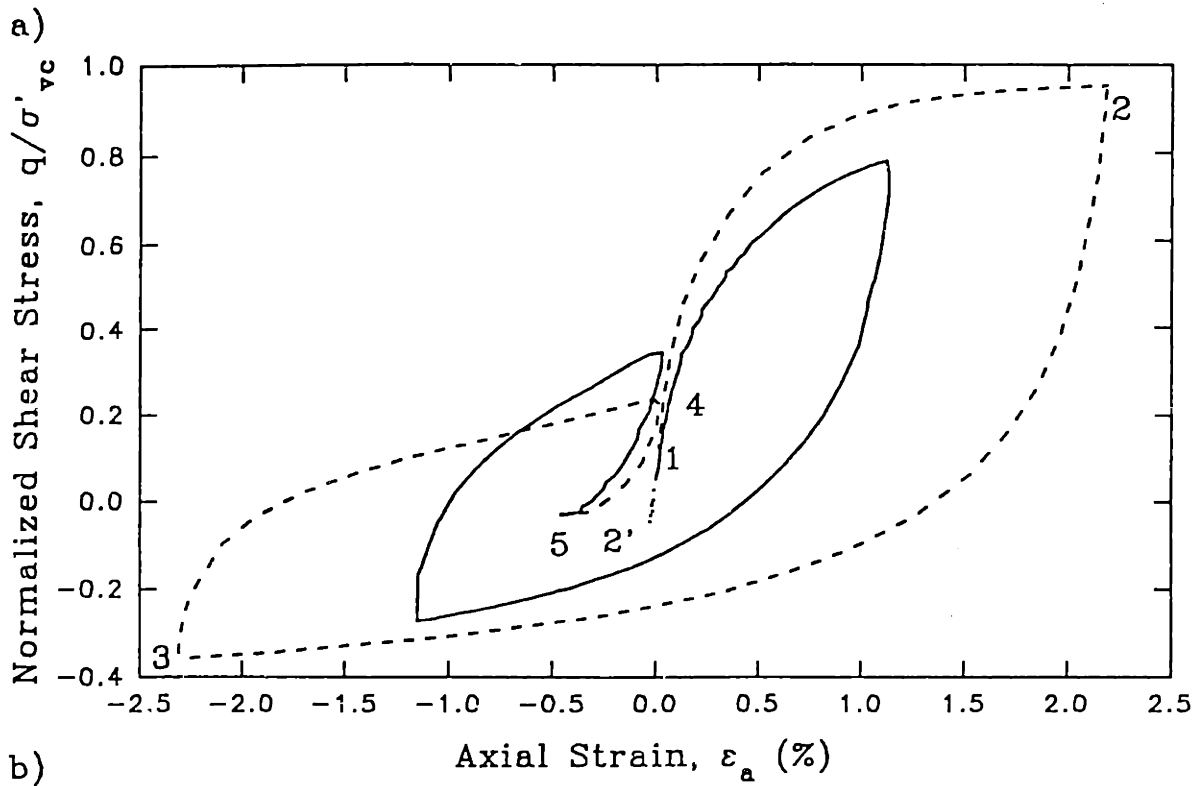


Figure 6.5: Stress Strain Curves (a) and Stress Paths (b) for PSA, ISA $\pm$ 1 and ISA $\pm$ 2 Disturbance of of OCR4 RBBC

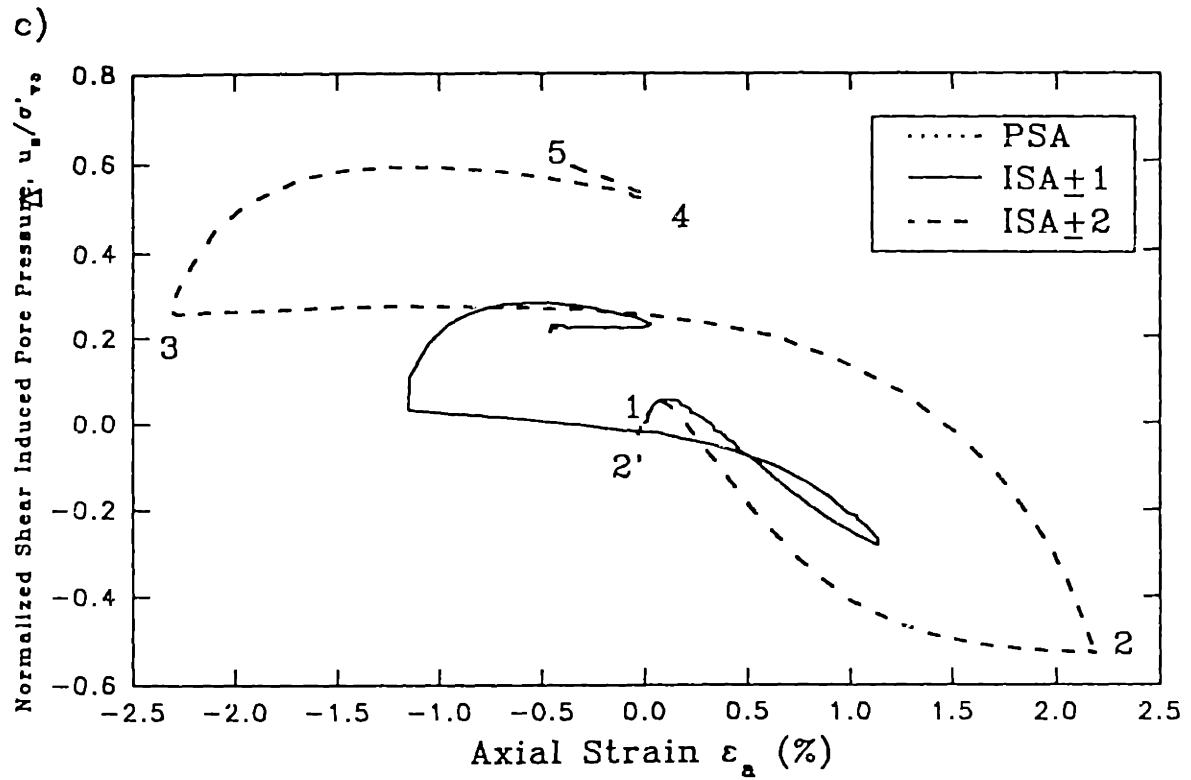


Figure 6.5: (c) Shear Induced Pore Pressure During PSA, ISA+1 and ISA+2 Disturbance of OCR4 RBBC

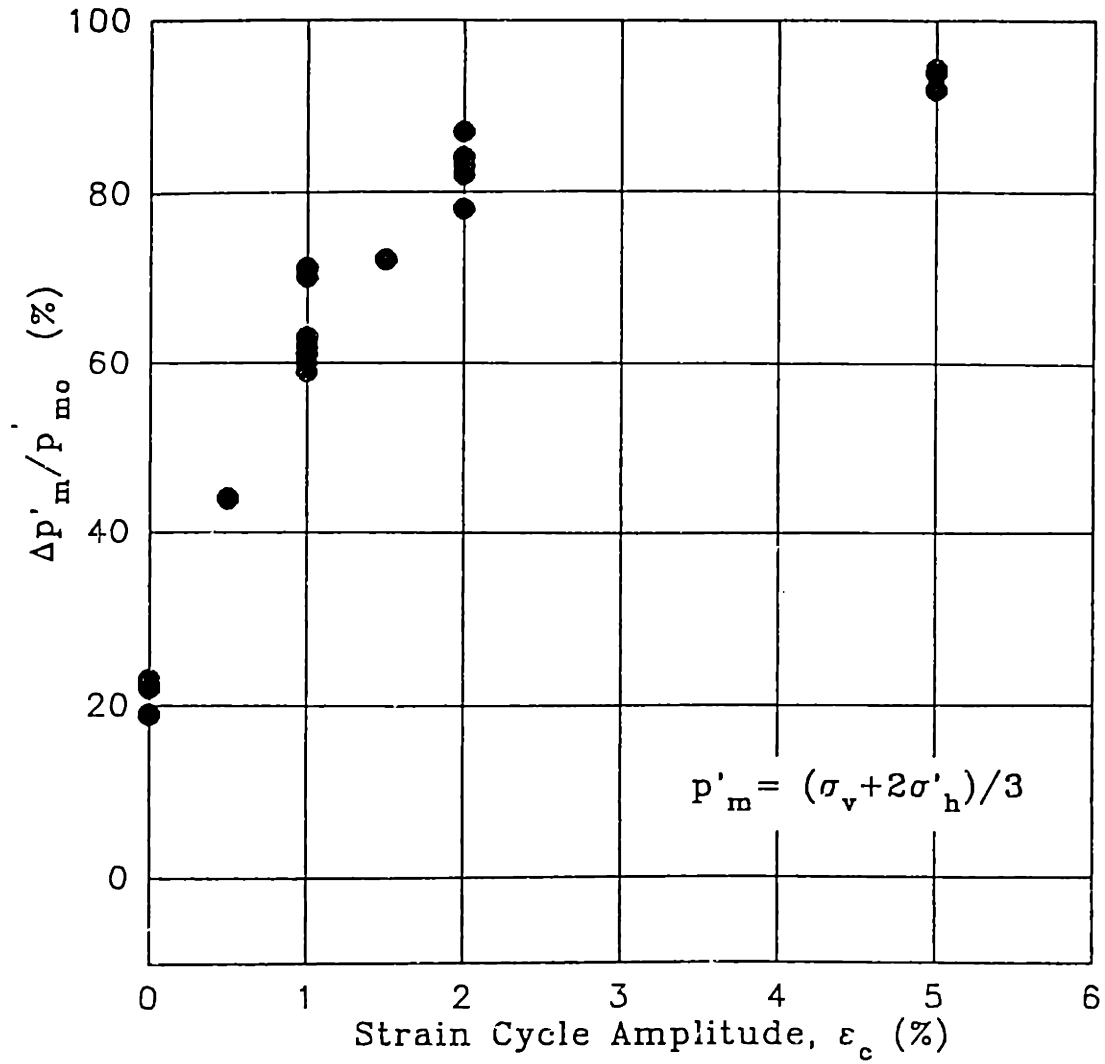


Figure 6.6: Loss in Mean Effective Stress due to PSA and ISA Disturbance for NC RBBC

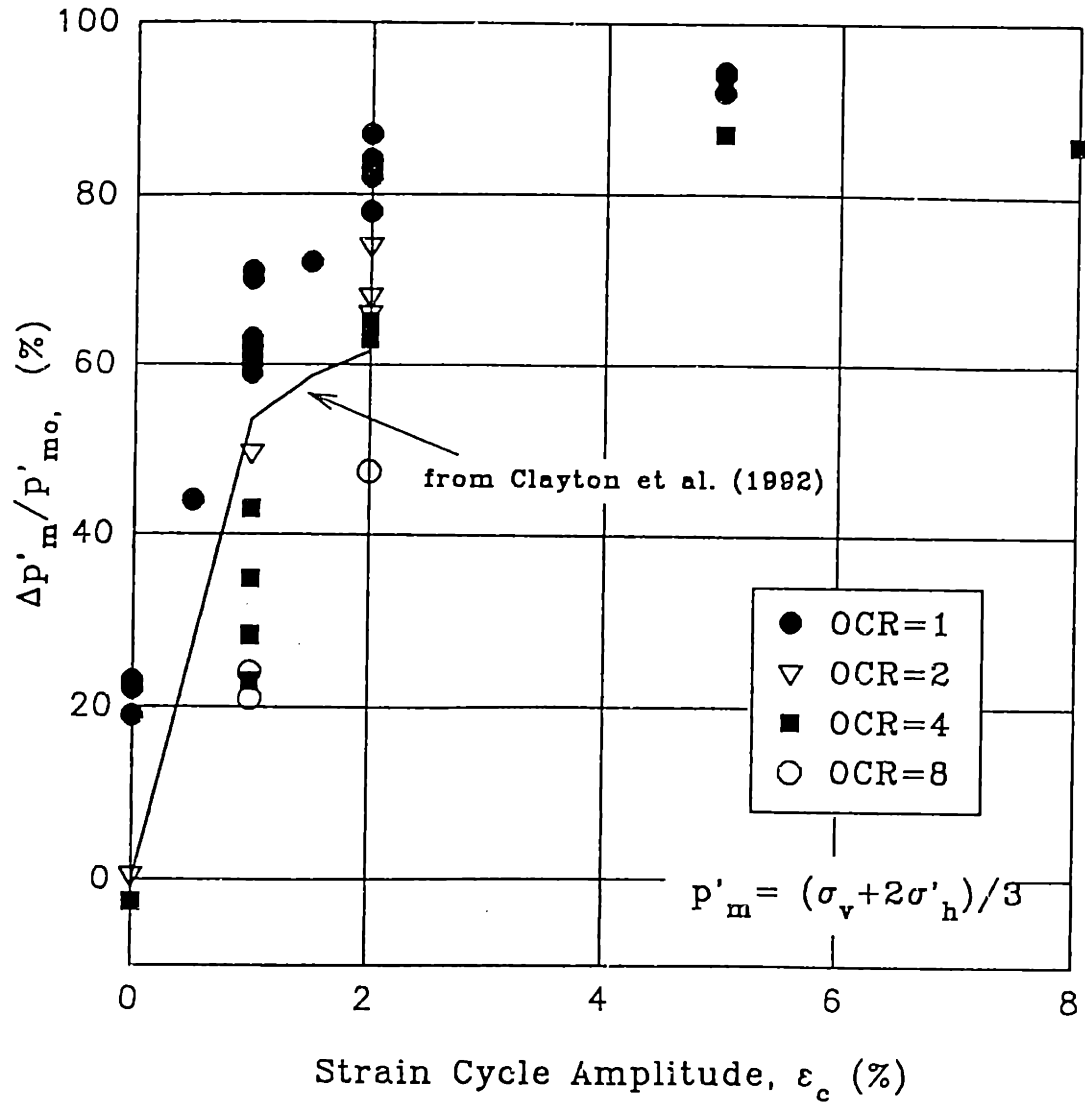


Figure 6.7: Loss in Mean Effective Stress due to PSA and ISA Disturbance for NC and OC RBBC

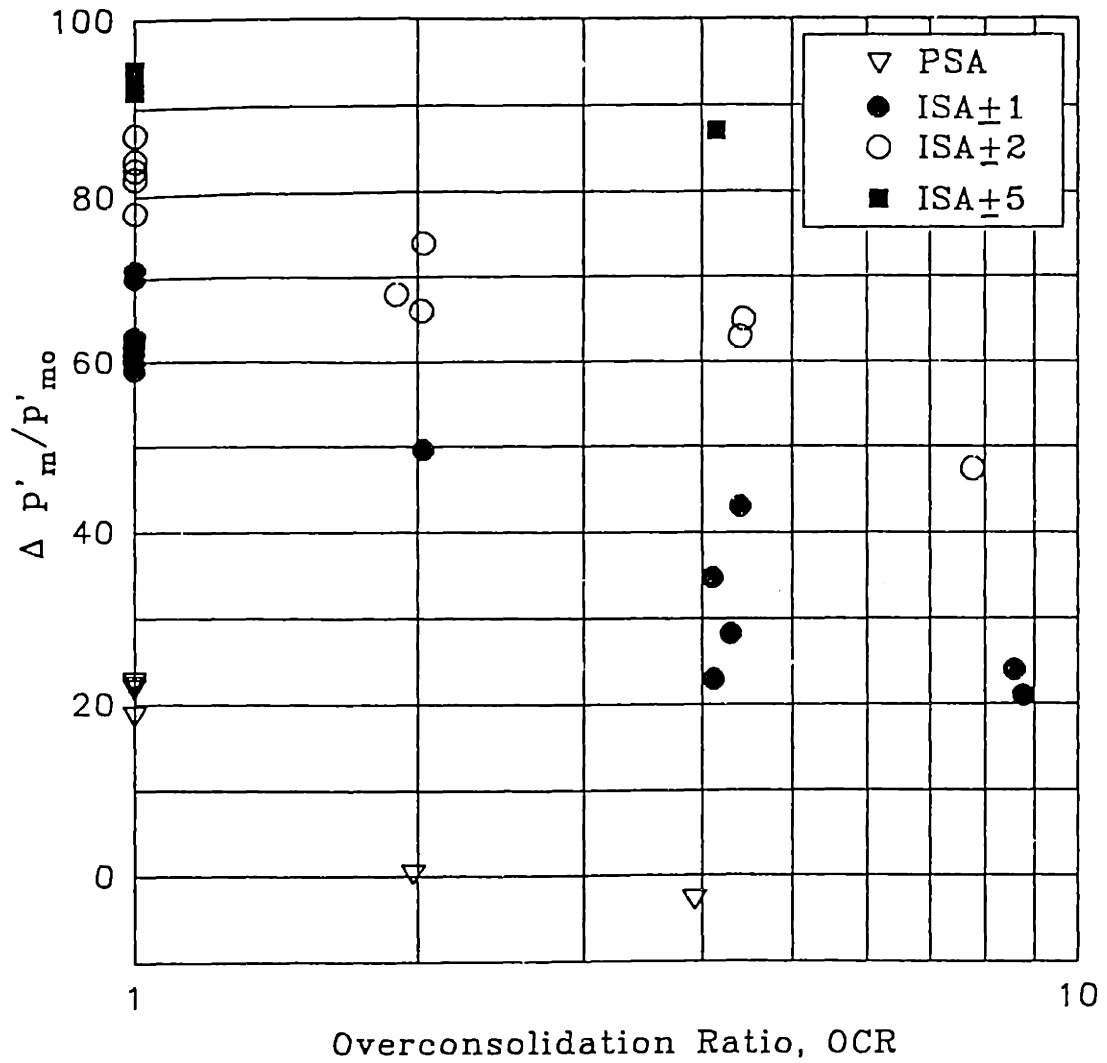


Figure 6.8: Loss in Mean Effective Stress due to Disturbance as a Function of the OCR and the Amplitude of the Disturbance Cycle

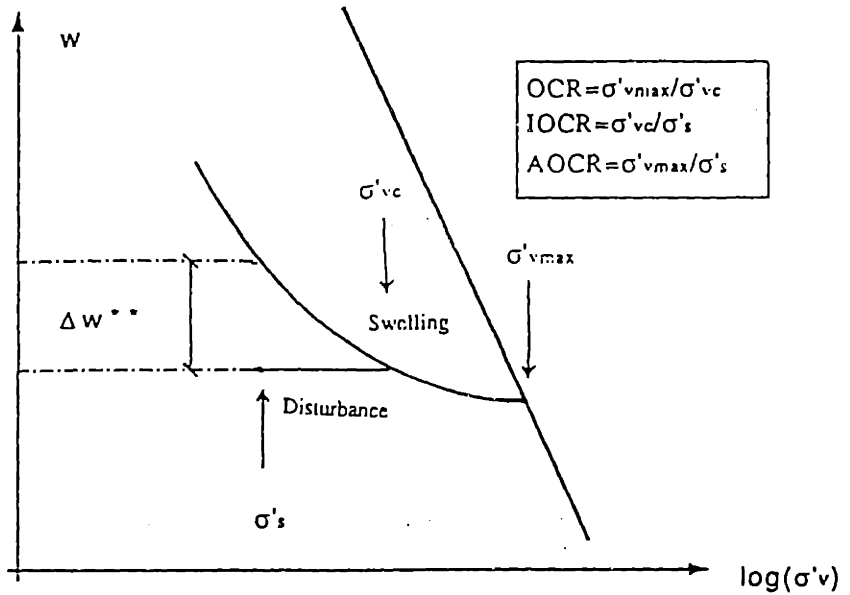
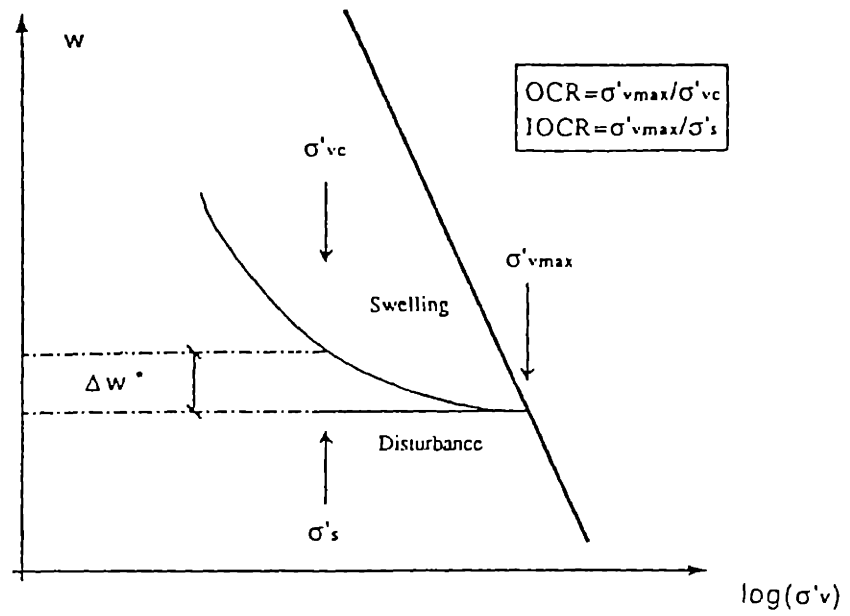


Figure 6.9: Schematic Representation of Effects of Swelling and Disturbance: (a) NC RBBC, (b) OC RBBC

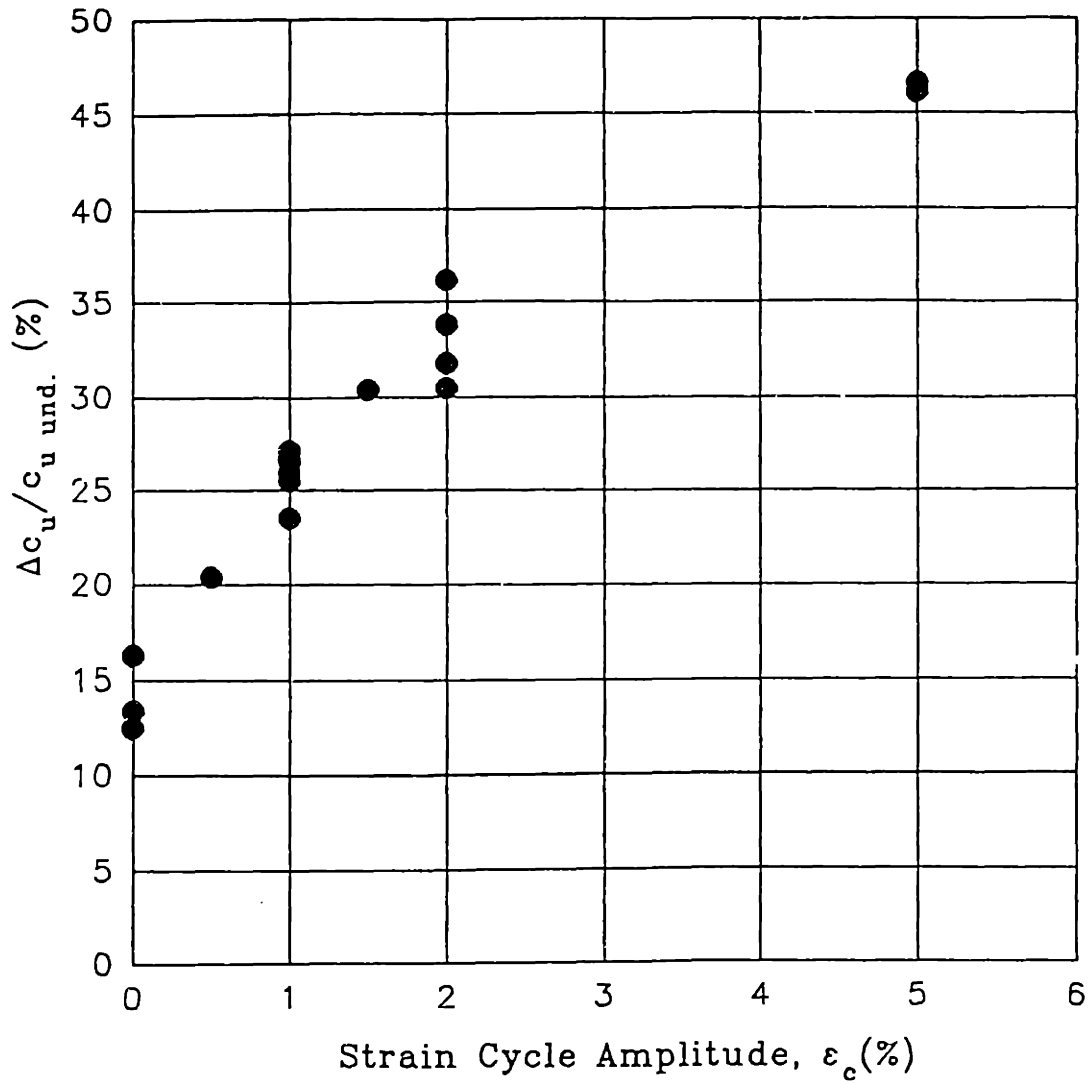


Figure 6.10: Decrease in Strength of NC RBBC due to PSA and ISA Disturbance



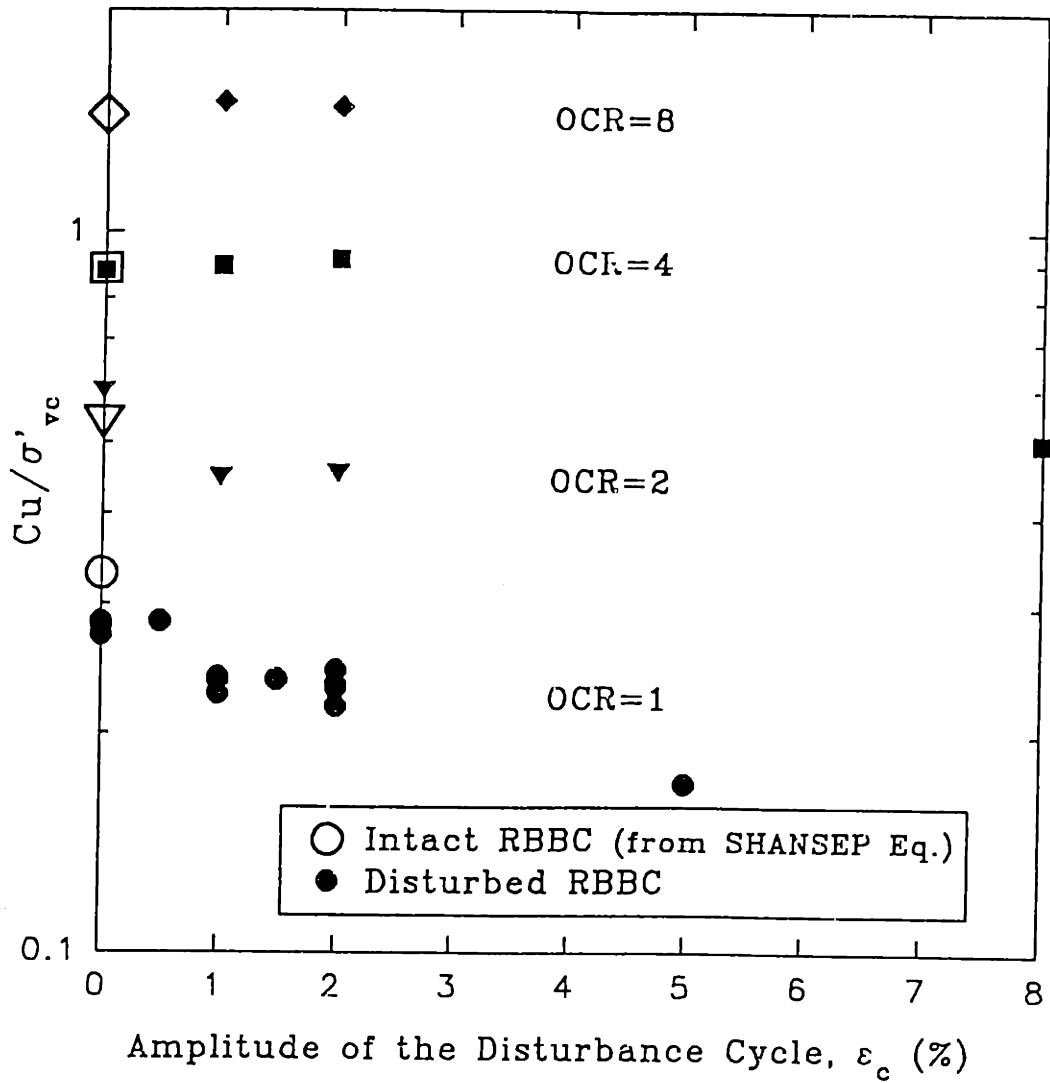


Figure 6.11: Effect of ISA and PSA Disturbance on the Undrained Strength of NC and OC RBBC.

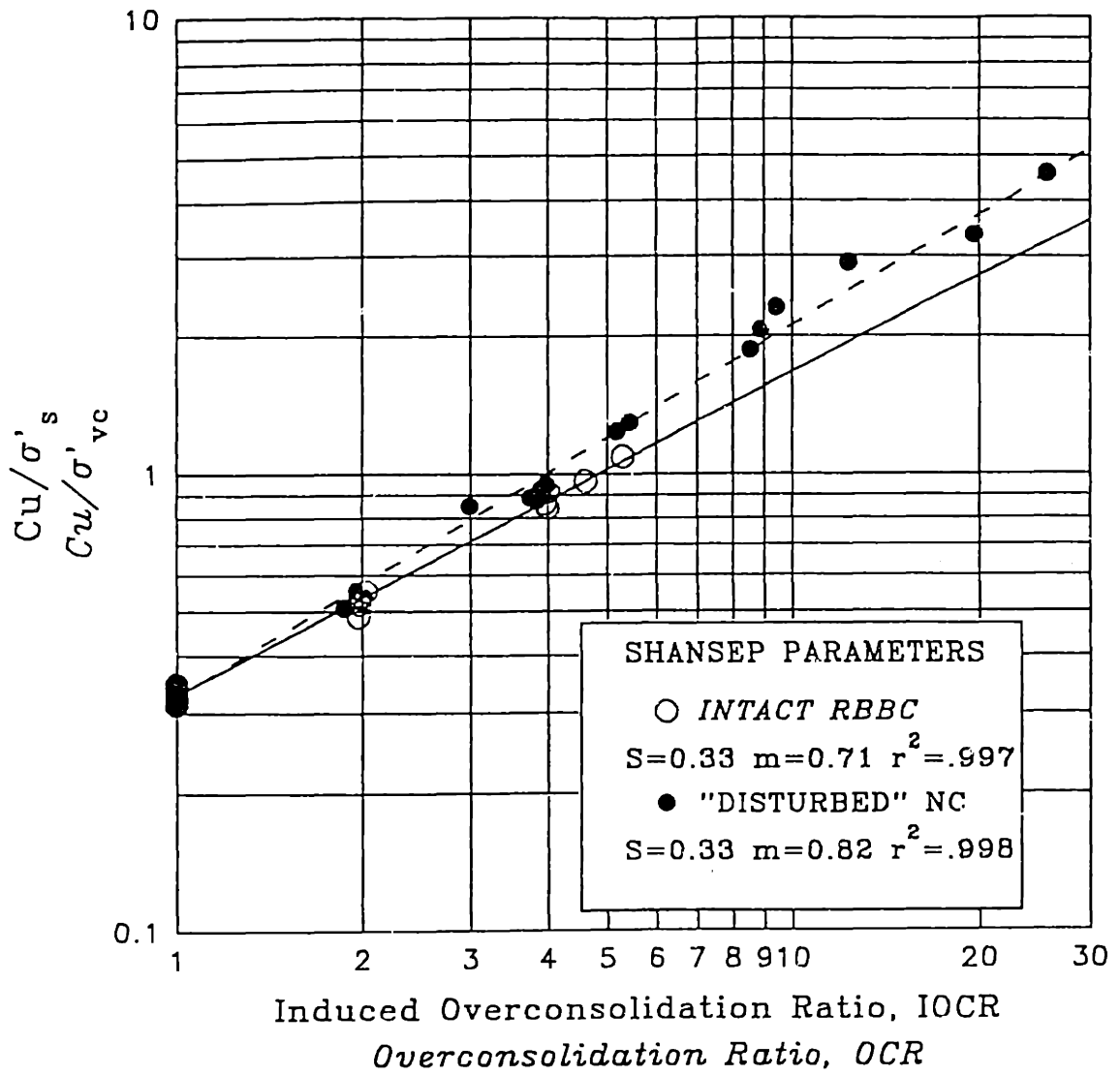


Figure 6.12: SHANSEP Relationship between  $C_u/\sigma'_s$  and IOCR for Disturbed NC RBBC

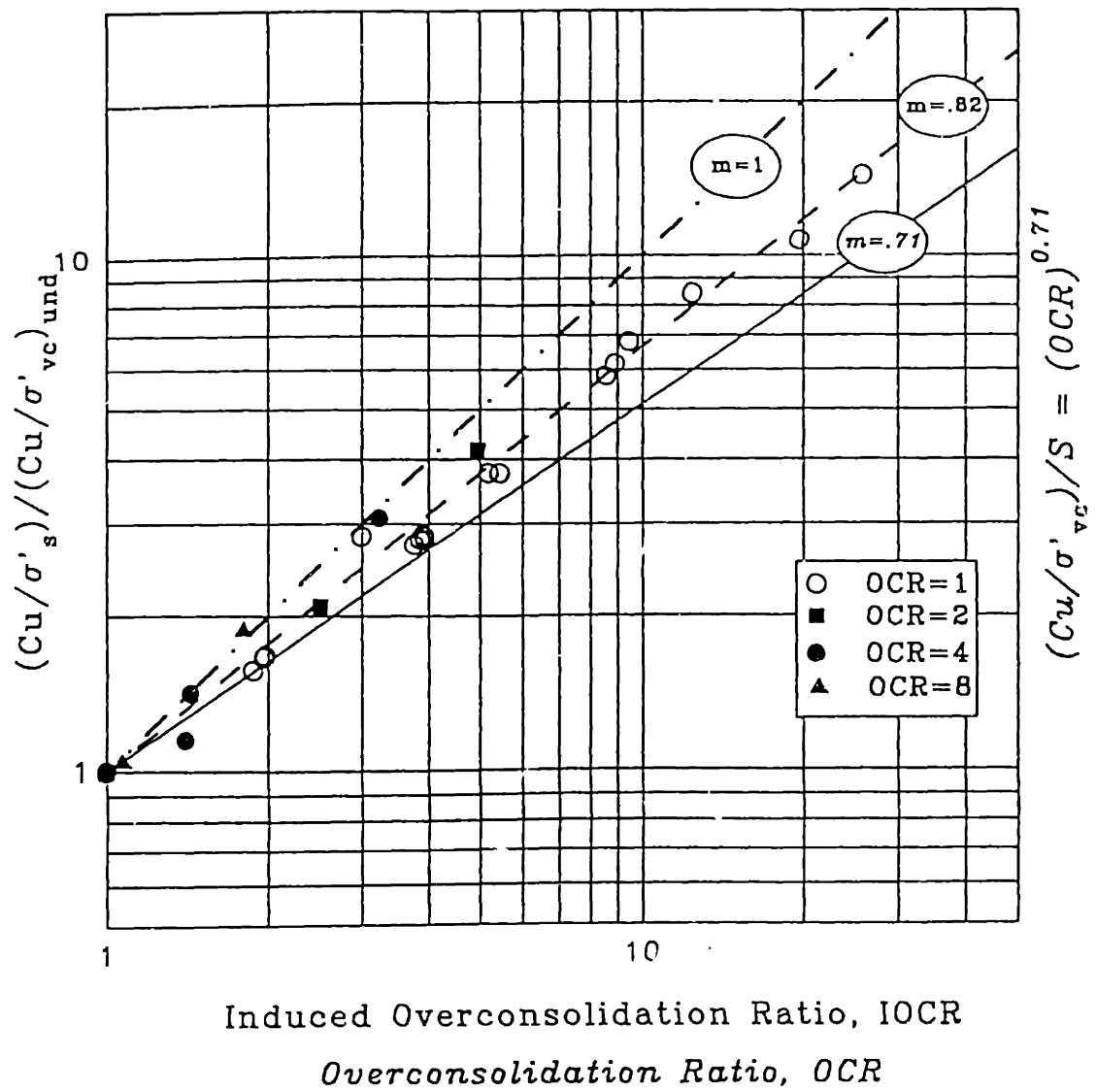


Figure 6.13: SHANSEP Relationship for Disturbed RBBC

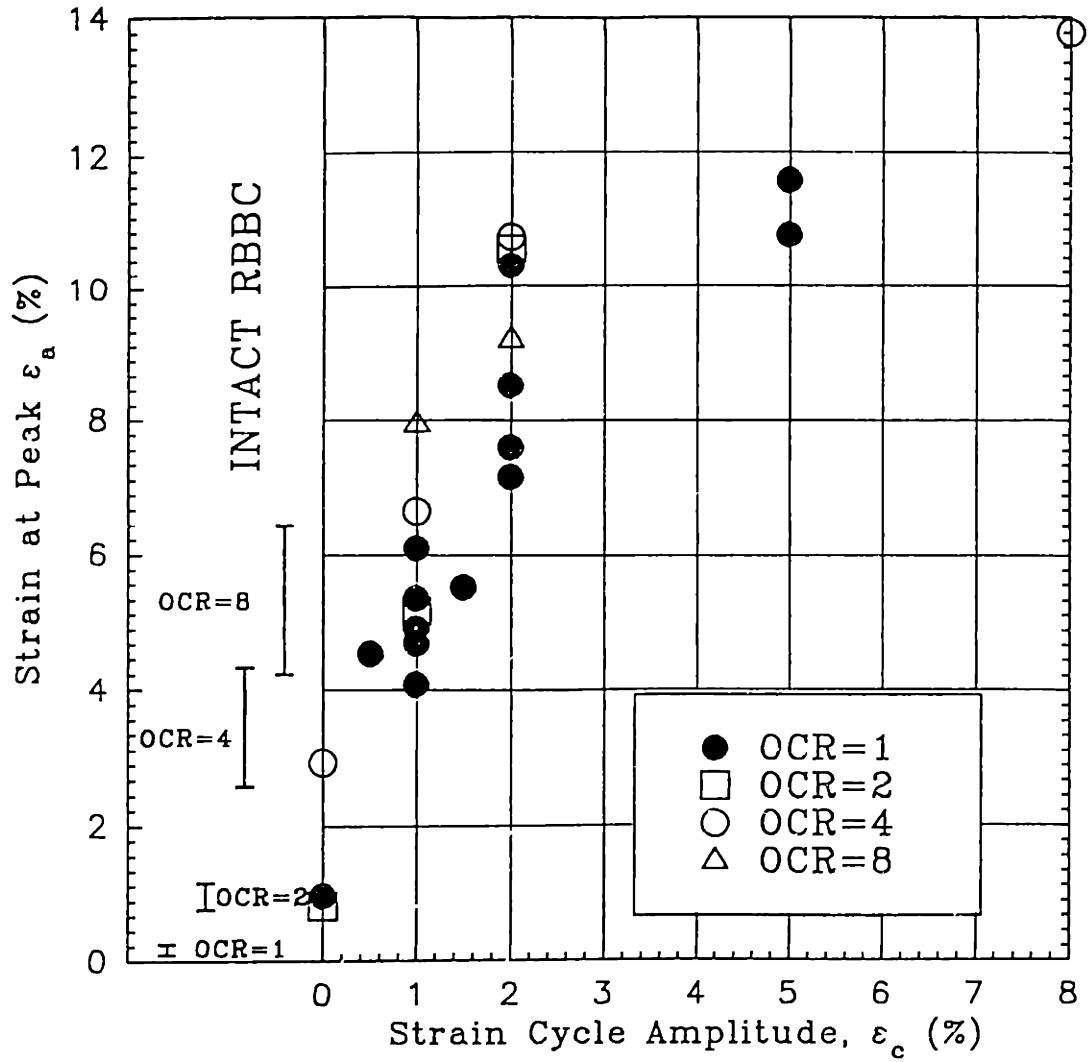


Figure 6.14: Strain at Peak after PSA and ISA Disturbance of RBBC

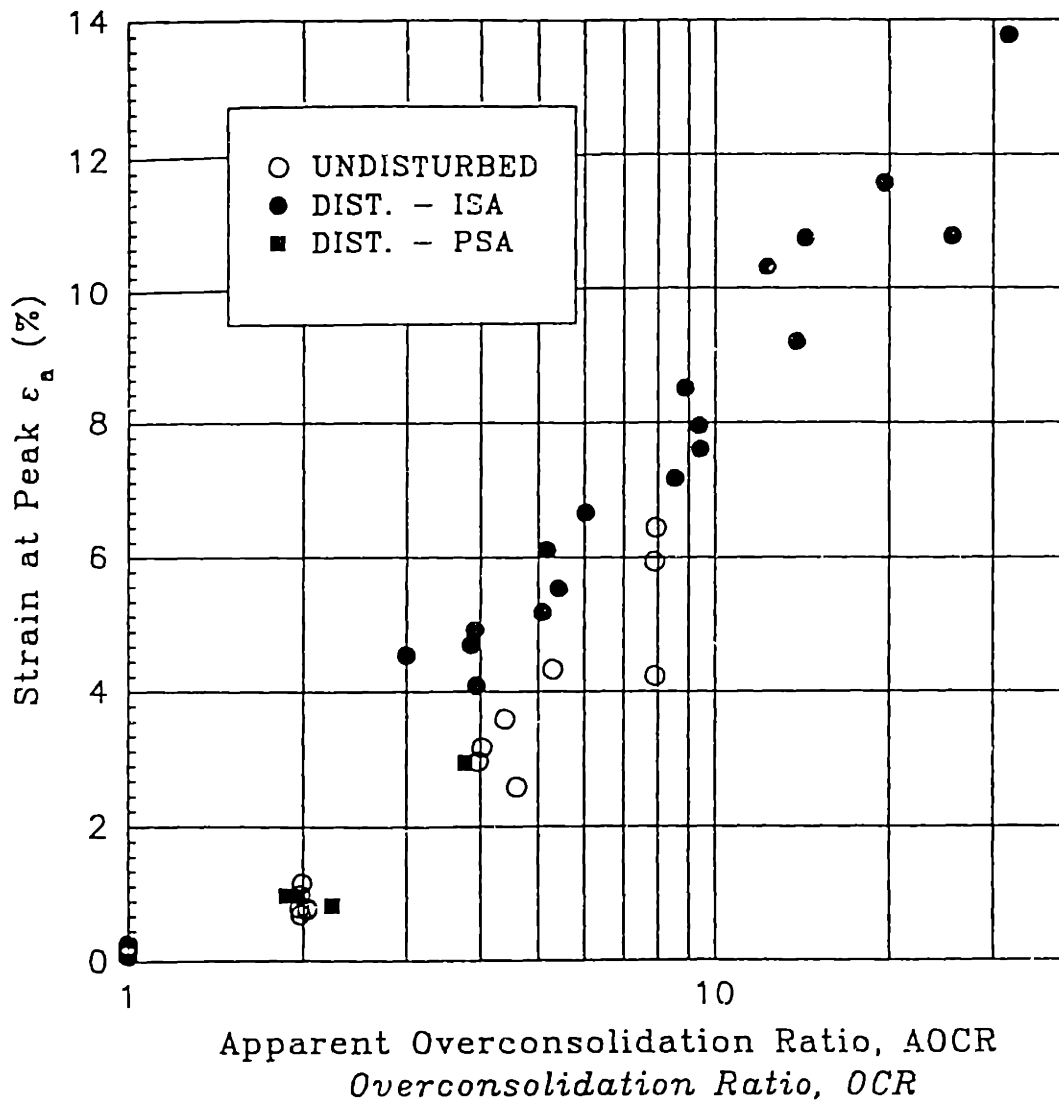


Figure 6.15: Strain at Peak versus AOOCR for Intact and Disturbed RBBC

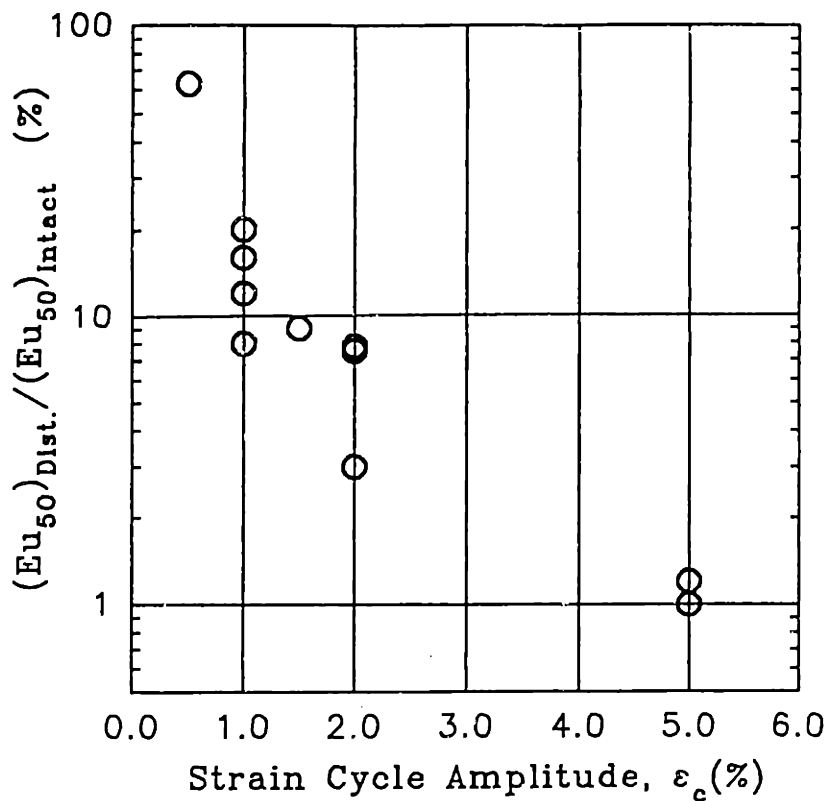


Figure 6.16: Effect of ISA Disturbance on  $Eu_{(50)}$  for NC RBBC

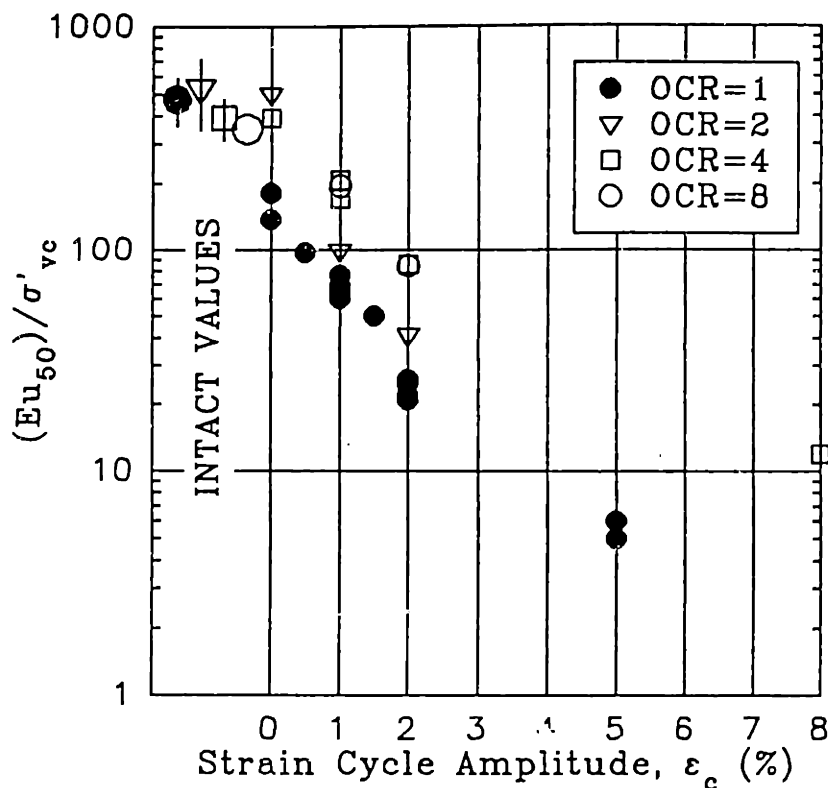


Figure 6.17: Decrease of  $Eu_{50}$  due to Disturbance in RBBC

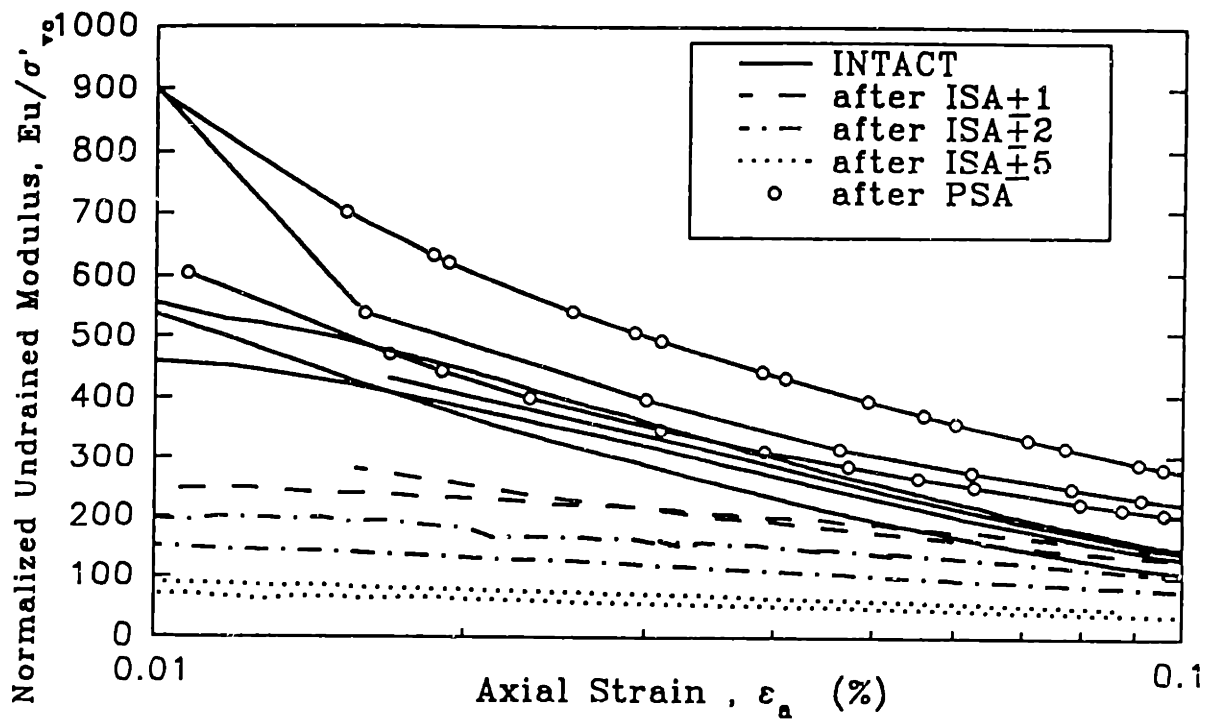


Figure 6.18: Effect of Disturbance on the Intermediate Strain Stiffness of NC RBBC

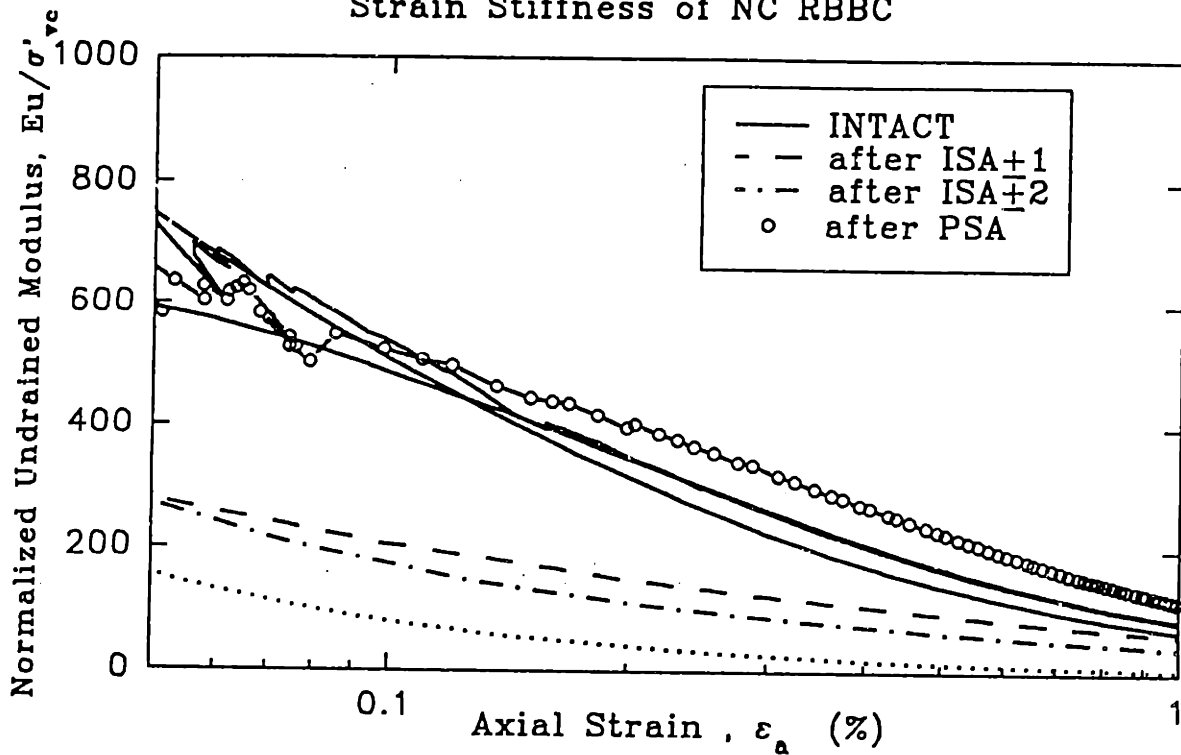


Figure 6.19: Effect of Disturbance on the Intermediate Strain Stiffness of RBBC with OCR=2

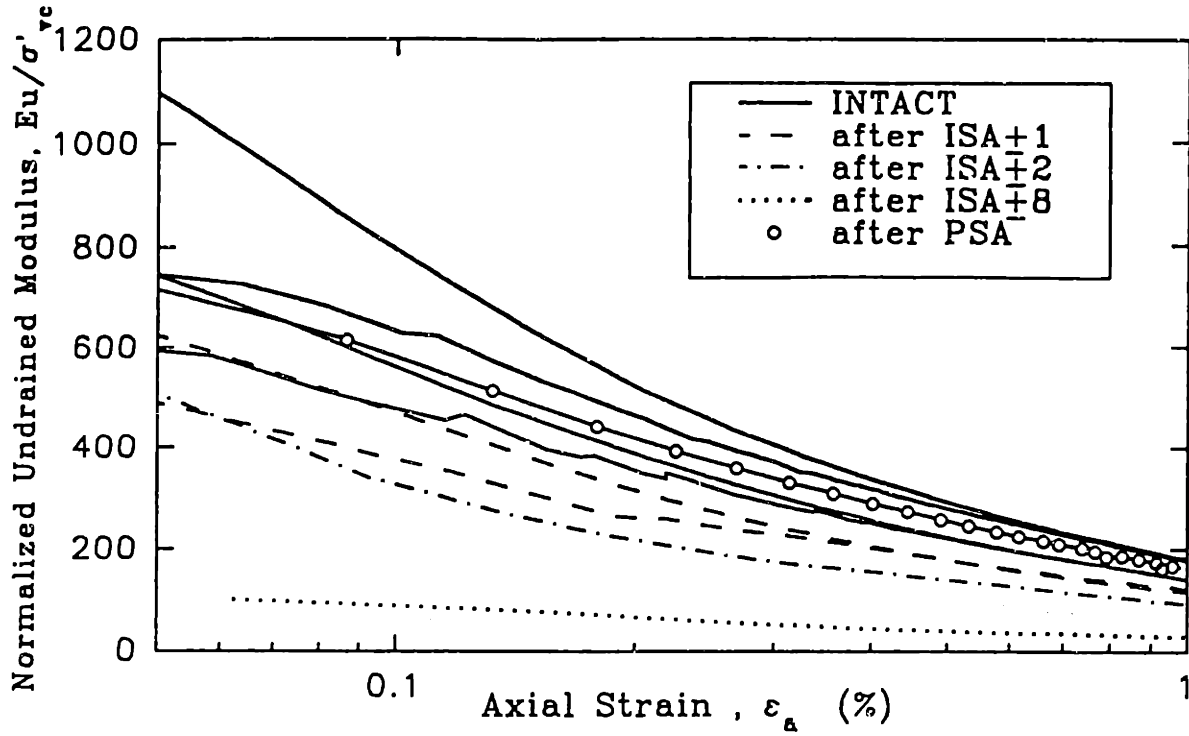


Figure 6.20: Effect of Disturbance on the Intermediate Strain Stiffness of RBBC with OCR=4



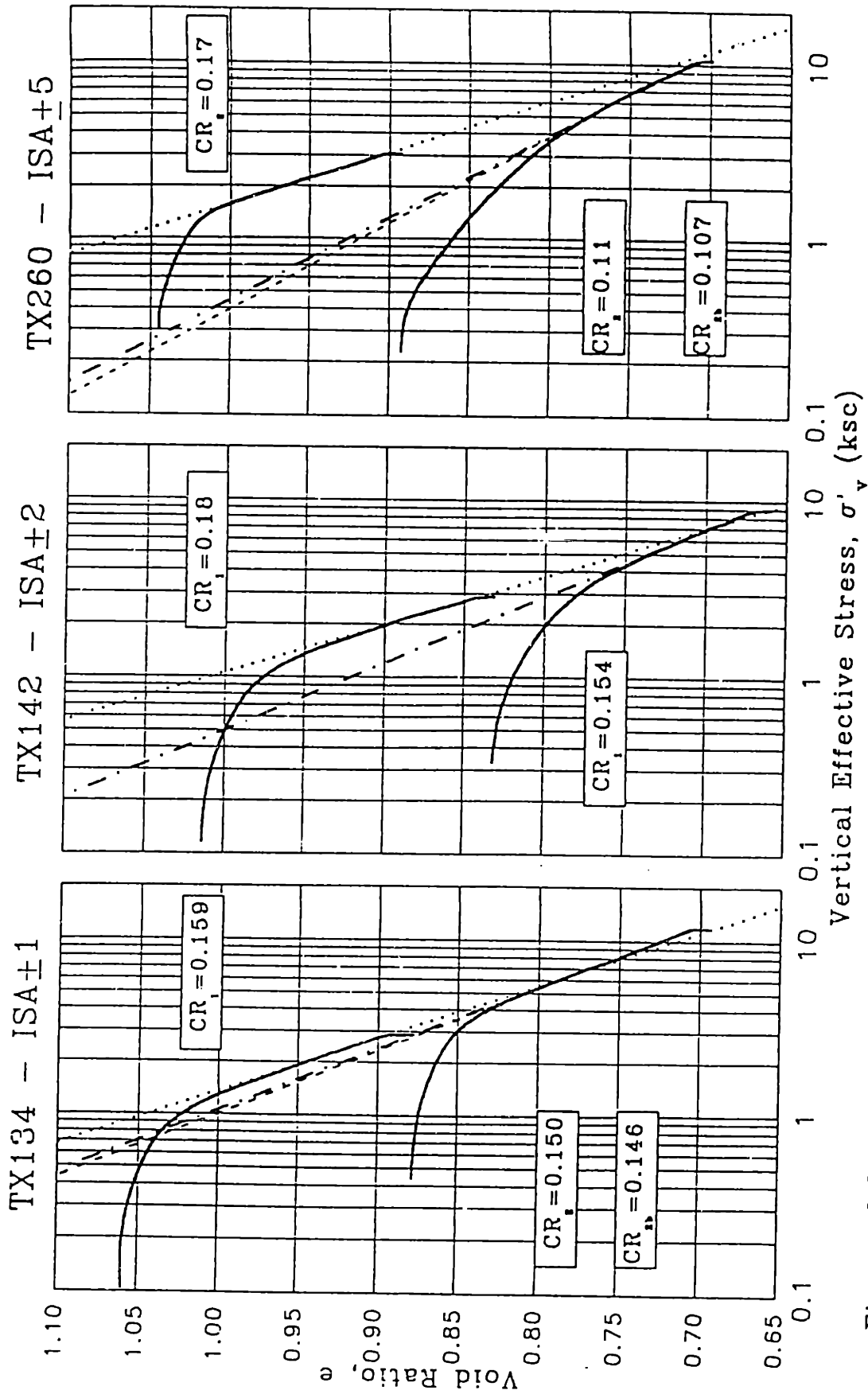


Figure 6.21: Effect of ISA Disturbance on the Compression Behavior of NC RBBC

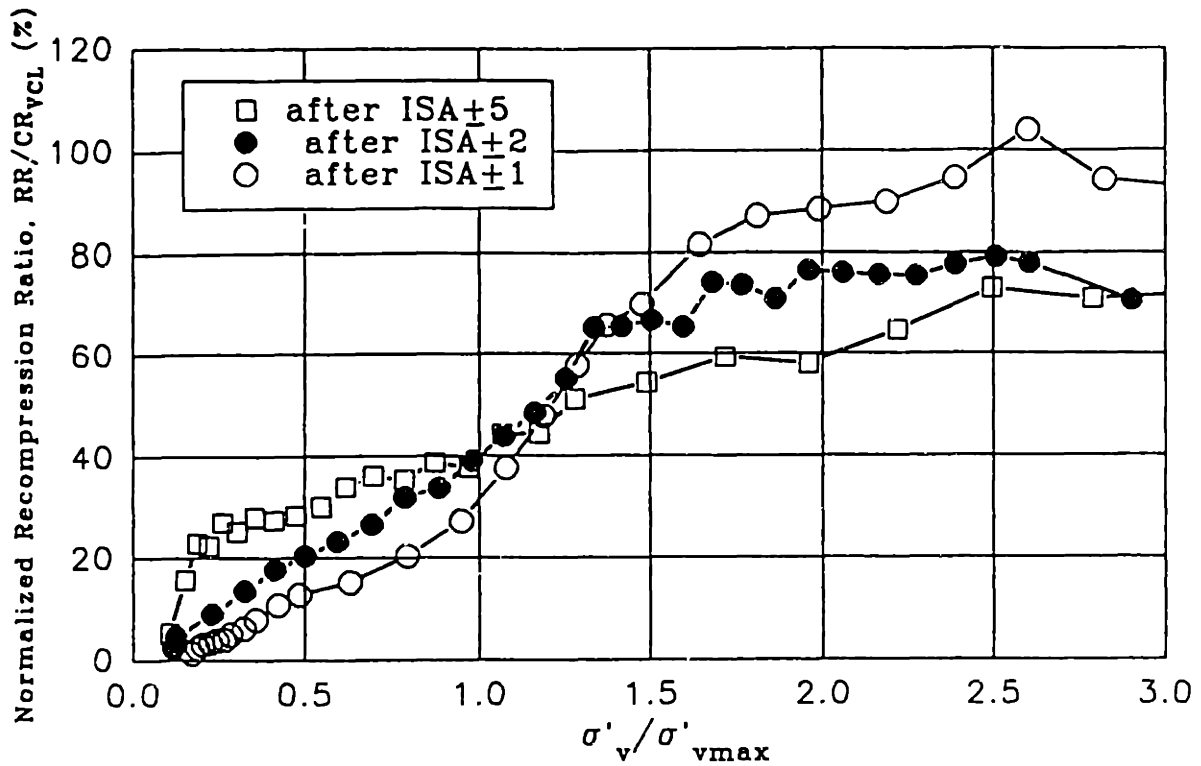


Figure 6.22: Effect of Disturbance on the Compression Behavior of NC RBBC

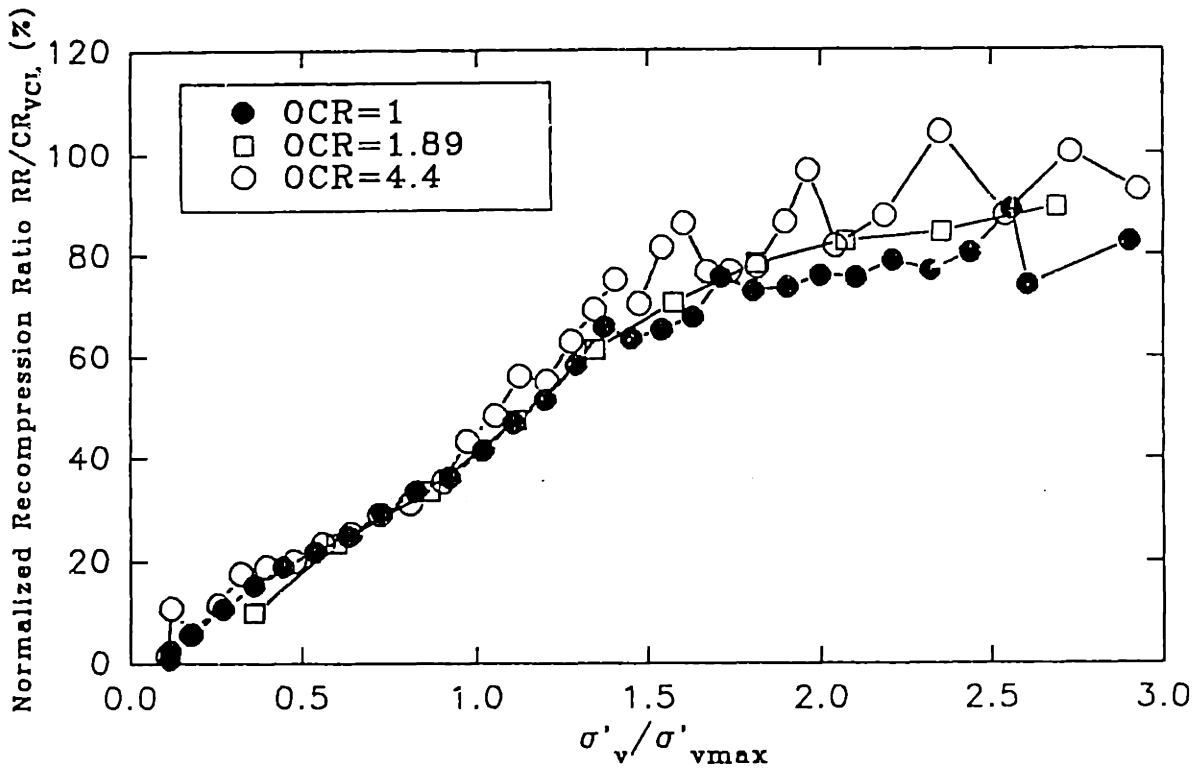


Figure 6.23: Effect of ISA+2 Disturbance on the Compression Behavior of RBBC (OCR=1,2,4)

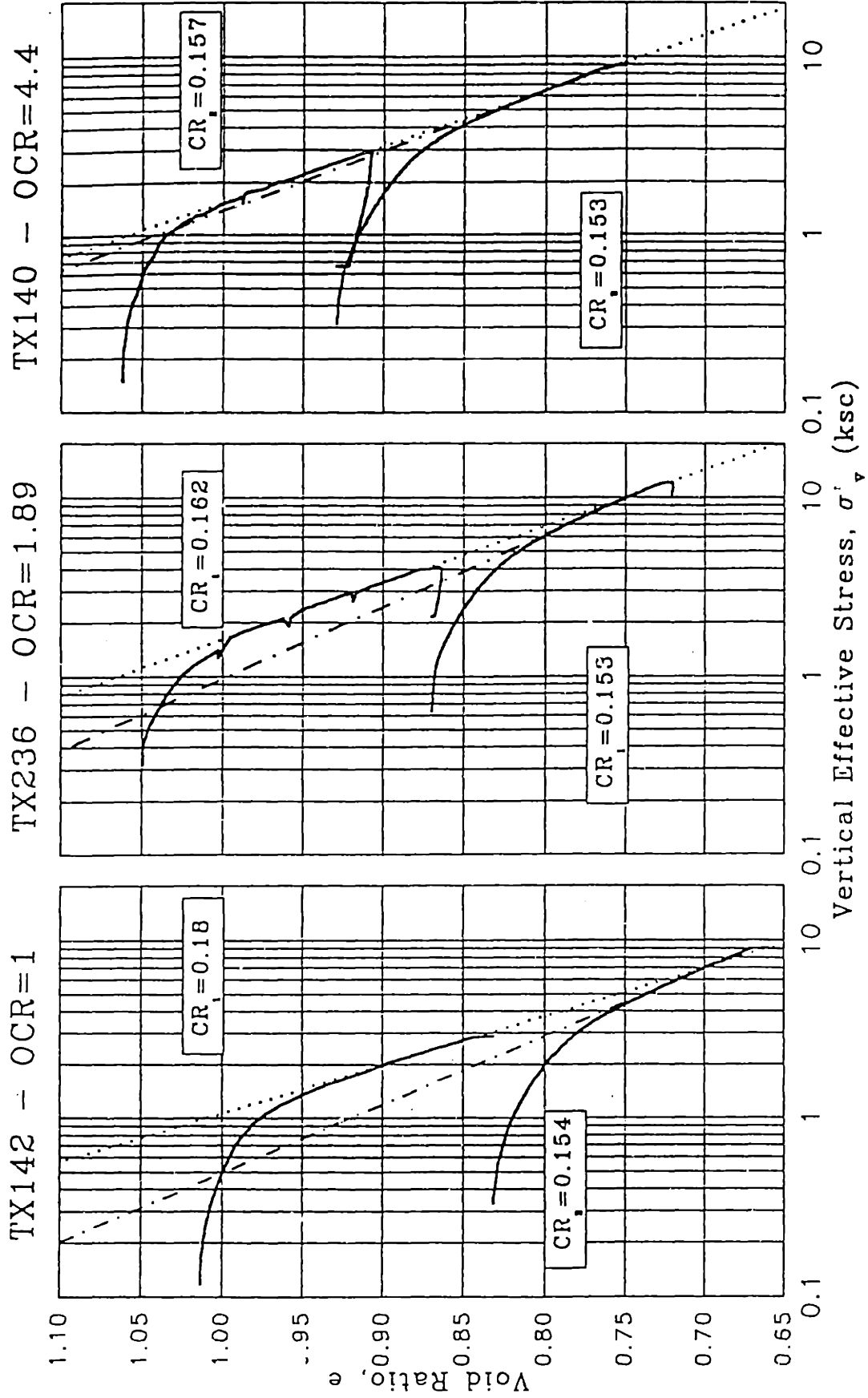


Figure 6.24: Effect of ISA±2 Disturbance on the Compression Behavior of RBBC with OCR=1, 1.89, 4.4

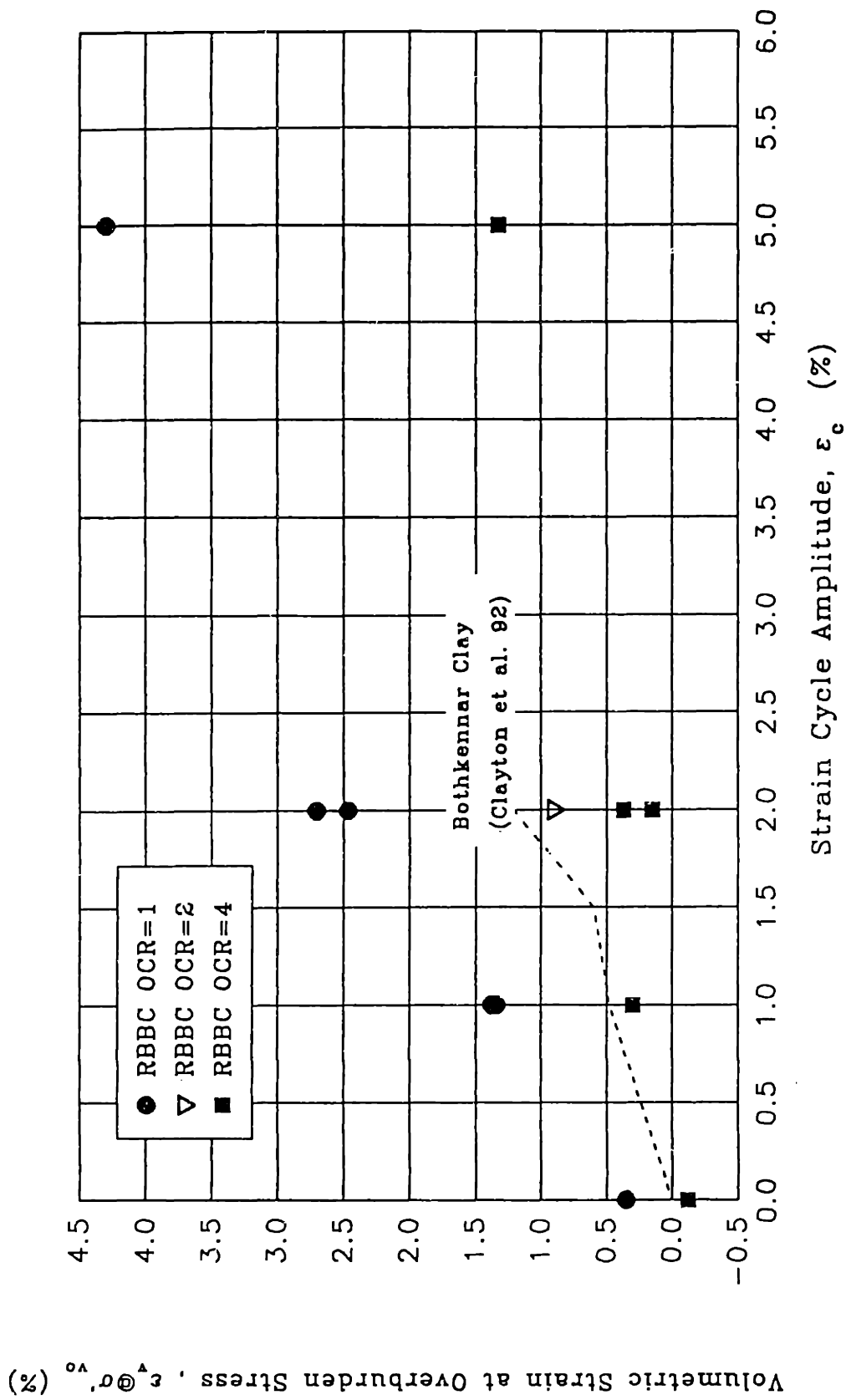


Figure 6.25: Volumetric Reconsolidation Strains after PSA and ISA Disturbance of RBBC

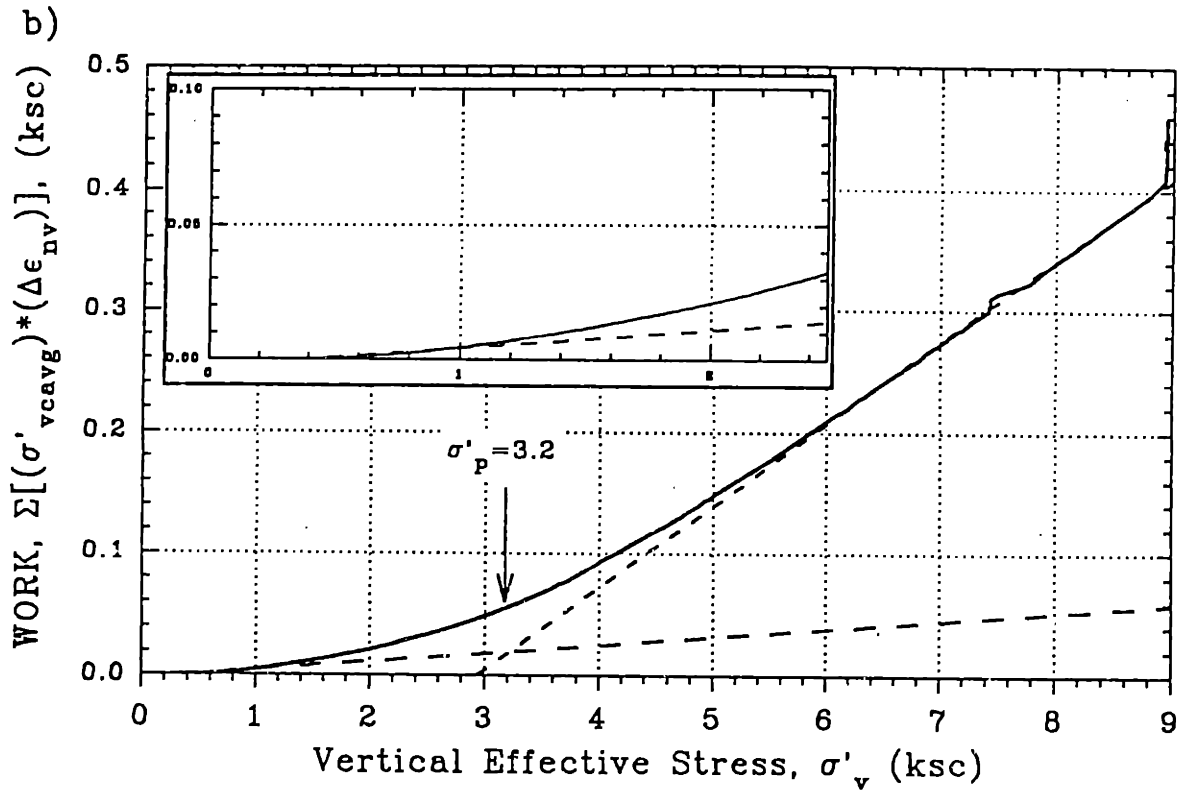
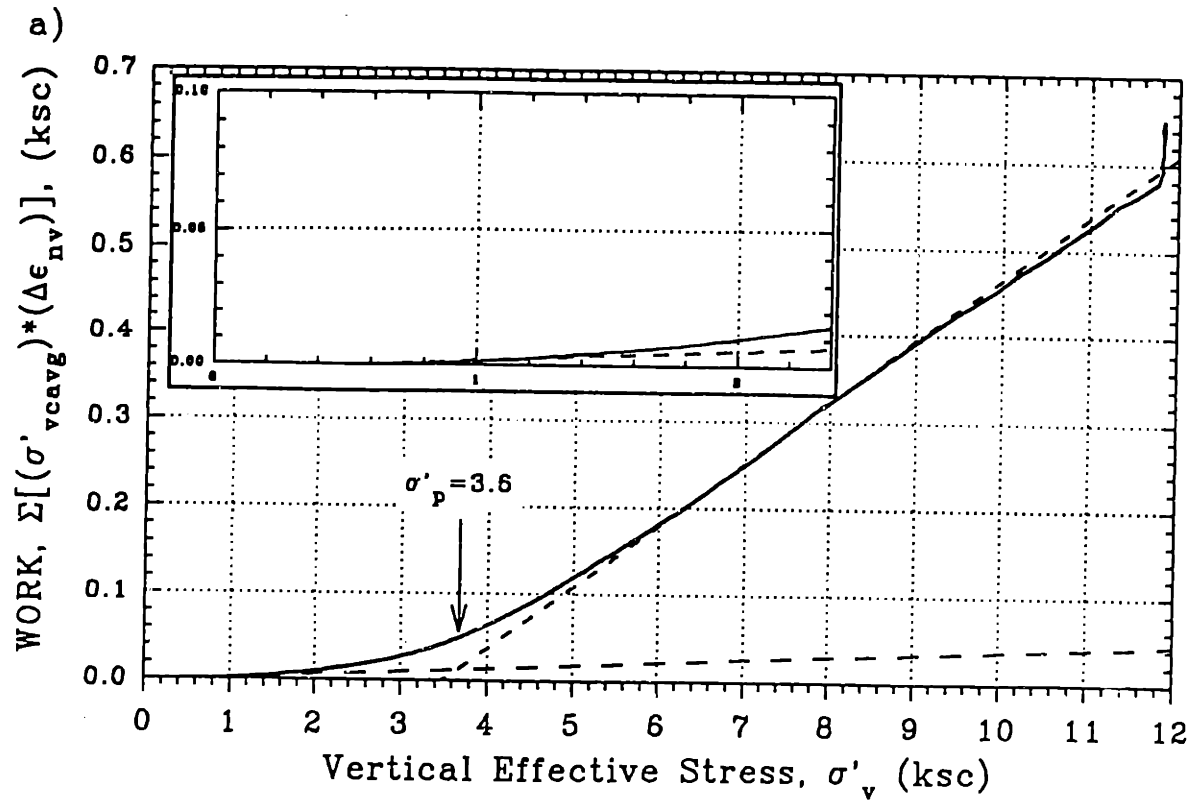


Figure 6.26: Determination of the Preconsolidation Pressure after (a) ISA<sub>+1</sub> (TX134) and (b) ISA<sub>±2</sub> (TX142) Disturbance of NC RBBC

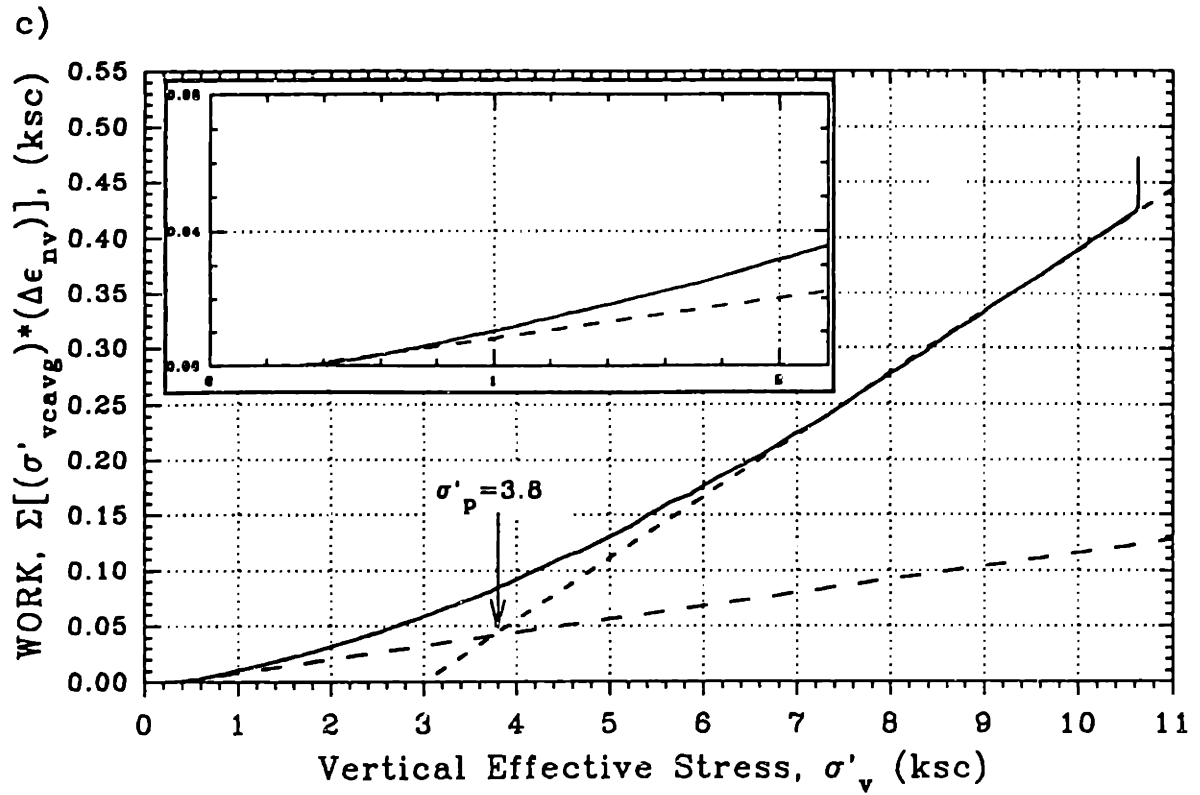


Figure 6.26c: Determination of the Preconsolidation Pressure after ISA $\pm$ 5 Disturbance of NC RBBC (TX260)

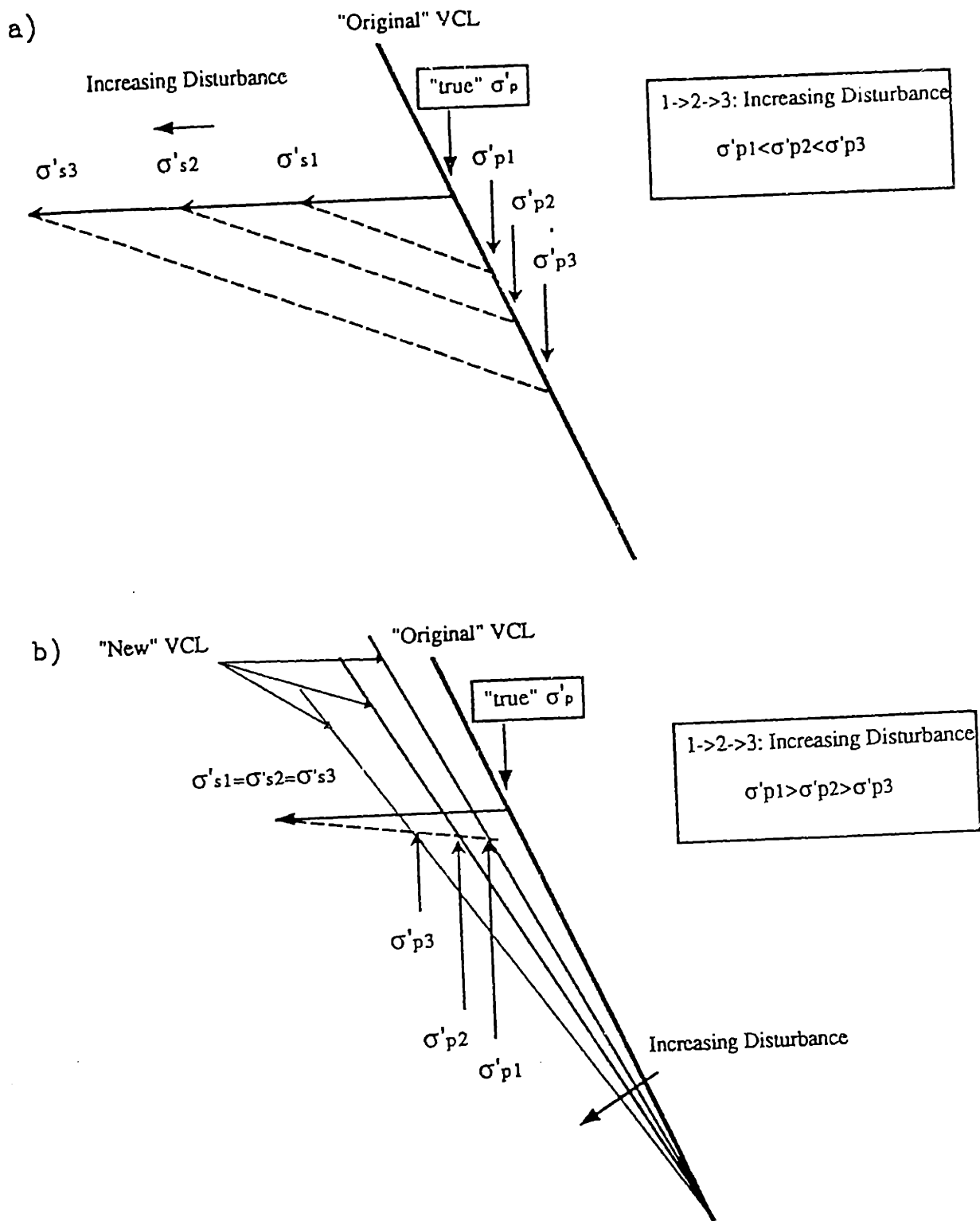


Figure 6.27: Simplified Models Describing the Effects of Disturbance on the Compression Behavior

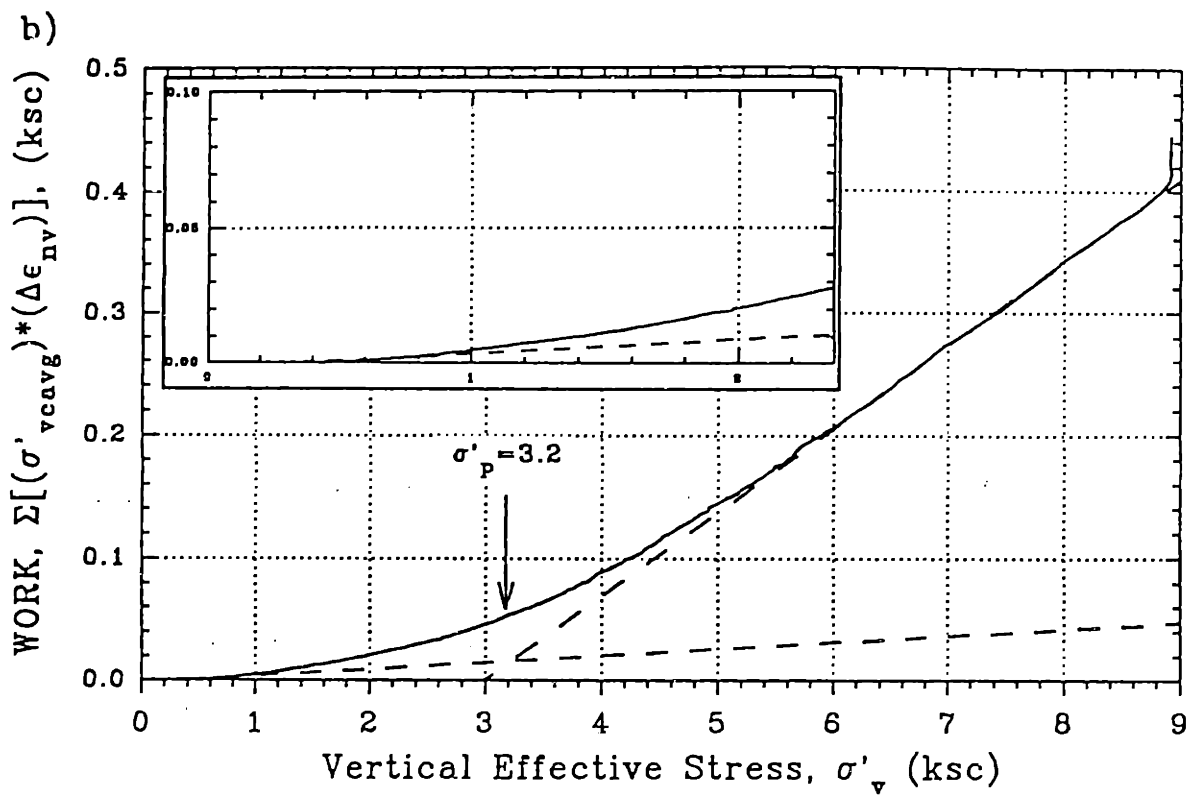
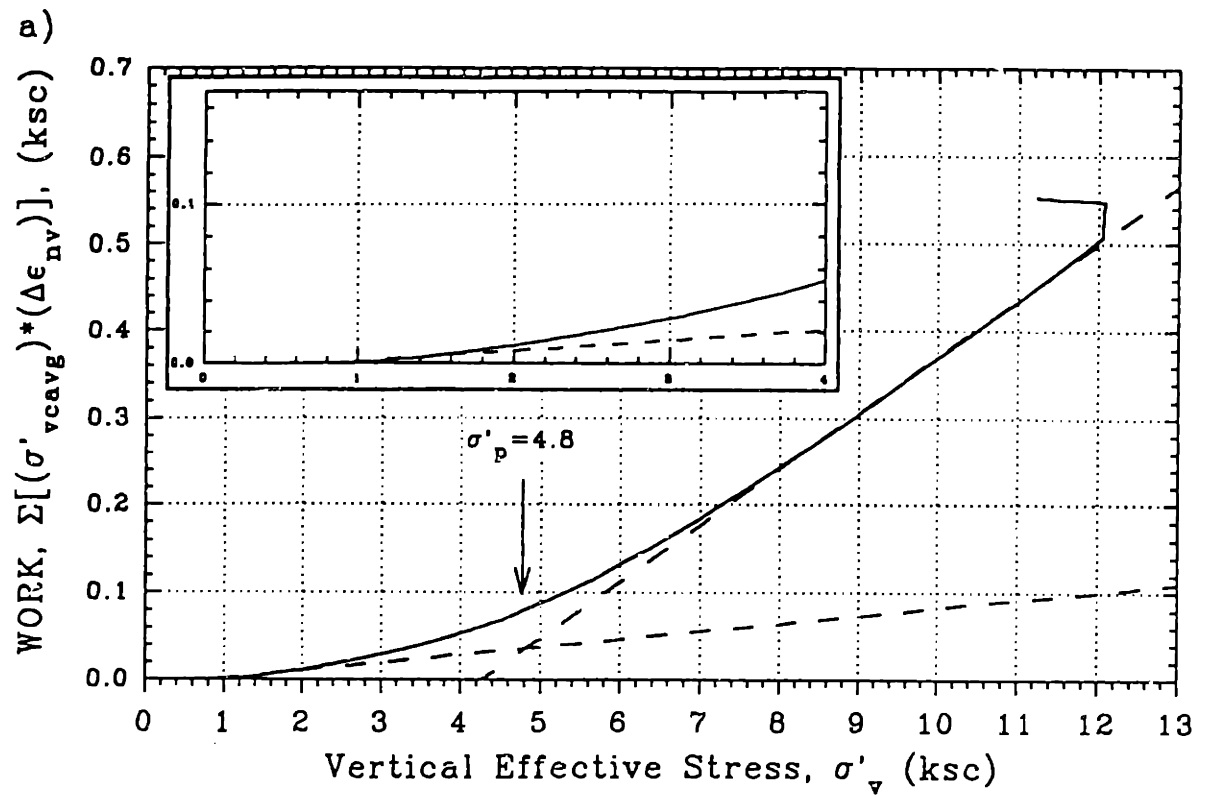


Figure 6.28 : Determination of the Preconsolidation Pressure after ISA $\pm$ 2 Disturbance of (a) OCR2 (TX236) and (b) OCR4 RBBC (TX140)



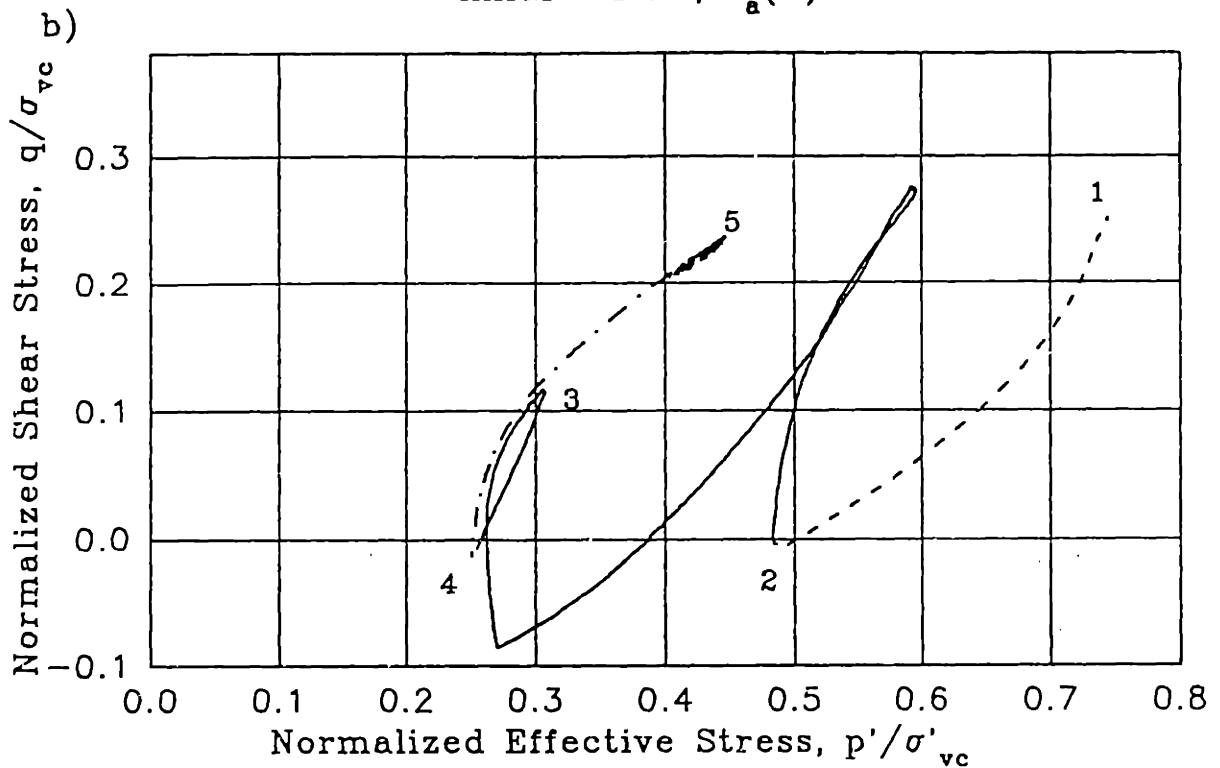
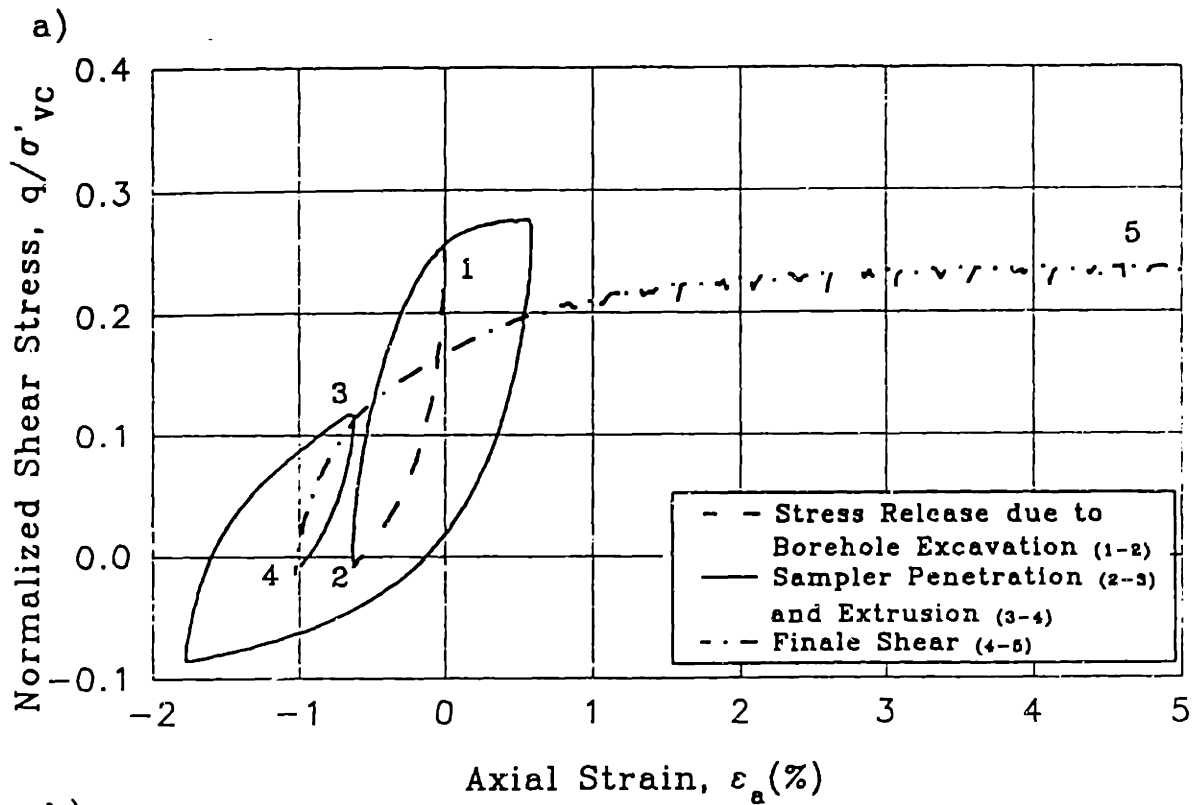


Figure 6.29: Special Test TX120 with Shear Stress Release Prior to  $ISA \pm 1$  Disturbance: (a) Stress Strain Curve, (b) Stress Path

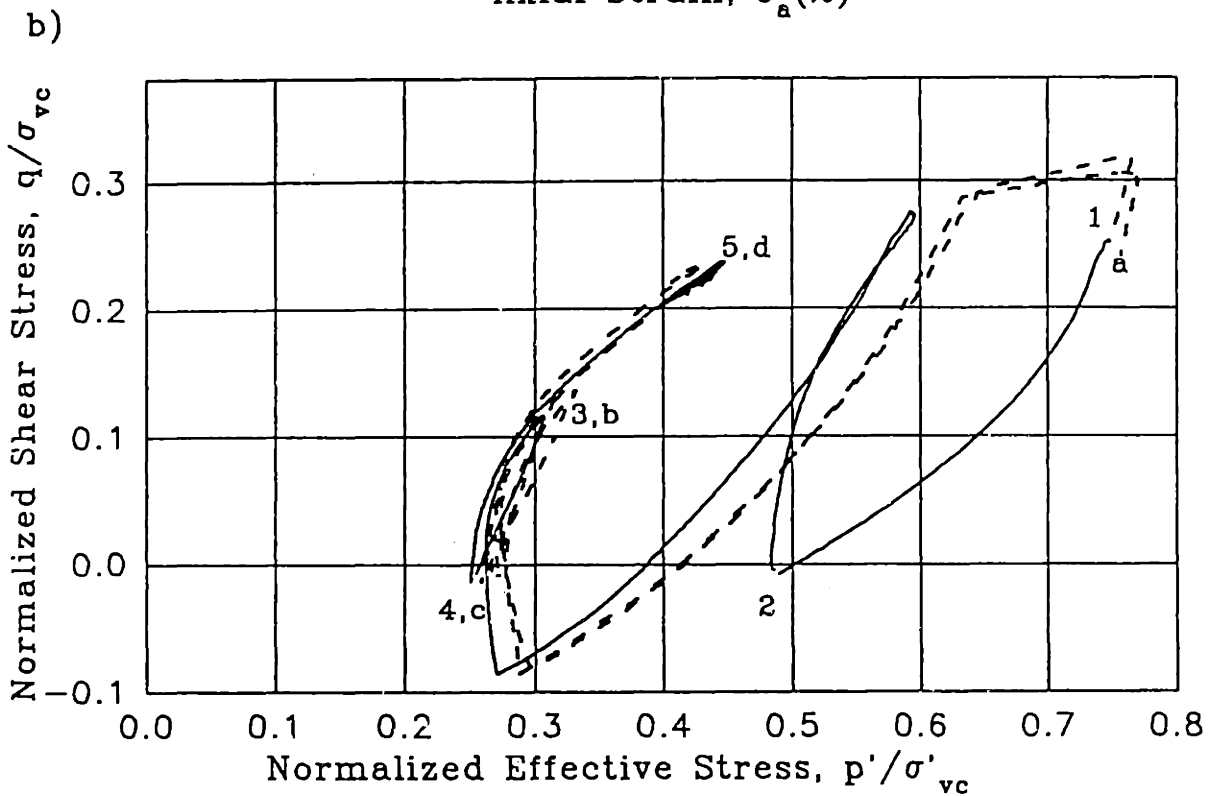
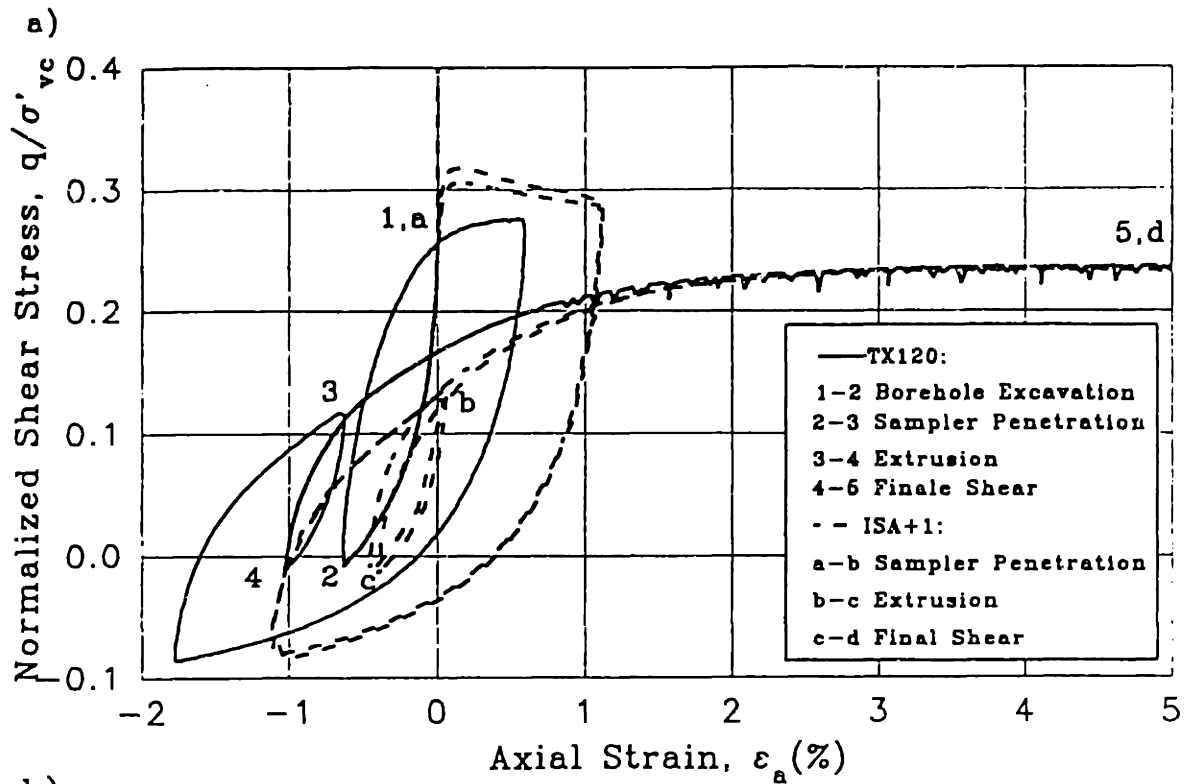


Figure 6.30: Comparison of TX120 with Two ISA $\pm$ 1 UU Tests: (a) Stress Strain Curves and (b) Stress Paths

# Chapter 7 Effect of Recompression and SHANSEP Reconsolidation on the Undrained Behavior of RBBC

## 7.1 Introduction

As discussed in Chapter 2, the selection of a suitable reconsolidation procedure represents a central issue in laboratory testing. In practice either the Recompression (Bjerrum 1973) or the SHANSEP (Ladd and Foott, 1974) procedure is used. However there is still large dissent on the most appropriate procedure to be used especially in the case of normally consolidated soil.

This research program has attempted to investigate the effect of the two reconsolidation procedures mentioned above, and described in Chapter 2, on the determination of the engineering properties of RBBC. This has been done by performing "Recompression" and "SHANSEP" Tests as defined in Chapter 4. In both cases the soil, starting from the "in-situ" conditions, is subjected to an undrained "disturbance phase" simulating the sampling operations (PSA or ISA). At the end of this phase the specimen is reconsolidated either back to the in situ stresses (Recompression) or well into the virgin compression range and then swelled to the appropriate OCR (SHANSEP) before being sheared in undrained compression. This final shear is considered representative of the behavior of RBBC after Recompression or SHANSEP reconsolidation and thus one can compare it to the "intact" behavior of RBBC.

This chapter examines the effects of the two reconsolidation procedures on the undrained behavior of RBBC and in particular on the undrained strength, strain at peak, and stiffness. The results presented are relative to a limited triaxial program conducted for NC (Recompression and SHANSEP) and OCR4 RBBC (Recompression). The data available show promising results but further testing is necessary to validate the observations made.

## 7.2 Recompression

### 7.2.1 General Undrained Behavior

Figures 7.1a and 7.1b compare the undrained behavior of NC RBBC in a PSA Recompression Test (TX211) with the intact behavior of the same soil. Also shown are the results for a UU test with equal disturbance. Similar comparisons for larger degrees of disturbance,  $ISA_{\pm 1}$  (TX213) and  $ISA_{\pm 2}$  (TX200), are presented in Figures 7.2a-b and 7.3a-b respectively. For the ISA tests the initial compression phase of the disturbance cycle is used as a reference of undisturbed behavior. The PSA test makes use of the same reference curves used for the  $ISA_{\pm 2}$  test due to the fact that both tests are characterized by the same pre-shear value of  $K_0$ .

The comparison of the Recompression (dotted lines) with the UU (dash-dotted lines) test results indicates that this reconsolidation procedure does partially recover the intact behavior of the soil: the strain at peak

decreases, the stiffness at the lower strains increases, and the shape of the stress path resembles much more that of an intact NC specimen.

The differences between the reconsolidated and the intact behavior are however still quite marked: the soil fails at a much larger strain, and strain softening is essentially eliminated in the ISA tests. Figures 7.1b, 7.2b and 7.3b also show that there are differences in the shape of the stress path followed by the soil during shear. After recompression, the stress paths appear much more rounded than those observed for the intact soil. As the level of disturbance preceding recompression increases so do the differences between the intact and the reconsolidated soil.

Most importantly Figures 7.1-7.3 indicate that recompression to the in situ stresses is consistently associated with an overestimate of the undrained strength of the soil. Especially for the higher magnitude of disturbance (ISA $\pm$ 2), the recompression test provides a highly unsafe estimate of  $c_u$ .

It must be pointed out that, due to problems encountered during testing, the "in situ" stresses were not targeted perfectly during the reconsolidation. The error in the vertical stress is minor: the "in situ" value is exceeded by 0.5% in the ISA $\pm$ 2 test, 2.5% in the ISA $\pm$ 1 test and 5% in the PSA test. The deviation of the horizontal stress from the "in situ" value is instead more marked (2%, 2.9% and 21% increase) leading to a significant difference in the pre-shear value of K (0.522 instead of the in situ value 0.513 for TX200, 0.594 versus 0.564 for TX213 and 0.591 versus 0.513 for TX211). In all cases at the end of recompression the soil has a larger K value than that for the in situ soil.

In Figures 7.4a and 7.4b respectively the stress strain curve and the stress path of an  $ISA_{\pm 2}$  Recompression test on RBBC with OCR equal to 4.23 are plotted in dotted lines. The undrained behavior of the same specimen during the ISA shearing to 2% is plotted with a dashed line. This curve provides a useful comparison for the early portion of the shear. The figure also presents, in solid lines, the results of a standard "Undisturbed" test on RBBC with OCR equal to 4.33, and one can judge the effect of the reconsolidation on the stress strain curve and the stress path at higher strains. The two intact curves are remarkably similar and indicate that in the ISA test the soil is very close to reaching the peak strength. The dashed-dotted line represents instead the results of a  $ISA_{\pm 2}$  UU test on RBBC with  $OCR=4.44$ .

After disturbance and recompression, the soil exhibits a stress strain behavior completely different from that of the intact soil. There is an initial yielding, at less than 0.5% axial strain, followed by some strain hardening to about 3% after which the stiffness of the soil decreases before reaching the limit strength. On the other hand it appears that the Recompression test provides an accurate estimate of the strength.

If one compares the stress strain of the soil after disturbance and recompression with that of the soil in the  $ISA_{\pm 2}$  UU test also shown in Figure 7.4a, the two curves appear extremely similar. The stress strain behavior of the UU test shows the same features just described for the Recompression test. Except for a slight increase in the stiffness at the smaller strains, it appears that recompression leaves the behavior of the OC soil unchanged compared to the end of disturbance. In fact in the case of  $OCR_4$  RBBC, this magnitude of disturbance does not lead to large

variations in the position of the soil element in the stress space. Consequently the reconsolidation path is extremely short and very small reconsolidation strains are measured (from Figure 6.23  $\epsilon_{rec} < 0.5\%$  for ISA $\pm 2$ ). For lower values of disturbance the reconsolidation is even more limited: for OCR4 RBBC, PSA disturbance actually leads to a limited increase of the effective stresses, and reconsolidation is associated with a slight increase in the water content ( $\epsilon_{rec} = -0.2\%$ ).

### 7.2.2 Undrained Strength

In the previous section, in discussing the results of the recompression tests, it was observed that the reconsolidation procedure leads to an overestimate of the undrained strength. Figure 7.5 plots this increase in undrained strength ( $c_{uREC} - c_{uINT}$ ) normalized by the intact value of the strength ( $c_{uINT}$ ) versus the amplitude of the disturbance cycle. As in the case of the "UU" tests the results for the PSA tests are plotted in correspondence to  $\epsilon_c = 0$ . The figure shows results for both NC and OCR 4 RBBC.

For the NC tests, the intact values are determined from the reference curves plotted in Figures 7.1-7.3. For the OC tests, two different approaches were taken to estimate  $c_{u(INT)}$  for the three tests presented. For the PSA test (TX238) and the ISA $\pm 5$  test (TX239) the undisturbed undrained strength was estimated through the SHANSEP relationship determined in Chapter 5 for Intact RBBC:  $c_u / \sigma'_{vc} = 0.33(OCR)^{0.71}$ . For the ISA $\pm 2$  test (TX224), the normalized shear stress at the end of the ISA compression to 2% is equal to 0.953 and already exceeds the value of  $c_u / \sigma'_{vc}$  estimated through the

SHANSEP equation (equal to 0.919 for OCR=4.23). A value of  $c_{uINT} = 0.953$  was chosen having observed that from Figure 7.3a it appears that at the end of the ISA compression the soil is very close to reaching the peak strength. Based on the results shown in Figure 7.5, it can be deduced that for both NC and OC RBBC, as the level of disturbance increases the recompression tests more severely overestimate the undrained strength of the soil.

In the case of NC RBBC the recompression technique leads to an unsafe estimate of the strength for any level of disturbance. The overestimate of the undrained strength is hardly noticeable (<1%) for the PSA test, but it becomes much more significant for the ISA tests, increasing from 8% for the ISA $\pm$ 1 test to almost 20% in the case of ISA $\pm$ 2 disturbance. Even though no Recompression tests were performed on NC RBBC for higher magnitudes of disturbance, most likely for larger disturbance the overestimate of the strength will be even greater. In the previous chapter it was shown that the reconsolidation strains, and therefore the reduction in water content, increased almost linearly with disturbance at least up to an amplitude of the ISA strain cycle equal to five. For the ISA $\pm$ 5 test, the reconsolidation strain was almost three times the value after ISA $\pm$ 2 disturbance. Based on this observation and on the fact that the undrained strength of RBBC appears to correlate very well with the water content, it can be hypothesized that, for example, an ISA $\pm$ 5 Recompression test could lead to an overestimate of  $C_u/\sigma'_{vc}$  as high as 50%.

As mentioned above, in all three of the NC tests, the specimens were not reconsolidated to the correct "in situ" value of the lateral stress ratio,



but to a larger value. Had the value of  $K$  been perfectly targeted, based on the relationship between the undrained strength and the lateral stress ratio presented in Chapter 5, one would expect a higher value of  $c_{uREC}$  leading to an even more unsafe estimate of the strength.

From the data plotted in Figure 7.5 one can compare the effect of the Recompression technique on NC and OC RBBC. While for the NC soil this reconsolidation technique provides a largely unsafe estimate of the strength, the undrained strength measured in the Recompression tests is quite accurate. For example, after the same level of disturbance ( $ISA+2$ ), recompression leads to overestimation of the undrained strength by 20% in the NC tests and by only 2% for the OCR4. It should be pointed out that for OCR4 RBBC after  $ISA\pm 2$  disturbance the UU test provided a satisfactory estimate of the undrained strength. This is to say that in this case the accuracy of the estimate of  $c_u$  provided by the recompression test is not due to the merits of the reconsolidation technique, but to the fact that the strength of the soil was not significantly damaged by this level of disturbance. The recompression technique needs to be validated for larger values of disturbance that are known to cause a significant decrease in the strength. Unfortunately, the effects of  $ISA\pm 5$  disturbance on the undrained strength of OCR4 RBBC have not been quantified and no Recompression test is available for  $ISA\pm 8$  disturbance which was shown to produce a large decrease in the strength (Figure 6. 8).

### 7.2.3 Strain at Peak

When analyzing the stress strains curves from the recompression tests, it was already pointed out that the intact stress strain behavior of the soil is not fully recovered through this reconsolidation procedure. The strain at peak measured in the recompression tests on NC RBBC is plotted in Figure 7.6 versus the amplitude of the disturbance cycle and compared with the values measured in the intact tests as well as in the UU tests. As expected, the strain at peak increases with the level of disturbance and is much larger than the values for the intact material. The strains measured in the Recompression tests are however, much lower than those measured in the UU tests and it appears that reconsolidation to the in situ stresses allows partial recovery of the stress strain behavior of the soil.

An equivalent plot for RBBC with  $OCR=4$  is presented in Figure 7.7. In this case, it appears that the reconsolidation technique does not reconstruct the structure of the intact material. Except for the PSA test, the peak strain measured during the final undrained shear for the recompression tests in fact largely exceeds the value measured for undisturbed RBBC with equal OCR. As anticipated in Section 7.2.1, no significant difference is observed between the values of  $\epsilon_{peak}$  of the recompression tests and those measured in the UU tests indicating that, for this value of the OCR, recompression does not substantially change the behavior relative to the UU tests.

#### 7.2.4 Undrained Stiffness

Figure 7.8 compares the stiffness behavior of Recompression tests on NC RBBC with the intact behavior of the same soil represented here by the curves for the first compression phase of ISA cycles for tests TX200 and TX213. For all three levels of disturbance, the curves relative to the final shear after recompression fall above those of the intact soil. At 0.01% strain the disturbed tests all show the same stiffness about 70% higher than the intact value. As the strain increases the more disturbed tests give a softer response until about 1% strain when they become stiffer due to the absence of any strain softening. Regarding the higher stiffness at the lower strains, the result of the PSA test is not surprising having shown in Chapter 6 that even without any reconsolidation (UU Test), the stiffness of the soil increased somewhat after PSA disturbance. It appears that in the ISA tests, the restructuring produced by the reconsolidation and the consequent decrease in water content, not only overcomes the effects of disturbance, but also leads to further increase of the stiffness.

The following three figures (Figures 7.9a-c) present, for each level of disturbance, a comparison of the modulus measured in the recompression tests with the stiffness typically observed in UU tests. At the lower strains reconsolidation to the in situ stress results in a marked increase of the stiffness and the effects of disturbance are erased even for the ISA<sub>±2</sub> test. The recompression tests also describe the post peak behavior more accurately than the UU tests.

The stiffness at intermediate strains of intact OCR4 RBBC disturbed and reconsolidated to the in situ stresses is compared in Figure 7.10 with

the behavior of the intact soil. For all levels of disturbance reconsolidation increases the stiffness at the lower strains (<1%) compared to the UU tests. In the PSA test the disturbance is very limited and after reconsolidation the stiffness of the soil slightly exceeds that of the intact material.

Reconsolidation has essentially no effect on the stiffness at larger strains. In the previous chapter it was pointed out that, for OCR4 RBBC, ISA $\pm$ 2 disturbance led to a significant reduction of the stiffness but only to a slight decrease of the effective stresses. Consequently, the benefit of reconsolidation is limited and it is not possible to recover the stiffness of the intact soil.

## **7.3 SHANSEP**

### **7.3.1 General Undrained Behavior**

Figures 7.11-7.13 compare the stress strain curves and the stress paths of intact NC RBBC with the curves of the undrained shear following SHANSEP reconsolidation after ISA $\pm$ 1, ISA $\pm$ 2 and ISA $\pm$ 5 disturbance, respectively. The dashed-dotted lines are the UU tests with equal degree of disturbance.

Before discussing the results it is important to point out that the variations in stress level must be taken into account when analyzing the differences between the shear behavior of intact RBBC and the behavior measured during the final shear of the "SHANSEP" tests. The data used to define the intact shear behavior of RBBC are based on tests in which the

vertical consolidation stress ranged from 3 to 4 ksc while all the "SHANSEP" tests are consolidated to 9 ksc or higher. The effects of stress level on the normalized behavior of RBBC have been investigated by Ahmed (1990) who performed DSS tests on NC RBBC with  $\sigma'_{vc}$  varying between 1.12 and 12 ksc. The data presented by Ahmed (1990) indicate that consolidation stress level has a significant effect on the strain at peak and on the normalized undrained modulus  $E_{u50}/\sigma'_{vc}$  but does not have much influence on the undrained strength. Unfortunately, no data of this type has been obtained for the behavior of RBBC in triaxial compression.

Further in the SHANSEP tests, after disturbance, the soil was reconsolidated to 3-4  $\sigma'_p$ . As pointed out in the previous chapter, especially for larger disturbance, this reconsolidation may not be sufficient to bring the soil back to the virgin compression line. The final shear would not then be representative of a truly NC soil.

Another aspect complicates interpretation of the results for NC RBBC. In Chapter 5 it was pointed out that the undrained strength, and to a lesser degree the strain at peak, were influenced by the pre-shear value of the lateral stress ratio. In particular, higher values of  $K$  led to a decrease in the undrained strength and to an increase of the strain at peak. Therefore some difference between the strength and the strain at peak after the SHANSEP reconsolidation and the corresponding intact values may arise if the  $K$  value after reconsolidation is different from the "in situ" value. The limited number of SHANSEP tests performed have not resolved if, and to what degree, disturbance affects  $K_0$ . Of the tests performed only the ISA $\pm$ 1 (TX134) and the ISA $\pm$ 2 (TX142) tests maintained perfect  $K_0$  conditions during the second consolidation. In the first case, the  $K_0$  prior to the final

shear was considerably higher (0.475 vs. 0.435) while in the second case it was virtually identical to the in situ value (0.444 vs. 0.445).

From Figures 7.11 and 7.12 it can be seen that for both the ISA $\pm$ 1 and ISA $\pm$ 2 SHANSEP tests, the reconsolidation procedure proposed by Ladd and Foott (1974) yields a realistic description of the general undrained behavior of NC RBBC including the small value of the strain at peak and some strain softening. Comments regarding the undrained strength are provided in the following section.

When a NC specimen is subjected to much more severe disturbance as in the case of an ISA $\pm$ 5 disturbance cycle (Figures 7.13a-b) it appears that even after reconsolidation to about  $3.2 \sigma'_p$  the effects of disturbance are very far from being erased, and it is possible that the soil has not reached the virgin compression line. In this case the higher stress level and the variation in the lateral stress ratio cannot explain the large modification in the undrained behavior of the soil. The stress strain curve of the final shear shows a much larger strain at peak and the absence of the strain softening.

### 7.3.2 Undrained Strength

In comparing the SHANSEP strength after disturbance with the intact value it is necessary to take into account the effect of the pre-shear value of the lateral stress ratio. When there is no variation in  $K_0$ , as for the ISA $\pm$ 2 test, the intact strength is underestimated by less than 3%. For the ISA $\pm$ 1 and ISA $\pm$ 5 tests, at the end of reconsolidation the  $K_0$  is higher than the "in situ" value (Figure 7.14). Making use of the relationship presented

in Figures 5.11 and 7.14, it is possible to compare the intact and the final shear undrained strength at a chosen value of  $K$ . When this is done for the tests just discussed it results that  $c_u/\sigma'_{vc}$  is underestimated by about 3 % in test TX142 and approximately 5% in both TX260 and TX134.

In conclusion, for all levels of disturbance, the SHANSEP tests provide a reasonable estimate of the undrained strength of NC RBBC. Further, when the strengths are corrected to account for the variation in  $K_0$ , it appears that after SHANSEP the undrained strength is very close to the intact reference value even for the higher level of disturbance. It remains to be understood if the increase in  $K_0$  observed in TX134 is a result of disturbance.

### 7.3.3 Strain at Peak

Figure 7.15 compares the strain at peak measured in the SHANSEP tests with those from the Undisturbed, the UU and the Recompression tests. From this figure it appears the SHANSEP  $ISA_{\pm 1}$  and  $ISA_{\pm 2}$  tests fall within the range of results of the Intact material. However, Figure 7.16 shows that both values of  $\epsilon_{peak}$  represent an upper bound in the trend between the strain at peak and the lateral stress ratio. The deviation from the trend is hardly significant and it is possible that it is due to the increased stress level.

In the  $ISA_{\pm 5}$  test the strain at peak is equal to about 1.0 % and largely exceeds the values measured in the case of intact NC RBBC. Ahmed (1990) reports that a stress level increase from 1 to 12 ksc produces a maximum increase of the strain at peak of about 100-120%. On the other

hand the results presented in Figure 7.16 indicate for  $K=0.533$  one should expect a value of  $\epsilon_{peak}$  less than or equal to 0.25%. The author believes that these two factors alone cannot account for the large value of  $\epsilon_{peak}$  measured in this test, and that for this level of disturbance, the stress strain behavior of the soil is still influenced by disturbance.

#### 7.3.4 Undrained Stiffness

Figures 7.17 plots the modulus versus the axial strain for the SHANSEP  $ISA_{\pm 1}$ ,  $ISA_{\pm 2}$  and  $ISA_{\pm 5}$  tests. In full lines are the curves relative to the first compression phase of the ISA disturbance for the same three tests, which represent the intact behavior. The following three figures (Figures 7.18-7.20) plot, for each level of disturbance the curve from the SHANSEP test (dotted line), the corresponding intact one (thicker solid line) and the results of one or more UU tests (dashed-dotted line).

The results of the lower strain modulus for the  $ISA_{\pm 1}$  and the  $ISA_{\pm 5}$  have to be discarded due to control problems which occurred during the early part of the undrained shear. The  $ISA_{\pm 2}$  test indicates that within the range of strains examined, the pre-peak stiffness of the NC soil is fully recovered through SHANSEP reconsolidation.

The larger strain stiffness is fully recovered for moderate disturbance ( $ISA_{\pm 1}$  and  $ISA_{\pm 2}$ ) but is overpredicted in the  $ISA_{\pm 5}$  test due to the absence of strain softening.



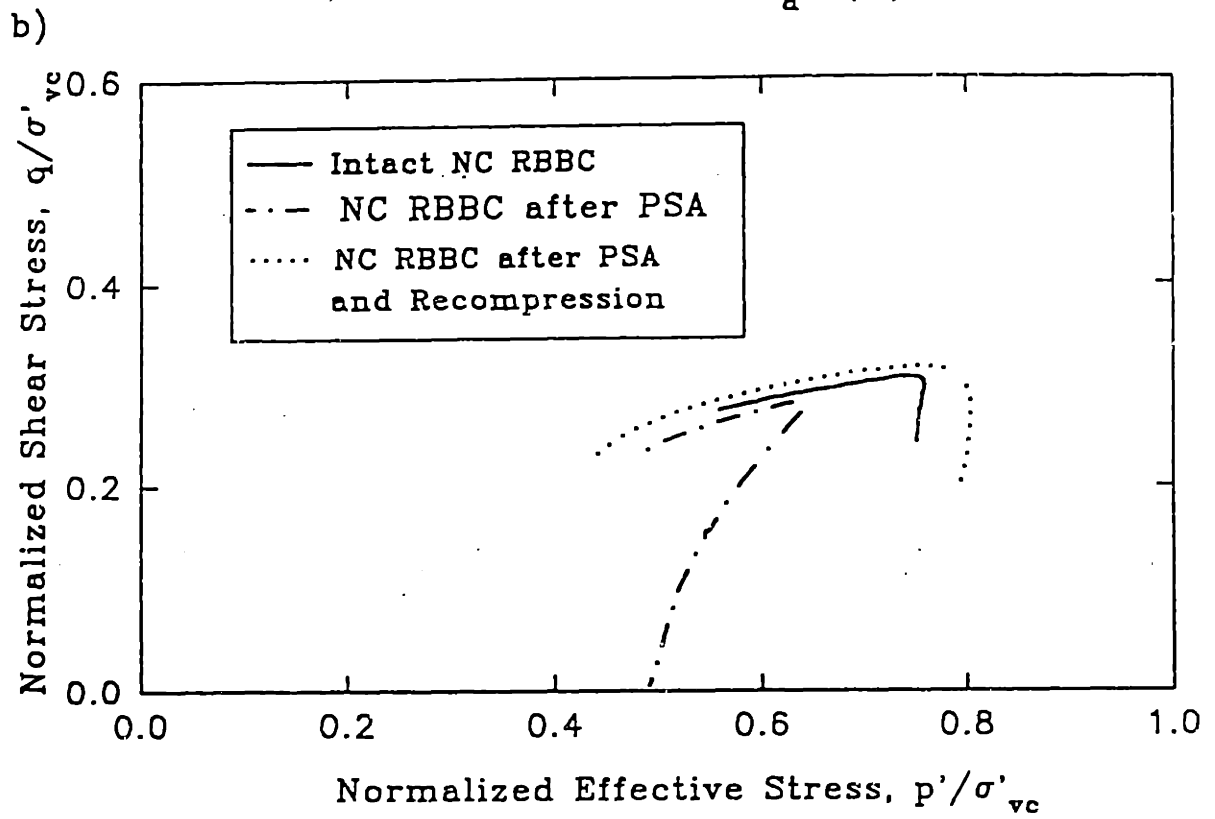
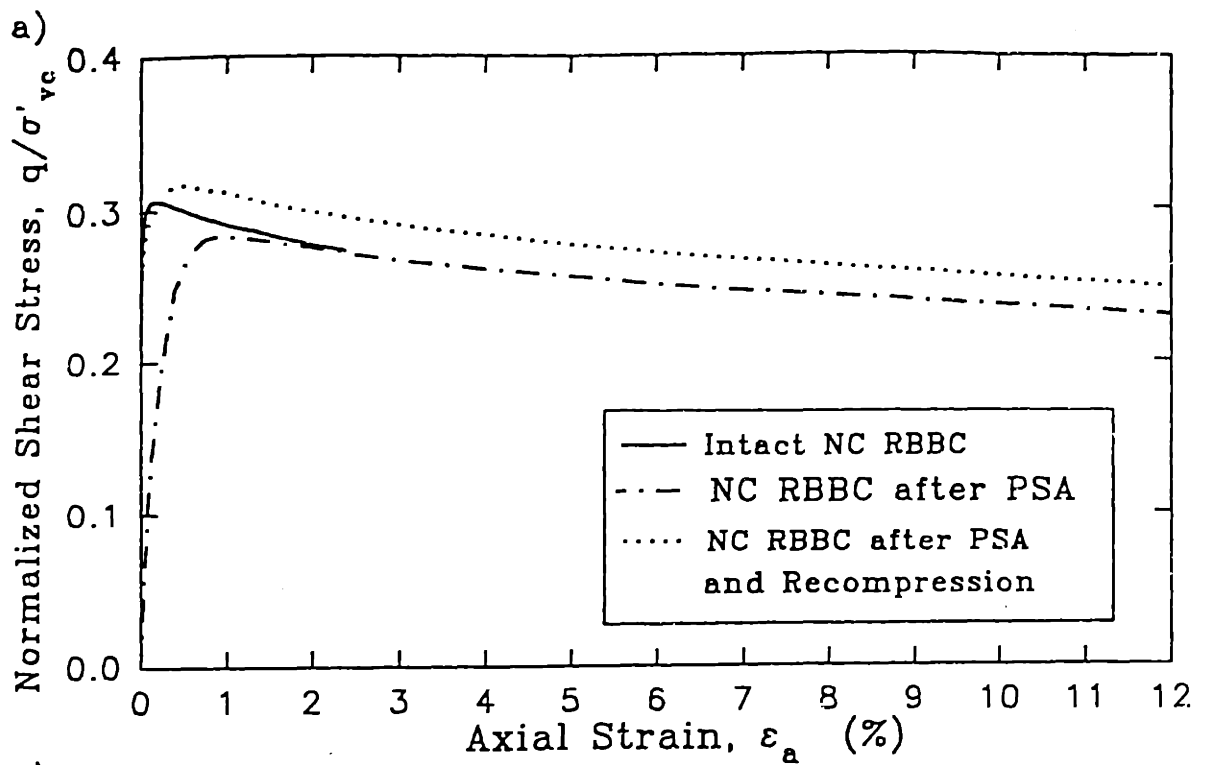


Figure 7.1: Effect of PSA Disturbance and Recompression on the Undrained Shear Behavior of NC RBBC: (a) Stress Strain Curve, (b) Stress Path

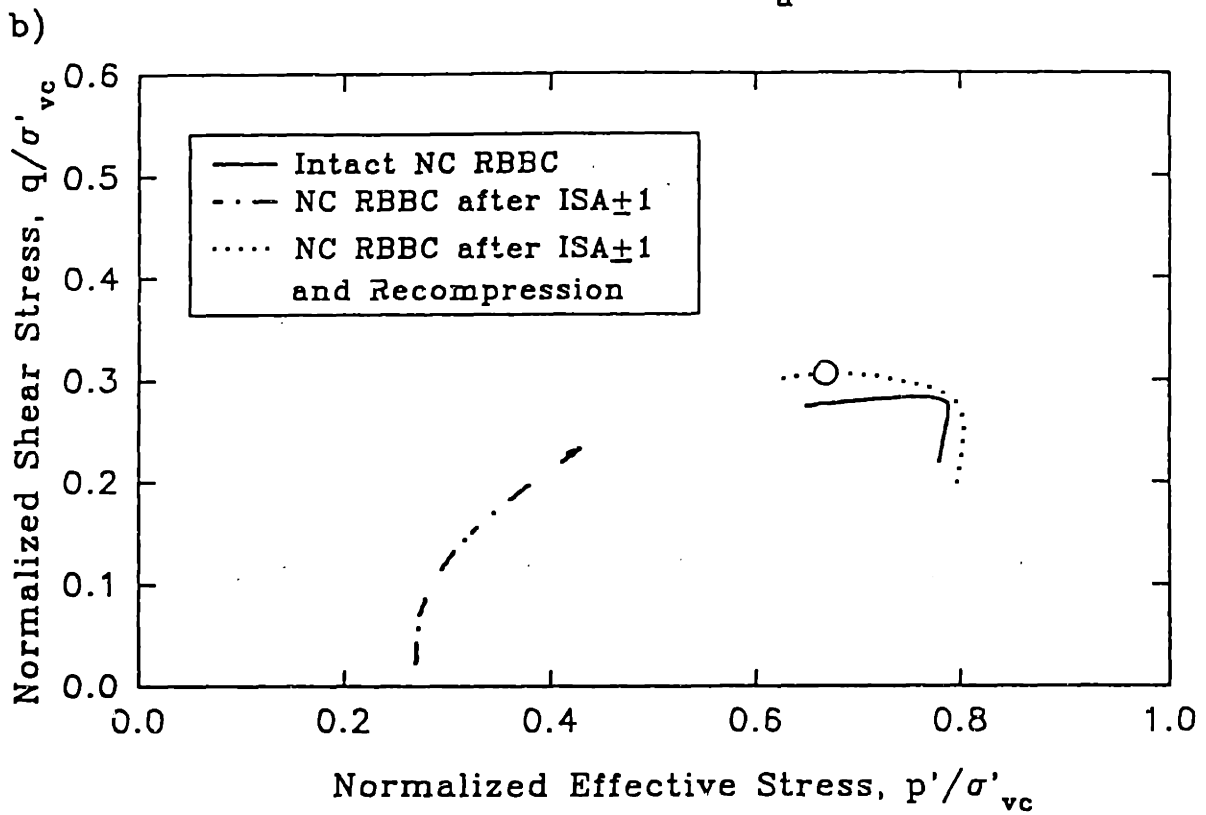
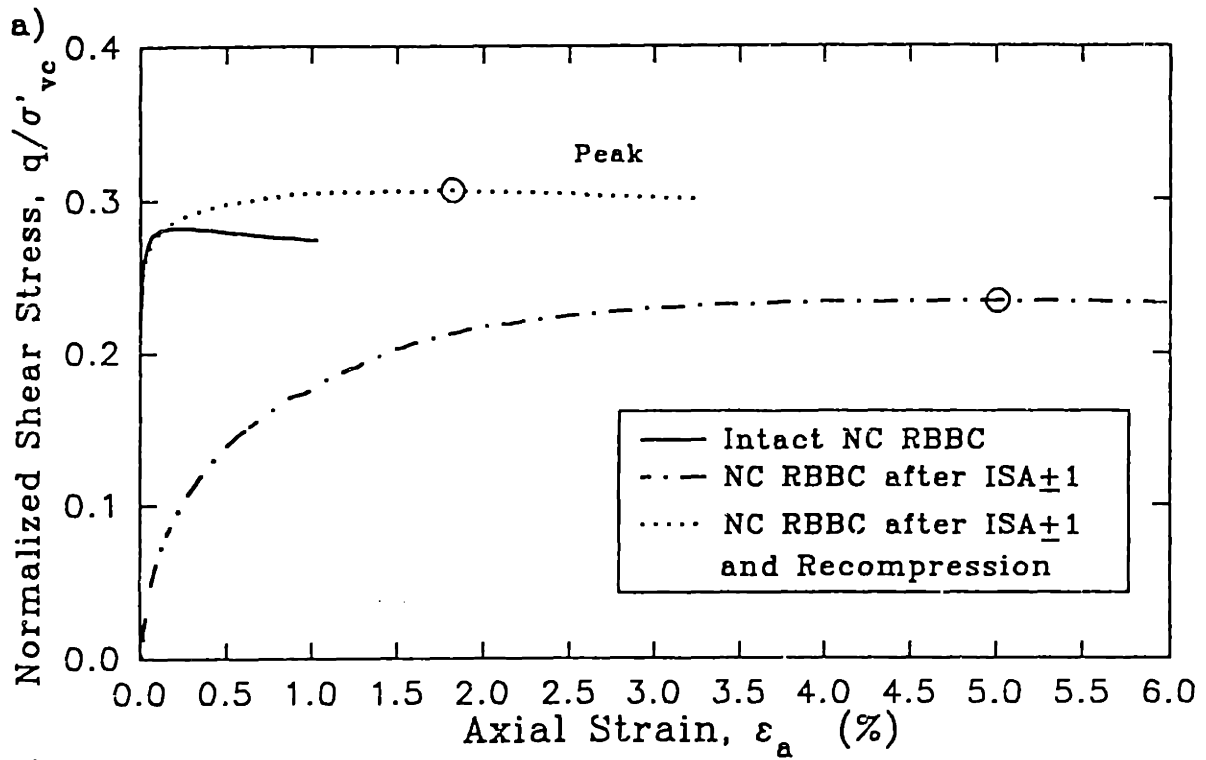


Figure 7.2: Effect of  $ISA_{\pm 1}$  Disturbance and Recompression on the Undrained Shear Behavior of NC RBBC: (a) Stress Strain Curve, (b) Stress Path

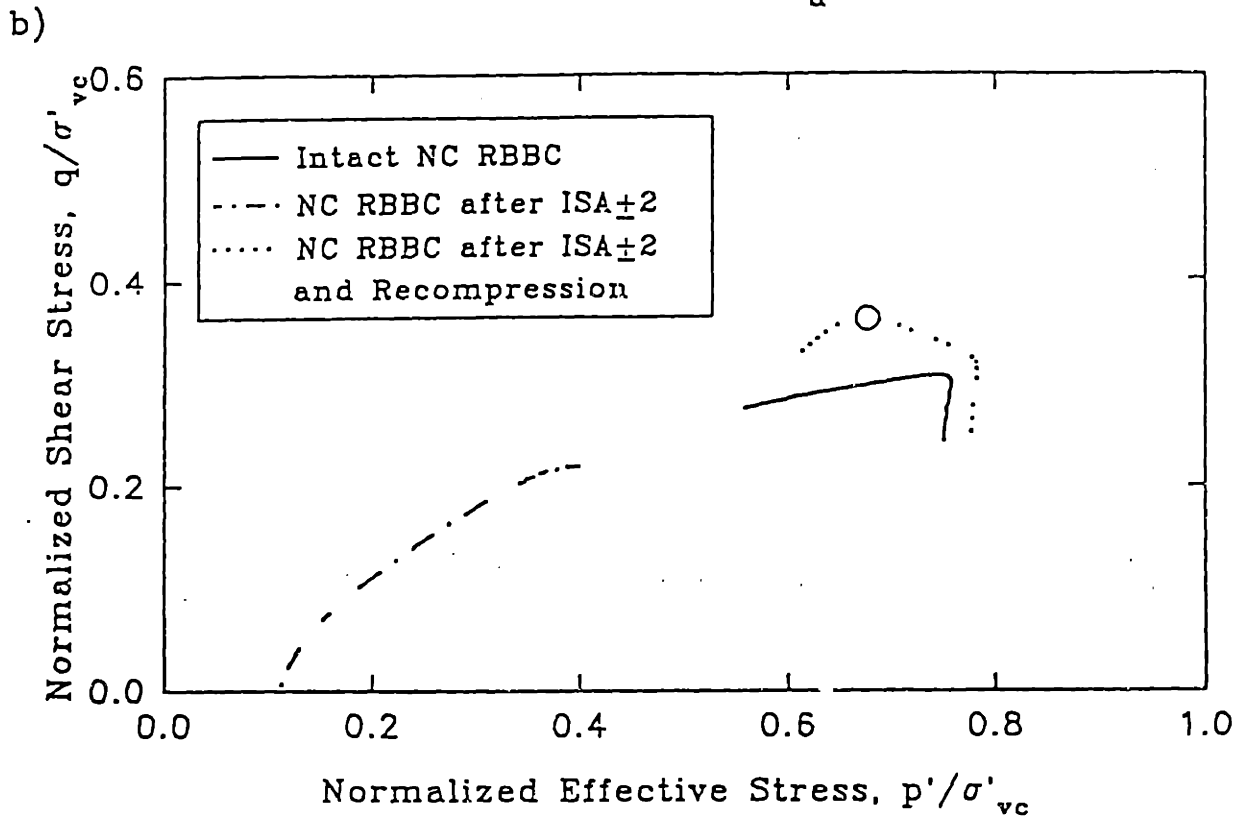
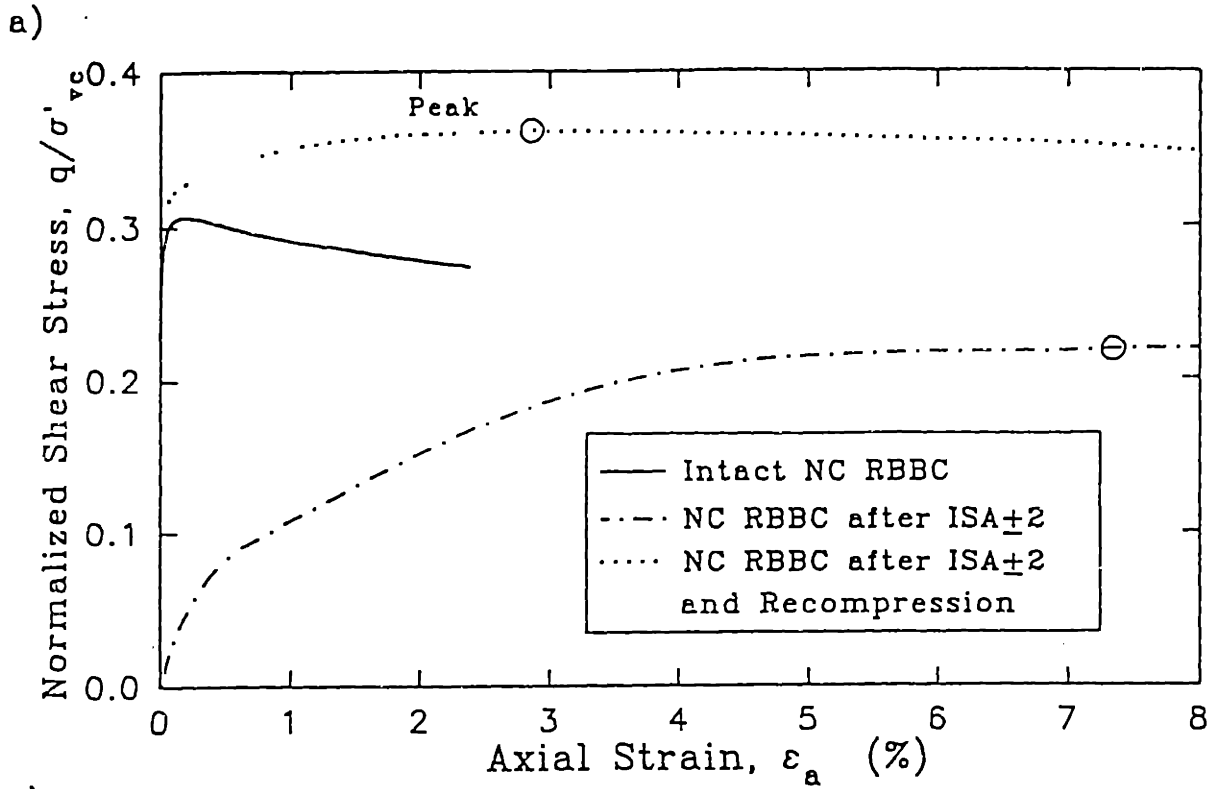


Figure 7.3: Effect of  $ISA_{\pm 2}$  Disturbance and Recompression on the Undrained Shear Behavior of NC RBBC: (a) Stress Strain Curve, (b) Stress Path

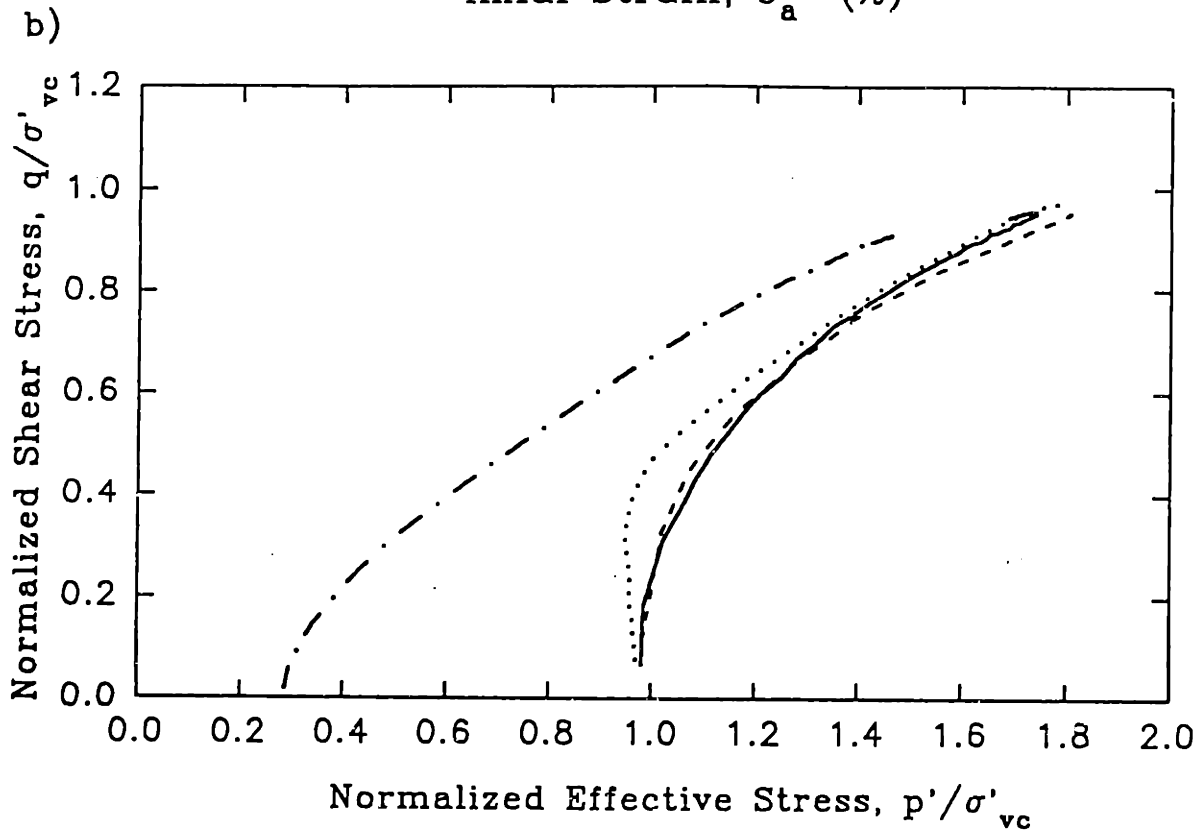
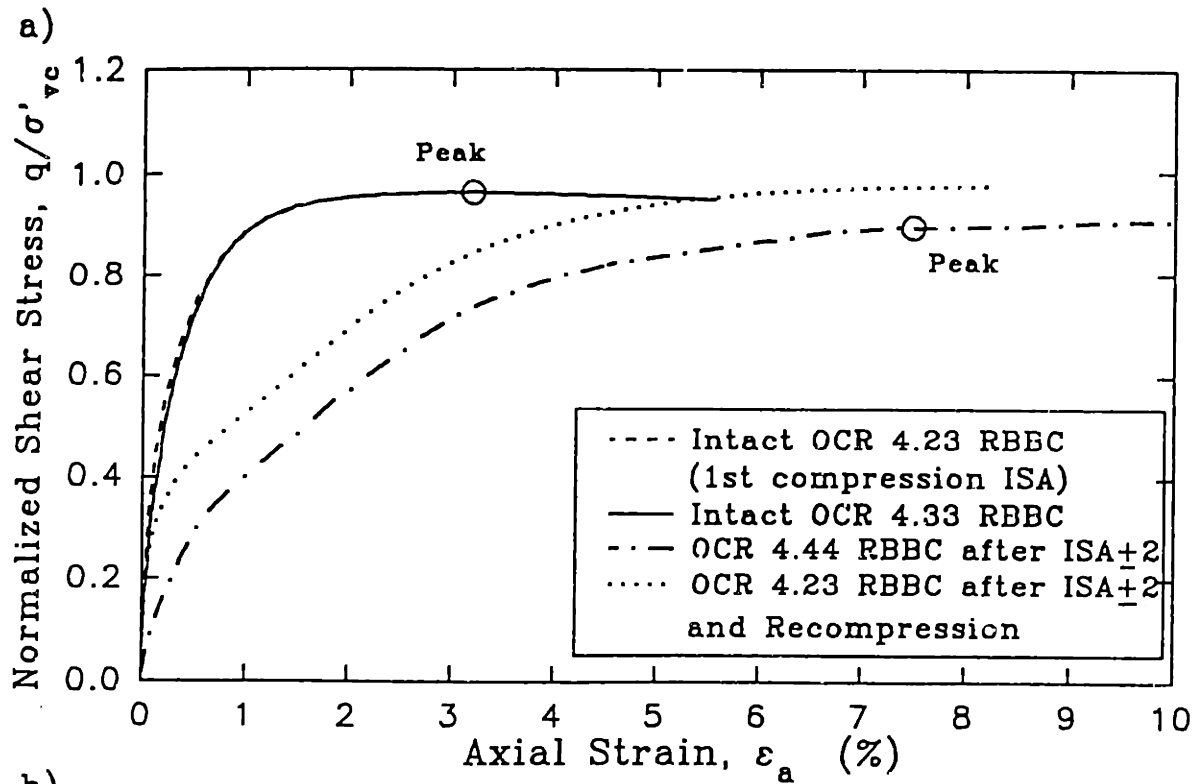


Figure 7.4: Effect of ISA $\pm$ 2 Disturbance and Recompression on the Undrained Shear Behavior of RBBC with Nominal OCR equal to 4: (a) Stress Strain Curve, (b) Stress Path

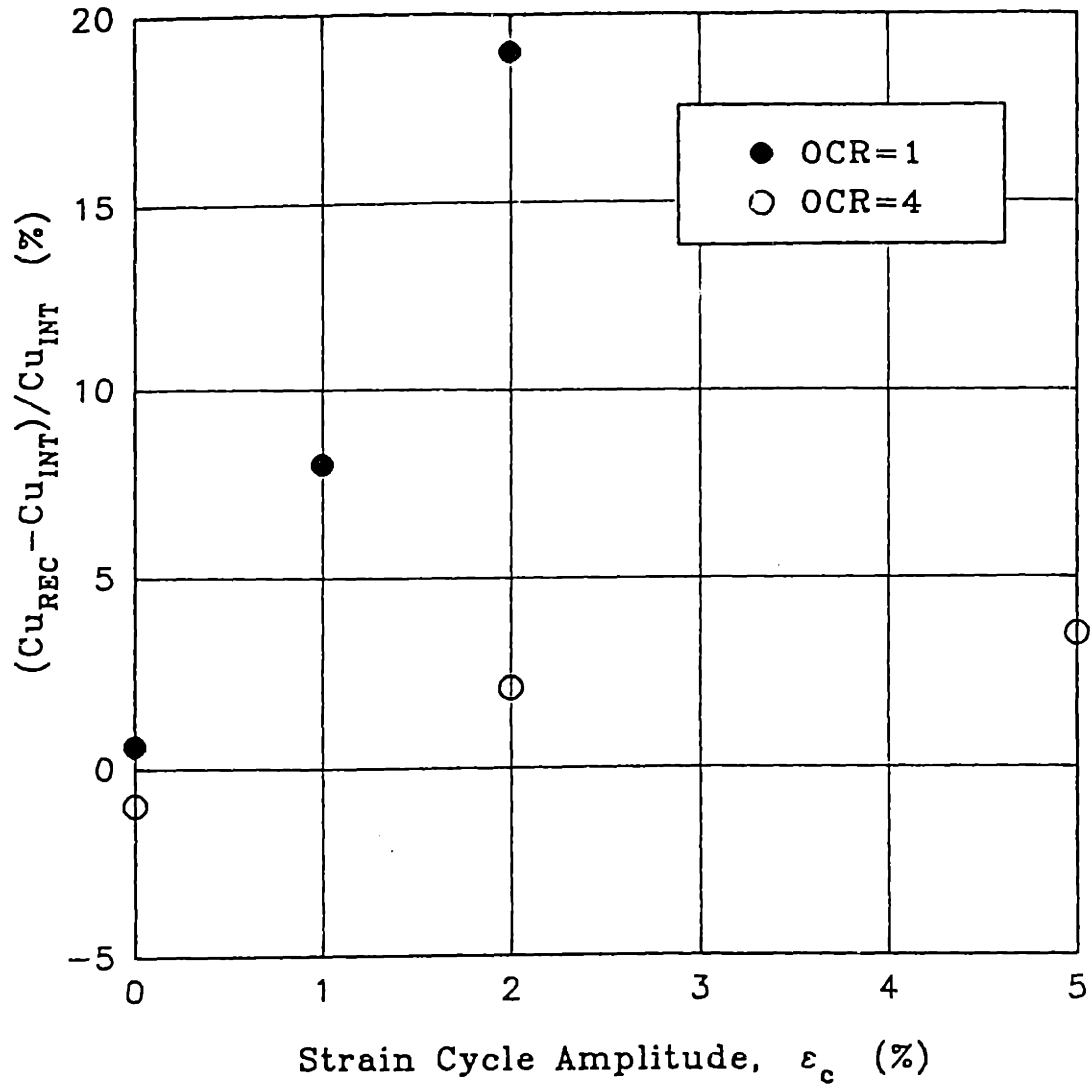


Figure 7.5: Change in Strength due to Recompression of Disturbed NC and OCR4 RBBC

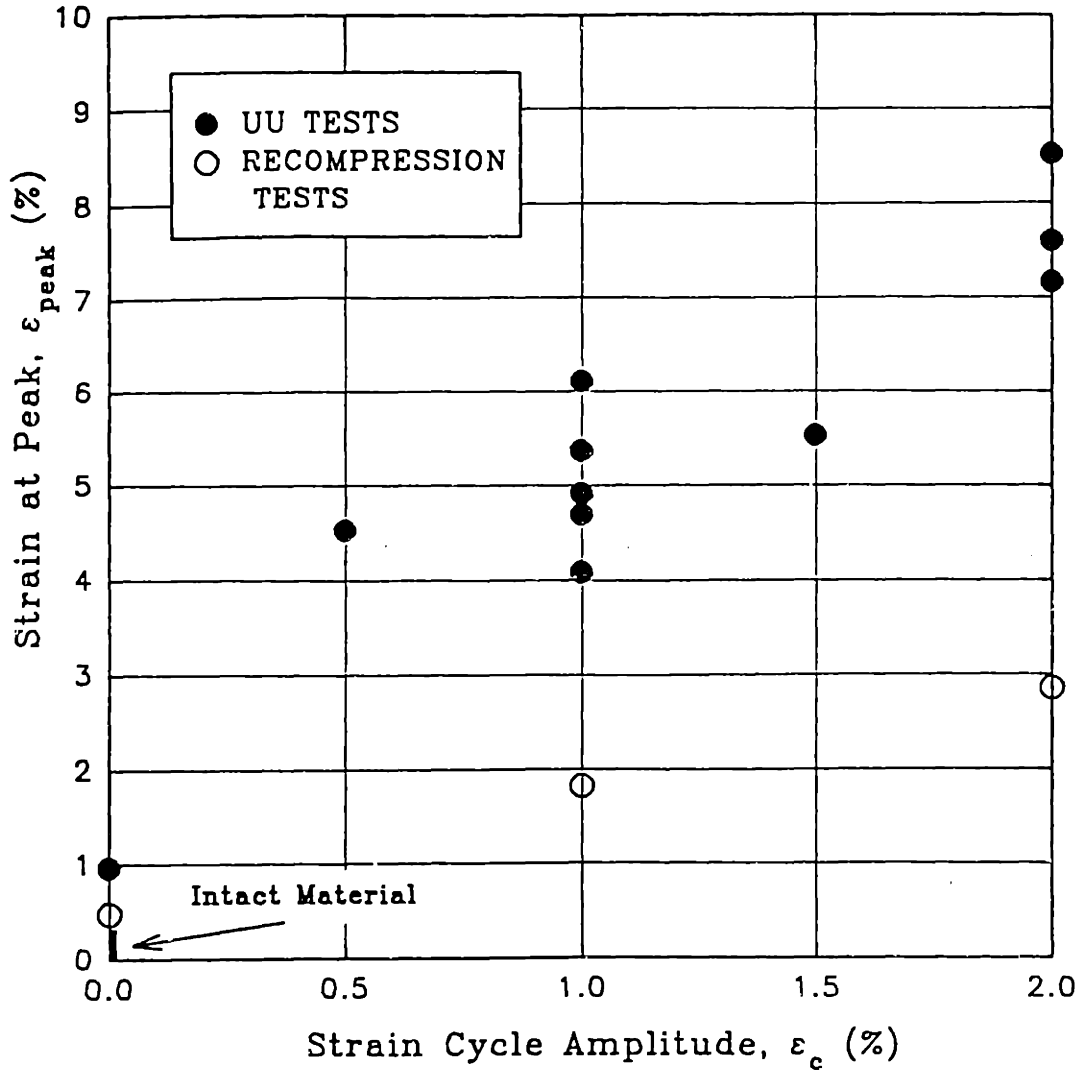


Figure 7.6: Strain at Peak from Undisturbed, UU and Recompression Tests on NC RBBC

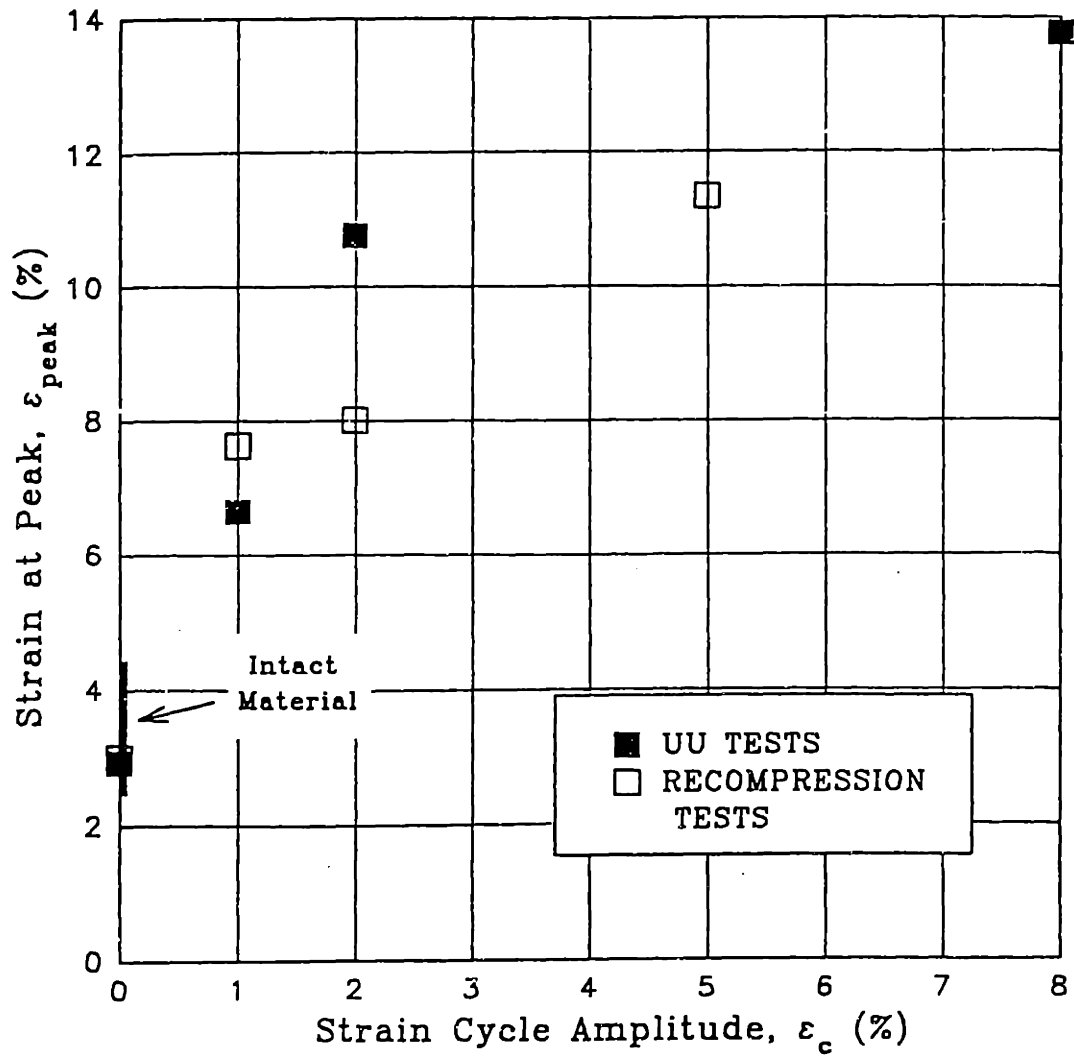


Figure 7.7: Strain at Peak from Undisturbed, UU and Recompression Tests on OCR4 RBBC

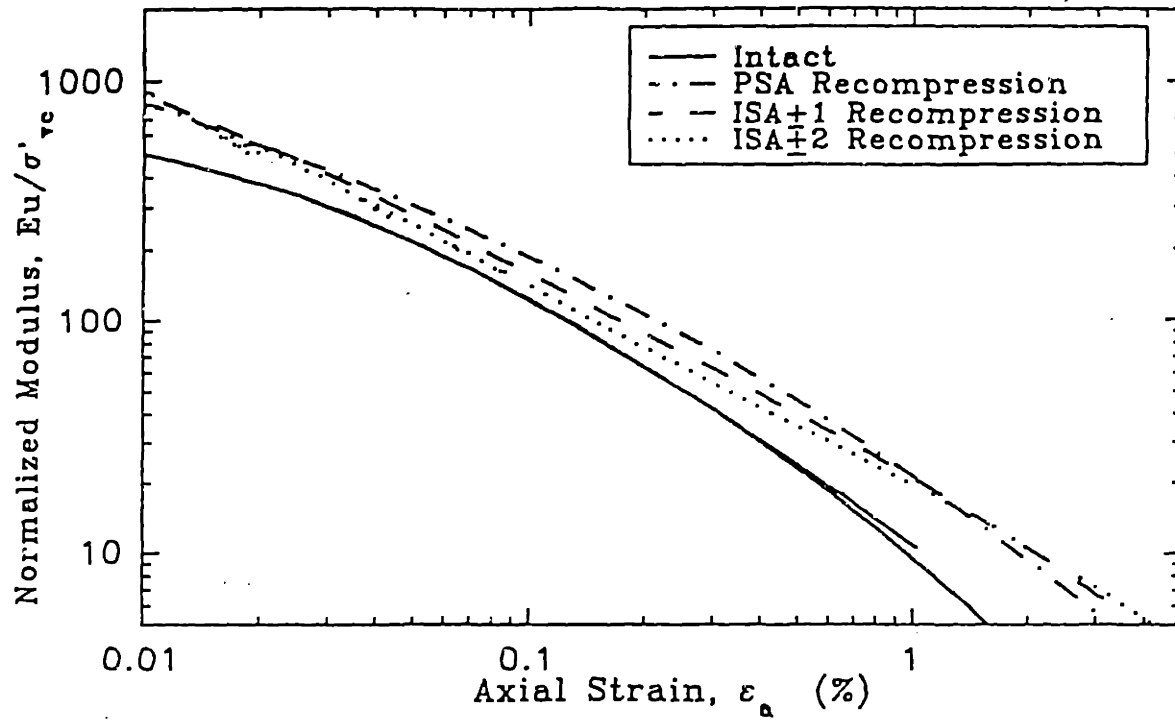


Figure 7.8: Effect of Disturbance and Recompression on the Stiffness of NC RBBC

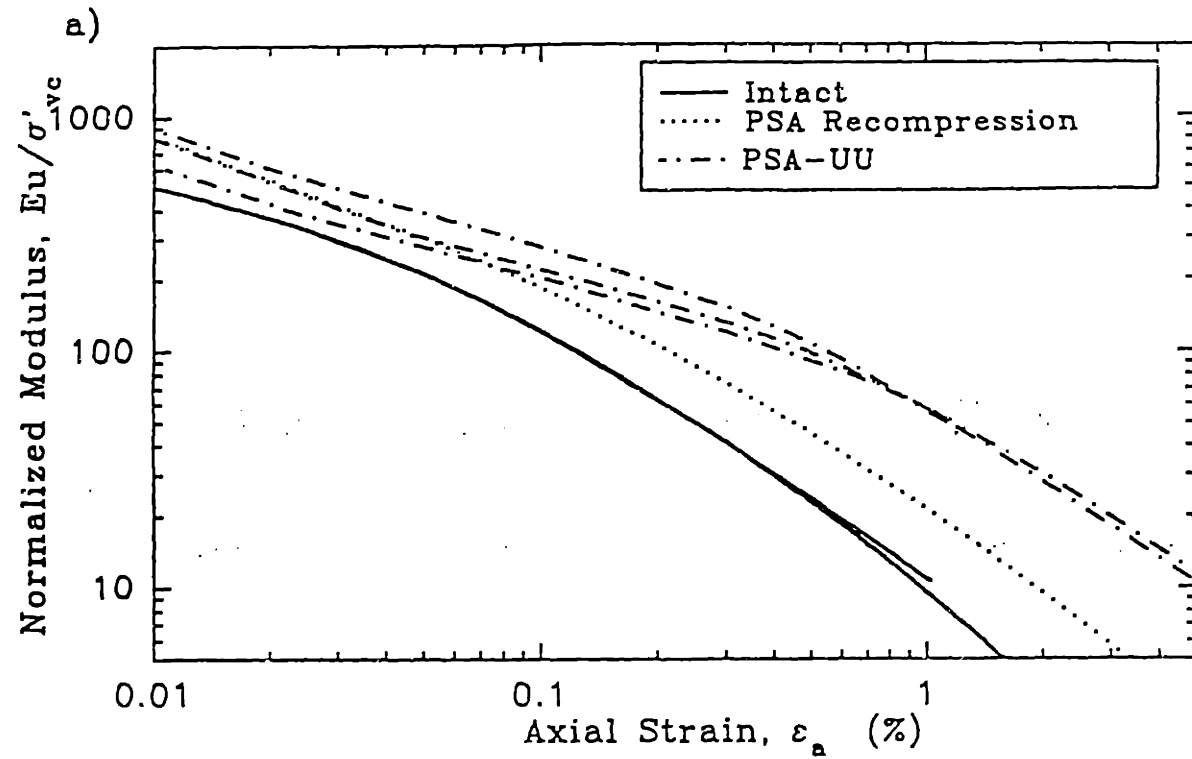


Figure 7.9: Effect of Disturbance and Recompression on the Stiffness of NC RBBC: (a) PSA



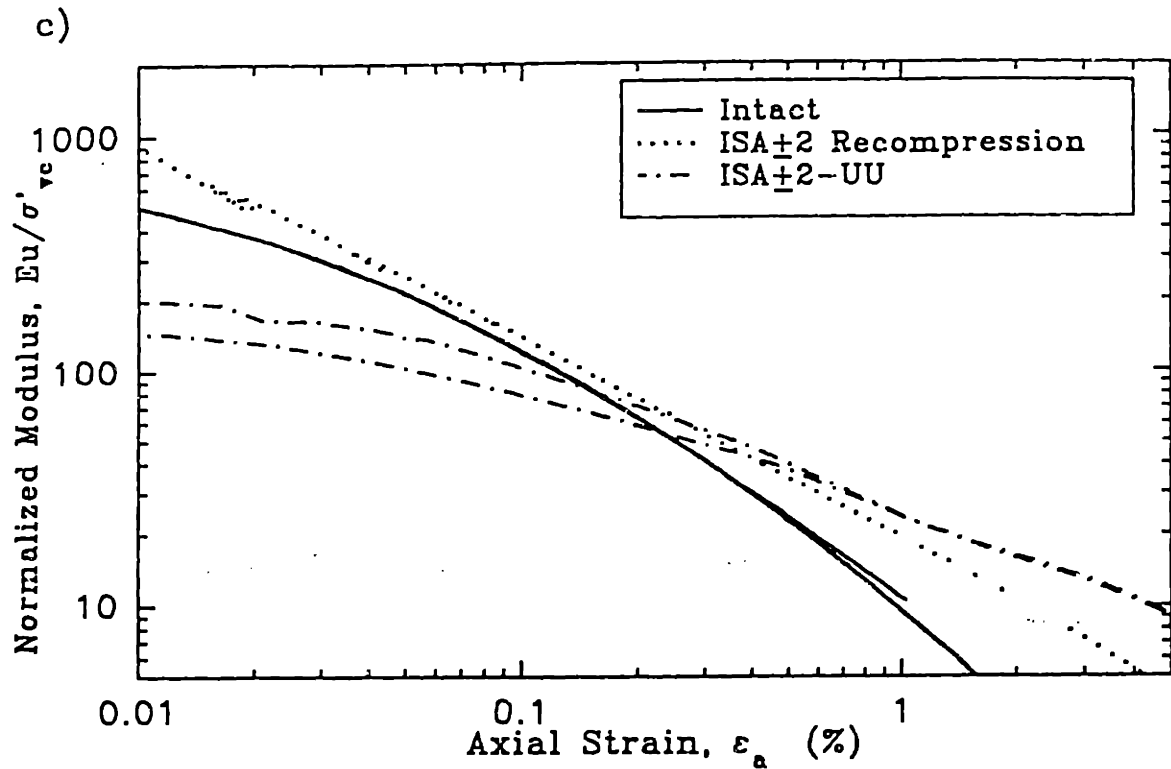
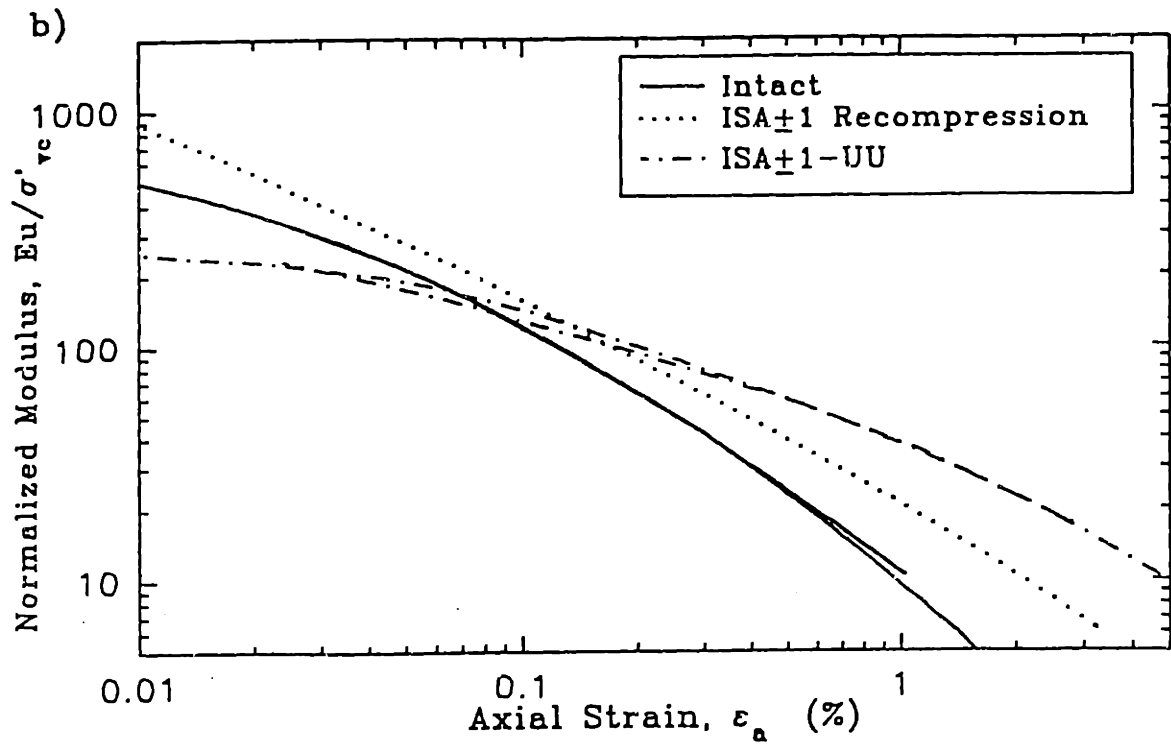


Figure 7.9: Effect of Disturbance and Recompression on the Stiffness of NC RBBC: (b) ISA $\pm$ 1, (c) ISA $\pm$ 2

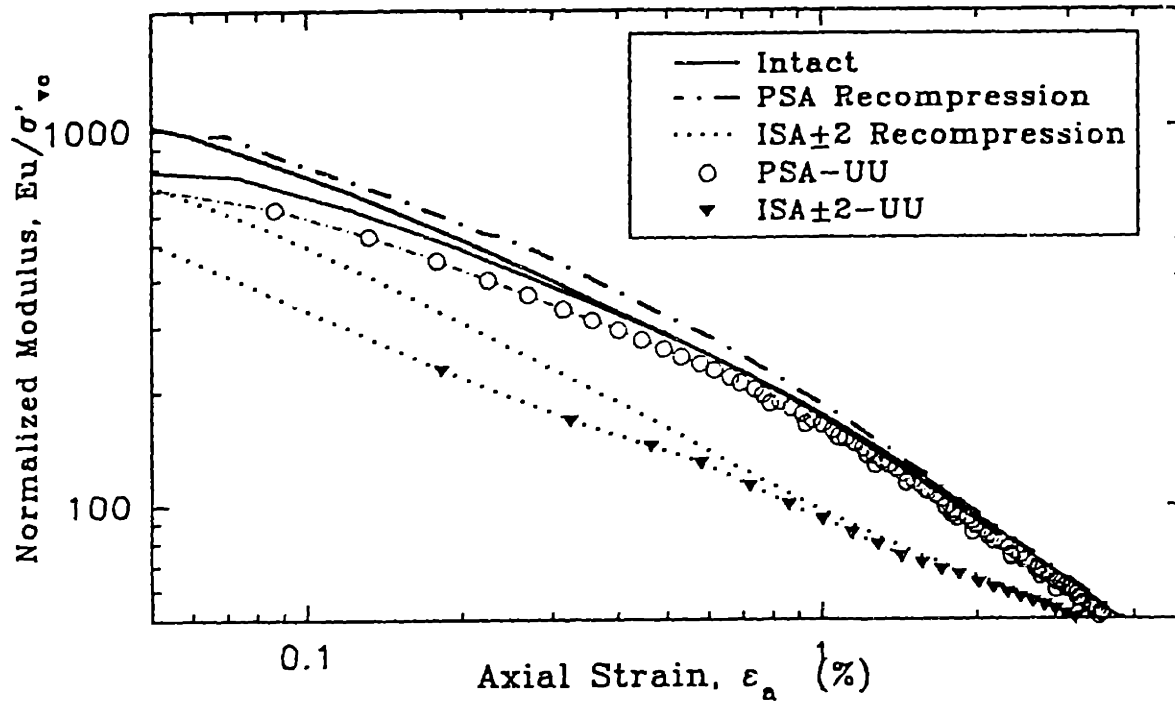


Figure 7.10: Effect of Disturbance and Recompression on the Stiffness of RBBC with Nominal OCR=4

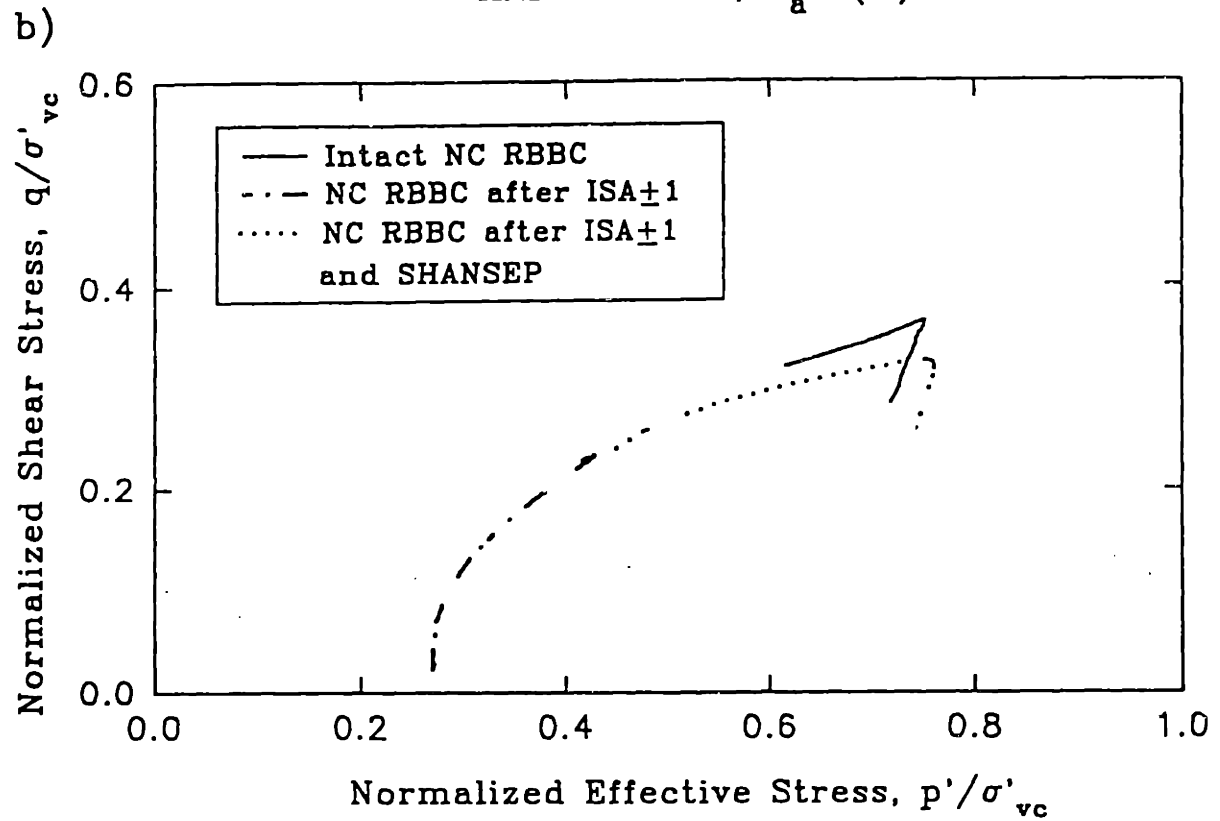
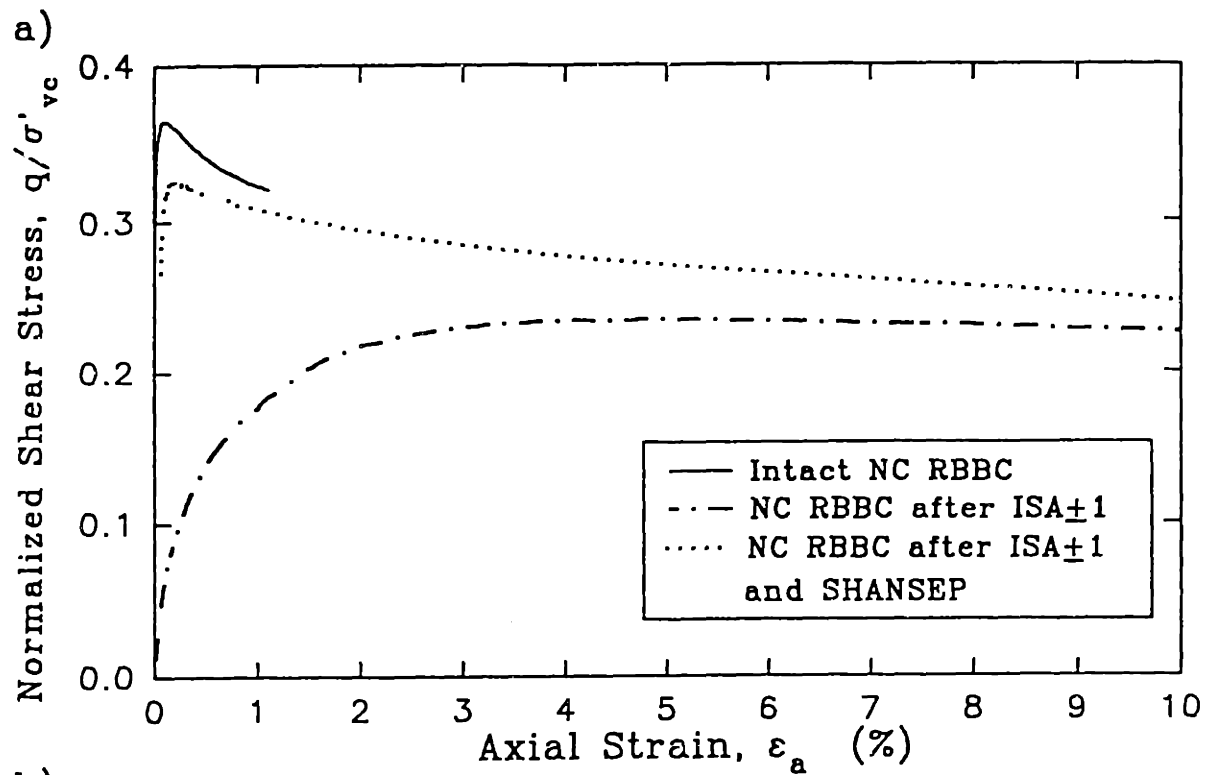


Figure 7.11: Effect of  $ISA_{\pm 1}$  Disturbance and SHANSEP on the Undrained Shear Behavior of NC RBBC: (a) Stress Strain Curve, (b) Stress Path.

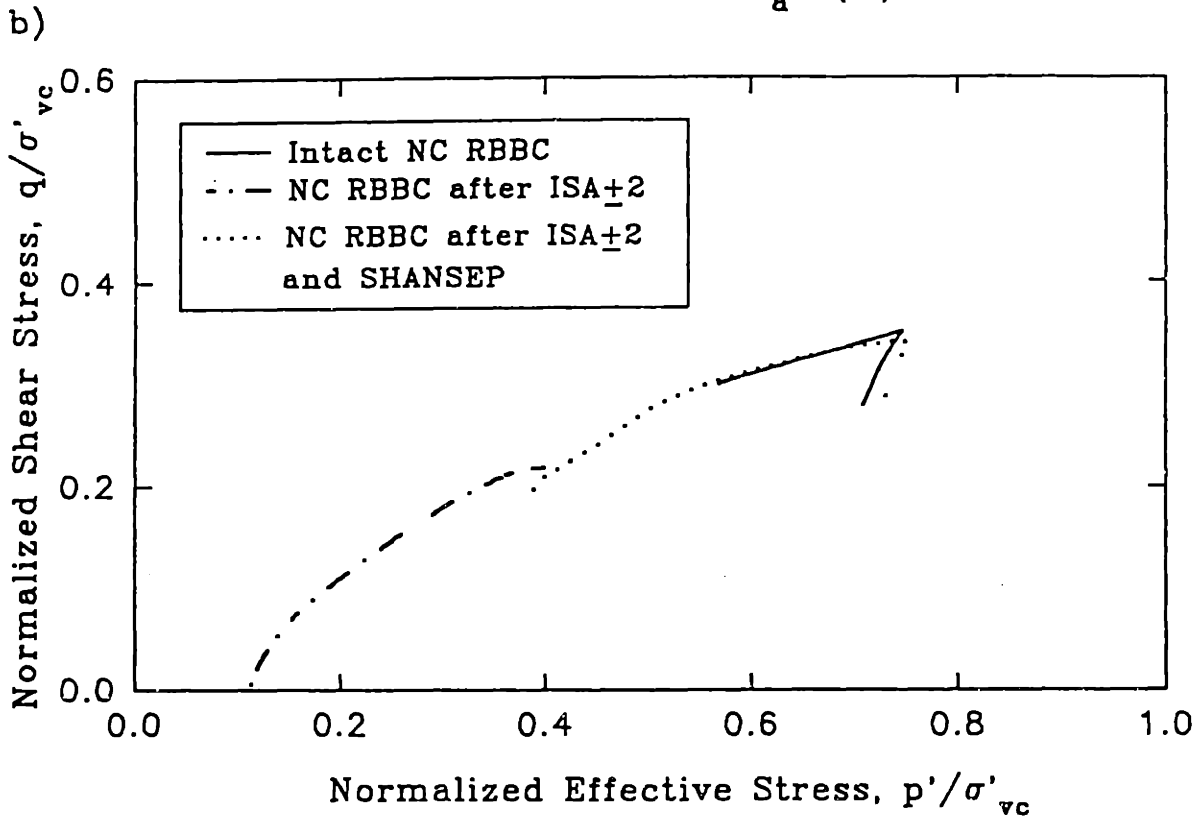
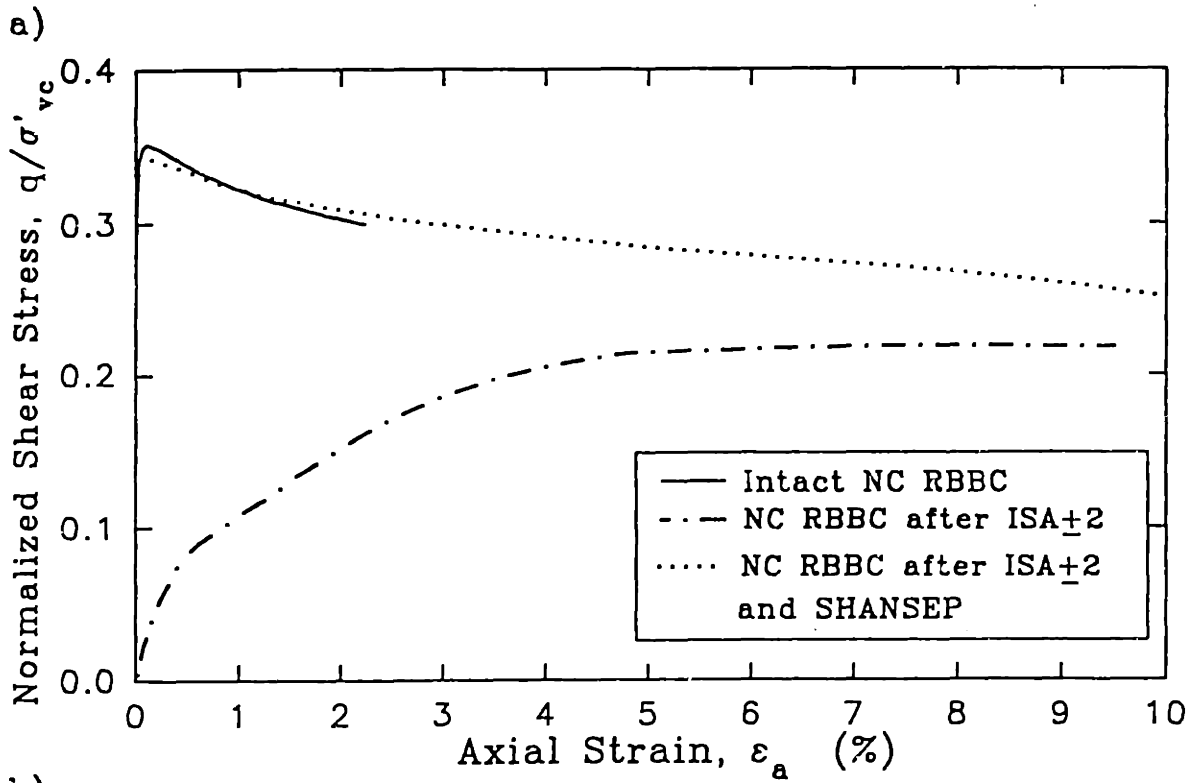


Figure 7.12: Effect of ISA+2 Disturbance and SHANSEP on the Undrained Shear Behavior of NC RBBC:(a) Stress Strain Curve, (b) Stress Path

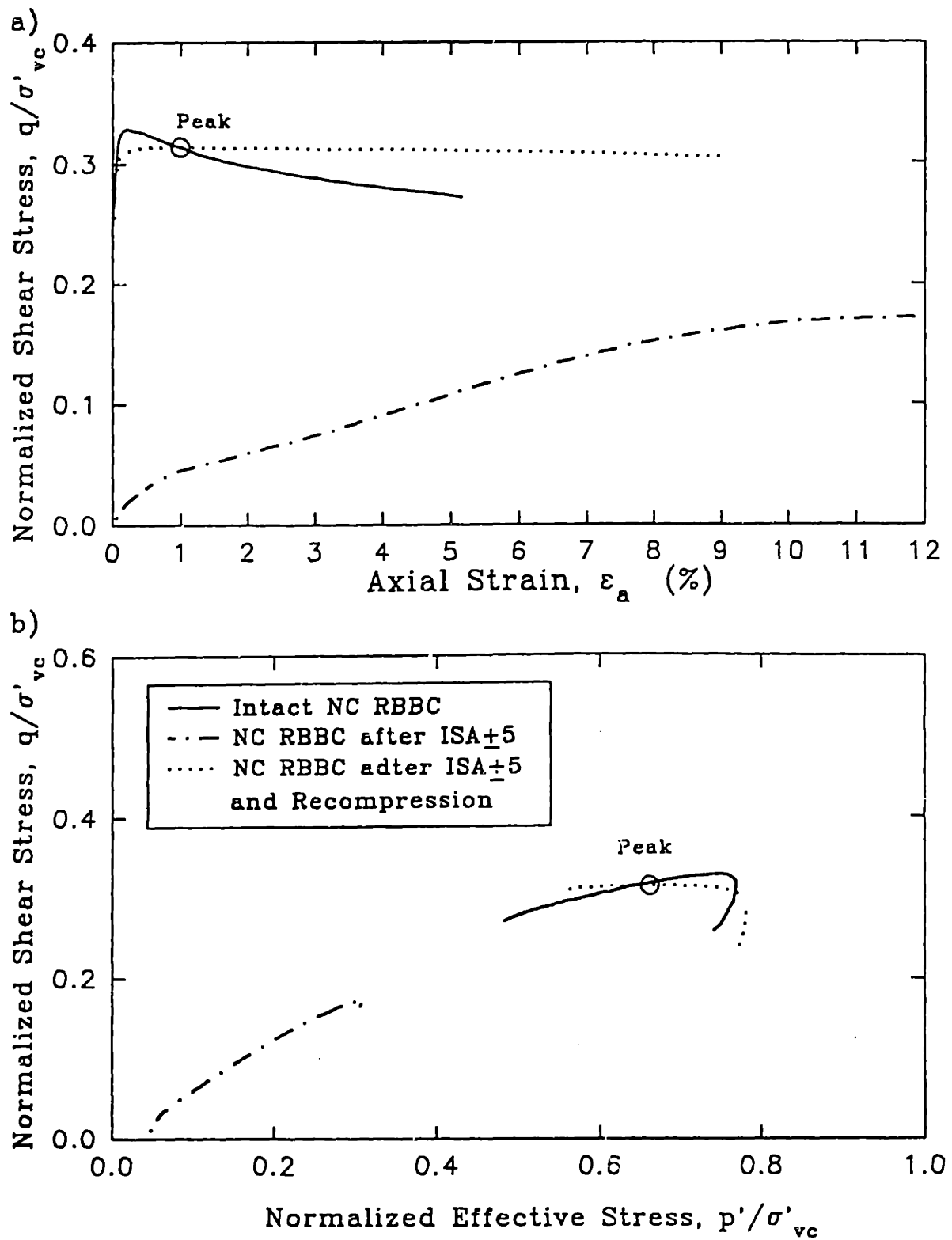


Figure 7.13: Effect of ISA $\pm$ 5 Disturbance and SHANSEP on the Undrained Shear Behavior of NC RBBC  
 (a) Stress Strain Curve, (b) Stress Path

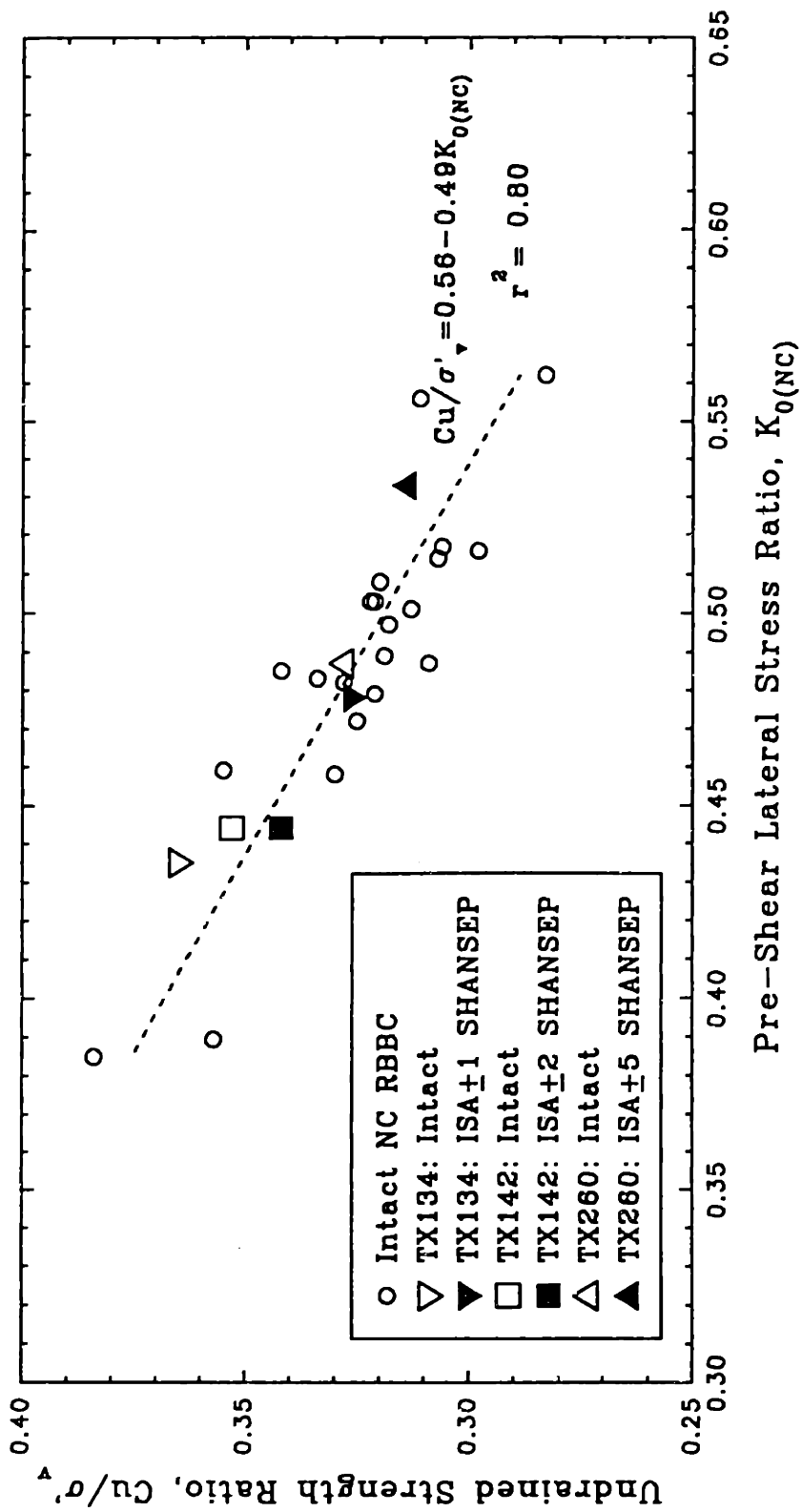


Figure 7.14: Applicability of the  $K_{0(NC)}$  vs.  $C_u/\sigma'_{vc}$  Relationship to the SHANSEP Tests

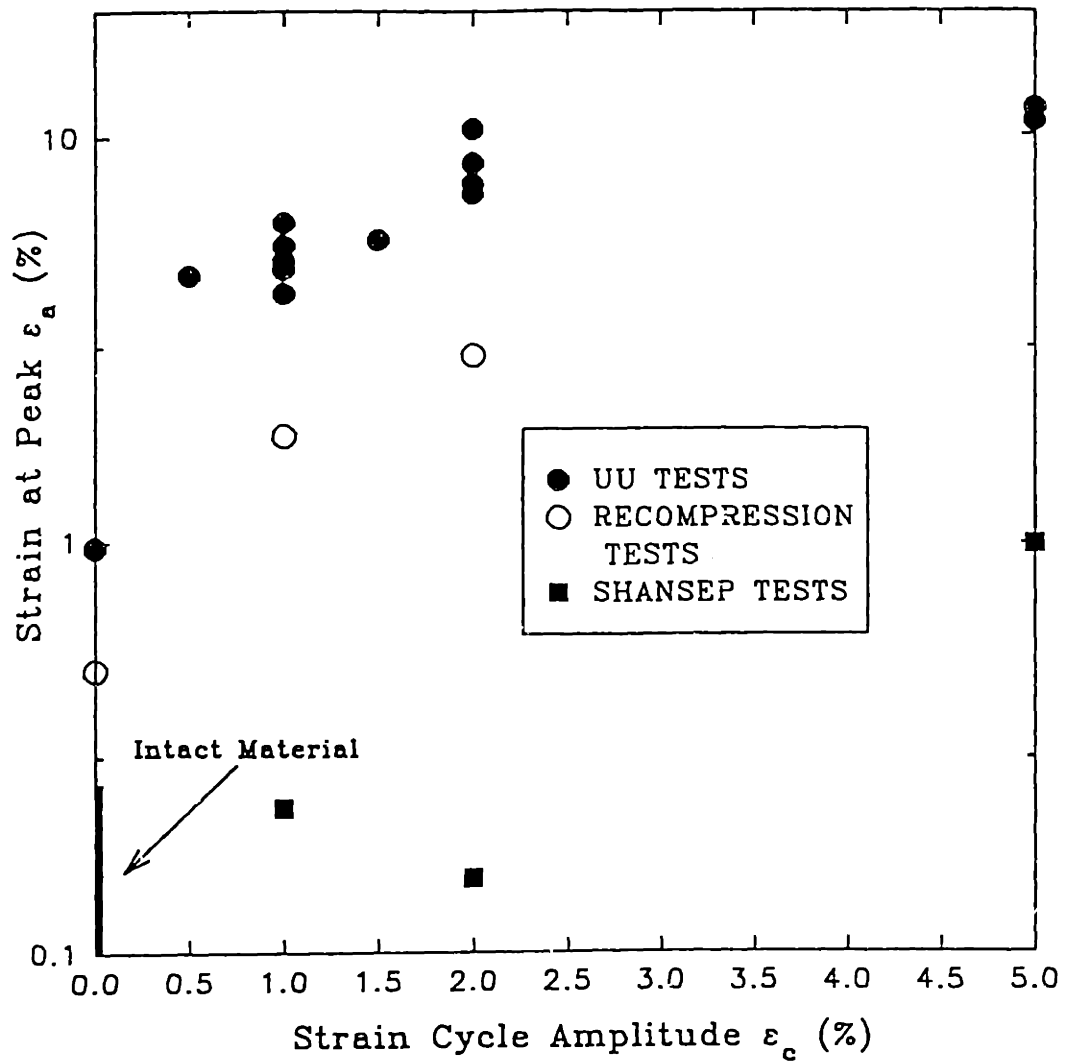


Figure 7.15: Strain at Peak from Undisturbed, UU, SHANSEP and Recompression Tests on NC RBBC

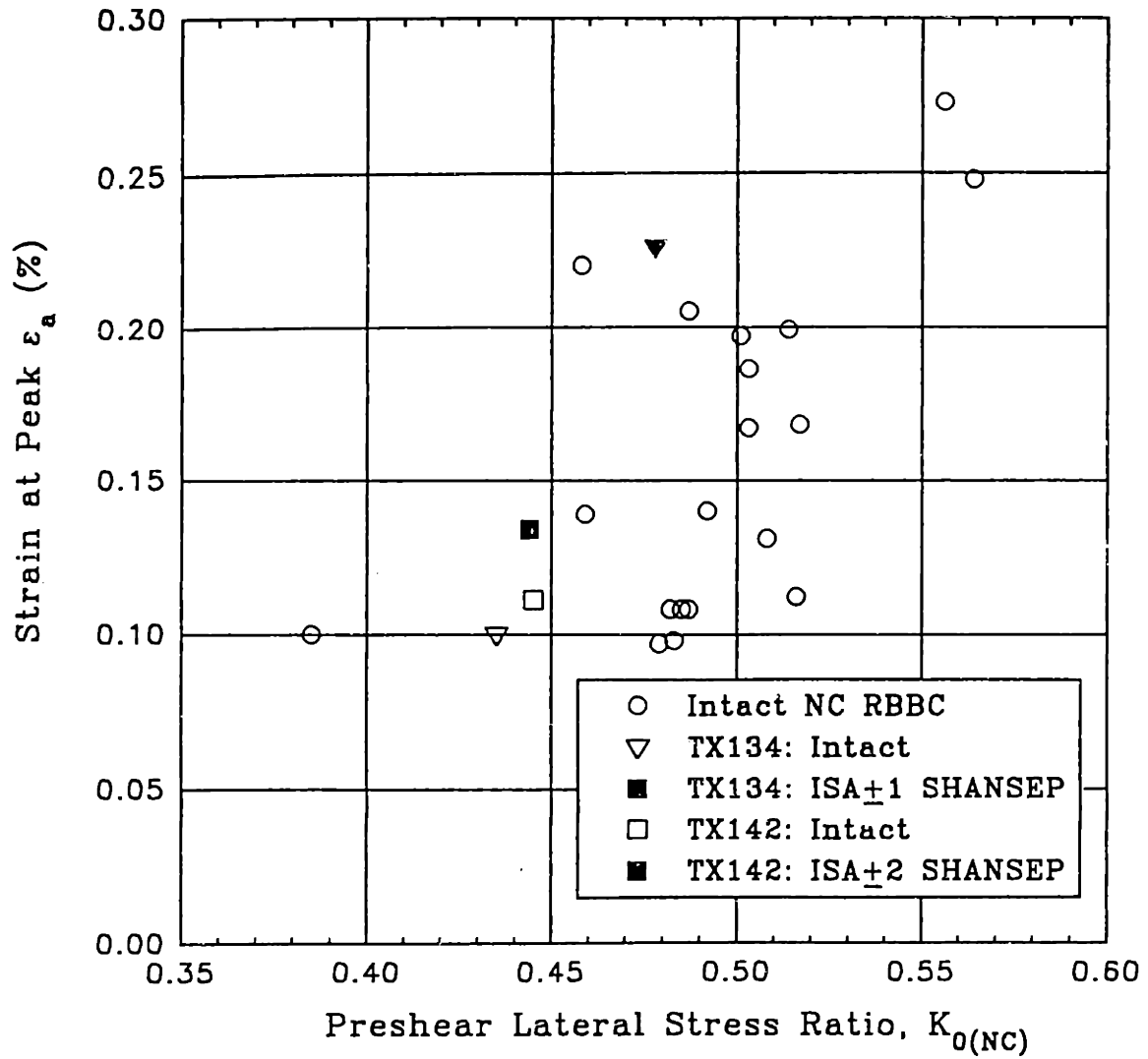


Figure 7.16: Validity of the  $K_{0(NC)}$  versus  $\epsilon_{peak}$  Relationship for SHANSEP tests



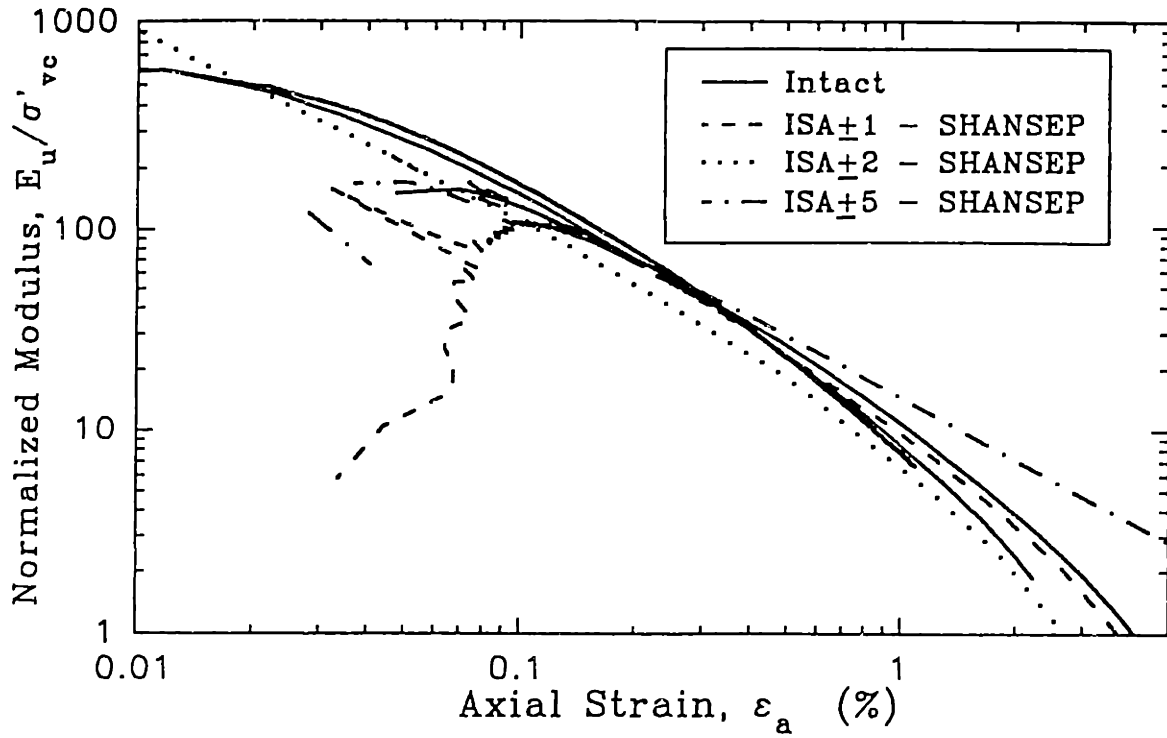


Figure 7.17: Effect of Disturbance and SHANSEP Reconsolidation on the Stiffness of NC RBBC

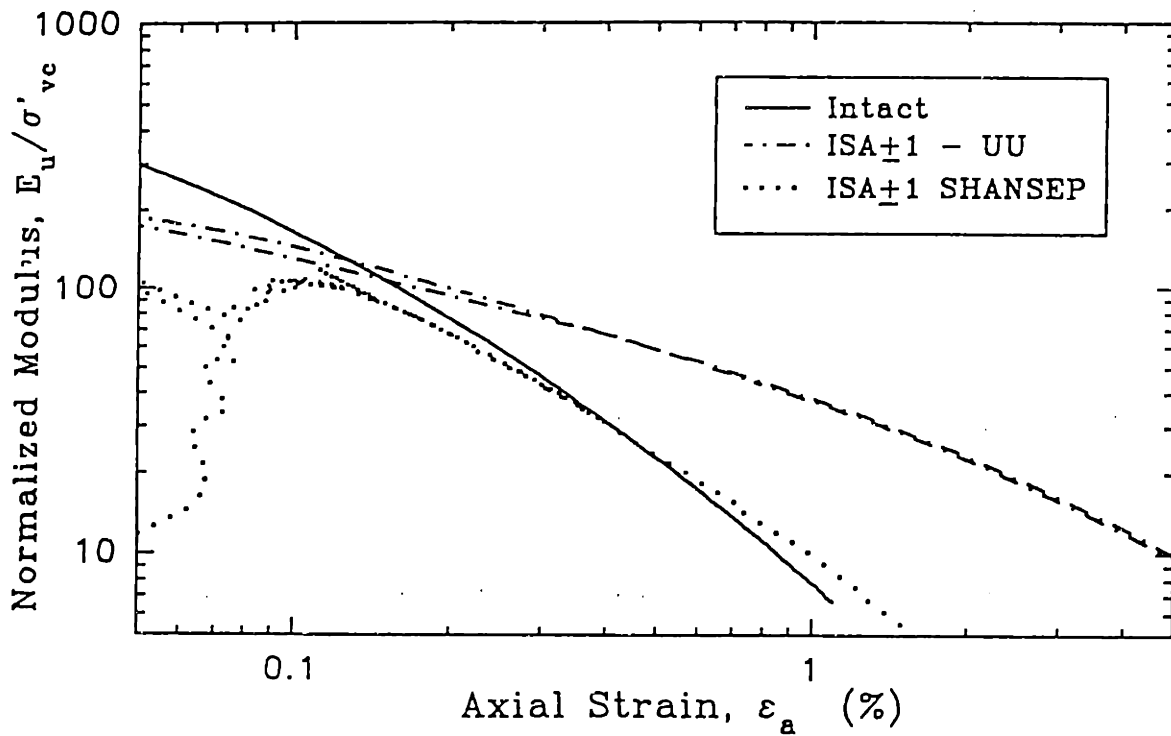


Figure 7.18: Stiffness for ISA+1 Disturbed SHANSEP test on NC RBBC

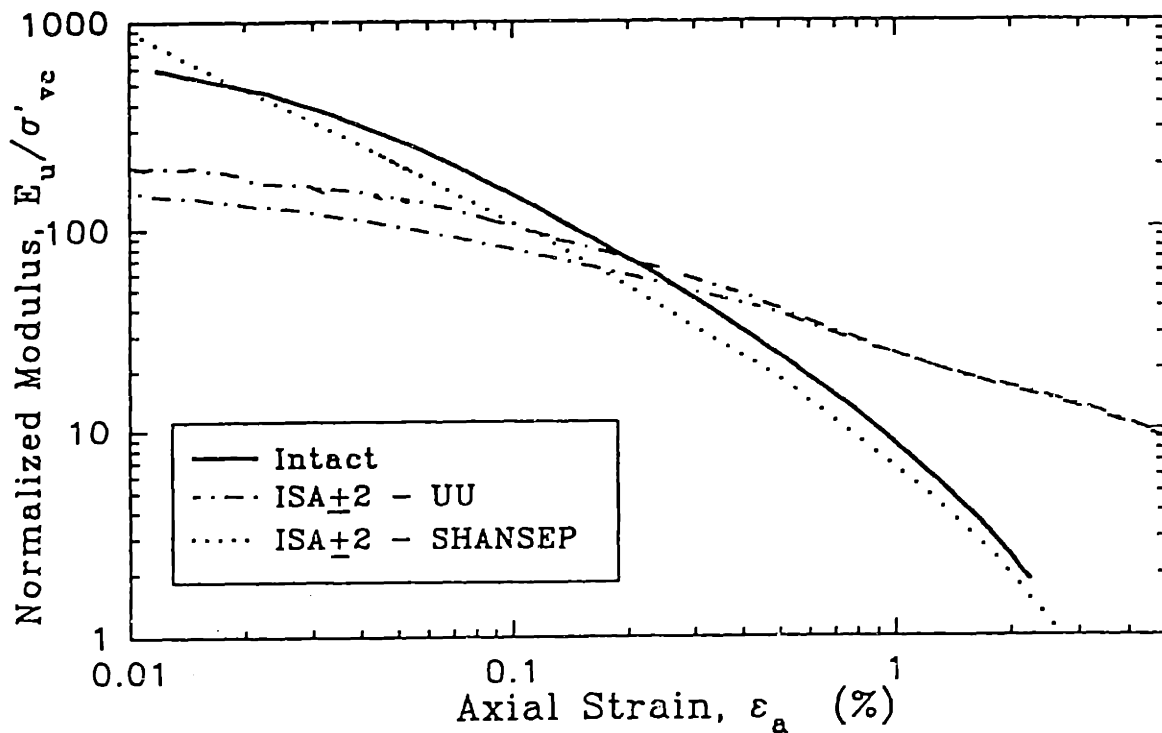


Figure 7.19: Stiffness for ISA±2 Disturbed SHANSEP test on NC RBBC

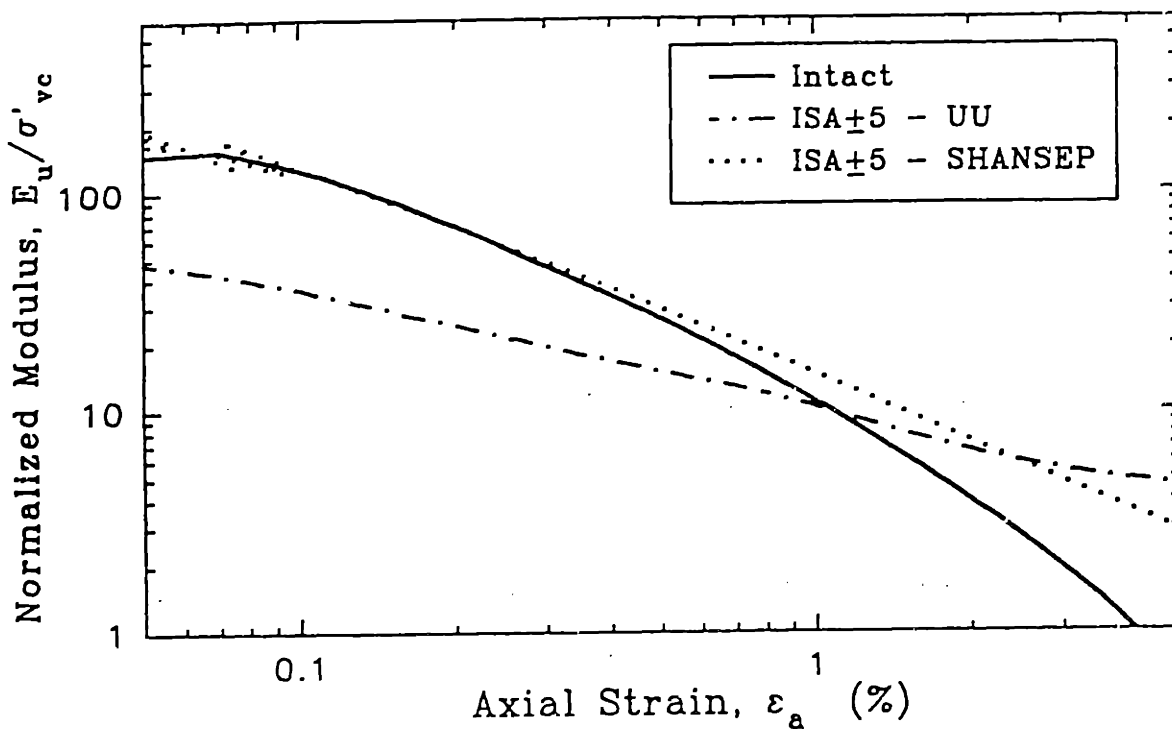


Figure 7.20: Stiffness for ISA±5 Disturbed SHANSEP test on NC RBBC

# Chapter 8 Summary, Conclusions and Recommendations

## 8.1 Introduction

This research investigated the problem of sampling disturbance by performing single element triaxial tests in which an intact specimen of RBBC was disturbed in accordance with the Perfect Sampling Approach (PSA) and the Ideal Sampling Approach (ISA). The testing program, entirely conducted on Resedimented Boston Blue Clay, consisted of a total of 46 triaxial tests of which the majority were performed on NC RBBC (27). The rest of the tests were performed on OCR2 ( 3 tests), OCR4 (13 tests) and OCR8 (2 tests). Existing data on RBBC were used to complement the results.

The tests have been classified in the following four categories: Undisturbed, Disturbed UU, Disturbed Recompression and Disturbed SHANSEP or  $K_0$ -consolidation tests. ISA tests were performed with amplitude of the disturbance cycle varying between 0.5% and 8%. The testing program focused on relating the variations of the engineering properties caused by disturbance to the magnitude of the strains imposed during disturbance.

The primary objectives of the research were to:

- a) Define the intact compression and shear behavior of RBBC for values of the OCR ranging from one to eight.
- b) Assess the effect of different types (PSA and ISA) and magnitudes of disturbance on the compression and shear behavior of the soil as a

function of its OCR.

c) Verify the advantages/disadvantages of using Recompression and SHANSEP reconsolidation to recover the intact behavior of the soil after disturbance.

## **8.2 Summary of the Results**

### **8.2.1 Intact Behavior of Resedimented Boston Blue Clay**

The intact behavior of RBBC was defined based on the results of this testing program as well as on data available for previous batches of RBBC.

The compression curves of all the tests during consolidation to 3-4 ksc and subsequent swelling were analyzed to verify consistency in the behavior of the soil and to determine the intact parameters of interest such as  $K_{0(NC)}$  and the slope of the virgin compression line, CR.

For the NC soil the results obtained from this testing program (during the undrained shear of the Undisturbed Tests and during the first compression phase of the ISA disturbance in the Disturbed Tests) yielded the information necessary to characterize the undrained shear behavior of the soil. For the other OCRs, extensive use was made of the results provided by Sheahan (1991).

#### ***Compression Behavior***

A value of the intact Compression Ratio of the soil was defined based on the slope of the compression curve in the range between 2.5 ksc

and the maximum stress, when the slope is constant and the soil is assumed to have reached the Virgin Compression Line. There appears to be some scatter (between 0.14 and 0.18) in the measured values of CR between specimens from different batches, which in most cases can be explained by differences in the index properties of the batches. There is also considerable variation of the strains at any given value of the stress.

The analysis of the consolidation results indicates a large scatter in the pre-shear value of  $K_0(\text{NC})$  which could not be linked to variation in the material index properties, the water content, the slope of the compression curve or the disturbance undergone by the triaxial specimen during set-up. The measured values of  $K_0$  range between 0.43 and 0.56. Due to the variation in  $K_0$  the position of the NC soil element within the stress space prior to shear varies considerably.

In a limited number of tests the specimens were consolidated to the maximum stress by stress path consolidation through which the horizontal and vertical stresses were targeted to obtain the desired value of the lateral stress ratio. The results for these tests indicate however that a precise definition of the pre-shear stress state of the soil is obtained at the expense of large modifications in the compression curve of the soil: not only can the stress history of the specimen no longer be evaluated, also the slope of the compression curve decreases substantially.

### ***Undrained Shear Behavior***

The analysis of the undrained shear results for Intact NC RBBC show that the soil fails at a very small strain and exhibits significant strain softening. As the OCR of the soil increases the undrained strength normalized by the consolidation stress and the strain at peak increase and

there is no strain softening. At large strains the stress paths of RBBC with OCR=1, 2, 4 and 8 all approach a common failure envelope.

For NC RBBC the undrained strength ratio is strongly influenced by the pre-shear value of the lateral stress ratio. This applies whether the soil is consolidated to the maximum stress in  $K_0$  conditions or following a constant  $K$  path. As the pre-shear lateral stress ratio increases the undrained strength decreases and the relationship between the two parameters, for  $K$  varying between 0.38 and 0.57, can be satisfactorily described through the following equation:  $S_c = 0.56 - 0.49 \cdot K$  ( $r^2=0.80$ ). Based on this relationship a technique was suggested to correct the values of  $(C_u/\sigma'_{vc})_{NC}$  to the same value of  $K$ . The variation in  $K$  does not affect the strength of the overconsolidated clay.

The relationship between the undrained strength and the OCR of the soil is very well described by the SHANSEP equation  $C_u/\sigma'_{vc}=S \cdot (OCR)^m$ .

The regression ( $r^2=0.997$ ) through the undrained strength results for RBBC with OCR equal to 1, 2, 4 and 8 provides the parameters  $S$  and  $m$  for the equation. The resulting values  $S=0.33$  and  $m=0.71$  are in excellent agreement with previous results (Sheahan 1991) on RBBC.

The strain at peak of the intact soil increases with OCR. For the NC soil it appears to be affected by the pre-shear lateral stress ratio. In particular it is observed that larger values of  $\epsilon_{peak}$  are measured as  $K$  increases.

The equipment used for this research allows reliable estimates of the

stiffness to be made for strains larger than 0.01-0.05%. At these low strains and before the NC clay strain softens, the normalized stiffness decreases with increasing OCR. Extremely scattered results were obtained for  $E_{u(50)}/\sigma'_{vc}$  the undrained modulus at 50% of the stress increment to reach failure and it wasn't possible to establish any trend with OCR.

## 8.2.2 Effects of Disturbance on the Undrained Shear Behavior of RBBC

### *NC RBBC*

PSA and ISA Disturbed UU tests with the strain cycle amplitude varying between 0.5% and 5% were performed on NC RBBC. The results of the ISA tests indicate that disturbance results in:

- a modification of the stress strain curve and of the stress path,
- a complete loss of the strain softening behavior.
- a reduction of the effective stresses,
- a reduction of the undrained strength,
- an increase in the strain at peak,
- a reduction of the normalized modulus  $E_{u(50)}/\sigma'_{vc}$ ,
- a decrease in the stiffness at the intermediate strains.

These effects can be observed in a consistent manner in all the ISA tests but they become more and more marked as the level of disturbance increases.

For the PSA tests all the above applies except that the soil after disturbance continues to exhibit some strain softening and does not show a decrease of the stiffness at the intermediate strains.

Comparison of the stress strain curves and the stress paths of the disturbed NC specimens with the corresponding curves determined for Intact OC RBBC indicates that the effects of disturbance are similar to those produced by swelling. In this sense the undrained decrease in stresses caused by disturbance was quantified in terms of an Induced Overconsolidation Ratio IOCR equal to the ratio between the vertical consolidation stress  $\sigma'_{vc}$  prior to disturbance and the vertical stress resulting from disturbance  $\sigma'_s$ .

The decrease in the undrained strength of NC RBBC produced by disturbance is very significant ranging from approximately 15% in the PSA tests to 45% in the ISA $\pm$ 5 tests.

The IOCR is related to the strength normalized by the end of sampling vertical stress  $\sigma'_s$  by an equation of the type:  $C_u/\sigma'_s = S \cdot (\text{OCR})^m$ . This "SHANSEP" equation describing the variation of strength for increasing IOCR is characterized by the same S parameter as the equation determined for the undisturbed soil and by a value of m equal to 0.82, indicating that a decrease in effective stress caused by disturbance produces a smaller change in the undrained strength than if the same change in stress is due to swelling.

The effect of disturbance on the strain at peak is very distinct for all levels of disturbance with  $\epsilon_{\text{peak}}$  increasing by 50 times after only ISA $\pm$ 1 disturbance. Comparison of the results of the UU tests with the Undisturbed Tests on OC RBBC indicates that:



- the increased value of  $\epsilon_{\text{peak}}$  in the PSA tests can be explained by the stress unload;
- the ISA disturbed NC soil exhibits a less brittle behavior than the intact OC material;
- in the ISA tests the increase in the strain at peak is due not only to stress unload but also to the restructuring of the soil caused by the large strains imposed during the disturbance cycle.

Due to the fact that disturbance causes such a marked modification in the stress strain behavior of the soil, the undrained modulus  $E_{u(50)}$  does not represent a reliable indicator of the effect of disturbance on the stiffness of the soil which can be assessed by comparing intact and disturbed behavior in the same range of strains. ISA disturbance causes a large decrease in the stiffness at the intermediate strains for all magnitudes of disturbance.

In the PSA tests the soil upon reloading is consistently stiffer than during the initial loading due to the fact that unloading to the hydrostatic conditions does not damage the structure of the material.

The effect of the stress unload caused by bore-hole drilling prior to penetration of the sampler was investigated through one NC test in which the soil specimen was unloaded to hydrostatic conditions prior to being subjected to ISA $\pm$ 1 disturbance. The results of this test, identical to those of the ISA $\pm$ 1 tests, indicate that limited stress release prior to tube penetration does not lead to further disturbance.

## **OC RBBC**

The results of the UU tests run on OCR4 RBBC after PSA disturbance indicate that due to the limited stress change and straining associated with the unloading to hydrostatic conditions, PSA disturbance causes negligible effects on the undrained strength, the strain at peak, and the stiffness of the soil. The same is true also for OCR2 RBBC except that PSA disturbance does cause a slight increase in the stiffness.

The ISA tests show instead that this type of disturbance is always associated with:

- a reduction of the effective stresses,
- a modification of the stress strain behavior,
- an increase of the strain at peak,
- a decrease in the stiffness at intermediate strains.

These effects are much less pronounced than in the NC tests and decrease with increasing value of the OCR.

The ISA tests on OCR 2 RBBC indicated also a decrease in the undrained strength for all values of disturbance. For higher OCR it appears that very significant disturbance is necessary to cause a decrease of the strength and that  $ISA_{\pm 1}$  and  $ISA_{\pm 2}$  disturbance leave the strength of the soil unchanged. It is likely that the "minimum" straining required to cause a significant degradation of the soil properties is related to the peak strain of the soil.

The stress strain behavior of the soil after disturbance indicates that also for OC RBBC disturbance produces effects similar to those caused by swelling and the decrease in stress caused by disturbance can be quantified by the IOCR.

Larger magnitudes of disturbance compared to the NC soil are necessary to produce the same IOCR. For the same value of IOCR the decrease in strength measured in the OC tests is lower than for NC clays.

The strain at peak appears to be the parameter more severely affected by disturbance for all values of OCR. As for the NC clay, the stress unloading alone is not responsible for the increase in the strain at peak.

PSA disturbance produces a slight increase in the intermediate strain stiffness of OCR2 RBBC, while it has no effect on the modulus of the OCR4 and OCR8 RBBC.

The effects of ISA disturbance are to decrease the stiffness at the intermediate strain. For increasing OCR the reduction of the modulus decreases.

### **8.2.3 Effects of Disturbance on the Compression Behavior of RBBC**

The limited number of tests in which the triaxial specimens were reconsolidated well past the in situ stresses after disturbance indicate that increasing amplitudes of imposed strains during disturbance are associated with:

- a more rounded compression curve,
- an increase in the slope of the recompression curve,
- a decrease in the compression ratio,
- increasing reconsolidation strains,
- increased uncertainty in defining the maximum past pressure.

It is has not been established if disturbance affects the normally consolidated lateral stress ratio.

For the same level of disturbance the effects of disturbance are less marked for increasing OCR.

The reconsolidation strains increase with level of disturbance but decrease for increasing OCR. Therefore they should be considered only as a means to evaluate the relative disturbance affecting tests performed on the same soil.

The limited results indicate that uncertainties in the definition of the preconsolidation pressure are associated with:

- the large reconsolidation strains that increase with disturbance;
- the fact that upon reconsolidation, due to disturbance, the soil is not able to reach the virgin compression line. For increasing disturbance the slope of the "disturbed" compression curve beyond the  $\sigma'_{vm}$  decreases.

Regardless of the OCR of the soil (1, 2 or 4) and of the level of disturbance (ISA $\pm$ 1, ISA $\pm$ 2, ISA $\pm$ 5) the maximum past pressure was estimated with an accuracy of 10 $\pm$ 5%, indicating does not significantly affect the stress history of RBBC. While the higher OCR tests yielded a better estimate of the maximum past pressure, for NC the most accurate determination of  $\sigma'_p$  was not associated with the lower level of disturbance.

All the best estimates of the preconsolidation pressure obtained by the Strain Energy method led to an overestimation of  $\sigma'_p$ .

#### **8.2.4 Effect of Recompression Reconsolidation on the Undrained Behavior of RBBC**

The results of the PSA, ISA<sub>+1</sub>, ISA<sub>+2</sub> Recompression tests performed on NC RBBC indicate that for NC clay this reconsolidation procedure:

- causes a decrease in water content,
- significantly overestimates the undrained strength of the soil by as much as 20% in the ISA<sub>+2</sub> test,
- grossly overestimates the strain to peak in the ISA tests,
- does not describe the post-peak strain softening of the soil,
- predicts a larger stiffness of the soil at the intermediate strains.

These errors increase as the level of disturbance increases.

The effects of Recompression on disturbed OCR4 RBBC are quite different due to the smaller increase in water content involved with the brief reconsolidation.

For OCR4 RBBC it appears that Recompression:

- provides an accurate estimate of the undrained strength for the level of disturbance considered, but
- describes very inaccurately the stress strain behavior of the soil, in particular significantly overpredicting the strain to peak,
- does not recover the intermediate strain stiffness for the ISA tests.

These last two effects become more significant for increasing magnitudes of disturbance.

### **8.2.5 Effect of SHANSEP Reconsolidation on the Undrained Behavior of NC RBBC**

The effectiveness of the SHANSEP reconsolidation techniques in recovering the intact behavior of NC RBBC was investigated for three levels of disturbance ( $ISA_{\pm 1}$ ,  $ISA_{\pm 2}$ ,  $ISA_{\pm 5}$ ).

For all levels of disturbance this reconsolidation procedure provides:

- a reasonable and safe estimate of the undrained strength of the soil,

If the disturbance is moderate this reconsolidation procedure leads to an accurate description of the stress strain behavior of the soil and of the post-peak stiffness of the soil. Greater disturbance ( $ISA_{\pm 5}$ ) causes a significant increase in the strain at peak and the absence of strain softening with consequent stiffer post-peak behavior. However much of the difference may be accounted with the inability of the soil to return to the intact VCL.

The limited results available also indicate that through SHANSEP reconsolidation, it is possible to recover the intermediate strain stiffness of the NC soil.

### 8.3 Conclusions

This research contributes to the understanding of sample disturbance by investigating the effects of PSA and ISA disturbance on the compression and shear behavior of NC and OC RBBC. Given that the level of disturbance on field recovered samples cannot be accounted for by the Ideal Sampling Approach, it is clear that in practice other factors will contribute to determining sample quality. However the work performed provides a useful framework to:

- quantify the effects of tube penetration and stress release,
- determine the sensitivity of soft soils to disturbance as a function of the OCR,
- determine which engineering parameters are most affected by disturbance,
- provide insight into which soil properties can be recovered through Recompression and SHANSEP reconsolidation.

Comparison of the behavior of RBBC after PSA and ISA disturbance indicates the following:

- the shear stress release simulated in the PSA tests produces limited damage on NC RBBC and negligible effects for higher OCRs;
- the decrease of the effective stresses and the restructuring caused by the large strains imposed during ISA disturbance cause a significant degradation of all the properties of NC RBBC;
- NC RBBC is more susceptible to disturbance than the OC clay: as the OCR of the soil increases larger magnitudes of disturbance are

necessary to produce the same degradation of the engineering properties.

This research proposes that it is possible to interpret some of the effects of sampling disturbance by comparing the undrained decrease in the effective stresses caused by disturbance to the drained stress unload occurring during swelling. In this framework, the normalized undrained strength  $c_u/\sigma'_s$  after disturbance has been successfully related to the IOCR through the "SHANSEP" equation  $c_u/\sigma'_s = S(\text{OCR})^m$ . For RBBC  $S=0.33$  and  $m=0.82$ . Sinfield (1994) has found that the same equation relating the strength and the IOCR applies after in-laboratory simulation of true field sampling, indicating that this relation does not depend on the drainage conditions.

The degradation of other parameters, such as the strain at peak, produced by ISA disturbance cannot be explained simply by the decrease of the effective stresses. It is concluded that the large strains imposed during the simulation of disturbance produce significant restructuring of the soil.

The tests performed present evidence that disturbance does not significantly affect the determination of the preconsolidation pressure which can be determined with an accuracy of  $10\pm 5\%$  for all levels of disturbance. Further it appears that sampling disturbance leads to overestimating  $\sigma'_p$ .

Disturbance affects the compression behavior of the soil by decreasing the compression ratio and increasing the strains at any stress level. For increasing disturbance the amount of consolidation required to



return to the virgin compression line increases with the magnitude of disturbance and decreases with OCR for the same disturbance.

Reconsolidation strains increase with disturbance but their magnitude depends on the OCR of the soil. It is therefore recommended that they be used solely as a means to evaluate the relative disturbance affecting tests performed on the same soil.

This research presents a preliminary investigation of the advantages and disadvantages of the two reconsolidation techniques generally employed.

Test results show that for NC RBBC, the Recompression technique results in an unsafe estimate of the strength by as much as 20% even for moderate disturbance. Therefore this technique is not recommended for low OCR soils. This reconsolidation procedure should only be considered reliable when assessing the undrained strength of a soft clay with OCR equal to or larger than 4. For all OCRs, Recompression yields an unsatisfactory description of the stress strain behavior of the soil.

Reconsolidation according to SHANSEP provides an accurate and safe estimate of the undrained strength of the NC soil for all magnitudes of disturbance. Further, for moderate disturbance SHANSEP reconsolidation also yields a realistic description of the intact stress strain behavior. Limited results indicate that the intermediate strain stiffness of NC RBBC is recovered through SHANSEP reconsolidation.

Test results indicate that stress relief due to borehole excavation does not affect the soil properties.

While contributing to the understanding of the effects of sample disturbance, the work performed has isolated aspects of the intact behavior of RBBC previously not understood. In particular it was shown that:

- within a wide range of values of  $K_0$  (0.38 to 0.57) there is a clear relationship between the pre-shear lateral stress ratio and the undrained strength of NC RBBC: as  $K$  increases,  $c_u/\sigma'_{vc}$  decreases;
- stress path consolidation produces a drastic variation of the compression behavior of RBBC obscuring the stress history and decreasing the compression ratio, but has no impact on the strength.

#### **8.4 Recommendations for Future Research**

The research performed has provided a basic understanding of the effects of PSA and ISA disturbance on the most significant properties of RBBC and has presented a preliminary assessment of the applicability of the Recompression and SHANSEP techniques to erase the effects of disturbance.

It is therefore suggested that future research be aimed primarily at completing the evaluation of the effects of PSA and ISA disturbance on OC RBBC. In particular, it appears important to:

- i) define the effects of Recompression on the undrained strength of OCR2 RBBC so to better define the range of OCR values for which this technique provides unsafe estimates of the strength;

- ii) verify the applicability of the SHANSEP technique to reconstruct the intact behavior of OC RBBC;
- iii) extend the analysis of the effects of PSA and ISA disturbance to clays with OCR as high as 16.

Second, future investigations should address the effects of PSA and ISA disturbance on soil properties which were not investigated in this research, including:

- i) the stiffness of the soil at small strains. At the same time, one should assess the effectiveness of Recompression and SHANSEP in recovering this parameter. For this purpose it is essential to perform on-specimen small strain stiffness measurements.
- ii) the lateral stress ratio of the soil. A precise assessment of this parameter could not be performed in this research due to the lack of radial strain measurements.
- iii) the shape and position of the bounding surface. Evidence for shrinking of the bounding surface due to sample disturbance has been presented by La Rochelle et al. (1981), Tavenas and Leroueil (1987) and Hight et al. (1992).

Third, it is suggested that additional tests be performed to validate some of the observations presented in this work. In particular, conclusive determination of the following behavioral points requires further investigation:

- i) the effect of SHANSEP reconsolidation on the intermediate strain stiffness;
- ii) the overestimation of the preconsolidation pressure caused by disturbance;
- ii) the inability of SHANSEP consolidation to recover the stress strain behavior of highly disturbed NC RBBC; and
- iii) the inability of the NC soil to reach the original virgin compression slope when reconsolidated after disturbance.

Both ii) and iii) require the soil to be consolidated to stresses much higher than those applied in this research. This can be achieved by either decreasing the sampling effective stress or employing high pressure triaxial cells.

Finally, it appears that additional insight into the effects of sampling disturbance could be obtained by

- i) conducting a limited testing program on natural material to verify how PSA and ISA disturbance affect the degradation of the engineering properties of a more structured material;
- ii) modifying the simulation of disturbance in the laboratory to also include variations of the water content during sampling.
- iii) performing an extensive comparison with field data to determine to what extent the PSA and ISA can account for the level of disturbance of block and tube field samples.

## References

- Adachi, K., Todo, H. and Mizuno, H. (1981), "Quality of Samples of Soft Cohesive Soil", *Proc. 10th Int. Conference on Soil Mech. and Fdn. Engrg.*, Stockholm.
- Ahmed, I. (1988), "Investigation of normalized behavior of Resedimented Boston Blue Clay using Geonor direct simple shear apparatus", Master of Science Thesis, Department of Civil Engineering, MIT, Cambridge, MA.
- Andresen, A. and Kolstad, P. (1979), "The NGI 54mm sampler for undisturbed sampling of clays and representative sampling of coarser materials", *Int. Symp. of Soil Sampling*, Singapore, 14-31.
- Atkinson, J. H., Allman, M. A., and Boese, R. J. (1992). "Influence of laboratory sample preparation procedures on the strength and stiffness of intact Bothkennar soil recovered using the Laval sampler." *Géotechnique* , 42, No. 2, 349-354.
- Atkinson, J. H. and Kubba, L. M. (1981), "Some effects of sample disturbance on soft clay." *Proc. 10th Int. Conf. Soil Mech. and Fdn. Engrg* , Stockholm 2, 423-426.
- Baligh, M. M. (1985). "The strain path method." *J. Geotech. Engrg.* , ASCE, 111(9), 1108-1136.
- Baligh, M. M., Azzouz, A. S., and Chin, C.-T., (1987). "Disturbance due to 'ideal' tube sampling." *J. Geotech. Engrg.* , ASCE, 113(7), 739-757.
- Becker, D. E., Crooks, J. H. A, Been, K. and Jefferies, M. G. (1987), "Work as a criterion for determining in situ and yield stresses in clays", *Canadian Geotech. J.* , 24 (1), 549-564.
- Berman, D. R. (1993), "Characterization of the engineering properties of Boston Blue Clay at the MIT campus," Master of Science Thesis, Department of Civil Engineering, MIT, Cambridge, MA.
- Berre, T., and Bjerrum, L. (1973). "Shear strength of normally consolidated clays." *Proc. 8th Int. Conference on Soil Mech. and Fdn. Engrg.* , Moscow, U. S. S. R., 1.1, 39-49.
- Bishop, A.W and Henkel, D. F. (1962), The Measurement of Soil properties in the Triaxial Cell, 2nd Ed., Edward Srnold, Ltd., London.

- Bjerrum, L. (1973). "Problems of soil mechanics and construction on soft clays: OSA Report." *Proc. 8th Int. Conference on Soil Mech. and Fdn. Engrg.*, Moscow, U. S. S. R., 3, 111-159.
- Broms, B. B. (1980). "Soil sampling in Europe: state-of-the-art." *J. Geotech. Engrg. Div. Am. Soc. Civ. Engrs.* , 106, No. GT1, 65-98.
- Budhu, M. and Wu, C. S. (1992), "Numerical analysis of sampling disturbances in clay soils', *Int. J. for Num. and Anal. Methods in Geomechanics*, vol.16, 467-492.
- Burland, J. B. (1990), "On the compressibility and shear strength of natural clays", *Géotechnique* , 40, No. 3, 329-378.
- Cauble, D. F. (1993), "The behavior of Resedimented Boston Blue Clay at OCR4 in cyclic and post-cyclic undrained direct simple shear", Master of Science Thesis, Department of Civil Engineering, MIT, Cambridge, MA.
- Chandler, R. J., Harwood, A. H., and Skinner, P. J. (1992). "Sample disturbance in London clay." *Géotechnique* , 42, No. 4, 577-585.
- Chin, T. C. (1986). " Open-ended Pile Penetration in Saturated Clays," PhD Thesis, Department of Civil Engineering, MIT, Cambridge, MA.
- Clayton, C. R. I., Hight, D. W., and Hopper, R. J. (1992). "Progressive destructuring of Bothkennar clay: implications for sampling and reconsolidation procedures." *Géotechnique* , 42, No. 2, 219-239.
- de La Beaumelle, Axel Christian Luc Angliviel (1991), "Evaluation of SHANSEP strength-deformation properties of undisturbed Boston Blue Clay for automated triaxial testing," Master of Science Thesis, Department of Civil Engineering, MIT, Cambridge, MA.
- Estabrook, A. H. (1991), "Comparison of recompression and SHANSEP strength-deformation properties of undisturbed Boston Blue Clay from automated triaxial testing," Master of Science Thesis, Department of Civil Engineering, MIT, Cambridge, MA.
- Georgiannou, V. N., and Hight, D. W. (Not yet published). "The effects of centre-line tube sampling strains on the undrained behaviour of two stiff overconsolidated clays."

- Germaine, J. T., (1982) "Development of the directional shear Cell for measuring cross anisotropic clay properties", Doctor of Science Thesis, Department of Civil Engineering, MIT, Cambridge, MA.
- Graham, J., Kwok, C. K., and Ambrosie, R. W. (1987). "Stress release, undrained storage and reconsolidation in simulated underwater clay." *Can. Geotech. J.* , 24, No. 2, 279-288.
- Graham, J. and Lau, S. L.-K. (1988). "Influence of stress-release disturbance, storage, and reconsolidation procedures on the shear behaviour of reconstituted underwater clay." *Géotechnique* , 38, No. 2, 279-300.
- Hight, D. W. (1993). "A review of sampling effects in clays and sands." *Offshore Site Investigation and Foundation Behaviour* , Society for Underwater Technology, Vol. 28, 115-146.
- Hight, D. W., Boese, R., Butcher, A. P., Clayton, C. R. I., and Smith, P. R. (1992). "Disturbance of Bothkennar clay prior to laboratory testing." *Géotechnique* , 42, No. 2, 199-217.
- Hight, D. W., Gens, A. , and Jardine, R. J. (1985), "Evaluation of geotechnical parameters from triaxial tests on offshore clay", *Proceedings of the Conference on Offshore Site Investigation*, London, England.
- Holtz, R. D., Jamiolkowski, M. B., and Lancellotta, R. (1986), "Lessons from oedometer tests on high quality samples", *J. Geotech. Engrg.* , ASCE, 112(8), 768-775.
- Hvorslev, M. J., "Subsurface exploration and sampling of soils for civil engineering purposes." Report on a research project of ASCE, U. S. Army Engineer Experiment Station, Vicksburg, 521 pp.
- Jamiolkowski, M., Ladd, C. C., Germaine, J. T., and Lancellotta, R. (1985). "New developments in field and laboratory testing of soils: Theme Lecture 2." *Proc. 11th Int. Conference on Soil Mech. and Fdn. Engrg.*, San Francisco, 1, 57-153.
- Jardine, R. J., St. John, H. D., Hight, D. W. and Potts, D. M. (1991). "Some practical applications of a non-linear ground model." *Proc. 10th European Conference on Soil Mech. and Fdn. Engrg.* , Florence, Vol. 1, 223-228.
- Kallstenius, T. (1958). "Mechanical disturbances in clay samples taken with piston samplers." *Royal Swedish Geotech. Inst. Proc.* , No. 16, 1-75.

- Kimura, T. and Saitoh, K. (1982). "The influence of disturbance due to sample preparation on the undrained strength of saturated cohesive soil." *Soils and Foundations* , Japanese Soc. of Soil Mech. and Fdn. Egrg., Vol. 22, No. 4, 109-120.
- Kimura, T. and Saitoh, K. (1984). "The effect of sampling disturbance on undrained strength of cohesive soils" *Geotechnical Engineering*, Vol. 15, 37-57.
- Kimura, T., Saitoh, K. and Nishihara (1983). "The effect of reconsolidation on undrained strength of normally consolidated cohesive soils" *Soils and Foundations* , Japanese Soc. of Soil Mech. and Fdn. Egrg., Vol. 23, No. 3, 27-38.
- Kirkpatrick, W.M. and Khan, A.J. (1984). "The reaction of clays to sampling stress relief. " *Géotechnique* , 34, No. 1, 29-42.
- Lacasse, S., Berre, T (1988) and Lefebvre, G. (1985), "Block sampling of sensitive clays", *Proc. 11th Int. Conference on Soil Mech. and Fdn. Engrg.*, San Francisco, 2.
- Ladd, C.C. (1986). "Stability evaluation during staged construction." Twenty-second Karl Terzaghi Lecture, ASCE Annual Convention, 537-615.
- Ladd, C. C. , and Foott, R. (1974). "New design procedure for stability of soft clays." *J. Geotech. Engrg. Div.* , ASCE, 100(7), 763-786.
- Ladd, C. C. and Lambe, T. W. (1963). "The strength of undisturbed clay determined from undrained tests." *Symp. on Laboratory Shear Testing of Soils* , ASTM STP 361, 342-371.
- La Rochelle, P., Sarrailh, J., Tavenas, F., Roy, M., and Leroueil, S. (1981). "Causes of sampling disturbance and design of a new sampler for sensitive soils." *Canadian Geotech. J.* , 18(1), 52-66.
- Lefebvre, G. and Poulin, C. (1979), "A new method of sampling in sensitive clay", *Canadian Geotech. J.* , 16(1), 226-233.
- Mesri, G. and Choi, Y. K. (1985), "Settlement Analysis of Embankments on Soft Clays", *J. Geotech. Engrg.* 111(4), 441-464.
- Mesri, G. and Godlewski, P. M. (1977), "Time and stress compatibility Interralationships", *J. Geotech. Engrg. Div.* , ASCE, 103(5), 417-430.



- Ortega, O. J. (1992), "Computer automation of the consolidated-undrained direct simple shear test", Master of Science Thesis, Department of Civil Engineering, MIT, Cambridge, MA.
- Santagata, M. C. and Germaine, J. T. (1994), "Simulation of sampling disturbance in soft clays using triaxial element tests: Supplementary data report", MIT Report R94-04, MIT Cambridge, MA>
- Seah, T. H., (1990) "Anisotropy of Resedimented Bostone Blue Clay", Doctor of Philosophy Thesis, Department of Civil Engineering, MIT, Cambridge, MA.
- Sheahan, T. C. (1991), "An experimental study of the time-dependent undrained shear behavior of Resedimented Boston Blue Clay using automated stress path triaxial equipment", Doctor of Science Thesis, Department of Civil Engineering, MIT, Cambridge, MA.
- Sheahan, T. C. and Germaine, J. T. (1992). "Computer automation of conventional triaxial equipment," *ASCE, Geotechnical Testing Journal*, Vol. 15, No. 4, pp. 311-322.
- Sinfield, J. V. (1994), "An experimental investigation of sampling disturbance effects in Resedimented Boston Blue Clay", Master of Science Thesis, Department of Civil Engineering, MIT, Cambridge, MA.
- Skempton, A. W., and Sowa, V. A. (1963). "The behaviour of saturated clays during sampling and testing." *Géotechnique* , 13, 269-291.
- Tavenas, F. and Leroueil, S. (1987), "Laboratory and in situ stress-strain-time behavior of soft clays: a state-of-the-art.", *Proc. Int. Symp. on Geotechnical Engineering of Sofs Soils*, Mexico City, Vol.", 1-46.
- Vaughan, P. R., Chandler, R. J., Apted, J. P., Macguire, and Sandroni, S. S. (1993). "Sampling disturbance - with particular reference to stiff clays." *Predictive Soil Mechanics*, Edited by Thomas Telford, London.
- van Eekelen, S. and van den Berg, P. (19920, 'Sample isturbance, numerical model and experiments", Delft Geotechnics, The Netherlands.
- Walbaum, M. (1988), "Procedure for investigation of sample disturbance using the direct shear apparatus", Master of Science Thesis, Department of Civil Engineering, MIT, Cambridge, MA.

